A multidisciplinary investigation of the relationship between *Pseudomonas syringae* and *Aesculus hippocastanum* bleeding canker

Omar A. Ahmed Alhamd

Thesis for submission towards the degree of Doctor of Philosophy

March 2020

Keele University

Abstract

Bleeding canker of *Aesculus hippocastanum* is caused by *Pseudomonas syringae* pathovar *aesculi*. The disease has rapidly spread through many countries, yet little is known about this potentially fatal disease. Climate change affects plant diseases directly, and abiotic and biotic stress adds to the pressure. In turn, the plant produces pathogen-induced defence responses at the genetic or proteomic level which are not well understood.

In this study, the transcriptome of *A. hippocastanum* phloem was sequenced using Illumina RNA-Seq technology. Many genes were identified, some of them known to have a relationship with wound stress in plants such as C86B1 which is involved in the stimulation of wound suberization. Some genes were up-regulated in infected trees, such as BGL17, but their functions are still unknown. Further studies are required to determine the roles of these genes in host defence.

An experimental investigation was conducted to explore the effect of selected environmental factors and nanoparticles on the bacteria and plants. Different levels of damage and drought stress have been studied. Some positive results were observed in reducing infection and activity of bacteria with low levels of drought stress (75% soil field capacity). The thermal shock was also applied to bacteria, which showed susceptibility to the rise in temperature.

The effects of four nanoparticles (NPs) at different concentrations were investigated *in vitro* and *in vivo*. Silver and cerium oxide NPs were synthesised and characterised using transmission electron microscopy and inductively coupled plasma optical emission spectrometry. NPs were applied to bacteria

strains, *A. hippocastanum* and two model plants (*Phaseolus vulgaris* and *Lycopersicon esculentum*). Titanium oxide and silver NPs showed significant antibacterial activity against several pathogenic strains of *Pseudomonas*. It was found that titanium NPs can have either a negative or a positive impact on bacterial and plant growth, according to concentration and species of plant.

Abbreviations

Abbreviations	Descriptions
16S rRNA	16S Ribosomal Ribonucleic Acid
ABA	Abscisic acid
BCHC	Bleeding canker of horse chestnut
BSA	Bovine Serum Albumin
CAN	Acetonitrile
CFC	Cetrimide Fucidin Cephaloridine selective supplement
CFU	Colony-forming unit
CBBG	Coomassie Brilliant Blue G-250
DAD	Disc agar diffusion
DEGs	Differentially expressed genes
CVI	Chronic venous insufficiency
DTT	Dithiothreitol
DW	Distil water
EDTA	Ethylenediaminetetraacetic acid
ETI	Effector-triggered immunity
ETS	Effector-triggered susceptibility
FA	Formic acid
FC	Soil moisture field capacity
FPLC	Fast Protein Liquid Chromatography
GM	Genetically Modified
HCLM	The horse-chestnut leaf miner
HCSE	Horse chestnut seed extract
HPLC	High-performance liquid chromatography
kDa	Kilodalton
LC-MS	Liquid Chromatography-Mass Spectrometry
LPS	Lipopolysaccharide
M	Molar
MAMPs	Microbial–associated molecular patterns
MeCN	Methyl cyanide (Acetonitrile)
MOPS	3-(N-morpholino) propane sulfonic acid
NB-LRR	Nucleotide binding-site leucine-rich repeat
nm	Nanometres
OD	Optical density
Pae	*Pseudomonas syringae* pv. *aesculi*
PAMPs	Pathogen–associated molecular patterns
PEG	Poly ethylene glycol
PRRs	Pattern-recognition receptors
PTI	PAMP -triggered immunity
PVPP	Polyvinylpolypyrrolidone
R-gene	Resistance gene
R-proteins	Resistance proteins
ROS	Reactive oxygen species

RT	Room temperature
SD	Standard deviation
SDS	Sodium dodecyl sulfate
SDW	Sterile distilled water
TCA	Trichloroacetic acid
TEMED	Tetramethylethylenediamine
TFA	Trifluoroacetic acid
Tris	Tris(hydroxymethyl)aminomethane
Triton X-100	Polyoxyethylene octyl phenyl ether
β-ME	β-Mercaptoethanol

Acknowledgements

First and foremost, I would like to acknowledge and thank **Dr Annette Shrive** my supervisor, **Dr Peter Thomas** my co-supervisor and **Professor Trevor Greenhough** my advisor, for your combined support, inspiration and guidance. Annette and Peter without your help and encouragement, I would not be complete this work, thank you so much.

I also would like to thank past and present our group, Will, Jamie, Jennifer, Harry, Sameer, Ian Burns, Emily, Henry, Ruben, Rob, for always being ready to help when needed and for being so much fun. Thank you all, especially when you supported me during my illness. You were my real family. I'm proud because I was with this friendly team. I will not forget you as long as I'm alive. Thanks for Billy for photographic assistance in the greenhouse.

Thanks to Dr. Sarah Green, Dr. Daniel, Dr Sarah, Dr. Clare and for all the support, advice, friendship, over the years and to the people in Life Sciences who have given me endless support and encouragement along the way.

I owe big thanks and gratefulness to all of the staff at Keele University; School of Life Sciences, a special thanks to Jayne Bromley, Ian Wright, Nigel Bowers, Ron Knapper, Lisa Cartlidge and Chris Bain for providing the facilities throughout the academic study. I extend my special thanks to Chris who kept our lab clean and tidy.

Deepest thanks to my mum and Dad and family and my kids who have been there for me waiting for me, thanks for your patience and long waiting – you kept me going. Thanks to anyone I have missed, your efforts have and always will be appreciated. I will remember you all.

Table of Contents

Table of Figures

Table of Tables

1 Chapter 1: Introduction

1.1 *Aesculus hippocastanum*

1.1.1 Classification and distribution of *Aesculus hippocastanum*

Aesculus hippocastanum is a large, deciduous tree belonging to the Sapindaceae family, which has only two genera *Aesculus* and *Billia* (George, 1951; Benson, 1979; Thomas *et al.*, 2019). The *Aesculus* genus ranges from shrubs to large trees. This genus contains about twenty-five species of woody deciduous trees and medium shrubs, most of them on the North American continent. They are natural to the temperate northern hemisphere and can be found in all three northern continents (Bean, 1970; Nelson *et al.*, 2007). In the *Aesculus* genus, *Aesculus hippocastanum* is the most common species found in the UK today (horse chestnut) with a widespread hybrid, *Aesculus* x *carnea* (red horse chestnut). There are also some species that are considered less familiar, such as *Aesculus flava* (Yellow Buckeye), *A. indica* (Indian Horse chestnut) and *A. parviflora* (Bottlebrush Buckeye) (Thomas, *et al.*, 2019; Bean, 1970; Phillips, 1978).

A. hippocastanum is usually found in the lowlands of Britain, reaching around 505 m altitude at Ashgill and 1300m in Sweden and Norway (Preston *et al.*, 2002; Bellini & Nin, 2005). It occurs at 218-1,485m in its original range in Bulgaria and Greece, and up to 1,600 m in Albania (Leathart, 1991; Avtzis et al. 2007; Walas *et al.*, 2018; Horvat *et al.*, 1974). In Greece, 72% of mature trees grow between 500 and 1000m and 35% of individuals and 31% of the populations are observed within 900 and 1000 m, (Tsiroukis, 2008). *Aesculus hippocastanum* is a mesophytic forest tree,

spreading in warm-temperate climates. The climatic requirements across the entire European continent are considered the main limitations of its distribution where precipitation is in the warmest and coldest quarters of the year and there is a wide range in annual temperature. These conditions appear to act essentially through low humidity, which was seen as the chief factor limiting distribution in areas such as the Mediterranean and urban areas, and through high soil moisture and low stomatal conductance. These requirements appear to be excellent in supporting horse-chestnut survival (Walas *et al.,* 2018). It is probable that the recalcitrant nature of the seeds (unorthodox seeds) i.e. their intolerance of desiccation, is the chief factor limiting *A. hippocastanum* naturally to moist sites and reveals why it can be successfully transplanted as seedlings into a wide range of climatic conditions from woodlands to harsh, dry urban areas (Horvat *et al.*, 1974).

To better understand and recognise of *A. hippocastanum* characteristics; it is useful to classify it entirely from the highest levels to the most accurate taxonomic or as what known tree of life and as the following:

Domain: Eukarya

Supergroup: Archeaplastida

Kingdom: Plantae

Subkingdom: Tracheobionta

Superdivision: Spermatophyta

Division: Magnoliophyta (Angiosperms)

Class: Magnoliopsida (Dicotyledoneae)

Order: Sapindales

Family: *Sapindaceae*

Genus: Aesculus

Species: *Aesculus hippocastanum*

(Thomas *et al.,* 2019; Ball *et al.*, 2011; George, 1951)

1.1.2 The Etymology of *Aesculus hippocastanum* L.

The commonest names are usually horse chestnut, buckeye, conqueror and fish poison (Fuller & McClintock, 1986; Nelson *et al*., 2007), the scientific name is *Aesculus hippocastanum*. The common name Horse-chestnut (often unhyphenated) may possibly belong to the Turkish people because they used the fruits of *A. hippocastanum* to treat breathing problems in horses or because the fruit looks like sweet chestnut (Gledhill, 2008; Herbert, 1985). In America *A. hippocastanum* is called the buckeye because its seed resembles the eyes of the buck (male deer) (Dutton, 1979) or was called fish poison as it used to be used to catch fish after killing them as a result of eating seed powder, which is toxic to fish (Nelson *et al*., 2007).

Aesculus hippocastanum is the most widely planted member of the *Aesculus* genus. It was brought to Britain in 1616 as an ornamental tree. The tree was also introduced into other parts of Europe as early as during the 15th century.

According to The National Woodland Inventory of Woodland Trees (NIWT), there are around 470,000 healthy *Aesculus hippocastanum* trees in the UK divided approximately to 432,000 in England, 29,100 in Scotland and 11,100 in Wales. However, this species is mostly planted in non-woodland places. Thus, most of the trees in the UK are probably not accounted for in any national woodland census, but are common along streets, in gardens and parks as amenity trees (Forestry Commission, 2015). *A. hippocastanum* is indigenous to southern Albania northern Greece, parts of Bulgaria, and Turkey at high elevations. It is also common in town parks, private gardens and especially on village greens in England, less commonly so in Ireland and Scotland (Thomas *et al.*, 2019).

1.1.3 Other species of *Aesculus*

The genus of *Aesculus* L. contains approximately 14 important species (Table1-1). Apart from the horse chestnut which is the only *Aesculus* species native to Europe, there are twelve other species of *Aesculus* that are found throughout the northern hemisphere, mainly in eastern Asia and eastern USA. There is also a single species native to western North America and another indigenous to north-western Mexico (Thomas, *et al*; 2019).

Table 1-1 Important species within the *Aesculus* genus. Data from Bean, 1970; Mitchell, 1974 and Thomas *et al.*, 2019.

Species of Hippocastanum Taxa	**Common name**	**Tree approximately height at maturity (ft.)**	**Native Range**
A. hippocastanum	Horse chestnut, Conker tree	25-100	S. Albania, N. Greece, Bulgaria
A. turbinata	Japanese horse chestnut	80-100	Japan
A. x carnea *	Red horse chestnut	30-50	Spread in Germany Hybrids between *A. hippocastanum* and *A. pavia*
A. parryi	Parry buckeye	30	Baja California, Mexico
A. glabra	Ohio buckeye	30-70	S.E. United States
A. flava	Sweet or yellow buckeye	25-88	S.E. United States
A. pavia	Red buckeye	90	S.E. United States
A. parviflora	dwarf buckeye bottlebrush buckeye dwarf horse chestnut	8-15	S.E. United States
A. sylvatica	painted buckeye	25 -65	S.E. United States
A. assamica		80	N. Siam, NW Indo-China, s. China, NE Pakistan, Bhutan
A. indica	Indian horse chestnut	Over 100.	N.W Himalayas
A. chinensis	Chinese horse chestnut	80-90	Eastern Asia
A. wilsonii	Wilson's horse chestnut		Central China
A. californica	California buckeye	30-40	western North America

* Besides this hybrid, there are several others of natural origin in North America that have been identified, such as *Aesculus x bushii* Schneid. And *Aesculus x mississppienis* Sarg. These hybrids can be very confusing and challenging to differentiate, and are of little horticultural importance (Bean, 1970).

1.1.4 Anatomical and morphological features

Anatomical features for the tree may offer opportunities for drawing out valuable information, but few studies give details of the anatomy of *A. hippocastanum*. The colour of the bark is dark grey-brown and older bark tears into long plates whose ends rise away from the trunk or into large scales to give a ribbed or fluted shape (Mitchell, 1974); it is habitually twisted in the right-hand direction. The branches usually occur in wide circles and can form a large, tall domed canopy. The large branches are upright with low spreading bases then sharply upturned ends. The stem of *A. hippocastanum* usually requires pruning to develop a sound structure.

Aesculus hippocastanum foliage forms on hardy twigs which are pale pink-brown or reddish-purple with oval buds set in pairs; dark shiny red-brown 2.5 x 1.5 cm. During the winter period, the outer scales are covered with a viscous resin to protect them from insects, pests and diseases (Figure 1-1 B). The lenticels are pale brown to grey (Herbert, 1985; Mitchell, 1974). *A. hippocastanum* has palmate compound leaves (a leaf with two or more separate leaflets) opposite, and stipules are absent (Benson, 1979; Forrest, 2006) In general, leaves consist of digitate 3-9 obovate leaflets usually consisting of five leaflets (George, 1951); 10-25 cm long; 2.5-10 cm wide, elliptical or obovate, broadest towards the abrupt point, tapering to a stalkless base, and bright, fresh green at first then becoming darker. The autumn colour is very variable, the trees become scarlet early, or gold or orange. In mid-September to early November all the leaves drop, leaving on the branch a scar that looks like a horseshoe. This mark, in fact, is the

remains of the vascular bundle. This is considered to be a clear diagnostic feature of the *Aesculus hippocastanum* tree in winter when the leaves drop, and the tree shoot become bare (Herbert, 1985; Mitchell, 1974). Most stomata on the *Aesculus hippocastanum* leaf are situated around the edge of the broadest parts of the leaflets (Thomas, 2014).

Figure 1-1 *Aesculus hippocastanum* flower and buds A: shows the inflorescence (image taken on Keele University campus in May 2017) B: shows the bud, The arrow indicates the top of the bud (image taken on Keele University campus in December 2017).

The flowers are polygamous (Radojevic *et al.*, 2000), appearing in large panicles to 0.3 m long (Fuller & McClintock, 1986) (Figure 1-1 A); bisexual, sometimes the upper flowers are unisexual having stamens but no pistil (George, 1951; Thomas *et al.*, 2019). The flowers are zygomorphic (bilaterally symmetrical) (Benson, 1979) and very abundant each year,

some trees flowering at the end of April to the beginning of June, but in general, they are flowering best in May. The flower consists of five separate sepals, 4-5 fringed, ciliate petals, unequal, imbricate, white petals with a blotch of colour at the base bright, which is at first yellow then changes to red in pollinated flowers. Some scholars consider this a sign to show that the flower has been pollinated (Bean, 1970; Mitchell, 1974). The stamens number between six to eight per flower and are slightly longer than the petals (Bean, 1970; Herbert, 1985). The flower has a hypogynous disc (Benson, 1979); the ovary is sessile (Hutchinson, 1959), and the newest flower is located toward the tip of the inflorescence (Herbert, 1985).

The fruit is spiny, green, leathery and spherical; it is around 6 cm in diameter (Figure 1-2A). The fruit splits when ripe and the seeds are ready to drop in September. The fruit contains one big or 2-3 small oval seeds. They are known as ‘conkers’ and may have a flat side; they are dark brown in colour, with a shining and smooth surface and have a large hilum with a light colour that looks like the pupil of an eye (McMillan, 1982; Mitchell, 1974) (Figure 1-2 B). The seed has two cotyledons (Bryan, 2010), the seed testa is coriaceous; cotyledons are thick, and often adherent face to face (Hutchinson, 1959). The average number of cleaned seeds per kilogram is 90 seeds (Thomas, 2014). The embryo is curved and there is no endosperm (George, 1951).

The tree’s approximate age of first fruiting is between 20 to 30 years (Thomas, 2014). The transverse section of trunk shows the conducting tissues (xylem, phloem) and it is straightforward to distinguish between them, but the phloem boundary with cortex is sometimes difficult to distinguish. Crystals of calcium oxalate are very common in the cortex,

especially clustered crystals with a few solitary crystals (Cutler, *et al.*, 1987; Herbert, 1985).

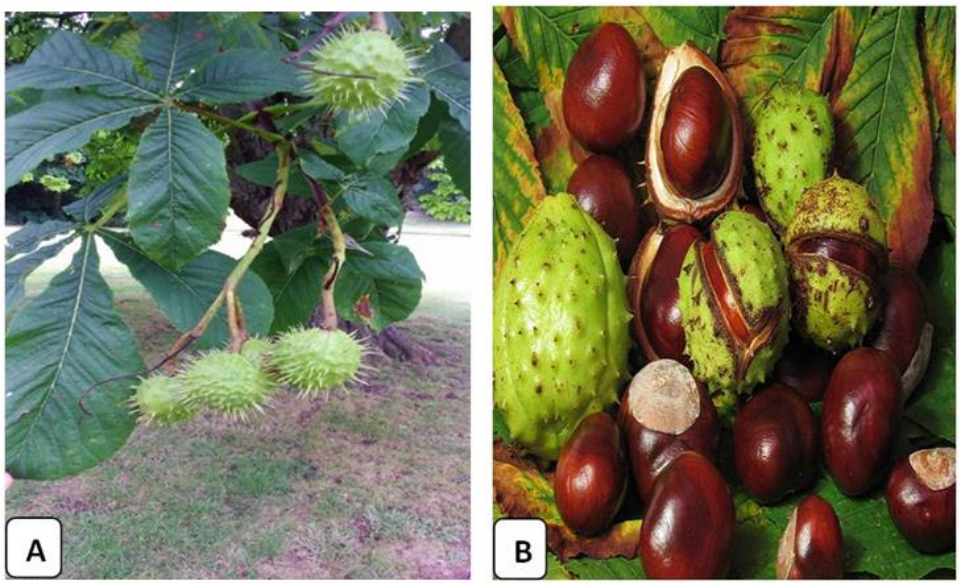

Figure 1-2 *Aesculus hippocastanum* fruits and seeds A: shows the leaves and the spiny fruit (image taken on Keele University campus in October 2016) B: shows the seeds and the capsules (image taken from Wikimedia, 2016).

Growth rings in the xylem are sometimes unclear; the walls of fibres are very thin, but the lumina of xylem conduits are very wide. The axial parenchyma is scattered. The parenchyma rays are usually uniseriate; vessels are individual or in pairs forming short radial chain; spiral thickening in the second wall is common (Cutler *et al.*, 1987).

1.1.5 Growth and environment requirements of *A. hippocastanum*

The type of seed germination in *Aesculus hippocastanum* is hypogeal (the cotyledons remains below the ground) (Thomas, 2014). The growth of buds starts in March or April. Trees grow for up to 300 years when they are not infected with the disease and are in good condition, but usually, the maximum age of a tree is about 150 years (Mitchell, 1974). The growing

point dies once it flowers and in the next year growth will be from the two buds behind the growing point (Thomas, 2014).

Aesculus hippocastanum grow quite well in any soil which is not too dry; the trees prefer deep, well-drained and wet soil, not too acidic. The tree is easy to cultivate, and seedlings readily transplant (Bean, 1970; Wilkinson & Mitchell, 1982). *Aesculus hippocastanum* also has the ability to tolerate a wide range of stressful conditions like wet clay, sandy soils and chalk, pollution and low light, but in severe winters shoots may be slightly damaged by frost (Tsiroukis, 2008). *A. hippocastanum* in its original range is usually restricted to humid but well-drained stony soil. In Bulgaria and Albania, horse-chestnut grows on calcareous soils (mostly or partly composed of calcium carbonate) derived from limestone. These medium-deep loams are slightly acidic on the surface and more alkaline at depth. *A. hippocastanum*, however, copes with being planted on a range of soils from heavy clay to nutrient poor sand and from acid to alkaline even if an optimum pH of 6.6 to 7.2 is recommended (Puchalski & Prusinkiewicz, 1975). *Aesculus hippocastanum* can withstand atmospheric pollution and grows well in polluted central cities in Europe. Leaves collected in polluted areas of mainland Europe can appear curved, small and brittle, though the degree of contamination causing this is not stated (Godzik & Sassen, 1970). The compound leaf in *A. hippocastanum* help to reduce excessive water loss when evaporative demand is higher than water supply (Thomas, 2014).

1.1.6 *Aesculus hippocastanum* uses and economic importance

1.1.6.1 Horse chestnut natural products and their pharmacological uses

Plant extracts have again become valuable as they are environmentally acceptable, easily obtainable, and renewable source for a broad range of required inhibitors. Horse-chestnut is essential as a source of many natural chemical compounds. The tree extracts are viewed as a rich source of naturally synthesised chemical compounds which are used in world pharmacopoeias and can be extracted by simple procedures at low cost (Bellini & Nin, 2004; Edwards *et al*., 2015).

Saponins and coumarins are the essential natural products of horse chestnut, but in addition to that, the tree has the ability to produce a variety of secondary products that are biologically and chemically active, which are mostly glycosides (Wilkinson & Brown, 1999).

The general structure of saponins is cyclic triterpene, steroid or steroidal alkaloid aglycones esterified to sugar or uronic acid moieties. These compounds make them amphiphilic in nature and because they are highly surface-active, many saponins form stable foams in aqueous solutions that emulsify in water similar to laundry detergent (Walthelm *et al*., 2001). Coumarins consist of simple coumarins, furanocoumarins, pyranocoumarins and substituted coumarins; coumarin is highly heterocyclic, highly oxygenated aromatic lactones (Sproll *et al*., 2008).

The medicinal properties of horse-chestnut natural products have been used for many centuries. In the past horse-chestnut preparations, chiefly from

seeds, were used in folk medicine as a treatment, cure and analgesic for many diseases including coughs, arthritis, rectal complaints, rheumatism, antipyretic, narcotic, tonic, and as a vasoconstrictor. They have also been used to treat backache, sunburn, neuralgia, haemorrhoids and whooping cough, although the essential phytochemical basis for these applications, were not known (Wichtl, 2004; Wilkinson & Brown, 1999).

The main use of *A. hippocastanum* is to reduce symptoms including leg swelling, leg cramps and heaviness as well as vascular problems (Pittler & Ernst, 2012), because this extract consists mainly of escins and a mixture of triterpenoid saponins (α- and β-escin) (Edwards *et al*., 2015; Pittler & Ernst, 2012). As well it is used for gastrointestinal disorders and bladder and fever (Newall *et al*., 1996; Sirtori, 2001).

A. hippocastanum is currently used in homeopathic medicine to treat a wide variety of conditions (Edwards *et al*., 2015). The seed extracts (HCSE) have been used in medicines to treat chronic peripheral vascular insufficiency (CVI) (Pittler & Ernst, 2012). The effectiveness of extracts against CVI and other oedemas is due to escin, which decreases lymphatic flow and alters the permeability of cell membranes that allows fluid to be reabsorbed. Besides this, escin increases blood flow and the vein tonic (elastic, contractile) properties of human saphenous veins without any noticeable effect on blood pressure (Sirtori, 2001). Furthermore, seed extracts are also used as a medicine for coughs and fevers (Curir *et al*., 2007).

Early studies suggested that water extracts have potent anti-inflammatory properties on cytokine responses via nuclear factor-κB-signaling pathway

inflammation process (Kim *et al*., 2015). The anti-inflammatory effects of *A. hippocastanum* L. for different pathogens have been reported. HCSE also has antifungal activity (Curir *et al*., 2007). According to some researchers, *A. hippocastanum* seeds extract (HCSE) is used in skin cosmetics to control sebum (blackhead) regulation and inhibit lipogenesis and is useful for clearing topical skin conditions and for postoperative oedema (Edwards *et al*., 2015; Zhang *et al*., 2014; Dudek-Makuch & Studzińska-Sroka, 2015). The seed extract may also be useful in treating some baldness cases (Bellini & Nin, 2004). The plant is as well used in cream production for haemorrhoid treatment (Gurel *et al*., 2013). Kimura and his group found the effectiveness of plant saponins as an antiobesity agent after treatment with wood ashes (Kimura *et al*., 2008). In addition, the seed extract is reported as being useful in treating some cancer cases (Patlolla & Rao, 2015).

1.1.6.2 *Aesculus hippocastanum*: other uses

The *A. hippocastanum* tree is particularly valued as an amenity shade tree, which has beautiful flowers and conker fruits that ripen in September (Bean, 1970; Forrest, 2006). *A. hippocastanum* also has value for biodiversity because it is considered a favourite food for squirrels, roe and red deer, and other woodland mammals. The flowers also provide pollen and nectar for honey bee and insects that live in the forest.

A. hippocastanum timber is reputed to be used in Europe for black powder charcoal (Von Maltitz, 2003). The wood has a tendency to be slightly weak, and for this reason, it was not used widely structurally (Mitchell, 1990). Conversely, it has absorbent properties that make it perfect for kitchen

utensils, vegetable and fruit storage trays and racks that keep the fruit dry and so prevent decay. It is also used for plywood, general turnery, interior trim and decorations, and handsome decorative veneers (Brashaw *et al*., 2012). Despite all the above uses, the timber of *A. hippocastanum* still has little economic value.

Some environmental specialists have also started to use *A. hippocastanum* as a bio-monitor because the tree grows very tall, contains large compound leaves, is deciduous and has the ability to accumulate trace elements (Šućur *et al.*, 2010; Tomaševič *et al.*, 2008; Yilmaz *et al.*, 2006).

Ground seeds have been used as a coffee substitute (Loenhart, 2002) and in combination with wheat flour as a strong glue in bookbinding (Bainbridge, 1984). It is recorded that giving horse-chestnut seeds to cows in moderation improves the yield and flavour of the milk (Loenhart, 2002). The fruit is also used in the traditional sport of conkers in many British regions. September and October are indubitably considered the best months for the sport when the seeds are collected (Mitchell, 1990).

1.1.7 Possible disadvantages of *A. hippocastanum*

In addition to the fact that the fruits are toxic to humans and some animals (high intake of HCSE is toxic) (Sirtori, 2001), the root may cause a widespread problem because they penetrate and clog sewers, drainage systems, and sometimes are considered harmful if it is planted very close to buildings because its root may invade the building's foundations but this damage is rare (Thomas, 2014).

1.1.8 The toxicity of *Aesculus hippocastanum* natural products

Although the plant has pharmacological and practical uses, many of the natural compounds of *Aesculus hippocastanum* are considered to be very toxic (Sirtori, 2001). The seeds and twigs are toxic. People may be unaware of the poisonousness of these species may eat the seeds thinking them one of the edible sweet chestnuts (*Castanea sativa*) (Nelson *et al*., 2007).

The *A. hippocastanum* seeds (conkers) have been classified by the Food and Drug Administration (FDA) as an unsafe herb (Rathbun & Kirkpatrick, 2007). The seed contains many components which have toxic properties such as glycosides, aescin (a complex mixture of saponins), nicotine, shikimic acid, rutin, and quercitin. A high dose from these is likely to be toxic to humans and some animals, or have undesirable side effects (Baibado & Cheung, 2010; Nelson *et al*., 2007). For example, aesculin and other compounds may interact with anticoagulants such as aspirin, increasing the risk of internal bleeding (Baibado & Cheung, 2010). *A. hippocastanum* seeds can also cause severe allergic reactions (Nelson *et al*., 2007). Some clinical studies considered the toxicity of *A. hippocastanum* is not very dangerous because the saponins are poorly absorbed, but with large exposures (high dose), gastrointestinal effects include vomiting, nausea, abdominal cramping, and diarrhoea. The toxicity can be removed by heat, so roasting horse-chestnuts instead of sweet chestnuts (*Castanea sativa*) is unlikely to cause great harm. Tannins and saponins can be removed by heating or leaching small slices in running water (Weiner, 1980).

1.1.9 *Aesculus hippocastanum*; a useful but troubled tree

As described above, the horse chestnut (*Aesculus hippocastanum* L.) is a large, vigorous deciduous, fast-growing tree (Thomas, *et al.*, 2019). It is a valuable, decorative landscape tree, highly regarded for its qualities as a shade tree, and it is useful in providing food for other species. It also provides many useful chemical products that are used in herbal medicine. The tree is most beautiful, particularly in May when covered with striking white flowers which are held in erect clusters somewhat similar to a candelabra that holds candles (Figure 1-1 A).

Aesculus hippocastanum was introduced into the UK in the late 16th century and was planted in both urban and countryside areas (Mitchell, 1990), with an estimated British population of 470,000 trees. The tree is commonly known as the horse chestnut, but it is not the same as the sweet chestnut (*Castanea sativa*). The latter is edible, but the raw horse chestnuts are poisonous and inedible; however, after special preparation to remove the toxins, they can become safer to use (Fuller & McClintock, 1986; Peirce, 1999). Over the past few years, a disease in the trees identified as bleeding canker has markedly increased and become a huge problem, especially in some parts of Europe (Cerezal & Gutiérrez, 2013; Green *et al.*, 2009) including Britain.

In general, trees play a crucial role in our planet, preserving the ecological equilibrium as well as providing the food sources of human beings and animals, as plant photosynthesis provides organic molecules for energy (food) for the whole ecosystem and they provide oxygen, required by most

organisms and many other benefits. The quick development of seriously pathogenic strains of this disease and other diseases has created a dangerous problem for public health and the British landscape. Moreover, the accurate and correct recognition of a particular disease such as bleeding canker, which appeared and spread very fast in a dramatic way, may help us to understand the biology of other severe diseases, which may damage other important plants or affect the animal or human directly or indirectly.

1.2 Diseases and pests of *A. hippocastanum*

In the past, *A. hippocastanum* was known as a tree that was resistant to diseases. However, within the last ten to fifteen years, issues of disease severity and symptoms have increased. These diseases will likely pose a threat to the survival of the tree in the future. New diseases have been detected like powdery mildew, anthracnose and bleeding canker (Talgo *et al*., 2012).

1.2.1 Bleeding canker

Bleeding canker of *A. hippocastanum* (BCHC) is considered the latest and most dangerous of the recently discovered pathogens (Green *et al*., 2009). The disease is caused by *Pseudomonas syringae* pv. *aesculi* (Pae) (Pánková *et al*., 2015); this is described in more detail in section1.3. The bacteria can infect a wide range of species (Horst, 2013a). The first external symptoms of infection happen on the main stem and branches, these symptoms are a gluey liquid oozing from the bark wounds of infected trunks (Figure 1-3).

The colour of this ooze is usually black or rusty-colour, sometimes yellow-brown (Steele *et al*., 2010; Webber *et al*., 2008). In dry summer conditions, the oozing may stop, and the exudate dries to form a dark, brittle crust under the point of the wound in the bark. Sometimes it looks like the fruiting bodies of wood-rotting fungi. Fungi may invade and stick out of the dead bark cracked surface, after which the bark peels away, revealing the internal bark below and the whole tree shows a yellowing of shoots and premature leaf fall. Furthermore, the leaves may become smaller, slimmer and more flaccid than the leaves of uninfected trees, before finally, the crown dies (Forestry Commission, 2015; Steele *et al*., 2010).

Figure 1-3 The *A. hippocastanum* trunk. The figure shows stem infected by *Pseudomonas syringae*. There is oozing outside the trunk (typical symptoms). The Arrow indicates a single lesion centred on the main trunk. (image taken on Keele University campus in September 2016).

The internal symptoms extend into the inner bark (phloem) under the bleeding patches. The wound usually contains dead or necrotic tissue, stained a brown-orange or purple with often a mottled zoned or wavy appearance. The symptoms are very similar to those caused by *Phytophthora* spp. however, this is considered to be uncommon in horse-chestnut (Webber *et al.*, 2008). The disease progression is very slow, but younger trees are affected by the disease more than those who are older and have a large diameter (Forestry Commission, 2015). In Europe the bacteria were first identified in the Netherlands in 2002 and since this year has been found in several European countries. According to Talgo *et al.*, (2012) the disease was detected in southwestern Norway in June 2010.

1.2.1.1 Leaf miner

The horse-chestnut leaf miner (HCLM) (*Cameraria ohridella*) is a tiny but extremely debilitating leaf-mining moth from the Gracillariidae family (Lepidoptera) (Pavan *et al.*, 2003). The disease was first detected in Macedonia in 1984 and since that time it has spread throughout most of Europe causing severe damage to *Aesculus hippocastanum* trees. *Cameraria ohridella* was first noticed in the UK in the Borough of Wimbledon in London in July 2002 and has since spread to many parts of South-East England (Straw & Bellett-Travers, 2004). From this original area of infestation, the moth has spread quickly, and it is now extant across most of central and southern England (Straw & Tilbury, 2006; Walas *et al.*, 2018).

The moth causes significant aesthetic damage, mainly in late summer when the leaves of *A hippocastanum* turn brown. Despite the sickly appearance of these infected trees, there is no evidence that this small moth kills the tree, although it affects photosynthesis by reducing leaf area (Percival & Banks, 2014) (Figure 1-4), and hence reduces seed weight and longevity. Reproductive capacity also may thus be reduced (Percival *et al*., 2011). The majority of damage caused by the moth happens very late in the growing season, so it does not affect the tree's performance (Percival *et al*., 2011), so there is no need to cut down and remove trees just because they are infected with *C. ohridella* (Tilbury & Evans, 2003). The larva of this tiny moth feeds inside the mine in the tree leaves between the lower and upper epidermal layers (Palisade layer), damaging the leaf tissue and stops growth. This spreads quickly across the whole leaf, and these mines become large patches. Finally, the leaf begins to dry, curls inwards and upwards at the edges, then drops off; when the new leaves have grown, once again they are infected by the moth.

Figure 1-4 *Aesculus hippocastanum* leaves infected by leaf miner. The figure shows leaves infected by leaf miner and the mine spread throughout the leaf. Arrows indicate to leaf miner lesions. (image taken on Keele University campus in October 2016).

The moth is about 0.5 centimetres long, with bright brown fore wings that have thin, silvery-white stripes. The hindwings (back wings) are dark grey contain long fringes at the ends. The female of moth can lay between 20 to 40 eggs individually on the upper surface of leaves, and after 2–3 weeks the eggs hatch. The larvae grow through five feeding larval instars (phases) and two prepupal (spinning) stages before the pupal stage (Tilbury & Evans, 2003). The first stage creates a small mine parallel to a leaf vein. In its third instar (phase) the larvae create a mine approximately 0.8 centimetres in diameter, which can spread for several square centimetres (Johne *et al.*, 2006). Four weeks after hatching the larva starts to pupate and except when hibernating as a pupa in the mine in the winter, after two weeks the adult emerges. In severe infection, the individual mines can grow together, and

almost the entire leaf area may be affected. Each year the moth has the ability to go through up to five generations, but if the weather is dry and hot, the moth goes through three generations only. The last generation of the year pupates for over six months so as to survive over the winter. The pupae have the ability to resist frost even at a temperature lower than −23 °C. This means the populations can increase despite severe cold (Tilbury & Evans, 2003). The dead spots caused by the *A. hippocastanum* leaf miner on the leaves are very similar to the spots caused by the fungus *Guignardia aesculi* but can be distinguished by the fungal infection usually being outlined by a bright yellow band which the mines lack (Tilbury & Evans, 2003). The leaf miner pupae can be distinguished from those of the *Phyllonorycter* genus because the *C. ohridella* pupae do not have first five abdominal sections (De Prins *et al*., 2003).

1.2.1.2 Anthracnose (leaf blight)

Anthracnose is a common leaf disease on *Aesculus hippocastanum* linked to the fungus *Glomerella cingulate* (Horst, 2013b). The fungus is aggressive toward most plants, causing leaves to turn brown. The infection occurs along the veins, midribs and petioles, although sometimes the infection appears at random across the leaf's surface. The infected trees can lose their leaves, but the disease rarely leads to the tree’s death. Pruning of shoots ususally affects tree survival and increase accidental infection by *G. cingulate* (Schwarze *et al*., 2000).

1.2.1.3 *Aesculus hippocastanum* scale

The horse chestnut scale (*Pulvinaria regalis*) is a common and widespread insect through most of the United Kingdom. Its origin is unknown, but it is thought to have arrived in 1960 to Europe and was first recorded in Britain in 1964 (Sengonca & Arnold, 1999; Strouts *et al*., 1995). This insect attacks the trunks or large branches causes visible circular white spots, sometimes looking like the dropping of birds or honeydew. This pest is generally found causing blemishing of the trees, cause amenity problems (Forrest, 2006).

1.2.1.4 Powdery mildew

Powdery mildew, caused by the fungus *Erysiphe flexuosa*, occurs on a vast range of hosts that includes many woody and herbaceous plants; such as apple, ash, horse chestnut, birch, boxwood, buckeye, cherry, crab-apple, dogwood, beech, elm, euonymus, hackberry, hawthorn, hickory, holly, honey locust, lilac, lime, maple, oak, pear, plane, plum, poplar, rose, willow, walnut, and the tulip tree (Tattar, 1989). Leaves become white or grey because the fungus spreads in the form of a powder or dust on top of the leaves (Tattar, 1989). The disease has spread quickly in different areas throughout Europe (Stankeviciene *et al*., 2010). The *A. hippocastanum mildew* was first recorded in Poland in 2000 (Stankeviciene *et al*., 2010).

1.2.1.5 Leaf Blotch

Leaf blotch is a fungal disease; the infection usually appears in early June, caused by *Guignardia aesculi* (Trigiano *et al*., 2006). The fungus attacks the leaves causing reddish or dull brown spots ringed with yellow; small

black fruiting bodies may appear within the spots. The leaves may finally turn brown and drop off before the proper time (Zimmermannová, 2003). Although disfiguring the foliage, this disease causes little long-term damage to the tree.

1.2.1.6 Wood rotting fungi

There are also many fungi which frequently cause wood rot and decay on mature trees, including species of *Ganoderma*, *Armillaria* and *Fistulina hepatica*, but these do not cause significant harm to *A. hippocastanum* (Horst, 2013a; Schwarze *et al*., 2000).

1.2.1.7 Dead and drooping shoots

Aesculus hippocastanum seed is considered among the most favoured food of squirrels, especially grey squirrels (*Sciurus carolinesis*). But these squirrels will also gnaw *A. hippocastanum* tips, shoots, bud, stem and bark causing noticeable damage, although not causing the death of the tree.

1.2.1.8 Leaf Scorch

Leaf scorch is an abiotic disease associated with poor weather such as high temperature and water deficiency. The leaves will turn brown and become thinner along the edges and may curl up. *A. hippocastanum* trees that are exposed to long rainy seasons or drought may develop leaf scorch; the disease also occurs in trees planted in soil infested with pathogenic organisms or near pavements or buildings which can reflect heat onto the tree (Horst, 2013a; Trigiano *et al*., 2006).

1.2.2 Overlap between diseases

There have been many studies on *Aesculus hippocastanum*, quite a few of which have focused on the interaction between pests and diseases (Lamichhane & Venturi, 2015). This is compounded in *A. hippocastanum* since it is a deciduous tree that is infected by many diseases in leafing period (Talgo *et al*., 2012). The mechanism of interaction between diseases in plants is largely unknown (Lamichhane & Venturi, 2015). Synergistic interactions between pathogens in humans happen through a number of mechanisms, for instance, chemical signalling which influences gene expression or by metabolic exchange/complementarity in order to improve the metabolic ability and avoid competition for nutrients (Frey-Klett *et al*., 2011). One study suggested that *C. ohridella* might be an active vector of bleeding canker disease, helping its spread from tree to tree and overlap between the two diseases might be happening (Straw & Williams, 2013).

Of all the pests and diseases faced by *A. hippocastanum* bleeding canker is the one that is likely to cause more severe damage and death in the foreseeable future. Therefore, the study of this bacterial disease is the most important issue in the long-term future of this species.

1.3 *Pseudomonas syringae*

Pseudomonas syringae is a Gram-negative, rod-shaped bacterium (Figure 1-5), with polar flagella (Horst, 2013a; Palleroni, 1984). The bacterium infects humans, animals, and plants. As a plant pathogen, it causes disease in hundreds of herbaceous and woody dicot and monocot species around the

world. It causes necrosis in leaves, stems, and fruit. It also can be found growing endophytically and epiphytically on plant foliage without generating any disease signs (Hirano & Upper, 2000). The infection was also reported on annual plants. By 2010 more than 50 known pathovars of *P. syringae* had been recognised (Bultreys & Kaluzna, 2010; Studholme, 2011). This large number of pathovars includes variations in *P. syringae* host range and symptomatology, providing an extraordinary opportunity to study virulence and host specificity (Gašić *et al.,* 2012; Hwang *et al.,* 2005). *Pseudomonas syringae* pv. *aesculi* has been placed under the *P. syringae* group based on 16S rRNA analysis (Anzai *et al*., 2000). The pathovar is named after the *Aesculus* tree, from which it was first isolated (Palleroni, 1984; Webber *et al*., 2008).

Very little is known about this pathogen's infection process, or about the genetic and physiological factors that cause it to be so extremely harmful (Green *et al*., 2009). The majority of the study on this pathogen and the disease it causes is limited to a visual description of the symptoms and to epidemiological studies. This pathogen was most probably introduced to Europe by importing infected nursery stock from India (Brasier, 2008). It became much more aggressive because of the humidity, severity of weather conditions and different host plants available (Green *et al*., 2009). All *Aesculus* species in Europe are susceptible to *P. syringae*, especially *Aesculus hippocastanum* and *Aesculus.* x *carnea*. In Europe, *P. syringae* pv. *aesculi* was first identified in the Netherlands in 2002 and since then has been found in several other European countries. Interestingly, the disease has increased

dramatically in the last few years, in particular, in the UK (Green *et al*., 2009; Palleroni, 1984; Sparks, 2014).

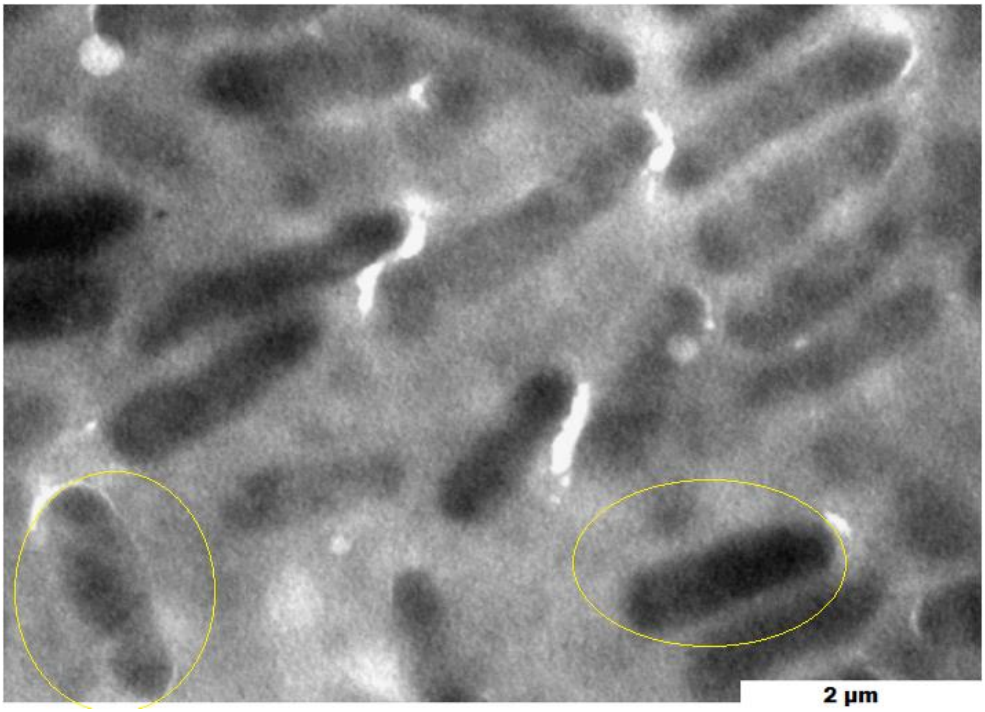

Figure 1-5 TEM images of *Pseudomonas syringae* pv. *aesculi*, bar size is 2 µm in image and analysis was done at 6 kV. The yellow circles indicate a single bacterial cell.

1.3.1 Bacteria spread and entry into trees

The *P. syringae* bacteria can invade a wide range of plants. The fast, global spread of *P. syringae* has caused bacterial cankers in many species and leads to a need for a deeper understanding of pathogen virulence and host specificity. *P. syringae* is spread in many ways, including by insects feeding on infected plants, or using contaminated pruning tools, or by water as it can be spread by rain. *P. syringae* prefers wet conditions, so is likely to increase in plants growing in wet conditions over the plants that grow in dry conditions (Kennelly *et al*., 2007). *Pseudomonas* bacteria enter the plant host in several ways. These bacteria do not have the ability to make ports in all hosts, as do

other types of bacteria or fungi (Agrios, 2005). In woody plants, there are many entry pathways for bacteria, including wounds caused by natural phenomena and human practices, or natural openings such as stomata, lenticels, hydathodes and trichomes (Agrios, 2005). The pathogen may use more than one port of entry, foliar pathogens that cause localised symptoms enter mainly through the stomata, although some of them also enter by broken trichomes or hydathodes (Hirano & Upper, 1990; Newton *et al*., 2012). The pathogens that cause woody parenchymatic diseases usually enter through wounds to woody tissues (Kamiunten *et al*., 2000; Young, 2004), while lesions on woody tissues allow direct entry into the vascular system. There is a relationship between the port of entry and the symptoms caused by *P. syringae* pathogens (Agrios, 2005), so that leaf symptoms do not occur on *A. hippocastanum* which is infected by *Pseudomonas syringae* pv. *aesculi* (Green *et al*., 2009). In horse chestnut, the role of lenticels as ports of entry has been confirmed (in addition to lesions) (Green *et al*., 2009) so that it is easy to find the bacteria in cortical tissues of infected trees. *Pseudomonas* also contains the Ina gene that enables the bacteria to cause frost damage to plants at temperatures above freezing and this feature is considered a route of entry by damaging epidermal cells, which act as gates or portals of entry for *Pseudomonas* (Morris *et al*., 2008).

The economic influence of *P. syringae* is increasing, with a resurgence of long-known diseases, including bacterial speck of tomato, and the appearance of new infections of importance as worldwide diseases, such as bleeding canker of horse-chestnut. Several pathovars cause long-term problems in trees, often through the production of deformities and cankers. Infections of annual crops are more sporadic and often produced by planting a contaminated seed. Many

reports record the seed-borne nature of *P. syringae*, but it is uncommonly adaptive (Mansfield *et al.*, 2012; Morris *et al.*, 2007).

1.4 Cure and Management of bleeding canker

Some research studies on *Aesculus hippocastanum* bleeding canker, across the world, have tried to find a cure for this disease, but currently, there is no biological or chemical active treatment available to cure or stop the progress of this disease. A recent study suggested a non-destructive heat treatment might stop disease progression (de Keijzer *et al*., 2012), but it is difficult to apply in the field. There are suggestions for limiting the spread of a tree's infection, such as not pruning infected trees, or if this is done, then using sterile tools. Pruned material be covered to isolate them during transportation before being burned in an appropriate place, or it should be burned on-site as soon as possible (Forestry Commission, 2015). If the bacteria have spread extensively through the entire trunk, the tree will undoubtedly die and will need to be felled. If main branches are infected and start to show weakness and die back, they should be removed, because dead or dying branches are likely to fall, and would pose a threat for humans or other animals, or cause damage to property (Forestry Commission, 2015).

1.5 Plant immunity

A potential method of controlling bleeding canker is through manipulation of plant immunity. Disease is the result of a dynamic, detrimental relationship between a pathogenic organism that interferes and changes the normal processes of cells or tissues in the plant (Trigiano *et al*., 2006). Plant disease resistance is critical in preserving food and amenity plants. As well,

it also provides necessary reductions in the agricultural use of water, land, fuel and other materials used in production processes. Plants have inherent disease resistance, but this resistance cannot always protect them or always be effective (Dangl *et al.*, 2013). Plant pathogens can spread quickly carried by wind, water, insects, humans and transport means. It is evaluated that diseases in general decrease plant crops by a tenth every year in more developed countries. It is estimated that 14% of the total global crop production has been lost because of plant diseases caused by fungi, bacteria and viruses (Agrios, 2005; Dangl *et al.*, 2013; Qaim & Zilberman, 2003; Trigiano *et al.*, 2006). Many plant diseases developed and caused large epidemics. These epidemics have an influence on human lives and distribution.

1.5.1 Defence means and resistance in plants

Plant diseases may be caused by biotic factors such as microorganisms or by abiotic factors such as drought, excessive temperature, lack of nutrients, ultraviolet radiation, pollution and oxygen absence (Aderiye & Omin, 2015). The abiotic stresses might increase in future because of global climate change.

Plants do not have a somatic adaptive immune system as in humans or animals, but they have many other external structural defences that discourage diseases such as plant cell walls and the plant cuticle, that act as physical barriers to prevent pathogens attack (Aderiye & Omin, 2015; Spoel & Dong, 2012). Also, antimicrobial chemicals, enzyme inhibitors, plant latex and other exudates act as chemical barriers to prevent pathogen

attack (Konno, 2011). Another study has also referred to hormones such as salicylic acid, jasmonic acid and ethylene and their roles in increasing the vitality of the plants and thus increasing resistance to diseases (Pieterse *et al*., 2009). There are also suggestions that leaf shedding might be a reaction that provides protection against diseases and pests (Williams & Whitham, 1986).

Researchers have studied the interactions in the binding of the bacterial lipopolysaccharide (LPS) with plant proteins, particularly lectins (De Schutter & Van Damme, 2015; Chrispeels & Raikhel, 1991). Another study reported the role of bacterial exopolysaccharide alginate, a co-polymer of O-acetylated ß-1,4-linked D-mannuronic acid and L-guluronic acid in the virulence of *P. syringae*. Another study found that when the plant is responding to environmental stress, this will affect gene transcription programs and therefore it will be difficult to establish a valid defence response. This is because transcription reprogramming happens by the harmony of many transcription factors and/or cofactors that function directly or indirectly to release or recruit RNA polymerase (Moore *et al*., 2011). All the above studies have shown that the plant's defence mechanism is diverse and overlapping a lot, depending on the type of plant and the environment and external factors surrounding it.

1.5.2 Plant immunity system

Plants have developed an immune system to defend against pathogenic organisms (Trigiano *et al*., 2006). Plants do not have a mobile defender cell; instead, they depend on the innate immunity of each cell and on

systemic signals coming from infection sites (Ausubel, 2005; Chisholm *et al*., 2006; Dangl & Jones, 2001). Plants have evolved two layers of innate immunity to defend against pathogen invasion: pathogen-associated molecular pattern or microbial–associated molecular patterns (PAMP or MAMP)-triggered immunity (PTI) and effector-triggered immunity (ETI) and with the presence of other elements such as carbon (Jones & Dangl, 2006; Park *et al*., 2015). PTI is activated in response to the recognition of PAMPs, for instance, flagellin of bacteria (Zipfel & Felix, 2005). Plants possess pattern recognition receptors (PRRs) such as flagellin sensing 2 (FLS2) in *Arabidopsis thaliana*. Pathogens try to combat PAMP-triggered immunity by sending effectors into host cells or outside the plasma membrane into apoplastic space, which can interact with host proteins to inhibit PTI, this causing an effector-triggered susceptibility (ETS) (Jones & Dangl, 2006; Truman *et al*., 2006). Jones and Dangl illustrated the immune system of the plant as a four-phased zigzag model (Figure 1-6) (Jones & Dangl, 2006).

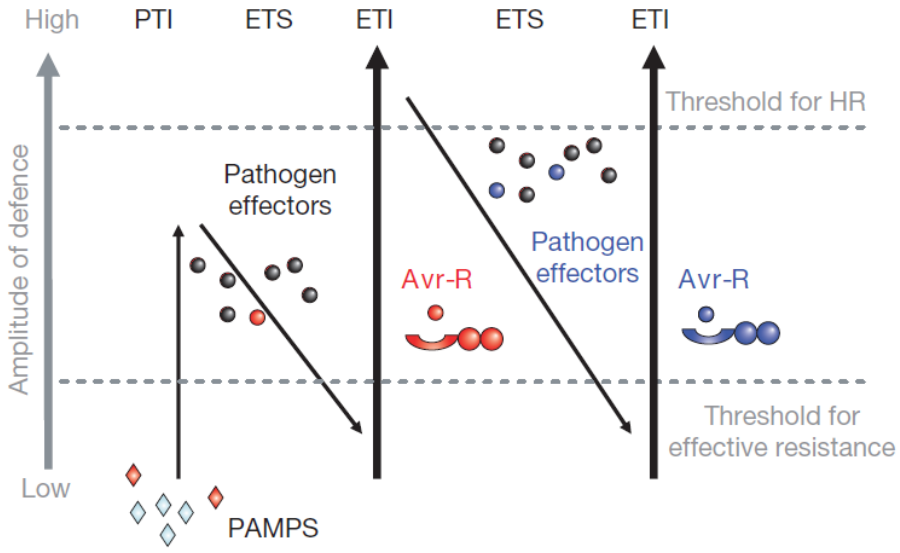

Figure 1-6 A zigzag model of the immune system. The figure shows the quantitative output of the plant immune system against pathogens. In phase 1, plants identify microbial/pathogen-associated molecular patterns (MAMPs/PAMPs, red diamonds) via PRRs to trigger PAMP-triggered immunity (PTI). In phase 2, successful pathogens deliver effectors that interfere with PTI, or otherwise enable pathogen nutrition and dispersal, resulting in effector-triggered susceptibility (ETS). In phase 3, one effector (indicated in red) is recognised by an NB-LRR protein, activating effector-triggered immunity (ETI), an amplified version of PTI that often passes a threshold for induction of hypersensitive cell death (HR). In phase 4, pathogen isolates are chosen that have lost the red effector, and perhaps obtained new effectors through horizontal gene flow (indicated in blue)—these can help pathogens to suppress ETI. Selection favours new plant NB-LRR alleles that can recognize one of the newly acquired effectors, resulting again in ETI (Jones & Dangl, 2006).

Phase I shows PAMP/MAMP are detected by PRRs, resulting in PAMP-triggered immunity (PTI) that can stop new pathogen colonisation. In phase 2, successful pathogens transport effectors that interfere with PTI, or else enable pathogen nutrition and dispersal, resulting in ETS. Phase 3 shows one effector (indicated in red in Figure 1-6) that is recognised by an NB-LRR protein (nucleotide-binding domain and a leucine-rich repeat protein), activating effector-triggered immunity (ETI), an amplified version of PTI that often passes a threshold for induction of hypersensitive cell death (HR).

Phase 4 shows pathogens evade ETI by diversifying effectors or gaining extra effectors through horizontal gene flow (indicated in blue) to suppress ETI through natural selection. The plant also evolves its repertoire of R genes (resistance genes), so that ETI can be triggered again to protect the plant from pathogens (Jones & Dangl, 2006). Plants can develop resistance to a pathovar by recognising PAMPs and launching or initiating an immune response, but the pathogen may find ways to destroy this immune response, leading to an evolutionary competition between the host and the pathogen (Baltrus *et al*., 2012; Ichinose *et al*., 2013; Lamichhane & Venturi, 2015).

1.5.3 Resistance genes

When the plants are challenged by a new disease they attempt to develop a resistance mechanism. This ability is an evolved mechanism known as resistance genes (R genes). These genes achieve plant disease resistance against pathogens by producing resistance proteins (R proteins), whose products allow the recognition of specific pathogen effectors, and also by direct binding or by recognition of the effector's alteration of a host protein (Jones & Dangl, 2006; Michelmore & Meyers, 1998).

There are dozens of specific genes (resistance-genes) that have been described for powdery mildew and rust diseases of the main crops. Most R-genes encode the nucleotide binding-site leucine-rich repeat (NB-LRR) proteins, which activate a defence to battle the disease (Collinge *et al*., 2008). The plant resistance gene and the pathogen avirulence-gene (Avr) must be matched so that the resistance gene can achieve resistance (McHale *et al*., 2006; Michelmore & Meyers, 1998; Nürnberger *et al*., 2004).

1.5.4 Transgenic engineered disease resistant plants

The term genetically modified (GM) is usually used to refer to plants modified using recombinant DNA technologies. Plants with transgenic/GM disease resistance against insect pests also increased food production, improved nutrition and health benefits, economic and environmental benefits and extended time fruit storage. This has been technically successful in commercial products, especially in maize (*Zea mays*) and cotton (*Gossypium hirsutum*) (Tabashnik *et al*., 2013). The transgenic strategies are achieved in different ways, such as by inserting genes that encode antimicrobial peptides or proteins. These genes come from plants or other organisms either in combination or alone. Other strategies involve detoxification to overcome pathogen signals or altering the recognition of the pathogen such as R-genes, etc. (Collinge *et al*., 2008). Most transgenic engineering was done to make plants resistant to insects and pesticides or to increase crop yield (Qaim & Zilberman, 2003).

1.6 Protein extraction from plant tissues

Protein study is considered to be an advanced technique because it is engaged in helping explain the function of genomes. The complete genome sequences of several organisms including some plant species are available only. Therefore, the proteomics field promises to fill the gap between cellular behaviour and genome sequence (Tabata, 2002; Frazier *et al.*, 2003). The measurement of protein amount is one of the fundamental and valuable parameters to study plant response against different interactions. Proteins are extracted from plant tissues for many reasons, including purifying a protein for

detecting the gene that encodes it as an indirect method to characterise the gene, to resolve proteins of the plant by polyacrylamide gel electrophoresis and in physiological studies to assay enzymes in a crude extract (Laing & Christeller, 2004). Extracting proteins from animal and plant origins are two separate things. While animal proteins can simply be obtained directly, in contrast extracting and dealing with plant proteins can be quite a challenge because plant proteins are more complicated to extract considering they are shielded by a rigid cellulose cell wall that contains several interfering agents and polysaccharides.

The main problems with plant tissues are low cellular protein content and the presence of enormous amounts of secondary compounds such as pigments, phenolics, lipids, and chlorophyll. Moreover, plant cells often have a large vacuole that contains secondary products, organic acids and proteinases. When these products are released from the vacuole as a result of the extraction techniques, these products may modify, degrade or inactivate proteins. These compounds will probably interfere and affect the protein extraction results (Méchin *et al.*, 2007).

The other challenge in a typical protocol is to remove the nucleic acid, which interacts with protein and shows bands with a reduced resolution and gives high background noise on the gel (Faurobert *et al.*, 2007). Additional difficulties to be considered are related to the instability of the analyte, when specific biomolecules are being analysed (Aurelio, 2007; de Magalhães & Arruda, 2007). It is challenging to maintain plant samples with high stability for further use, in particular if these samples belong to vegetal parts (leaf or green stem). Also, the presence of a highly abundant amount of different

proteins complicates the extraction. It is estimated that the chloroplast alone contains between 2,500 to 5,000 proteins (Park, 2004). Therefore, there is no perfect protocol or even a single soluble cocktail solution compatible that works for all conditions and all plant types or organs (Jorrín-Novo *et al.*, 2015; Aurelio, 2007). In studies of proteomics, it is known that sample preparation is often still the most critical step, because it is usually time-consuming, complicated, and also often responsible for mistakes in the final results (Jacobs *et al.*, 2001; Vasconcelos *et al.*, 2005). The typical extraction method should reproducibly catch the general store of proteins available, and simultaneously, reduce contamination and degradation by non-proteinaceous compounds. However, in general, with the most recalcitrant plants or those that contain chlorophyll, researchers have used phenol or acetone methods to extract and precipitate protein (Jorrín-Novo *et al.*, 2015).

1.7 Environmental conditions, diseases, and the trees

Plant defences, including the immune responses which are designed to protect plants, are influenced by the vigour of the plant, which in turn can be affected by environmental conditions and pollution (Baucom & de Roode, 2011).

Over recent years clear impacts of pollution or climate change on trees have been observed as a result of human activities on the natural environment which are taking place at the present time. Accordingly, disease incidence in plants and animals has increased (Agrios, 2005;

Newton *et al*., 2012). It is essential for those who study plant diseases to understand the role and impact of the environment and pollution.

The most common reasons for plant diseases are often misunderstood. This is because they may be caused by pathogens that are not easily seen (Webber *et al*., 2008) and because the diseases result from complex interactions between the plant defences, pathogens, and the environment (Trigiano *et al*., 2006). The disease triangle visualises this complex interrelationship and clarifies the perfect balance between the variables that are required for disease appearance and spread (Figure 1-7). A good understanding of these variables might contribute to finding more effective agents against these pathogens (Newton *et al*., 2012). Within the triangle, the environment includes all conditions favouring disease such as water availability, temperature, ozone, CO_2, extreme events, etc. The pathogen factors include virulence, abundance, etc. The emissions of chemical elements and pollutants into the atmosphere have increased because of human activities. Studies show that some trace chemical elements (lead, cadmium, copper, chromium, etc.) are spread widely in the environment and interact with different natural components, to cause a threat to human health and the environment (Nowak *et al*., 2014; Petrova *et al*., 2012).

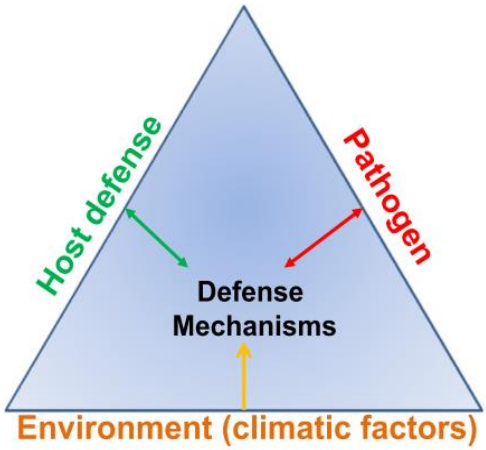

Figure 1-7 The disease triangle. The figure illustrates the vital role of defence mechanisms in the interaction between the host, the environment and pathogen (Newton *et al.*, 2012).

Aesculus hippocastanum trees are considered to be sensitive to pollution. The trees also have the ability to absorb and accumulate many trace chemical elements from the soil and air. This feature certainly reduces the vitality of the trees and consequently reduces disease resistance because these accumulations are accompanied by changes in structural and physiological features (Tomaševič *et al.*, 2008). One study illustrated a pollution effect on the leaf structure of *A. hippocastanum* (Şchiopu *et al.*, 2011); another study found that air pollution has a definite effect on the stomatal density of wild *A. hippocastanum* (Oljača *et al.*, 2009), so environmental stress stimulates stomatal opening more than usual, thus increases the chances of infection with pathogenic microorganisms. A different study found the climate change (especially rising temperatures) in the United Kingdom over the past six decades has led to accelerating flowering and leafing in *A. hippocastanum*, by 7.7 days and 4.9 days respectively (Sparks *et al.*, 2000; Sparks & Smithers, 2002). Climate change may make plants more susceptible to disease through its influence on plant fitness through gene expression (Garrett *et al.*, 2006) or

could change rates and stages of development of the pathogen, alter host resistance and result in changes in the physiology of host-pathogen interactions (Coakley *et al*., 1999). The movement of plants and plant products, between different regions by humans is now generally thought to be the cause of developing pathogens and pests, because the change in environmental requirements for the pathogen and plant may cause weakness in the plant thus providing better conditions for the pathogen (Boland *et al*., 2004; Cerezal & Gutiérrez, 2013).

1.8 Abiotic stress

Plant growth is considerably influenced by environmental abiotic stresses, such as drought stress, damage stress, low temperature, high salinity and biotic stresses, such as pathogen infection. Plants respond and adapt to these stresses in order to survive.

1.8.1 Drought stress.

Plants have developed a host of response mechanisms to enable survival under severe circumstances. In general, abiotic stress effects have a negative impact on living organisms in a particular environment. The non-living variable must affect the environment outside its natural range of variation to adversely affect the invader organism performance or particular physiology in the organism in a vital way (D-Vinebrooke *et al.*, 2004). However, about, one-third of the earth's area is desert and semi-desert, while occasionally unexpected climatic droughts often happen in most other land areas (Fang & Xiong, 2015). Drought stress is one of the wide-ranging and most critical environmental conditions. Abiotic

stresses cause important threats to agriculture, germination and affect the development and growth of plants (Bray, 1997; Vilagrosa *et al.,* 2012). Drought stress is the main reason for crop loss worldwide, decreasing yields by as much as 50% (Boyer JS, 1982; plants & 2000, 2000). Water deficiency can be fatal to plants and lead to massive social difficulties and economic losses and, along with temperature, determines the global distribution of major vegetation biomes. According to the Intergovernmental Panel on Climate Change report (IPCC) drought frequencies are supposed to increase globally over the next 50 years, and there will be rising shifts in rainfall patterns (Street *et al.,* 2006). The influence of drought stress is expected to be complicated by the fact that it associates with other factors, such as atmospheric gas levels, increases in temperature and humidity.

Gene expression in drought stress has been studied with microarray analysis for different species of *Populus*; for example, *P. deltoides* and *P. trichocarpa* (Street *et al.*, 2006). Many transcriptions factors are involved in the drought stress response such as Nuclear transcription factor Y subunit B-3, Late embryogenesis abundant protein 4 and Zinc-dependent alcohol dehydrogenase (Xiaowen Ma *et al.,* 2015; Umezawa *et al.,* 2006). Gene expression in many plants is changed, and different genes are expressed to react to water deficiency stress. The pathway from stress to physiological and biological responses and next to drought tolerance is complicated and not yet completely figured out. It is involved in protein synthesis and biochemical pathways expressed by various genes (Neill & Burnett, 1999). On the other hand, there are several species of plant such as *Weinmannia crassifolia* and *Clethra cuneata*, that do not experience drought stress to a level as it induces stomatal closure.

Under drought stress, proteins in living cells sustain damage such as the disruption of their native structure and have difficulties in keeping their activity. In order to survive, cells need to activate processes of protein repair and avoid non-native protein aggregation (Wang *et al.*, 2004). So, protein is considered one of the primary biochemical parameters that respond to drought stress. It was found that water channel proteins are essential in drought stress because they are involved in the control of the water state in the live cells (Assmann & Haubrick, 1996; E. A. Bray, 1997). Usually, when the damage is irreversible, then the degradation of the cell would take place in plant (Campalans *et al.*, 1999; Bartels & Sunkar, 2005).

Drought stress is also responsible for changing the physical features and chemical composition in the cell wall, such as wall extensibility (Campalans *et al.*, 1999). This can prevent cell development and also decrease the leaf area (Bray, 2004; Nonami & Boyer, 1990). A previous study on *A. hippocastanum* reported that paclobutrazol-induced drought tolerance was connected with decreased biomass, tree height, leaf area and transpiration, and increased stomatal resistance (Percival & Noviss, 2008). In order to know the region or surface that needs to be exposed to sunlight, there are many genes expressed during drought stress, such as proline-rich-proteins and s-adenosylmethionine synthetases which encoded and accumulated in the plant (Colmenero- Flores *et al.*,1997; Ingram & Bartels, 1996).

1.8.1.1 Drought and woody plant

In regard to the impact of drought stress on trees, water stress is also a crucial factor for plant health in particular with perennials and woody plant, and the predicted increase in the frequency of drought events in the UK will have implications for forest health in various areas of Britain (Green & Ray, 2009).

The impacts of drought stress on trees have been studied, and it is known that that changes in the physiological condition lead to changes in physical condition, growth, and plant chemistry. Resistance and tolerance to the drought stress also affects pests and pathogens, which invade hosts as well. The most extreme effect of water stress on trees is death. This often happens as a result of severe symptoms of direct damage. Many tree mortality cases have recently been associated with drought (Allen *et al.,* 2010; Anderegg *et al.,* 2013).

The biggest threat to UK forests is expected to be that of a rising severity and frequency of drought. The reasons for this belong to two causes. Primarily, severe impacts on drought-sensitive species in established plantations are likely to be widespread, especially in southern and eastern Britain. Furthermore, though most current forestry tree species will remain suitable across much of Britain, it may be essential to enter plant new drought-tolerant species in particularly drought-prone areas (Broadmeadow, Webber, & Ray, 2009). A drought happening in Scotland in 2003, for instance, caused 14 – 20 % mortality in Sitka spruce and other conifers at some sites in north-east Scotland, while many surviving trees showed differing levels of physical damage (Green *et al.,* 2008; Green & Ray, 2009). However, unlike much of the mainland Europe countries, the drought's influence across the UK was almost modest.

The main mechanisms behind tree death as a response to drought stress remain mostly unexplained, and it is possible that a mixture of mechanisms come together to cause the death of the tree. However, the core mechanism is hydraulic deterioration in tree tissues (Anderegg *et al.*, 2013). It is known that drought induces stomatal closure, and that means close of an easy port for the entry of bacteria or invader organism. A previous study on the hydraulic performance of *Populus tremuloides* (Aspen) under drought conditions, found that hydraulic damage not only continued but increased in dying trees over multiple years, with a minimal indication of recovery (Anderegg *et al.*, 2013).

In addition to plant death, as a result of drought stress, there are many further symptoms of direct damage on trees can be seen, such as foliage wilting, browning and leaf premature abscission (Warren *et al.*, 2011; Green & Ray, 2009).

Moreover, drought and raised CO_2 have been confirmed to have a strong relationship on leaf senescence and abscission, with increased responses when both come together (Warren *et al.*, 2011). However, other levels of stress may be useful in reducing the degree of infection and delaying the invader organism. A recent study observed that lettuce plant's (*Lactuca sativa*) response to peroxidase, superoxide dismutase and malondialdehyde activity during the drought stress condition was disrupted by using CeO_2 NPs (nanoparticles) 1000 mg/kg (Gui *et al.*, 2015).

Structural and physiological changes to the plant caused by drought may affect parasites or invader organisms directly by a change in nutrition quality and capability to feed, or indirectly by a variation in signals and host selection. Decreased growth by cell enlargement is the first factor to be affected by

moderate water stress (Hsiao *et al.*, 1976). Accordingly, decreased tissue growth is possible in droughted plants; leaves are thicker, waxier, and smaller, possibly making it more difficult for the invader organism to infiltrate and feed on the host plant (Pritchard *et al.,* 2007). However, the response to drought stress in a plant is a sophisticated process, which includes thousands of protein-coding genes and biochemical, molecular mechanisms.

1.8.2 Damage stress

A plant often suffers from mechanical wounds and damage, and this mostly leads to oxidative damage. Physical damage is an important form of abiotic stress that can significantly compromise food quality and also elicit a series of pathological and physiological responses (Tosetti *et al.,* 2014; Singh, *et al.,* & Sharma, 2009). However, very little work has been recorded on interpreting and documenting the damage stress that occurs during fresh-cut processing, packaging and natural conditions such as rain, hail, wind, insects and other organisms (Mittler, 2002).

For plants and all aerobic organisms, oxygen is a crucial factor. It is essential for standard growth and development, but continuous exposure to oxygen can result in cellular damage and finally death. This is because molecular oxygen is continually reduced within cells to several forms of reactive oxygen species (ROS) sometimes called active oxygen species (AOS) (Hirt & Shinozaki, 2004). However, plants show a high changeability in their response to damage and in sensitive species, exposure causes severe oxidative damage stress in terms of enhanced hydrogen peroxide (H_2O_2) accumulation, lipid peroxidation and change of non-enzymatic and enzymatic antioxidant mechanism (Singh *et*

al., 2009; Singh *et al.,* 2007). Hydrogen peroxide and superoxide free radical anion (O2.-) in particular react with different cellular components to give rise to chronic or acute damage. This damage is enough to prompt cellular death in plant cells, ROS are produced in high amounts by both inducible and constitutive ways, but under ordinary situations, the redox balance of the cell is maintained by the constitutive activation of a wide range of antioxidant mechanisms that have evolved to remove reactive oxygen species (Hirt & Shinozaki, 2004; Singh *et al.*, 2009).

Many environmental stresses and endogenous stimuli disturb or perturb the redox balance by increased ROS production or decreased antioxidant activity, such that oxidative stress follows. In response to increased ROS, the expression of genes encoding antioxidant proteins is induced, as well as that of genes encoding proteins associated with a wider range of cellular rescue processes. In addition, it is increasingly clear that ROS also has signalling roles outside of oxidative stress. The damage stress and regulation redox balance in plant cells is a complex process overlapping with cellular responses to ROS and the possible signalling mechanisms, developmental and physiological processes in the plant (Hirt & Shinozaki, 2004; Rejeb, Pastor, & Mauch-Mani, 2014).

When the tissue is wounded, it becomes susceptible to pathological and physiological responses. Therefore, fast wound-healing is essential including wound-induced suberin (natural protective polymer) as an emergency protective healing-screen layer. This layer is produced on wound surfaces. Suberization may be the most essential process in some plants such as potato tuber (Lulai, 2007). The first step of suberization, indicated as primary suberization, involves a closing layer formation whereby suberin biopolymers

accumulate in the cell walls at the wound surface. The secondary step, indicated as secondary suberization, involves wound periderm development whereby the afresh formed cells below the closing layer become suberized (Graça, 2015; Lulai, 2007; Tao *et al.*, 2016).

1.9 Nanotechnology

Nanoparticles can help the plant cope with pathogens such as bacteria and fungus and play an essential role with poor environmental conditions such as drought and physical damage, in other words, nanoparticles accumulation is increased in response to different biotic and abiotic stresses or vice versa (Ashkavand *et al.*, 2015; Hernandez-Viezcas *et al.*, 2016).

1.9.1 Nanotechnology and nanoparticles

The concept of nanoparticles was initially adopted in 1959. Feynman defined the value of employing individual atoms using larger machines to creating smaller machines (Feynman, 1959). The term "nanotechnology" was first used in 1974 at the Tokyo Science University, by Norio Taniguchi. Now, the term refers to these technologies that deal with bodies at the level of nanometres (Whatmore, 2006; Taniguchi, 1996). Nanotechnology is derived from the Greek word, which means one billionth or dwarf. This is one of the fastest developing technologies of our time and is a multidisciplinary science, which includes biology, chemistry, biomedicines, targeted drug delivery, and engineering. Additionally, it has become a promising and multipurpose field for designing novel materials with improved features and possible applications in diseases therapy (Cox *et al.*, 2017; Khan *et al.*, 2017; Servin *et al.*, 2015;

Siddiqui *et al.,* 2015). This technology has revolutionised healthcare and agricultural and antimicrobial application. Nanoparticles (NPs) are generally smaller than a hundred nanometers; therefore, they can interact with biological particles on the surface of the cells as well as inside the cells.

NPs have unique physicochemical properties such as large surface area to volume ratio, different surface structure, enhanced reactivity, etc. that differ distinctively from those of their molecular and bulk counterparts. These properties typically result also from the small size, chemical composition, surface structure, stability, shape, and agglomeration of the nanoparticles (García-Sánchez, *et al.,* 2015; N. Li, 2015; Mousa *et al.,* 2018).

The mechanism or manner of how engineered nanoparticles (ENPs) influence bacteria and plants is general inadequately understood but it is reported that these come from the production of reactive oxygen species (ROS), cause damaging cell membranes, damaging DNA, synergistic effects, and other cell effects. Whether these impacts occur from the presence of ENPs or/and from the discharged ions, is largely unknown (Prabhu & Poulose, 2012). It is possible that ENPs also affect the gene expression for protein synthesis during development, or induce stress response proteins associated with self-protection (Mushtaq *et al.,* 2008; Wang *et al.,* 2008). Another study has reported that the uptake of the necessary components in addition to ENPs by plants, may improve photosynthetic performance by a mechanism that implements energy to soil microbes, which in turn promotes higher amounts of nutrients to be used by plants (Siddiqui *et al.,* 2015; Wang *et al.,* 2013).

There are a number of ways, based on various features, that NPs can be classified. Initially this includes, based on their chemical composition, organic (carbon-containing) and inorganic NPs, or they can be further divided according to their origin into two main groups (Figure 1-8); natural and anthropogenic NPs (human activity or made) which, in turn, can be subdivided into engineered and incidental NPs (Nowack and Bucheli,2007; Bhatt and Tripathi, 2011).

Today, NPs are produced with different structure and size, enhancing their physical, biological, and chemical characteristics as opposed to natural Nano counterparts. Nanoparticles can now be reliably produced from NP solutions by exerting particular pressures; such structures include triangular rods, spheres, hexagonal snowflake-like three-dimensional morphologies and octahedrons (Nadagouda *et al.*, 2009; Siddiqui *et al.*, 2015).

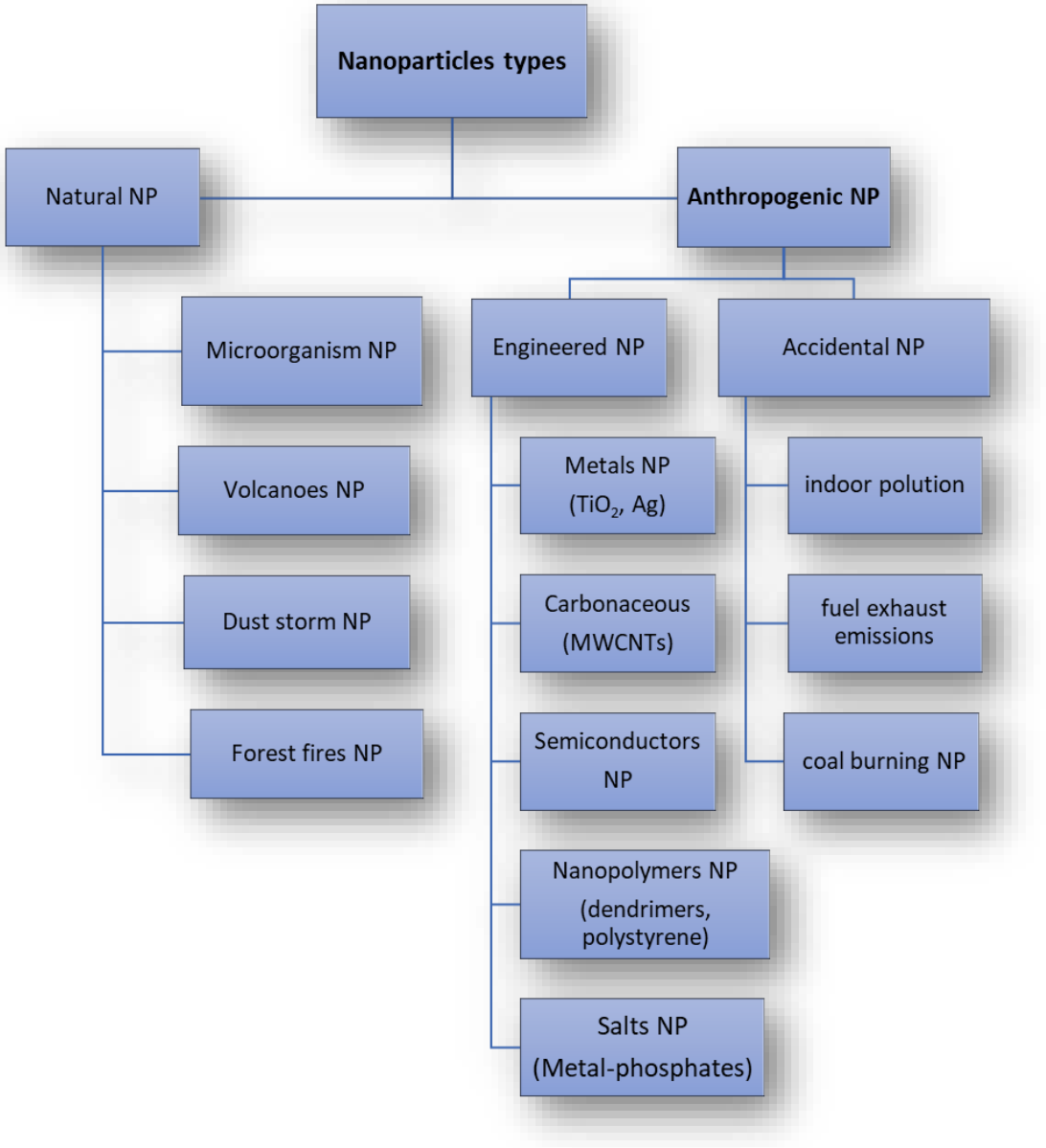

Figure 1-8 An outline of the several main types of nanoparticles in the environment.

1.9.2 Metal nanoparticles

Metal NPs have gained considerable attention in past years and have become a focal point of NP research because of their complex chemical and physical properties, which differ significantly from their bulk equivalents. Moreover, metallic NPs can be readily synthesised with significant control over desired

properties such as size, shape, and composition (Kawamura et al. 2013). Metal NPs are now widely employed in agricultural and biomedical sciences (Khan *et al.,* 2017; Conde *et al.* 2012).

The transition of metals to nanoscale length changes both their chemical and physical features, which can be tuned by controlling parameters such as shape, size, structure composition. Novel size-dependent properties (magnetic, optical, electrical, and chemical) emerge, which turn them to the building parts of nanostructures can be used for many technological fields (Guo & Wang, 2011). Reducing the size of NPs does not always support catalytic optimisation. Also, the catalytic activity does not always scale linearly with a particle surface area. NP toxicity does not correspond linearly to reducing particle size. For example, Cu NPs are more toxic to living cells than bulk Cu (on a micrometre scale), partly because Cu NPs cause increased mitochondrial damage. In contrast, bulk TiO_2 causes more serious DNA damage than TiO_2 NPs, and there is no significant difference between the limited toxicity caused by bulk Fe or NP of Fe (Karlsson *et al.,* 2009).

However, some metal NPs such as silver, gold and iron oxide, have a long history of safe use, especially in the clinical field. Because of their natural instability, surface engineering of these particles before introduction into biological environments is highly demanded (Auffan *et al.,* 2009; Häfeli *et al.,* 2009).

1.9.3 Role of Nanoparticles in Plants

Nanoparticles in agriculture are applied chiefly as fungicides, disinfectants, and fertilisers, for improving plant growth (Priester *et al.,* 2012). However, there

are unpredictable results concerning their effects, sometimes they are beneficial or harmful to plants and depending on the type of plant and the type of nanoparticles. The positive or negative impact of nanoparticles would generally be under the control of several factors which can work combined or alone, including their size, shape, or other characteristics (Morales-Díaz *et al.,* 2017; Siddiqui *et al.,* 2015; Tripathi *et al.,* 2017). An interesting and crucial factor is the possibility of such particles entering the food chain of humans or other organisms (Gui *et al.,* 2015; Rico *et al.,* 2011; Siddiqi & Husen, 2017).

The main route of entry of NPs in plant tissues is absorption through the root system. In 2012, studies of *Cucumis sativus* fruit using micro-X-ray fluorescence (μXRF) and micro-X-ray absorption near edge structure (μXANES) revealed that TiO_2 NPs are capable of entering the vascular system of cucumber roots and were even translocated to the leaves and accumulated in the leaf trichomes (Servin *et al.,* 2012).

Reports are confirming that there is increased toxicity of silver NPs compared to metallic silver ions, which indicate that silver ions are more toxic to bacterial cells if present in the form of NPs (Fabrega *et al.,* 2010). The negative influence of silver NPs are also reported on algal reproduction due to subsequent stimulated imposition of oxidative stress (Fabrega *et al.,* 2010; Ribeiro *et al.,* 2014).

In conclusion, the effect of nanoparticles varies according to their types and their chemical and physical properties as well as the concentration used, as many nanoparticles are directly involved in the food industry such as food processing, nutritional supplements, biodegradable. (Chellaram *et al.,* 2014; He & Hwang, 2016).

1.9.4 Bacteria and nanoparticles

The effects of ENPs on bacterial or other microorganism are being analysed from many angles, but the obvious effect on the bacteria is indirect, often depending on the growth medium (environmental effect). Regarding an environmental aspect, the possible toxicity of ENPs discharged to the environment is under evaluation. Scientists are trying to manipulate ENPs cytotoxicity to produce antibacterial surface coatings (Yang & Kim, 2013; Zhang *et al.,* 2018). Usually, exposure of soil microorganisms to ENPs could happen directly by the application of contaminated water onto soil or indirectly through root exudation of ENPs taken up by plant stem or leaves or decomposition after the death of the plant (Wang *et al.,* 2012; Chunjaturas *et al.,* 2014). Some types of nanoparticles, especially silver, titanium and copper showed a remarkable antibacterial effect. The most positive results were with small nanoparticles between 5-25 nm (Agnihotri & Mukherji, 2014; Nair & Chung, 2014). It is known that different strains of bacteria have different responses to ENPs. Therefore, the type of bacteria is also an important factor that must be taken into account when studying the influence of ENPs on bacteria. The mechanism of how ENPs affect microbes is in general poorly known but has been reported to involve damaging DNA, damaging cell membranes, production of ROS, and other effects on the medium of growth (Parbhu and Poulose, 2012).

1.9.5 Nanoparticles in the environment

The abundant use of NPs in different fields of science and their behaviour in the environment has boosted the concerns within the scientific community

about their fate and performance (Khan *et al.,* 2017; Siddiqui *et al.,* 2015; Wigginton *et al.,* 2007). However, the current levels of accumulation of ENPs in the environment are not well identified (Sun *et al.,* 2014). The concern comes from the present or future effect of these ENPs on the natural environment and their potential impacts on living organisms including plants. (Siddiqui *et al.,* 2015; Wigginton *et al.,* 2007). However, understanding NP fate and behaviour in the environment and soil is highly challenging because of the compound potential of interactions between physical and chemical factors of the surrounding environment, and the general absence of enough particle detection policies for environmental patterns (Servin *et al.,* 2015; Sharma *et al.,* 2015). There is also a lack of tools that can monitor and quantify their concentration and release in the environment (Gottschalk and Nowack, 2011; Gottschalk et al.,2009). The essential point with using NPs is that the surrounding environment determines the activity of nanoparticles in large and effective way.

The release of ENPs may happen over long or short periods, and as an individual or sizeable amount. When ENPs are released, it can be in their original or new form or some changes in their physicochemical characteristics can happen, leading to different behaviours and potential toxic effects in the environment (Bour *et al.,* 2015; Whatmore, 2006).

The essential manner that rules nanoparticles behaviour in water environments are dissolution and aggregation, determined by surface properties and size of the materials which are mainly dependent on environmental factors such as water availability, temperature, pH, ionic strength, particle concentration, and NPs features such as size, surface charge, coating agents, crystallinity, shape

and composition (Keller *et al.,* 2017; Khan *et al.,* 2017; Liu & Lal, 2015; Spielman-Sun *et al.,* 2017; Dunphy Guzman *et al.,* 2006). Usually water containing nanoparticles is absorbed by the plant from the soil.

The impact of some metal nanoparticles on soil bacteria or other microflora could be significant. The antimicrobial features of Cu and Ag NPs are well documented. This antimicrobial feature, in turn, affects the soil environment and then plant (Cho *et al.,* 2005; Espenti *et al.,* 2016). For example, uptake of CeO_2 NP into roots and root nodules was found to reduce nitrogen fixation potentials and cause weakened soybean growth (Priester *et al.,* 2012). The uptake of Fe_3O_4 and Ag NPs has also reduced mycorrhizal and clover (*Trifolium repens*) biomass (Feng *et al.,* 2013). Usually, an organic matter-coated natural metal or naked metal nanoparticles display less toxicity than NPs that are surface-coated with polymers or other surfactants (Sharma *et al.,* 2015).

However, regardless of the benefit of nanoparticle applications, the lack of enough objective information concerning the possible environmental and health hazards needs to be addressed adequately in advance. This is especially important given a growing indication that NPs can be detected and discharge in the environment and their amounts are predicted to increase in the future (Liu, *et al.,* 2016; Gottschalk and; Sun *et al.,* 2014).

1.10 Aims and objectives

It is clear that *Aesculus hippocastanum* is an important tree in temperate areas both for its impacts on other species and its aesthetic appeal. Yet it faces many challenges, especially from bleeding canker caused by the bacterium *Pseudomonas*. However, the plant will have internal defences to this disease and to other damaging agents such as drought and physical damage. This is undoubtedly linked to changes in genes and proteins involved in the immune response. The overall aim of this thesis is to investigate if these genes and proteins that change can be identified. It is also unknown whether nanoparticles can directly affect the bacterium or not. Due to the overlap of environmental factors with genetic factors, pathogen and host, the current study attempts to cover a wide variety of aspects related to plant, environment and pathogen.

The main aims and hypothesis of this thesis can be summarised by the following questions:

1. Which genes and gene functions respond to bleeding canker? Levels of genes expression will be compared to determine plant response to infection.
2. How do environmental factors affect plant infection or bacteria survival? The drought stress, damage stress, temperature and pH will identify which factors bacteria respond to or which induce different plant responses.
3. Is bleeding canker affected by nanoparticles? Are there any effects on bacteria or side effects on the plant or human food? The widespread use of nanoparticles has started receiving increased attention because of the knowledge gaps regarding their fate in the plant, effects on bacteria and the possible impact on human food.

The central objectives of the thesis can be outlined as follows:

1. To increase in particular knowledge about proteins and genes involved in defence against bleeding canker of *A. hippocastanum*. So far little is known regarding the disease.
2. To find out an easy, typical and reliable protocol to extract protein from *A. hippocastanum* leaves, especially as there is no previous study about this plant.
3. To investigate how drought and damage stress affects *A. hippocastanum* and model plants growth and estimate if they have any inhibitory or catalytic effect for the proteins involved in bleeding canker disease or *P. syringae* bacteria.
4. To find gene(s) associated or involved with bleeding canker disease or *P. syringae* bacteria and identify the proteins that produce.
5. To characterise the Ag and CeO2 NPs which were produced in this study.
6. To assess the impact of different NPs on *A. hippocastanum* seed germination and model plants (as control plants).
7. To provide quantitative information about the behaviour, location, toxicity and accumulation of different nanoparticles on *A. hippocastanum* and model plants used in this study.
8. To estimate the effect of different NPs on total dry biomass of the *A. hippocastanum* and model plants and assess any downstream effects on plant growth.
9. To investigate the effect and behaviour of the different nanoparticles core size and type on *Pseudomonas syringae* bacteria.

2 Chapter 2: Effect of environmental stress on bacteria and plants.

2.1 Introduction

Environmental conditions usually change dramatically throughout the plant's life cycle. These changes influence growth, reproduction, seed germination, and plant development. Abiotic stresses such as drought, salinity, high light and damage each will be recognised by the host plant, and responses happen (Hasegawa *et al.*, 2000; Leslie *et al.*, 2013; Yigit, *et al.*, 2018). Many studies have recorded that different genes respond to cold, high salinity and drought stress at the transcriptional level of plant and bacteria, such as nuclear transcription factor Y subunit B-3, expansin-like A2 gene and late embryogenesis abundant protein 4 (Abuqamar, *et al.*, 2013; Basu, *et al.*, 2016; Lee *et al.*, 2004; Liu, *et al.*, 2016; Ma *et al*., 2015).

In recent decades, environmental variation has increased because of global warming and human activity, and there is continuing concern about the effects that environmental factors may have on the life of our planet (Hardoim *et al.*, 2015; Nowak *et al.*, 2014). It is known that plant growth under environmental stress conditions is more complex and a highly dynamic process than growth under normal conditions. The plant must adapt to the conditions and respond to it because the plant cannot move and change its position as with animals or humans (Aroca, 2013; Garrett *et al.*, 2006; Konno, 2011). Plant growth is stringently regulated to allow stable structures and leads to a recognisable habit of species, even when the individuals develop under various environmental requirements. At the same time, growing plants are very dependent on their

immediate environment. The environment gives suitable conditions for active growth, and a vital role of growth is to obtain new resources from the environment. Consequently, growth must react to environmental conditions to optimise resource use efficiency (Garrett *et al.,* 2006; Hirano & Upper, 1990; Walter *et al.,* 2009). The critical side of the environmental factors, that they are influenced in more than one direction by affecting the host and the pathogen organism at the same time. (Bello, 2018).

Drought stress (water deficiency) is one of the significant weaknesses of global agricultural production due to the complexity of water-limiting conditions and altering climate, posing a threat to food security, closely associated with damage stress (Aroca, 2013; Feki & Brini, 2016; Hasheminasab *et al.,* 2012; Parida, *et al.,* 2007). It is estimated that total global water consumption has tripled over the last 50 years, and this foreshadows potential drought in the future. Drought not only causes massive agricultural production damages but also contributes to ecological disasters, such as land desertification. Plant species have developed a series of mechanisms and strategies at the physiological, biochemical, molecular, cellular and morphological levels to conquer drought stress or low water availability (Fang & Xiong, 2015; Khan *et al.,* 2017) including: drought escape, drought avoidance, drought tolerance and drought recovery (Fang and Xiong, 2015; Fang & Xiong, 2015). Drought escape happens when plants develop quickly and reproduce before drought situations become critical, i.e. they avoid drought-induced damage by quickly completing their full life cycles (Wood, 2005; Kooyers, 2015). In the case of drought avoidance, plants avoid the influence of drought by raising water use efficiency (WUE) by reducing transpiration through morphological

modification or physiological mechanisms, reducing vegetative growth, or increasing root growth during transient stages of drought stress (Kooyers, 2015). Among the four components of drought resistance, drought avoidance and drought tolerance are the two primary mechanisms for drought resistance conferred by plants.

The basic mechanism of drought stress tolerance adopted by plants is usually osmotic adjustment by accumulating organic compounds inside cells, such as proline, mannitol, betaine, inositol, fructan, glycine, trehalose, and inorganic ions. This leads to an increase in their concentration in the cells, reducing the osmotic potential, and enhancing cell water retention in response to water stress (Basu *et al.*, 2016; Vilagrosa *et al.*, 2012; Fang & Xiong, 2015; Rhodes & Samaras, 1994). Proline, for example, has powerful hydration abilities. Its hydrophilic part is able to bind to water molecules while it's hydrophobic part can bind to proteins, allowing proteins to better interact with water to improve their solubility and to limit protein denaturation from dehydration under osmotic stress conditions. Proline acts not only as a cytoplastic protecting agent for cell structure and enzymes but also for reducing cell acidity and regulating the redox potential (Basu *et al.*, 2016; Fang & Xiong, 2015; Percival & Noviss, 2008).

Coping with abiotic stress is based on multiple molecular processes involving many genes and signalling pathways. The transcription abundance of a considerable number of genes with different functions changes under drought stress conditions; many of them are not yet fully known (Garrett *et al.*, 2006; Bartels and Sunkar, 2005). External drought stimuli are perceived by sensors on the membrane which have not been well-characterised, and then signals are

passed down through multiple signals transduction pathways, producing the expression of drought adaptation and drought-responsive genes. A variety of secondary messengers (such as abscisic acid (ABA), Ca^{+2}, diacylglycerol, phosphoglycerol, and reactive oxygen species (ROS)) and transcriptional regulators play significant roles in various signal transmitting pathways (Lawlor, 2012; Leslie *et al.*, 2013; Zhu, 2002; Xiong *et al*., 2002).

However, *Aexsculus hippocastanum* is often considered to be highly influenced by environmental factors and unsuitable for dry urban areas due to its moderate sensitivity to drought in comparison to other plants (Snieskiene *et al.*, 2011; Petrova *et al.,* 2014; Yigit *et al.,* 2018; Roloff *et al.,* 2009). Therefore, drought may be seen as a stressor in this tree. Additionally, little is understood about whether *Pseudomonas syringae* bacteria can tolerate different conditions in the external environment (away from the host) and survive or retain its pathogenicity *(Laue et al*., 2014). Therefore, to ignore the environmental factors in any study related to plants is probably not neutral or logical.

2.2 Aims and Objectives

Aesculus hippocastanum is an important tree in temperate areas for its impacts on other species, its aesthetic appeal and some medicinal uses, yet it faces many challenges, especially from bleeding canker caused by the bacterium *Pseudomonas syringae*. However, the plant will have internal defences to this disease and to other damaging agents such as drought and physical damage. But it is largely unknown what proteins are involved in reacting to stress caused by external environmental conditions, which are likely to be similar to those produced by infection with bacteria. Therefore, the main aims and hypothesis of this chapter as attempts to understand how environmental factors may affect European *A. hippocastanum* and *P. syringae* and control plant susceptibility to *P. syringae* infection. Model plants were also used since they could be grown faster and earlier than *A. hippocastanum*, allowing more treatments to be investigated.

The main objectives of this chapter can be summarised as the following points:

1. To determine the effect of different levels of drought stress on the growth and protein content of *A. hippocastanum* and model plants. Estimate if the drought stress has any inhibition or stimulation influence on *P. syringae* bacteria causing bleeding canker disease in horse-chestnut.

2. Investigate whether artificial damage to *A. hippocastanum* and model plants increases the chance of infection or causes any effects on the plant's growth and protein content.

3. Test whether different strains of *P. syringae* can survive outside the host in different levels of pH and temperature (heat shock) for extended periods and whether they still retain their pathogenicity.

2.3 Materials and Methods

2.3.1 Chemicals and Solutions.

All chemicals and reagents used were of analytical quality. All glassware and non-disposable plastics were washed with tap water and rinsed three times with deionised water and dried in the oven at 60^{o}C prior to use unless otherwise stated.

2.3.2 Plant Material and Growing conditions

2.3.2.1 Seed Collection, growth and establishing model plant systems

Wild seeds of *A. hippocastanum* were collected in October 2016 from intact trees (with no visible lesions or marks of infection) and infected trees bearing lessions produced by Pseudomonas syringae at several sites on Keele University Campus, Staffordshire (53°00'05.4"N 2°16'27.3"W, 53°00'06.1"N 2°16'24.2"W and 52°59'57.5"N 2°16'16.6"W). The locations of target trees were recorded with a GPS Garmin Navigation System (GPSMAP,62, Garmin.Ltd.). Some of the seeds were stored in a refrigerator at low temperature (4 ± 1 °C) inside polyethylene bags for eight weeks to break seed dormancy, before planting them. The rest of the seeds were sown immediately in two-litre plastic trays containing compost (6 seeds/tray). Trays were covered with filter paper sheets for three days to initiate germination in darkness. Two weeks after germination, the germination value (GV) was calculated, and the seedlings of the experimental plants were transplanted into one-litre black plastic pots (1 seed/pot) containing compost (Clover, quality peat products,

Limited, UK) and peat (Irish Moss Peat, Limited, UK). Then pots were placed into a controlled environment in the greenhouse where the seedlings were grown under controlled photoperiod (8:16 h light: dark), a temperature of 21°C, humidity around 75% and maintained with sufficient water or according to the experiments. The environmental conditions inside the greenhouse were controlled using a TOMTECH HC160 auto-environment control computer system.

Model plants used were *Phaseolus vulgaris* 'Compass' (dwarf French bean) and *Lycopersicon esculentum* 'Ailsa Craig' (tomato). Seeds were obtained commercially from Suttons Seed company and used directly after rinsing in distilled water several times. Seeds were grown according to the above procedure. The seedlings were irrigated to field capacity and grown for four weeks before doing any treatment. The plant pots were also irrigated approximately once a month (57ml) with half-strength Hoagland's solution (hydroponic nutrient solution) in the watering regime, to keep a nutrient balance (Hoagland and Arnon 1938). The ingredients for Hoagland's solution are provided in Appendix 1.

2.3.2.2 Seed moisture content

Seed moisture content was determined before washing according to the International Seed Testing Association (ISTA) protocols. Five groups of seeds, each including ten solid, clean, healthy and apparently live seed were cut with a sterile scalpel into approximately 3 x 3 mm cubes and mixed as quickly as possible to reduce drying. Then 10 g of cut seeds (fresh weight) were dried in an oven at 105 ± 1 °C for between 18–24 hours or till two consecutive

weighings gave a constant weight. Then the final dry weight was taken, and moisture percent of seed was calculated by applying the following formula (Gosling, 2007).

$$\text{Moisture content (as \% fresh weight)} = \frac{(\text{fresh weight [g]} - \text{dry weight [g]})}{\text{fresh weight [g]}} \text{X100}$$

2.3.3 Bacterial strains and their sources

Experimental *A. hippocastanum* and model plants were inoculated with bacteria-specific for each species. Stock cultures were grown in the lab to provide the inoculum. They were prepared as described below. The original inoculum to make up stock cultures was obtained from Sarah Green (Forest Research, Edinburgh) (Table 2-1).

Table 2-1 *P. syringae* bacterial strains used in this study. The table shows the different species of pathogenic *P. syringae* bacteria and their source.

Isolate bacteria No.	Isolate No.	Bacterial Isolate species	Isolate source	Isolate reference
S1	2171	*P. syringae* pv *aesculi*	Eglinton Park, Irvine, Scotland	-
S2	2202	*P. syringae* pv *tomato*	NCPPB, York, UK	2563
S3	2200	*P. syringae* pv *phaseolicola*	NCPPB, York, UK	3613
S4	K2016	*P. syringae* pv *aesculi*	Keele campus, Staffordshire,	-
S5	2193	*P. syringae* pv *aesculi*	Winchester, England	-
S6	2250	*P. syringae* pv *aesculi*	Perth, Scotland	-
S7	2187	*P. syringae* pv *aesculi*	Lockerbie, Scotland	-
S8	2249	*P. syringae* pv *aesculi*	Budleigh Salterton, Devon, England	-

2.3.3.1 King B medium

Bacteria strains were incubated in King B medium (KB medium). To prepare it, all ingredients (Table 2-2) were combined and boiled with agitation for approximately three minutes to ensure the ingredients were sterilised, mixed and the agar was dissolved. Then they were cooled to around 25 °C (77 °F), and the final pH was adjusted with 0.1 M HCl and 0.1 M NaOH to pH 7.2 ± 0.2 at 25°C. Then the medium was autoclaved for 15 min at 121 °C and cooled to 25°C. Antibiotic Cetrimide Fucidin Cephaloridine selective supplement (CFC) at 70 mg/ L (Sigma–Aldrich) was added after autoclaving and mixed well, then about 20 ml was poured into tubes (tubes were inclined to give half butt and half slant for longer storage). To prepare the Petri dish media, around 30 ml of medium was poured into 9 cm Petri dishes which were covered immediately. Once the agar solidified, plates were kept upside down in a refrigerator until used. Inoculation by bacteria took place after the dishes were rewarmed to room temperature. For preparing the broth (liquid) medium, the agar was excluded from the mixture, detailed in Table 2-2.

Table 2-2. The composition of King B medium used in the isolation, cultivation and for the detection of Fluorescein of *Pseudomonas syringae*.

Ingredients	**Amount**
Casein peptone	10.00 g/l
Meat peptone	10.00 g/l
Dipotassium phosphate (K_2HPO_4)	1.50 g/l
Magnesium sulphate ($MgSO_4$)	1.50 g/l
Glycerol	10.0 ml/l
Agar	15.00 g/l
Distilled/deionized water	1000 mL
Final pH 7.2 ± 0.2 at 25 ºC	

2.3.3.2 Preparation of bacteria dilution series

Dilution series of bacteria were prepared in ten sterile glass test tubes to obtain dilutions containing approximately 10^3 to 10^4 CFU/ml. 100 µl of each of these ten tubes was removed and spread onto a 9 cm Petri dish containing 30 ml of solid King B agar medium. The Petri dishes were directly transferred to the incubator and kept at 21 ± 2 °C for 3-4 days. After bacteria growth, counting the number of bacteria forming a unit colony (CFU) was carried out on the surface of the Petri dishes. Counting was stopped after 5-6 days. The sample plates were examined for the presence of typical *P. syringae* colonies by comparison with the positive control plates, which were directly isolated from the mother isolation. All dilution series were carried out in the sterile condition conditions of an airflow bacterial culture hood.

2.3.3.3 Culture media preparation and culturing

The pathogenic bacteria *P. syringae* pv *aesculi* 2171, *P. syringae* pv *tomato* 2202 and *P. syringae* pv *phaseolicola* 2200 (Table 2-1) were used in this study for artificial inoculation. Freeze-dried mother samples of bacteria (from -80 °C glycerol stocked medium) were revived by streaking onto 9 cm Petri dishes containing fresh solid King's B medium agar and grown for three days at 21 ±1 °C. A single colony was selected and picked up by a clean loop and suspended in liquid King's B medium to grow at 21 ±1 °C on a rotary shaker speed of 150 rpm for 48 h. When the bacterial growth reached the late log phase of growth (OD600 0.5 to 1.0), bacteria were diluted to 10^4 CFU/ml in 10 mM $MgCl_2$ for the seedling inoculation (see 2.3.3.2 above). Control was established by inoculating plants with 10 mM $MgCl_2$ (Katagiri *et al.*, 2002). Usually, the total volume of the flasks for liquid culture was at least 3 to 4 times greater than the volume of King B medium to allow enough aeration. Antibiotics (CFC) and other supplements were added where required. All bacteria experiments were carried out under sterile conditions in an airflow bacterial culture hood. Mother strains were stored at -80 °C, and sub-culturing of bacteria on fresh King B medium performed monthly or when required.

2.3.3.4 Pathogen growth, reproduction and inoculation

For the injection application, *A. hippocastanum* and model plants (*L. esculentum* and *P. vulgaris*) were inoculated 10 cm above ground level by syringe (in bark) with 100µl of bacteria suspension (10^4 CFU/ml) (see 2.3.3.3 above). The injection site was covered with “Parafilm” to avoid external

contamination and to prevent dehydration of the plant at the injection site. For every injection, a new clean disposable syringe (with a needle) was used to prevent cross-contamination between inoculated samples. Inoculated plants were then incubated in the greenhouse under a long-day condition (16 hours light and 8 hours dark, 21-23 ºC, 75% humidity).

2.3.3.5 Wild *Pseudomonas syringae* pv. *aesculi isolation*

A wild strain of *P. syringae* pv *aesculi* was obtained from Keele campus. Bacterial isolations were collected from the main trunk around 1.5 meters above the soil. Small pieces (about 5 millimetres long) of necrotic tissue from infected sites (with visible lesions) were taken from the phloem tissues. The tissue was sterilised externally using ethanol alcohol 70 %, left to dry for a few minutes and incubated on a solid medium of nutrient agar for 48 hours. After this, they were tested to make sure that they were free of any contamination. The tissues were macerated in sterile water, streaked on fresh solid King's B medium agar and incubated at 21 ±1 °C for 3-4 days. All bacteria experiments were carried out in the sterile conditions of an airflow bacterial culture hood.

2.3.4 The effect of pH and temperature on *P. syringae* survival

Bacteria were grown in the KB medium at a range of alkaline and acidic pH levels between 3 to 11 for 1, 2 and 4 days. The same protocols required for bacteria growth on the liquid and solid media were followed as described above (see 2.3.3.3 above and 2.3.3.4 above).

The survival of bacteria at different temperatures was also examined on the liquid KB medium by exposing the bacteria to a temperature ranging between 0 to 80 ^{o}C in bathwater for 1, 5 and 15 minutes, respectively. Following this, the growth of bacteria was completed at 21 ±1 °C on a rotary shaker speed of 150 rpm for 3-4 days.

2.3.4.1 Alamar blue microplate assay (viability of bacteria assay)

Bacterial cells were grown as described previously (2.3.3.3 above). After pH or heat treatment (see 2.3.4 above), 10% volume of Alamar blue (Resazurin) reagent (Thermo Scientific) was added to each well of the samples. All samples were protected from light (by covering with aluminium foil) and incubated for 4-5 hours at 25 ^{o}C with the Alamar blue reagent. Media alone was used as a negative control. Light absorbance was then measured using a 96 well plate reader with a GloMaxplus® Multi Detection System (600nm as the reference). The percentage viability of bacterial cells was calculated by the % light reduction of Alamar blue reagent and by comparing treatments using bacterial cells (pH and heat shock) with untreated control cells.

2.3.4.2 Bacteria identification

2.3.4.3 Biochemical and nutritional test determinations

To ensure that *P. syringae* was being used in the above experiments, the identity of the isolates was characterised and confirmed based on antibiotic resistance, Gram staining test, colony growth and morphological characters on solid agar medium, detection of Fluorescein and finally Sanger sequencing. The generation of fluorescent pigment under longwave ultraviolet light (366

nm) on KB medium was examined at two days after incubation, and final counts of fluorescent and total colonies were made after 4-5 days of incubation. Fluorescent colonies were transferred to KB medium, and the absence of cytochrome c oxidase was verified by streaking some of the 48 h cultures with a sterile loop or sterile toothpick on filter paper imbibed with a fresh solution of 1% tetramethyl-phenylenediamine dihydrochloride (Morris *et al*., 2008).

2.3.5 Bacteria re-isolation from seedling tissues and pathogenicity test

The re-inoculation test by bacteria was carried out to confirm the pathogenicity of the *P. syringae* pv. *aesculi* isolates on *A. hippocastanum* and to ensure that the bacteria were still able to infect the host after experiments of bacteria survival at different levels of pH and temperature. Re-isolations of *P. syringae* were performed at the margins of lesions within phloem in the main stem, and tissue was macerated in sterile water using a sterilised Dounce tissue grinder 7 mL complete, streaked on medium KB medium. The pathogenic nature of each bacteria and the specific plant was determined by following the artificial inoculation method for inoculation of the healthy plants again by follows the same previous procedure for re-inoculation (2.3.3.4) (Green *et al.*, 2009; King *et al*., 1954). Re-inoculation tests were also carried out by re-injecting intact plants with isolated bacteria, and also by swapping high concentrations of different strains of bacteria with the model plants to ensure the incidence of infection or not.

2.3.6 Sequence analysis and primer design

The primers used were V4 Forward (GTGCCAGCMGCCGCGGTAA) and V4 Reverse (GGACTACHVGGGTWTCTAAT). Primers were designed online by using the NCBI- Gene Bank database and were ordered from the Eurofins company. After PCR (PCR is explained in detail in Section 4.3.5.10) additional Sanger sequencing of the suspect strains was carried out in collaboration with the Eurofins company. The Sanger preliminary annotation was carried out using Blast (NCBI) (http: www.ncbi. nlm.nih.gov/Blast/).

2.3.7 Inoculated plants response to drought stress

The drought stress treatment was initiated four weeks after planting (one week from inoculation by bacteria). Four irrigation treatments were applied, abundant irrigation (100% non-water-stressed as a control plant) and three other stress levels at 75, 50, and 25% of field capacity (full watering). All seedlings were then grown in the greenhouse under a long-day condition (16 hours light and 8 hours dark) at 21-23 ºC. Humidity inside the greenhouse was uncontrolled but showed limited fluctuation around 75%. Each treatment was replicated four times. After harvest, the dry weights, fresh weights, shoot heights and root lengths were measured. Each pot was routinely and regularly weeded throughout, the experiment to avoid losing plant water. Simple anatomical examinations also were carried out on plant tissues under an optical microscope to determine the extent or areas of lesions.

2.3.8 Water deficiency monitoring

Soil moisture was estimated and monitored with a Delta-T Theta Probe ML2 (Delta-T Devices Ltd.) connected to a Delta-T HH2 soil moisture sensor. The unit of measurement was volumetric water content (VWC) as a percentage (%Vol). This measure was used to confirm that the same soil moisture conditions were created during the whole study after field capacity (FC) was calculated.

2.3.9 Inoculated plants response to damage stress (Oxidative damage).

After five weeks from germination (one week from inoculation by bacteria), four damage levels were made using a cork borer (5.0 mm diameter) in plant leaf lamina amounting to 1, 3, 5 and 10% of the total area; major leaf veins were avoided (Figure 2-1). All seedlings were then grown in the greenhouse under a long-day condition as described above (see 2.3.7 above). After harvest, the dry, fresh weights, shoot heights and root elongations were measured. The leaf area was likewise determined using Image J software (version 1.52 a). Each treatment was replicated four times. Simple anatomical examinations were also carried out as mentioned in 2.3.7 above.

Field studies of damage stress were carried out at Keele University Campus, Latitude: 53°00'05.3"N, Longitude: 2°16'27.0"W. The study did not include protected or endangered species so no specific permissions were required for this location/activity. The damage stress study was carried out on single intact branches of the tree ranging from 1.5-2 metre above ground and without any artificial inoculation with bacteria. The same treatments of damage were

carried out as described above. Also, some leaves were pricked using a small syringe needle containing bacteria on the leaves of studied plants. Spraying bacteria was also applied on the leaves of some plants which were treated with damage stress after covering stems and soil with plastic cling film during application. The field trials were performed using three replicates and without any bacteria treatments.

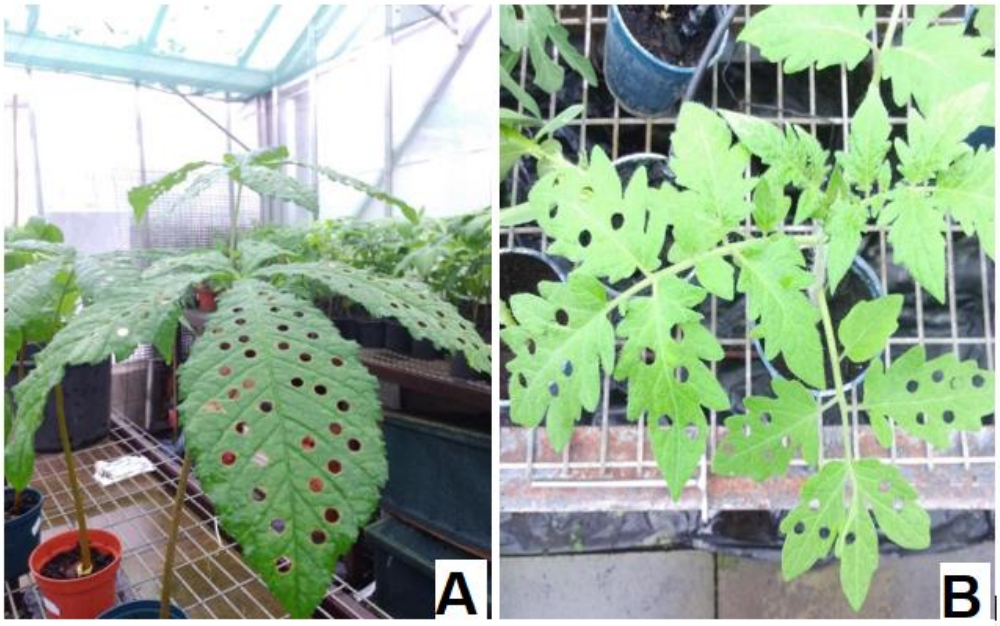

Figure 2-1 The damage stress treatments. The figure shows damage stress treatments 10%. A: leaves of *Aesculus hippocastanum*. B: leaves of *Lycopersicon esculentum*. The image was taken at the greenhouse of Keele University.

2.3.10 Measuring the effects of drought and damage on biomass, plant height and root length (Plant vitality assessments).

When the experiments were finished (at harvest time, six months from germination) root and shoot tissues were collected from the greenhouse. The plant height (mm) and root length (mm) was determined as the length from the

soil surface (base of the main stem) to the highest fully-grown leaf in the canopy and from the growth point to the root endpoint, separately by flexible tape measure (mm). The root hairs and root nodes were examined to check for any differences. The dry weight was used to analyse the effects of the damage and drought stress on plant biomass. The plant roots and shoots at harvest day were separately cut and weighed for the fresh weight (FW), then dried in an oven at 80 ± 5 ˚C for 24 hours and again weighed to register dry weight (DW) (Dwivedi *et al.*, 2015; Le Van *et al.*, 2016). Some seedlings of *A. hippocastanum* were left for the next season for purposes of examination and monitoring.

2.3.11 Protein extraction and quantitation methods

2.3.11.1 Preparation of leaf samples to extract proteins

For all protein extraction procedures, frozen or dried leaves were ground to a fine powder using a pre-chilled porcelain mortar and pestle in liquid nitrogen. All samples were dried because of the limited space available until used in the assays. In all trials, dried samples were used; frozen samples were used only to compare and find a better method to save samples in terms of the protein content. Lysis and buffer solutions were prepared by mixing stock solutions of their components that were kept in a fridge, except some of the components such as dithiothreitol (DTT) were freshly prepared, and the solutions which contained toxic components were prepared in a fume cupboard.

2.3.11.2 Detergent protein extraction

For this protocol 500 mg of ground tissue was suspended in 3 ml of ice-cold extraction buffer consisting of 0.2M MOPS (3-(N-morpholino) propane sulfonic acid), 5% PVPP (Polyvinylpolypyrrolidone), 1% Triton X-100, 10% glycerol, 20 µl protease inhibitor cocktail (Sigma), 2mM DTT (dithiothreitol). Protease and DTT were added on the day of use. All the components were mixed quickly for 1 min and sonicated for 3 min. The extract was then filtered immediately through a nylon mesh (micro cloth from Merck KGaA, Germany), and squeezed by hand to remove cell wall and other remains. After that, the extract solution was centrifuged at 1400 g for 25 min at 4°C. The supernatant was poured carefully, and the pellet was extracted again with buffer solution, filtered and centrifuged again (any unstable pellets were discarded). Finally, the supernatant was combined with the previous supernatant and stored at -20 °C until further use (Laing & Christeller, 2004).

2.3.11.3 TCA/Acetone protein extraction

The procedure was developed from a previously published protocol with some minor modifications as follows:

The plant leaves (500 mg) were homogenised and dissolved in 1 ml of ice-cold extraction buffer consisting of 10% TCA, 2% β-ME. The sample was sonicated for 3 min, then kept overnight at -20 °C for precipitation. Next day, the tissue mixture was spun at 10000 g for 15 min at 4°C. The supernatant was decanted, and the precipitates were washed three times using ice-cold acetone and vortexing, then the precipitate was dried at room temperature (but not over-

dried), and so remained slightly damp. This precipitate was dissolved in 3 ml of the lysis buffer consisting of 2 M thiourea, 7 M urea, 4% chaps 1% DTT, then stored at -20 °C until use (Wu & Wang, 1984; Cilia *et al*., 2009). In parallel, other trials were carried out by changing the molarity of urea (5, 7, 9 M) and with or without sonication.

2.3.11.4 Phenol protein extraction

In order to extract protein from the leaves, 500 mg of ground leaves were suspended in 1.5 ml of extraction buffer consisting of (500 mM Tris-HCl, 700 mM sucrose, 50 mM EDTA, 100 mM KCl pH was adjusted to 8.0 by HCl), vortexed and incubated by shaking vigorously for 10 min on ice (this step was performed at low temperature to limit protease activity). Next, an equal volume of Tris-saturated phenol was added, and the solution was incubated on a shaker for 10 min at RT; afterwards, the sample was centrifuged for 10 min at 5500*g* and 4°C. The upper layer (phenolic) was transferred to a new tube.

Then 3 ml of extraction buffer was added, the sample was shaken for 3 min, then centrifuged at 5500 g for 10 min at 4°C. The top layer (phenol) was collected into a new tube; 4 volumes of precipitation solution consisting of 0.1 M ammonium acetate in cold methanol was added. The tube was shaken by overturning it many times, and then incubated for at least four hours or overnight at 20 °C. Then the sample was pelleted by centrifuging at 5500 g for 10 min at 4 °C.

After spinning, the pellet was washed three times with cooled precipitation solution and lastly with chilled acetone. After each washing step, the sample

was spun at 5500 g for 5 min at 4 °C. Finally, the pellet was dried under vacuum and stored at -20 °C until use (Faurobert *et al*., 2007).

2.3.12 Protein quantitation via Bradford Assay.

Total protein concentrations were estimated from the leaf samples by using the Bradford method assay (Bradford, 1976; Hammond & Kruger, 2009). The reagent was prepared by dissolving 20 mg of Coomassie Brilliant Blue G-250 (CBBG) in 25 ml of 95% ethanol. The solution was mixed with 50 ml of 85% phosphoric acid, and then the volume was completed to 500 ml with distilled water (DW). The solution was filtered through filter paper (Whatman No.1) and then stored at room temperature. The absorbance was measured at 595 nm after 5 min and before 1 hour using a Nanodrop 1000 Spectrophotometer. Ten serial dilutions were prepared between the concentrations 0 to 11.2 mg/ml using bovine serum albumin (BSA Sigma), and a standard curve was created. Every protein sample was measured in triplicate, and the total protein in unknown samples was calculated.

2.3.13 Preliminary characterisation of protein by SDS-PAGE

SDS-PAGE (Sodium Dodecyl Sulfate Polyacrylamide Gel Electrophoresis) was carried out according to the method of Laemmli (1970) using 15% resolving gels with a 4% stacking gel buffer to resolve proteins. Total protein samples were treated with a sample buffer for SDS gels (13.15% of 0.5 M Tris pH 6.8, 26.3% glycerol, 2.1% SDS, 0.01% bromophenol blue, 5% β-mercaptoethanol) at a 1:1 ratio and heated to 95 °C for five minutes before loading. Molecular weights of the samples were determined using a low range

molecular weight marker (Bio-Rad). Samples and molecular weight marker were loaded into the gel wells, and electrophoresis was run at 200 V at room temperature until the blue dye reached the bottom (about 45 minutes), using a Power Pac Basic power supply (Bio-Rad) electrophoresis system. Gels were visualized by staining them with Coomassie stain, with bands developing after 30 minutes - 1 hour on a shaker.

2.3.14 In-gel digestion protocol

All chemicals and materials which were used were from Sigma, water and acetonitrile (both HPLC-grade) were from VWR/Fisher. Keratin is a major issue with in-gel digestions so that a pre-cast gel (Mini-PROTEAN® TGX™/Bio-Rad) was used to avoid any contamination.

2.3.14.1 Solutions and buffers used during protocol

Firstly, the following solutions were prepared:

Ambic Stock (ammonium bicarbonate): 50 mM NH_4HCO_3 (100 mg/25 ml) (will be used for all other Ambic preparations). 25 mM NH_4HCO_3 (25 mg/25 ml). Dehydration buffer consists of 25 mM NH_4HCO_3, 50% acetonitrile (ACN) (dilute Ambic stock 1:1 v.v. with MeCN). Extraction buffer consists of 50% ACN + 0.1%TFA (Trifluoroacetic acid) or Formic Acid (made next day).

Then the appropriate Coomassie Brilliant Blue stained SDS-PAGE bands were cut out from the gel into small pieces about 1 mm^2 using a clean scalpel blade (performed in a sterile laminar hood; gloves and sleeve covers were used). The gel bands were cut into small cubes to increase the surface area to volume

ratio. The pieces were then placed into labelled Eppendorf tubes. Enough dehydration buffer was added to cover the gel pieces (100ul or more, depending on how big the pieces were), vortexed and left for 10 mins. After this time the supernatant was extracted (a gel loading pipette tip was used) and discarded (this waste should be blue). The above two steps were repeated three times (3 washes). The gel pieces started to shrink and appeared opaque (due to losing their CBB blueness). Following this, 100% ACN was added to the gel pieces, vortexed and incubated briefly (~3 minutes) to dehydrate the gel pieces. Then the gel pieces were dried in a Savant Speed Vac for 15-30 min to complete dryness (gel pieces were smaller and white).

2.3.14.2 Reduction and Alkylation steps

The reduction process involved adding 30 μL (or enough to cover) and ten mM DTT in 25 mM NH_4HCO_3 to gel pieces (prepared fresh), then incubated for 45 min at 56 ^oC with shaking. The supernatant was removed and discarded. After that 55mM iodoacetamide (ICH_2CONH_2) in 25mM NH_4HCO_3were prepared near the end of the 45m incubation process.

For the alkylation process, iodoacetamide as above was added to cover the gel pieces and incubated at RT for 1 h in the dark, and the supernatant was discarded. Then the gel pieces were washed in 25mM NH_4HCO_3:50% ACN for a few minutes, the wash solution removed and then was dried in the SpeedVac to complete dryness (~ 20 min).

2.3.14.3 Trypsin digestion process

Fresh trypsin solution was added to cover the gel pieces (lyophilised trypsin powder was dissolved in water to obtain 1µg/ul concentration) (kept at -20'C). Trypsin was diluted 1/50 in 25mM NH_4HCO_3. The volume needed was calculated based on 5-10 ul/band (see below), a little extra was added to have a residual negative Tip-only control. Then a sensible (~7 ul) volume was added to gel pieces (usually 5-10 ul, depending upon original band/spot size and band staining intensity), and they were incubated on ice for a few minutes until gel pieces were partially rehydrated. Enough 25mM NH_4HCO_3were added to cover the gel pieces and incubated overnight (~16 hours) at 37 ^oC.

2.3.14.4 Extraction process

5 ul extraction buffer (50% ACN +0.1%TFA) were added to gel pieces to stop any remaining trypsin activity, the supernatant was then removed and kept in a new labelled Eppendorf tube. Gel pieces were covered in extraction buffer, vortexed and left for ~10 min (wash step). The supernatant was pooled together with that from the previous step and the wash step was repeated. The pooled extract was dried in the SpeedVac to complete dryness. Then the collected fractions were combined together, dried down in a SpeedVac and stored at -20 °C until further use (Hellman *et al.,* 1995; Rosenfeld *et al.,* 1992).

2.3.14.5 LC-MS characterisation

Dried extract fraction was dissolved in 0.1% formic acid, and the sample was placed in a clear glass (screw thread) vial for LC-MS. The sample calibration standard (5 µl, containing glu-1-fibrinopeptide) was introduced into a nanoflow

HPLC (Dionex Ultimate 3000, Thermo Fisher Corporation, Hemel Hempstead), and concentrated on a C18 trapping column (Acclaim PepMap100, ID 300 µm, length 5 mm, particle size 5 µm, pore size 100 Å, Dionex) at 30 µl/min, followed by separation on a C18 main column (Acclaim PepMap100, ID 75 µm, length 15 cm, C18 particle size 3 µm, pore size 100 Å, Dionex) using a binary gradient solvent A (0.1% F.A, 5% CAN) solvent B (0.1% FA, 95% ACN) at a split flow rate of 0.35µl/min.

The HPLC system was coupled to a hybrid quadrupole-time-of-flight mass spectrometer Q-TOF Premier (Waters Corporation, Wilmslow and Cheshire). Mass spectra were obtained using nanoflow electrospray ionization MS (nESI-MS), MS survey scans were acquired from 500 to 1600 m/z in the positive ion mode. Product Ion spectra were generated for precursors per survey from M/Z 50-200. HPLC performed at 200 Femto BSA trypsin digest. Data were acquired and processed by MassLynx (version 4.1; Waters Corporation).

2.3.15 Statistical Analysis

Four replicates of each treatment and concentration were used. The data in the Figures and Tables in this study are given as means. Error bars describe the standard error of the mean (SEM). Statistical analysis was performed using the GraphPad Prism statistical package (version 7) to determine the difference between the treatments. One-way analysis of variance (ANOVA) was used. Differences between values were considered statistically significant differences at $P \leq 0.05$.

2.4 Results

2.4.1 Seed moisture content and germination

The moisture content of seeds was measured to estimate the seeds ability to germinate and produce intact plants, and to estimate the viability of the seed. The moisture content of the *A. hippocastanum* seeds was between 41% and 45% (Figure 2-2). However, seed germination of all seeds was excellent, with the germination rate of seeds exposed to low temperatures to break the dormancy at approximately 97% compared to 93% for non-exposed seeds (planted directly in soil). Germination of the seeds exposed to a low temperature to break dormancy also occurred more quickly, taking about two to three weeks compared with seeds planted directly in the soil. There was no difference in the moisture content between seeds belonging to healthy trees and seeds belonging to trees which showed bleeding canker symptoms. Both groups of seeds had high germination, and no significant difference was seen between them.

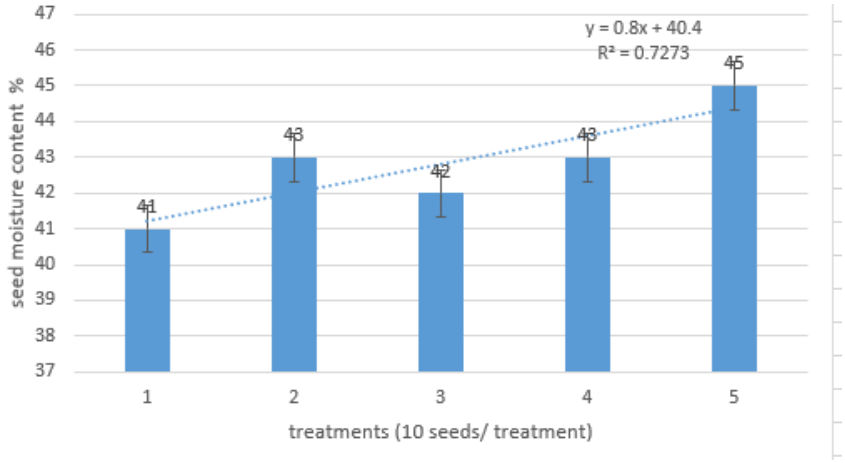

Figure 2-2 Seed moisture content. The figure shows the total moisture content of *A. hippocastanum* seeds. Treatments values are given as mean error bar represents the standard error of the mean ± SEM (n=10). 1-5 on the x-axis represent different experiments.

2.4.2 Plant vitality and infection assessments

As previously described (2.3.3.4 above) plants were inoculated with bacteria. In general, bacterial infection in seedlings was not very severe compared to trees that grow in nature, maybe because the disease needs a more extended period to develop and become more pathogenic or because of the presence of the disease without interference from other diseases or pests such as the larvae of leaf miner since in the greenhouse these were excluded and any plant showing other symptoms was isolated.

No lesions or symptoms were observed on leaves or buds (just on bark) throughout the time of study growing period. All lesions happened on the bark of the woody branches and seldom on leaf petioles or central veins. If the disease developed on leaves, the spots faded away after several days and left traces on the leaf looking like dead stiff tissue (Figure 2-3). The lesions formed in the entire phloem and cortex causing cankers, but there was no indication or sign of necrosis in the xylem tissues.

Figure 2-3 *A. hippocastanum* leaf inoculation with bacterial suspension (*Pseudomonas syringae* pv. *aesculi* 2171). The figure shows the infections were fading away after several days leaving on the leaf rust-red dead stiff tissue.

To determine whether the bacteria could cause infections on the leaves after damage treatments, inoculation and spraying treatments using bacteria were carried out. Based on the results, there is no record of any infection by the bacteria when using a spraying method on the stems or leaf through the lenticels or stomata. To determine the initial infection sites of *P. syringae* pv. *aesculi*, assessments were carried out on stems of artificially infected *A. hippocastanum* seedling showing typical bleeding canker symptoms such as quick defoliation compared with untreated plants, bark cracking and stem bleeding and dieback of some seedlings in the second year after the inoculation. The artificial inoculation also caused a dark strip that spread with the bark under the stem epidermis towards the bottom and showed no symptoms on the xylem (Figure 2-4).

Figure 2-4 Artificial inoculation of an *A. hippocastanum* stem. The figure shows a dark strip that spread along the bark under the stem epidermis towards the bottom. In the figure, an active lesion appears with black oozing. The blue arrow indicates the bacterial growth route. The yellow arrow indicates the central lesions.

In the second year, some of the wounds remained as cracks and were ineffective (no oozing) despite the presence of bacteria in some of them as confirmed by the re-isolation of bacteria and its development on the selective medium and then compared with the original bacterial strain (Figure 2-5). The same thing happened in the field or with the wild trees during monitoring bleeding canker disease of *A. hippocastanum* where some of the injuries were active and then became inactive or vice versa (activity restored after a period more than eight months).

Simple anatomical examinations were carried out on plant tissues to verify the existence of any symptoms of the bacterial infection. Based on the results, no signs of infection or lesion on xylem or leaves were observed six months after inoculation; the lesions were only observed on phloem tissues.

To study the susceptibility of the plant to infection with bacteria, the plants (horse chestnut, beans and tomato) were inoculated with specialised pathogenic bacteria for these plants and also with non-specialized bacteria separately. Unlike *A. hippocastanum*, most of the infection in *P. vulgaris* and *L. esculentum* happened on the leaves and sometimes on stems and fruits.

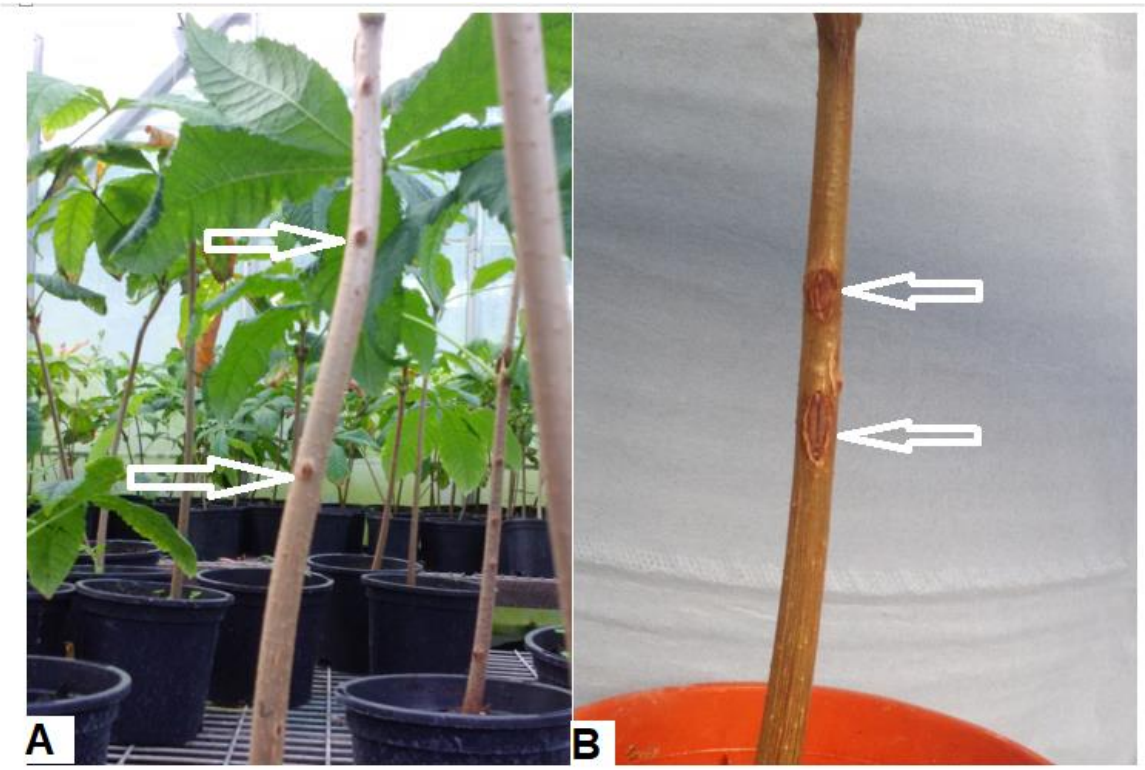

Figure 2-5 The effects of inoculation by *P. syringae* pv. *aesculi* on seedling of *A. hippocastanum*. **A**: shows lesion evolution beginning on a stem (arrows). **B**: shows inactive lesion after plant recovery or bacteria lose their pathogenicity for some reason (arrows).

2.4.3 Protein extraction and estimation.

To determine an appropriate procedure for the extraction of the total soluble protein from the plant's leaves, several methods were tried as mentioned in

2.3.11 above. The total protein content and nature of the precipitants (pellets) extracted reflects the efficiency of the extraction method and, therefore, we can anticipate how easy they will be to dissolve or to use later in the SDS–PAGE. The precipitants which were obtained from samples extracted by the detergent-protein protocol were greenish in colour, difficult to handle, viscous in nature and not easy to solubilise in the buffer. The pellets obtained from the TCA/Acetone protocol were opaque white in colour, slightly viscous, grainy in nature, easy to handle and easy to solubilise in the buffer. The precipitants from the Phenol protein extraction protocol were grainy, non-viscous, easy to solubilize in the buffer and gave pellet those were bright white in colour. Therefore, the TCA/Acetone method was chosen. The results of SDS-PAGE analysis were shown in Figure 2-6.

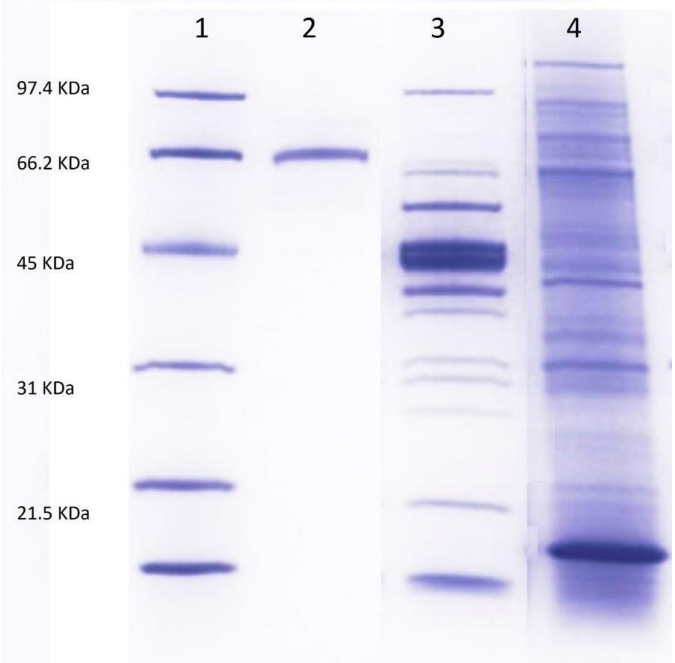

Figure 2-6 SDS–PAGE analysis of total soluble protein of *A. hippocastanum* leaves. Total protein was extracted by using different methods. The gel was visualized by CBBG (Coomassie Brilliant Blue G-250). An equal amount of protein (20 µl) was loaded in each well. Lanes 1 contain molecular weight markers. Lane 2 contains samples extracted using Phenol protocols. Lane 3 contains protein samples extracted using TCA. Lane 4 contains protein samples extracted using a detergent protocol.

2.4.4 Protein identification via Liquid Chromatography-Mass spectrometry

Mass spectrometry is one of the most accurate and sensitive techniques for analysing protein samples. The protein was extracted from the SDS-PAGE gel and digested, and then subjected to LC-MS/MS analysis (as described in section 2.3.14). The result of in-gel digestion of protein from *A. hippocastanum* leaves showed there is a very high abundance of specific proteins in the general proteome (Figure 2-7) especially ribulose-1, 5-bisphosphate carboxylase/oxygenase (rubisco). Also, the large chain of peptide matched with a sequence large chain (fragment) belonging to *Aesculus carnea*; this species is a hybrid of *A. hippocastanum* and *A. pavia* (Straw & Tilbury, 2006). Many other proteins including ATP synthase, were also identified. In summary, these results show that RuBisCO was the main protein constituent in the horse chestnut leaf.

RBL_BURIN	Ribulose bisphosphate carboxylase large chain (Fragment) OS=Bursera inaguensis GN=rbcL PE=3 SV=1
ATPB_ACRAL	ATP synthase subunit beta, chloroplastic OS=Acrocomia aculeata GN=atpB PE=3 SV=1
RBL_CITSI	Ribulose bisphosphate carboxylase large chain OS=Citrus sinensis GN=rbcL PE=3 SV=1
ATPB_NICBI	ATP synthase subunit beta, chloroplastic OS=Nicotiana bigelovii GN=atpB PE=3 SV=1
RBL_NICDE	Ribulose bisphosphate carboxylase large chain OS=Nicotiana debneyi GN=rbcL PE=3 SV=1
RBL_JUSOD	Ribulose bisphosphate carboxylase large chain (Fragment) OS=Justicia odora GN=rbcL PE=3 SV=1
RBL_CHAVU	Ribulose bisphosphate carboxylase large chain OS=Chara vulgaris GN=rbcL PE=3 SV=1
RBL_HALCL	Ribulose bisphosphate carboxylase large chain (Fragment) OS=Halesia carolina GN=rbcL PE=3 SV=1
RBL_FAGEA	Ribulose bisphosphate carboxylase large chain OS=Fagopyrum esculentum subsp. ancestrale GN=rbcL PE=3 SV=1
RBL_CAJCA	Ribulose bisphosphate carboxylase large chain OS=Cajanus cajan GN=rbcL PE=3 SV=1
RBL_CHLAT	Ribulose bisphosphate carboxylase large chain OS=Chlorokybus atmophyticus GN=rbcL PE=3 SV=2
RBL_JASSU	Ribulose bisphosphate carboxylase large chain (Fragment) OS=Jasminum suavissimum GN=rbcL PE=3 SV=1
RBL_CORLA	Ribulose bisphosphate carboxylase large chain (Fragment) OS=Corynocarpus laevigatus GN=rbcL PE=3 SV=2
RBL_STRNX	Ribulose bisphosphate carboxylase large chain (Fragment) OS=Strychnos nux-vomica GN=rbcL PE=3 SV=1
RBL_PIPCE	Ribulose bisphosphate carboxylase large chain OS=Piper cenocladum GN=rbcL PE=3 SV=1
RBL_FLERU	Ribulose bisphosphate carboxylase large chain (Fragment) OS=Fleroya rubrostipulata GN=rbcL PE=3 SV=1
RBL_COFAR	Ribulose bisphosphate carboxylase large chain OS=Coffea arabica GN=rbcL PE=3 SV=2
RBL_BEAGR	Ribulose bisphosphate carboxylase large chain (Fragment) OS=Beaumontia grandiflora GN=rbcL PE=3 SV=1
RBL_ANTHE	Ribulose bisphosphate carboxylase large chain (Fragment) OS=Anthospermum herbaceum GN=rbcL PE=3 SV=1
RBL_EQUAR	Ribulose bisphosphate carboxylase large chain OS=Equisetum arvense GN=rbcL PE=3 SV=1
RBL_ERICA	Ribulose bisphosphate carboxylase large chain (Fragment) OS=Eriodictyon californicum GN=rbcL PE=3 SV=1
RBL_DEPGR	Ribulose bisphosphate carboxylase large chain (Fragment) OS=Deppea grandiflora GN=rbcL PE=3 SV=1
RBL_VIGUN	Ribulose bisphosphate carboxylase large chain OS=Vigna unguiculata GN=rbcL PE=3 SV=1
RBL_LOBSP	Ribulose bisphosphate carboxylase large chain (Fragment) OS=Lobelia sp. GN=rbcL PE=3 SV=2
RBL_CUSSA	Ribulose bisphosphate carboxylase large chain OS=Cuscuta sandwichiana GN=rbcL PE=3 SV=1
ATPB_CHLVU	ATP synthase subunit beta, chloroplastic OS=Chlorella vulgaris GN=atpB PE=3 SV=1
RBL_ARGDE	Ribulose bisphosphate carboxylase large chain (Fragment) OS=Argyrochosma delicatula GN=rbcL PE=3 SV=1
RBL_PTEVI	Ribulose bisphosphate carboxylase large chain (Fragment) OS=Pteris vittata GN=rbcL PE=3 SV=1
ATPB_ANEMR	ATP synthase subunit beta, plastid OS=Aneura mirabilis GN=atpB PE=3 SV=1
ATPB_DICAN	ATP synthase subunit beta, chloroplastic (Fragment) OS=Dicksonia antarctica GN=atpB PE=3 SV=2
RBL_STAPU	Ribulose bisphosphate carboxylase large chain OS=Staurastrum punctulatum GN=rbcL PE=3 SV=1
RCAA_HORVU	Ribulose bisphosphate carboxylase/oxygenase activase A, chloroplastic OS=Hordeum vulgare GN=RCAA PE=2 SV=1
RBL_VITSX	Ribulose bisphosphate carboxylase large chain (Fragments) OS=Vitis sp. GN=rbcL PE=1 SV=1
ATPBM_HEVBR	ATP synthase subunit beta, mitochondrial OS=Hevea brasiliensis GN=ATPB PE=2 SV=1
ENO_ALNGL	Enolase OS=Alnus glutinosa GN=PGH1 PE=2 SV=1
ATPA_BUXMI	ATP synthase subunit alpha, chloroplastic OS=Buxus microphylla GN=atpA PE=3 SV=1
ATPBM_ARATH	ATP synthase subunit beta-1, mitochondrial OS=Arabidopsis thaliana GN=At5g08670 PE=1 SV=1
ATPA_CHAVU	ATP synthase subunit alpha, chloroplastic OS=Chara vulgaris GN=atpA PE=3 SV=1
RUBB_BRANA	RuBisCO large subunit-binding protein subunit beta, chloroplastic OS=Brassica napus PE=2 SV=1
PSBO_HELAN	Oxygen-evolving enhancer protein 1, chloroplastic OS=Helianthus annuus GN=PSBO PE=1 SV=1

Mascot Score Histogram

Ions score is -10*Log(P), where P is the probability that the observed match is a random event.
Individual ions scores > 30 indicate identity or extensive homology (p<0.05).
Protein scores are derived from ions scores as a non-probabilistic basis for ranking protein hits.

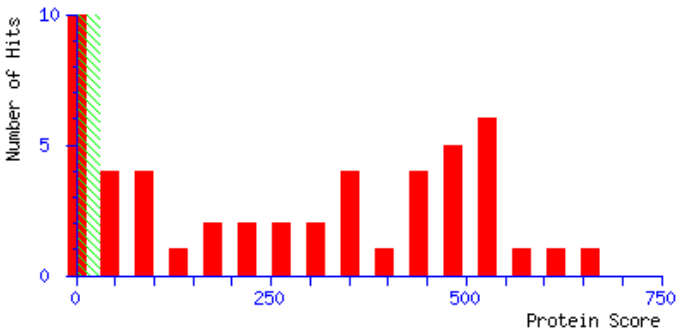

Figure 2-7 Matching of peptides to sequence database and Mascot Score Histogram. The figure shows a small part of peptides matching from top matching hits.

2.4.5 Effect of drought on *A. hippocastanum*

To determine drought stress effects on growth and protein content of the *A. hippocastanum* and model plants, drought stress experiments were carried out. The extraction of total protein was carried out using the TCA-Acetone protein extraction method (TCA), and the estimation of protein content was done following the method of Bradford (1976). The results reveal that following drought stress, total leaf protein increased significantly at 75% field capacity, but with the 25% FC treatment, there was significantly reduced the amount of total protein ($P<0.05$). The comparison of the mean values of the leaf protein revealed that the irrigated treatment had, in general, the highest protein content and the non-irrigated treatment had the lowest leaf protein, and there were no differences with controls that were inoculated with its specific bacteria). The results showed no apparent effects for 50% treatment (water deficit) on the protein content of inoculated *A. hippocastanum* seedlings (Figure 2-8).

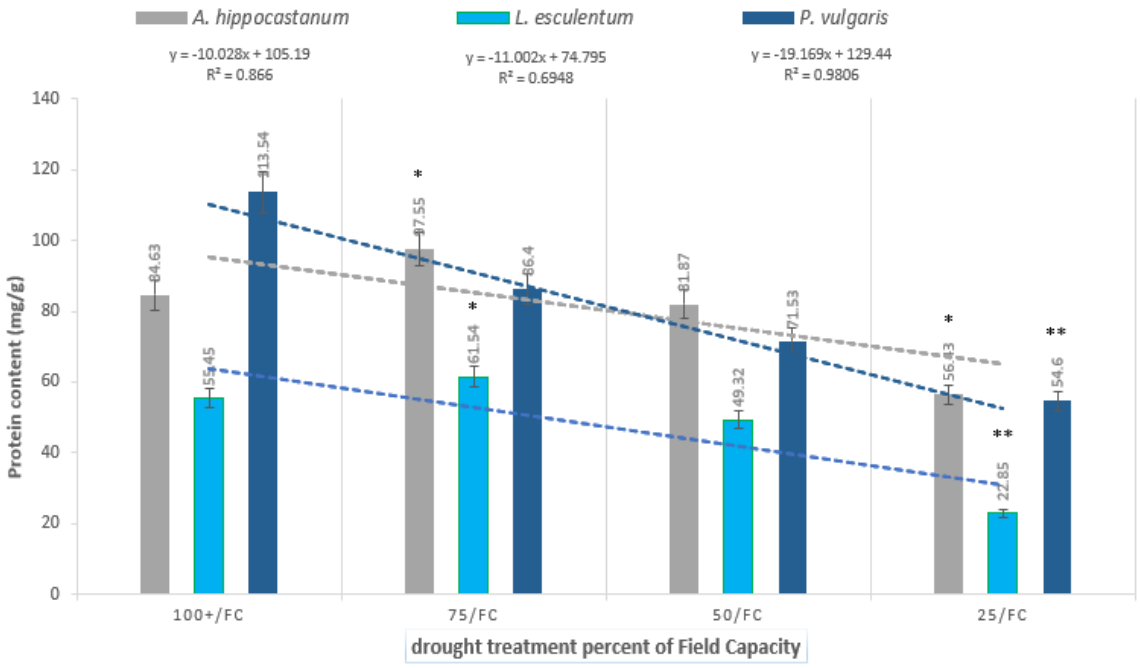

Figure 2-8 The effect of drought stress treatments on the total protein content. The figure shows the total leaf protein concentrations of *A. hippocastanum* and model plants with different drought stress treatments. Values are given as means and the error bars represent the standard error of the mean ± SEM (n=4). Asterisk(s) above bars indicate significant difference at $p < 0.05$. FC represents soil moisture at field capacity. All samples were inoculated by each specific *P. syringae* (S1, S2 and S3).

The exposure of *A. hippocastanum* to different drought stress treatments showed there was an apparent influence on protein content with treatment of 50% and 25% of FC on root elongation and height of shoot. On the other hand, there was a significant decline in dry shoot weight when compared with the control plants (Figure 2-9).

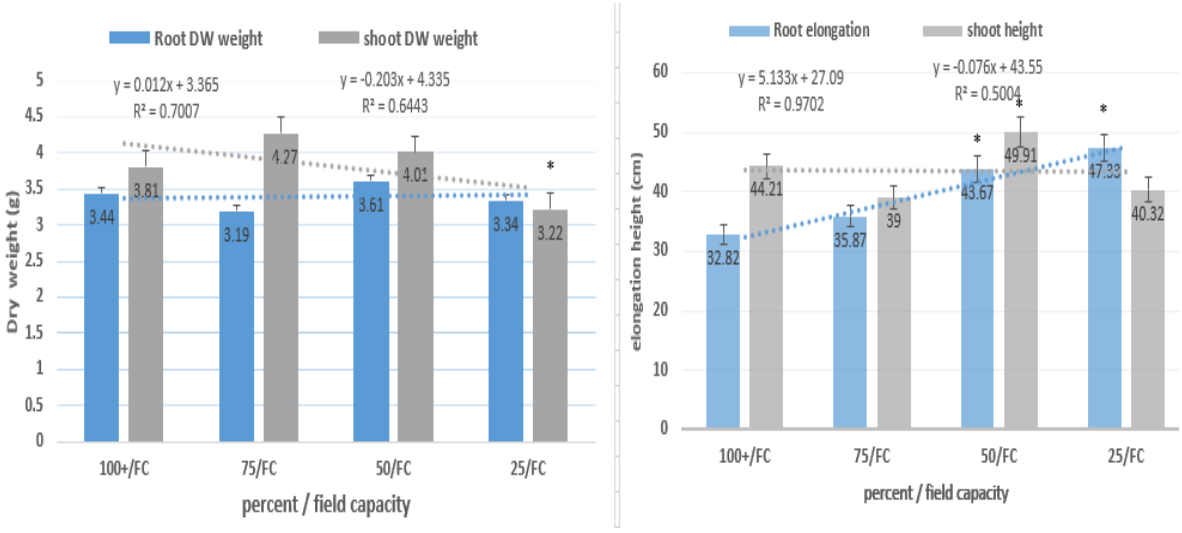

Figure 2-9 The effect of drought stress on *A. hippocastanum* seedlings growth and biomass. The figure shows the effect of drought stress on roots and shoots dry matter, root elongation and shoot height of *A. hippocastanum*. Values are given as means and the error bars represent the standard error of the mean ± SEM (n=4). Asterisk(s) above bar indicate significant difference ($p < 0.05$). FC represents soil moisture field capacity. All seedlings were inoculated by *P. syringae* pv *aesculi* 2171.

Generally, the stem assessments showed there was a decrease in the development of *A. hippocastanum* infections in the seedling in particular with the 75% treatment in conjunction with drought stress. At the same time, severe drought stress treatment had a negative effect on plant growth and development. The number of lesions clearly decreased over time or in some cases, a lack of infection was reported in the *A. hippocastanum* plants which were exposed to drought stress.

2.4.6 Effect of drought on the model plants

The use of plant models is useful when the test plant is a long-lived perennial which has not previously been studied, as in *A. hippocastanum*. The results showed that the total leaf protein of *L. esculentum* was significantly increased

with the moderate treatment of 75% field capacity and negative with other treatments. With regard to the effect of drought stress on *P. vulgaris* (the common bean), there was no significant increase in the treatments. On the contrary, there was a significant decrease especially with severe drought (25%) (Figure 2-10).

Exposing *P. vulgaris* to drought stress resulted in a significant decrease in the dry weight at the treatment at 25%. In contrast, with the 50% treatment a significant effect was observed on elongation root, but the height of the shoot decreased significantly and reached 21.16 cm compared to the control of 28.7 cm ($P<0.05$) (Figure 2-10). The number of bacterial infections also clearly decreased over time, especially in the tomato plants which were exposed to drought stress; in contrast, no significant change was seen with the bean plants. The results also showed a significant increase in root growth of both model plants at the lowest water treatment ranging from 15 to 25%. The number and shape of nodules on *P. vulgaris* roots did not show any variation between the control and roots of drought treated plants. Except in the severe droughts treatments, the number of root nodes was reduced to nearly half of the control samples.

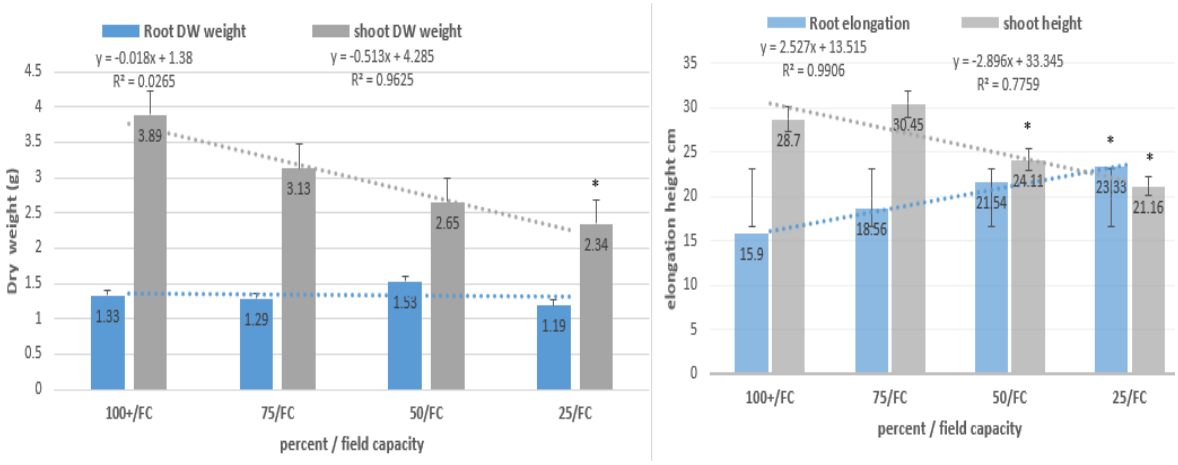

Figure 2-10 The effect of drought stress on *P. vulgaris* seedlings growth and biomass. The figure shows the effect of drought stress on roots and shoots dry matter, root elongation and shoot height of *P. vulgaris*. Values are given as means and the error bars represent the standard error of the mean ± SEM (n=4). Asterisk(s) above bar indicate significant difference ($p < 0.05$). FC represents soil moisture field capacity. All samples were inoculated by *P. syringae* pv *phaseolicola* 2200.

Exposing *L. esculentum* to drought stress resulted in a significant increase in the dry weight at the 75% treatment. On the other hand, there was a positive effect with 75% and 50% treatment on root elongation and shoot height where the increase was significant. They have reached at treatment 25% 44.33 and 66.56 on elongation root and height of shoot, respectively (Figure 2-11).

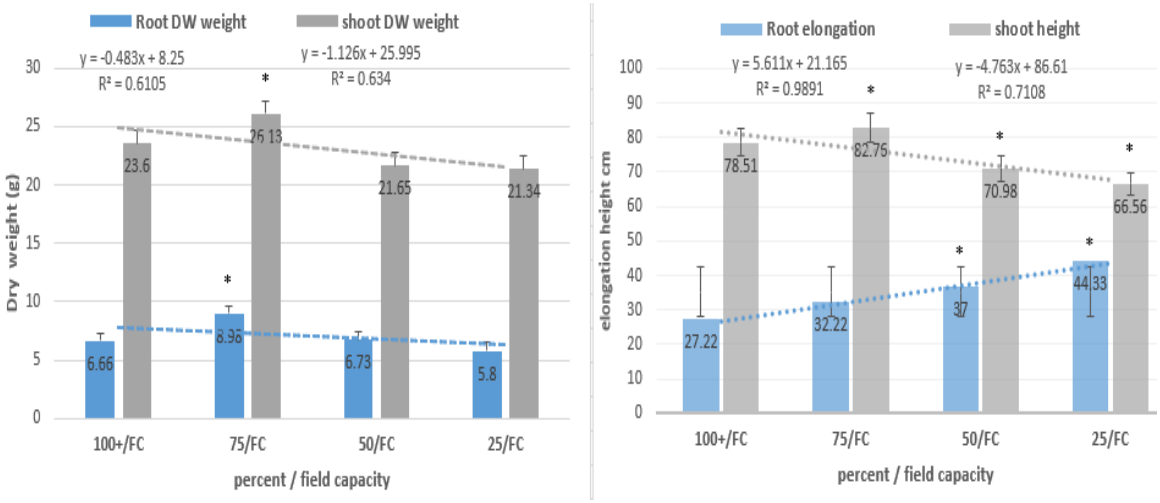

Figure 2-11 The effect of drought stress on *L. esculentum* seedlings growth and biomass. The figure shows the effect of drought stress on roots, shoots dry matter, root elongation and shoot height of *L. esculentum*. Values are given as means and the error bars represent the standard error of the mean ± SEM (n=4). Asterisk(s) above bar indicate significant difference ($p < 0.05$). FC represents soil moisture field capacity. All samples were inoculated by *P. syringae* pv *tomato* 2202.

2.4.7 Effect of damage stress on *A. hippocastanum* field and greenhouse studies

The field studies of damage stress were carried out at Keele University Campus. The damage stress was carried out on single intact branches without any artificial inoculation with bacteria. During the study period (six months), there were no visible lesion or symptoms by bacteria recorded, although there are many trees infected at the same site or close to the experimental site.

The protein contents estimated are critical physiological parameters in plant development. In terms of the effect of damage on *A. hippocastanum* leaf protein, there was no clear response to the effect of damage. However, there

was some apparent increase and decrease with different treatments, but the values were not significant. (Figure 2-12).

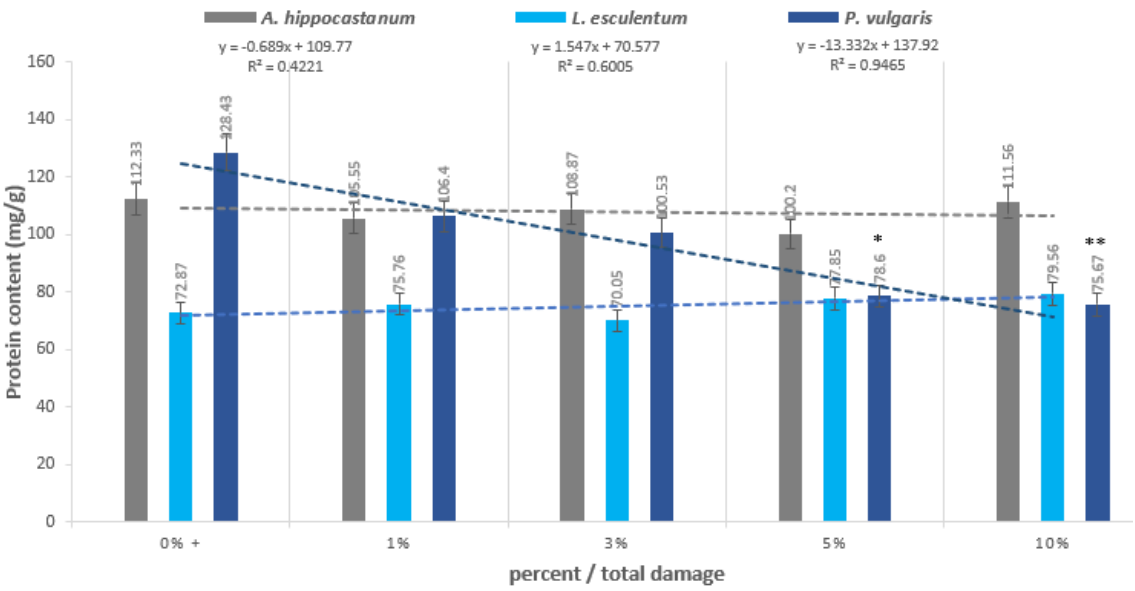

Figure 2-12 The effect of damage stress treatments on the total protein content. The figure shows the total leaf protein concentrations of *A. hippocastanum* and model plants with different damage stress treatments. Values are given as means and the error bars represent the standard error of the mean ± SEM (n=4). Asterisk(s) above bar indicate significant difference ($p < 0.05$). FC represents soil moisture field capacity. All samples were inoculated by each specific *P. syringae* (S1, S2 and S3).

In terms of the effect of damage stress, there was an apparent decrease in the dry weight of the stems and roots, but the values were not significant. There was also an apparent increase in the length of the root and plant height, but the values were also not significant, except for the rise in the height of the shoot at the treatment of 10% damage of the total leaf area where the increase was significant (Figure 2-13).

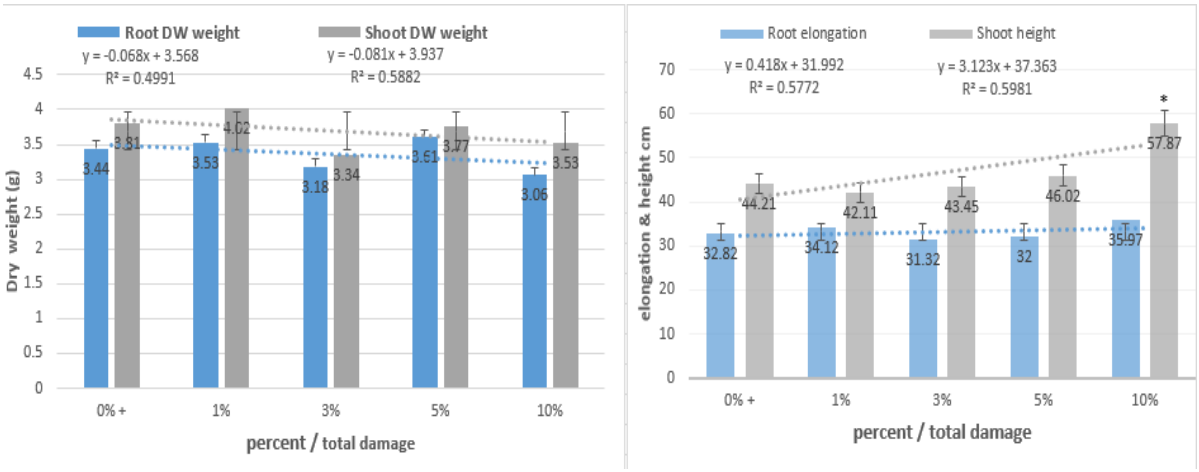

Figure 2-13 The effect of damage stress on *A. hippocastanum* seedlings growth and biomass. The figure shows the effect of damage stress on roots, shoots dry matter, root elongation and shoot height of *A. hippocastanum* seedlings. Values are given as means and the error bars represent the standard error of the mean ± SEM (n=4). Asterisk(s) above bar indicate significant difference ($p < 0.05$). FC represents soil moisture field capacity. All samples were inoculated by *P. syringae* pv *aesculi* 2171.

2.4.8 Effect of damage stress on the model plants

The protein content of the tomato plant showed no response to damage. For bean plants, however, there was a significant decrease in the concentration of protein in treatments of 5% and 10%, reached 39% and 41% respectively (Figure 2-12).

There was no significant effect of damage stress in bean plants on the dry weight of the stems and roots. However, there was a significant decrease in shoot length with 10% damage of total leaf area, where the length of the shoot decreased by 22.9% (Figure 2-14). The number and shape of the root nodules did not show any variation between the control and roots of damaged plants.

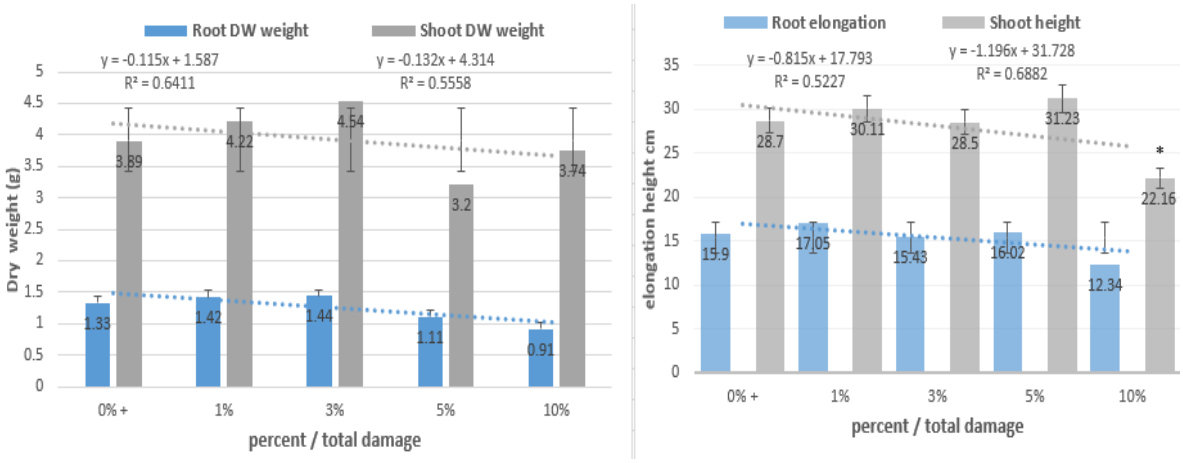

Figure 2-14 The effect of damage stress on *Phaseolus vulgaris* growth and biomass. The figure shows the effect of damage stress on roots, shoots dry matter, root elongation and shoot height of *P. vulgaris*. Values are given as means and the error bars represent the standard error of the mean ± SEM (n=4). Asterisk(s) above bar indicate significant difference ($p < 0.05$). FC represents soil moisture field capacity. All samples were inoculated by *P. syringae* pv *phaseolicola* 2200.

Regarding the effect of damage stress on tomato plants, there was no significant change in the dry weight of the stems and roots. However, there was a significant increase in the length of the shoots with the treatment of 10% damage of total area, where the length of the shoot increased by 23.5%.

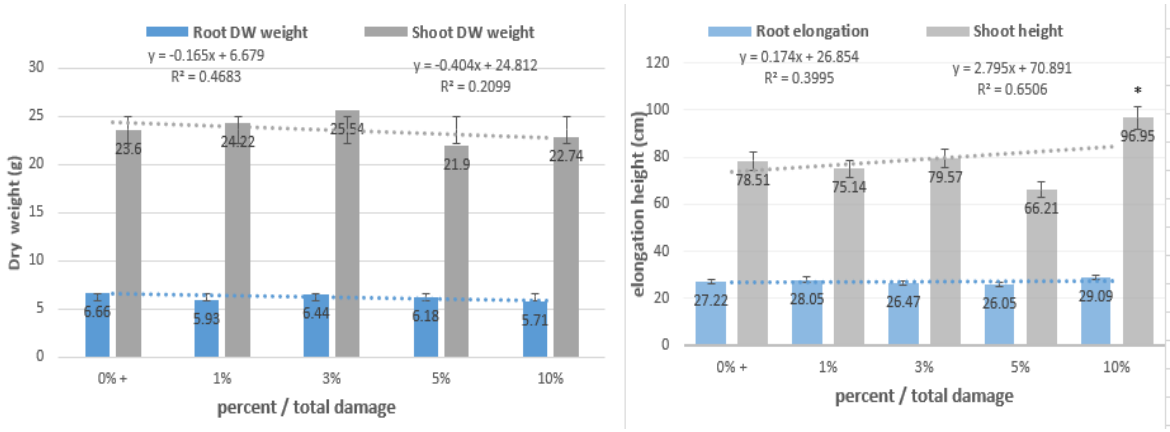

Figure 2-15 The effect of damage stress on *Lycopersicon esculentum* growth and biomass. The figure shows the effect of damage stress on roots, shoots dry matter, root elongation and shoot height of *L. esculentum*. Values are given as means and the error bars represent the standard error of the mean ± SEM (n=4). Asterisk(s) above bar indicate significant difference ($p < 0.05$). FC represents soil moisture field capacity. All samples were inoculated by *P. syringae* pv *tomato* 2202.

Regarding the relationship between drought and damage stress in this study, and if there is any interference between them, nothing was seen or reported.

2.4.9 Bacteria population and identification of viable cells

All the bacterial strains showed a positive response towards oxidase reaction. In regard to producing fluorescent pigment to identify fluorescent cultures, *P. syringae* was streaked on King's medium B amended with 50 mg/l CFC. The finding revealed that all strains studied showed an ability to produce a green-yellowish fluorescent pigment that fluoresces under longwave ultraviolet light (366 nm). There was no difference in the intensity of the fluorescence with the exception of the strains *P. syringae* pv *phaseolicola* 2200 and *P. syringae* pv *aesculi* 2249, which did not fluoresce under longwave ultraviolet light (Figure 2-16). On the other hand, the strains *P. syringae* pv *aesculi* 2171 and *P. syringae* pv *tomato* 2202 exhibited an intense fluorescence compared to other

strains. Fluorescence pigments were detectable at pH between 5.0 to 8.0 on KBA medium.

The isolated bacterial strains were recognised and systematically classified based on their morphology in culture and size. The produced colonies were creamy white and round-shaped. The mean colony size of the bacteria was 4.22, 2.20 and 1.73 mm for strains *P. syringae* pv *tomato* 2202, *P. syringae* pv *phaseolicola* 2200 and *P. syringae* pv *aesculi* 2171, respectively (Figure 2-17). All *P. syringae* pv *aesculi* isolates showed lower viscosity than *P. syringae* pv *tomato* and *P. syringae* pv *phaseolicola* when were transferred by loop when sub-culturing. The identity of all suspect colonies was confirmed by a pathogenicity assay on host seedlings of the intact plant.

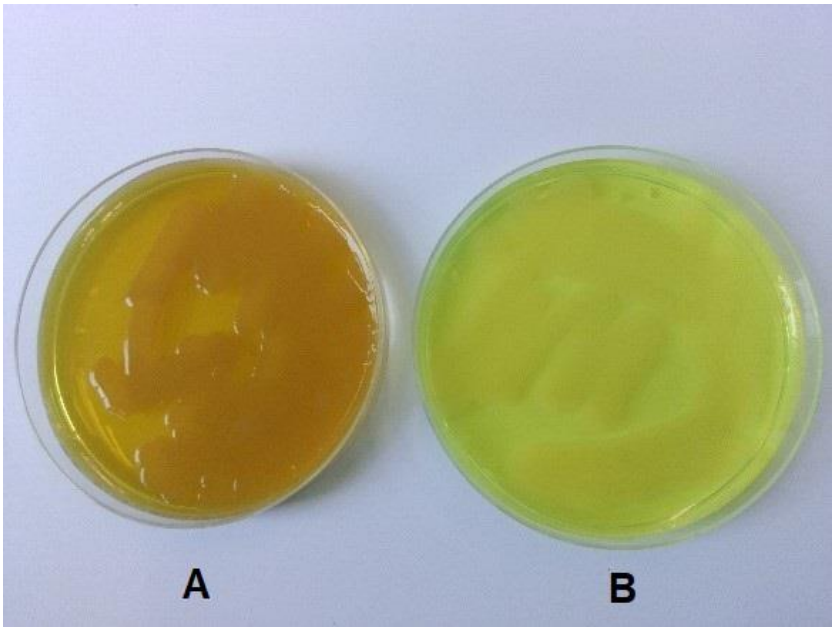

Figure 2-16 The *Pseudomonas syringae* fluorescent strain test. The figure shows a non-fluorescent *P. syringae* pv *phaseolicola* strains (A) and a fluorescent *P. syringae* pv *aesculi* 2171 (B), both under normal light.

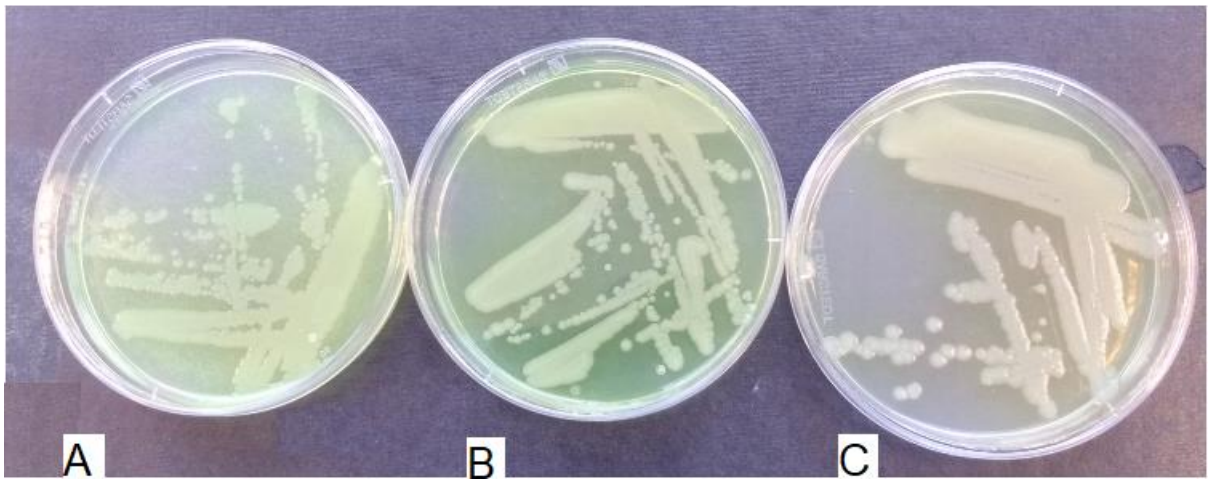

Figure 2-17 Pure culture of different *P. syringae* strains. A: *P. syringae* pv tomato 2202. B: *P. syringae* pv *phaseolicola* 2200. C: *P. syringae* pv *tomato* 2171, growing on agar plate shows different sizes and shapes of colonies after one day of incubation at 21 °C.

The survival of bacteria to heat shock was tested using a range of temperature between 0 to 80 °C in broth KB medium. Statistical significance was

determined using a one-way ANOVA analysis. Each value was compared to the control (optimal growth temperature of 21 ± 1 °C). The results of the growth of bacteria exposed to heat shock for 5 min were strongly associated with all strains except a small difference in the tolerance of the growth of strains No. S1 (*P. syringae* pv *aesculi* 2171) and S6 (*P. syringae* pv *aesculi* 2250) which showed better growth. The same two bacterial strains above (S1 and S6) showed better tolerance and resistance and were able to survive at high temperatures which reached 40 to 60 °C for 5 min, where the growth rate ranged from 10 to 30%. In contrast, the bacteria S2 (*P. syringae* pv *tomato* 2202), S3 (*P. syringae* pv *phaseolicola* 2200) and S8 (*P. syringae* pv *aesculi* 2249) were very sensitive to temperatures raised above the optimum temperature of growth (20 °C). The growth of most bacteria was stopped at temperatures 70 °C and above (Figure 2-18).

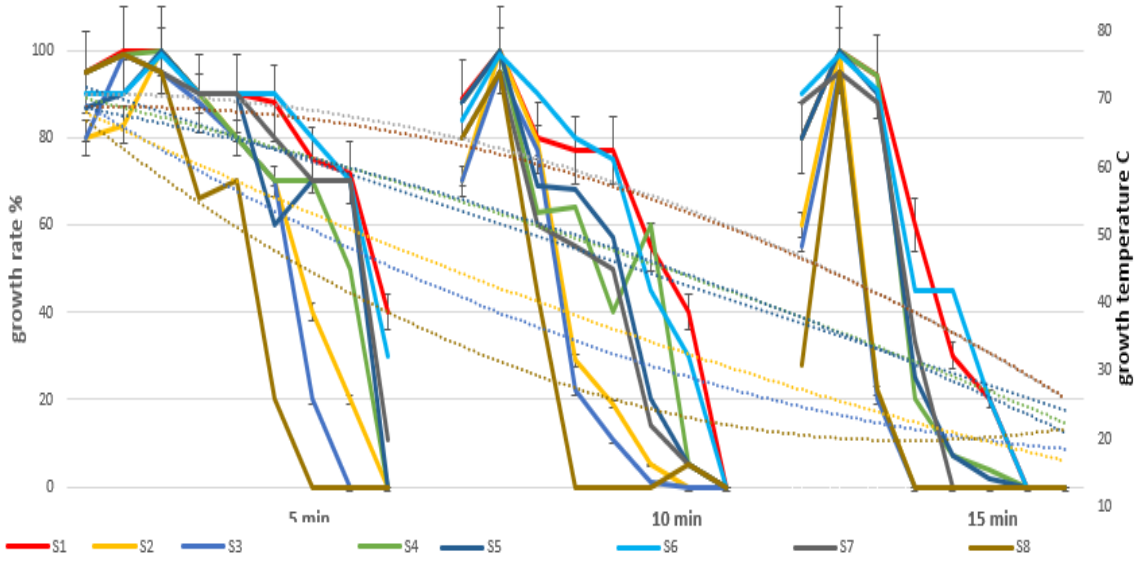

Figure 2-18 The effect of different temperature on bacterial growth. The line chart shows growth percentage of surviving *P. syringae* after challenging with different temperature growth for 5, 10 and 15min after which the bacteria were grown in KB broth media until reaching exponential growth phase. Bacteria were measured at OD600 colony forming units were determined. S1 to S8 represent isolates bacteria No. as mentioned in Table 2-1. Statistical significance was determined using a one-way ANOVA analysis.

When plants were re-infected with surviving bacteria (pathogenicity test), after being exposed to 60 ºC and above for 5 minutes, the bacteria did not produce any disease symptoms. Moreover, plants re-inoculated with the surviving bacteria, exposed to 50 ºC for 10 and 15 minutes, also did not show any disease symptoms.

To study the effects of different pH levels on *P. syringae* growth, bacteria were exposed to a range of pH between 3 to 11 on broth and agar medium. In all trials, the percentage of surviving *P. syringae* bacteria was calculated relative to the number of bacteria with pH 7 (optimal bacteria growth pH). The results of exposing bacteria to different levels of pH did not show any significant difference except the high sensitivity and growth was reduced in

strains S1, S2, and S8, when the pH was raised or dropped slightly away from the optimal pH 7 (Figure 2-19). When the pathogenicity test was used, all treatments showed symptoms of infection except S8 (*P. syringae* pv *aesculi* 2249).

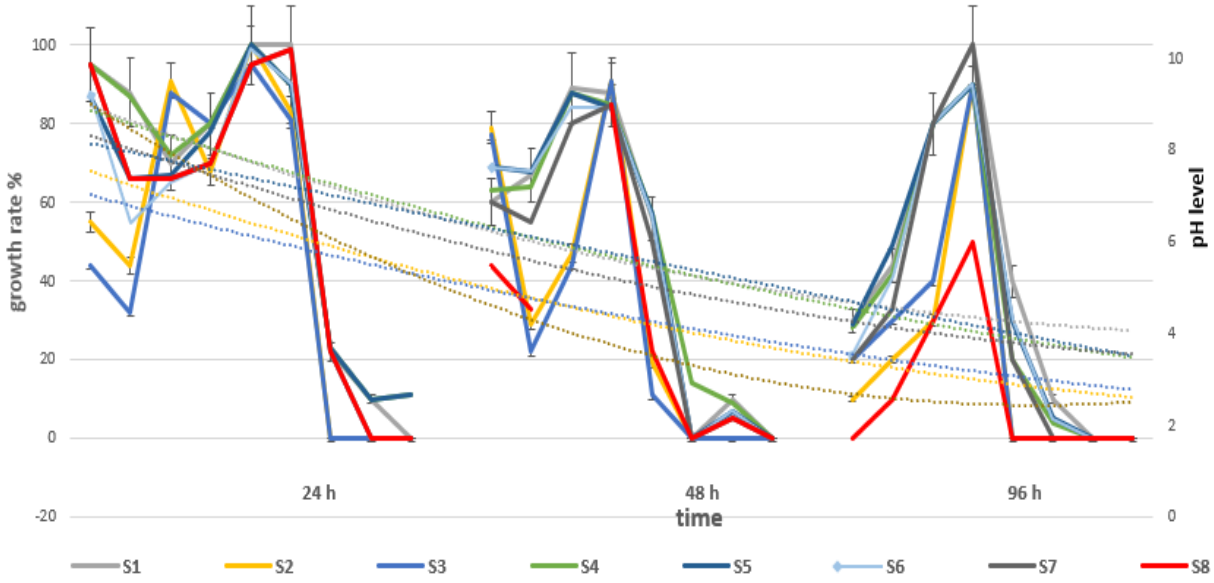

Figure 2-19 The effect of pH on bacterial growth. The line chart shows growth percentage of surviving *P. syringae* after challenge with different pH level for growth with 24, 48 and 96 hours. Bacteria were grown in KB broth media until reaching exponential growth phase. Bacteria were measured at OD600 colony forming units were determined. S1 to S8 represent isolates bacteria No. as mentioned in Table 2-1. Statistical significance was determined using a one-way ANOVA analysis.

2.4.9.1 Pathogenicity test

Pathogenicity tests were carried out by re-injecting intact seedlings of *A. hippocastanum* and the model plants with isolated bacteria to make sure that the plant has a susceptibility to bacteria. In general, and according to the statistical analysis of results, the culture population of the viable bacterial cells was affected by both pH levels and growth temperature. Main effects of pH level were seen on solid medium concentration, and changes in pH

significantly decreased the bacterial population. However, the interaction effect between the growth and the pH levels was not significant.

The results of the pathogenicity tests showed that *A. hippocastanum* has a susceptibility to bacteria by swapping different strains of bacteria to make sure of the occurrence of infection or not. The results of the pathogenicity tests also showed that the bacteria have the ability to infect only the plant to which it is specific to and cause symptoms of the bacterial disease. Moreover, high concentrations of bacteria were used with the model plants (more than 10^7 cell/m) which would be expected to overcome any slight host resistance. The identification of suspect isolates was confirmed by inoculation into intact seedling. All inoculated *P. syringae* isolates caused lesion and necrosis between 2 to 4 weeks from the inoculation.

2.4.9.2 16S rRNA sequence analysis

The results of the partial sequence analysis of the 16S rRNA gene of most isolates indicate that the identity of bacteria matched more than 85% of the sequences of *P. syringae* stored in the NCBI GenBank database (version: BLASTN 2.10.0+).

2.5 Discussion

2.5.1 Seed moisture content

Seed moisture content is usually described as the weight of water, represented as a percentage of the fresh weight (Gosling, 2007), assuming that any reduction in weight reflects moisture loss. This moisture content is a useful

parameter to show the viability of seeds and their ability to germinate. Usually, most tree seeds can be stored for a longer time at lower moisture contents (6–8% moisture content for most spruces and pines, 10–15% moisture content for most firs, cedars, cypresses and broadleaves) but some trees have recalcitrant seeds, such as *A. hippocastanum*, sweet chestnut, oak, and sycamore, where seeds start to die below 40% moisture content (Gosling, 2007). Seed moisture study is essential especially with the seeds of perennial plants which have recalcitrant seeds, which need a long time to grow and where non-germination would result in the loss of an experiment or study for the entire season. The percentage of water in the seeds also indicates the ratio of the elements present in the soil due to osmotic pressure, as found in previous studies where there is an essential relationship between nutrients in plants, soil elements and moisture content of seeds (Garrett *et al.,* 2006; Hirt & Shinozaki, 2004; Rejeb *et al.,* 2014; Thalmann, Freise, Heitland, & Bacher, 2003; Tolaymat, Genaidy, Abdelraheem, Dionysiou, & Andersen, 2017). The moisture content of seeds had no effect on germination in this study, as evidenced by the growth of all or most of the seeds. Moisture content was, however, lower compared to other studies on *A. hippocastanum* trees (Salleo *et al.,* 2003; Thalmann *et al.,* 2003). Another study showed the close relationship between low concentrations of nanoparticles and the moisture content of peanut seeds (Li *et al.,* 2015). However, the finding in this study (see 2.4.1) is consistent with the other studies with different plant species (Cervantes & Emilio, 2006; Hernandez-Viezcas *et al.,* 2016; Kingdom, 1978; Li *et al.,* 2015).

2.5.2 Plant vitality assessments

Bacterial infection symptoms in the studied plants were not as severe as with trees growing in the wild. Here the percentage of dead plants did not exceed 5%, after artificial bacterial inoculation, which is considered very low when compared with infected plants that grow in nature, maybe because the disease needs a more extended period to develop and become more pathogenic (Green *et al.*, 2009; Percival & Banks, 2015) or because of the absence of other diseases and pests such as the leaf miner from the greenhouse. Any plant showing symptoms of other pests or diseases were removed from the greenhouse to prevent infection transmission to intact plants. This was done in previous studies such as Percival and Banks (2014). The result of leaf inoculation showed that no severe bacterial infections were on the midrib or veins and the infection recovered (faded and vanished) from the lamina a few days after appearing, maybe because the leaves contain some aromatic substances that prevent the growth of bacteria and lack abundant lignin which is considered stimulating to bacteria growth (Avtzis *et al.*, 2007; Dudek-Makuch & Studzińska-Sroka, 2015; Green, 2012). Another explanation may be due to the genetic pathways which the bacteria have for the degradation of plant-derived aromatic compounds such as lignin derivatives, aromatic glucoside and other phenolic compounds. It is possible that these pathways enable *P. syringae* to use aromatic substrates as carbon sources particularly those derived from the woody plant's tissues (Green *et al.*, 2012; Kim *et al.*, 2015; Baibado & Cheung, 2010).

The results of bacterial infection shows that artificial inoculation caused a dark strip that spread with the bark under the stem epidermis towards the bottom of the plant. The results also showed there were no symptoms in the xylem. Possibly, this is a sign of the downward transmission of bacteria through the sieve element or parenchyma cells of the phloem, which is the direction of the flow of sugars that are produced in the leaves. The presence of bacteria was confirmed by re-isolation and its development on selective medium and then compared with the original bacterial strain. The findings in this study are consistent with the results of past studies by Steele *et al.* (2010) who found that lesions developed in the cortex and phloem and extended into the cambium to cause cankers, but there was no evidence of necrosis in the xylem tissues.

The study on *A. hippocastanum* (main plant) was performed in parallel to the study of the model plants since *A. hippocastanum* is a perennial tree and takes time to grow. Therefore, *L. esculentum* and *P. Vulgaris* were chosen as model plants because seeds germination and seedling growth are faster than in *A. hippocastanum*. They also have economic value for the food and agriculture industry. They have the ability to mature and form flowers and fruits in several weeks, whereas *A. hippocastanum* needs several years to produce flowers and fruits. The susceptibility of these model plants to *P. syringae* was reported elsewhere. Furthermore, the results of the model plants could be related or compared to the main plant to discover and avoid any experimental mistakes, as there are not many previous studies about the main plant.

2.5.3 Protein content assessment

A. hippocastanum is considered to be a recalcitrant plant because the plant contains many phenolic compounds (Otajagić *et al.*, 2012). Therefore, the protein extraction method is more laborious than with other regular plants. There is also a need to find an economical, reproducible and straightforward protein extraction procedure for proteomics studies because there are many samples that need to be tested. In terms of the quantitative analysis of each method, the detergent protocol gave the higher protein yields, then TCA protocol and finally the Phenol protocol. This is possibly due to the fact that the detergent protocol did not remove all interfering substances which probably affected the result.

SDS-PAGE electrophoresis is a useful and straightforward technique that separates proteins according to their various molecular weights for analytical studies and distinguishes them in comparison to molecular weight markers (Chernyshenko, *et al*., 2016; Rabilloud *et al*., 2009). The result obtained in the current study show that the TCA/Acetone protocol was better than the detergent protocol, especially with 7M urea and showed higher protein resolution bands on the gel when compared with the other two methods, maybe because of the urea enhanced solubility of precipitated proteins besides the other components (Zhang *et al*., 2011).

In the comparison of phenol and TCA/acetone extraction protocols, both methods were effective in extracting proteins from leaf tissues, but the TCA/Acetone protocol with sonication was more efficient because the bands were more apparent, removing interfering substances that cause smearing,

deformation and interference in the bands, and resulted in the highest quality gels with less background smearing. In spite of the fact that the pellets obtained from phenol protocol were more easier to handle than TCA/acetone, the main difficulty in TCA/ Acetone protocol was to keep samples during extraction at a low temperature, then maintain protein samples between 20 to 25 °C to avoid urea precipitation (Méchin *et al*., 2007). Possibly washing the acetone and phenol in the TCA/acetone and phenol protocol allowed clearing of the sample from interfering substances which were dissolved in the acetone, as acetone allows solubilisation of the pigments, lipids, and terpenoids possibly present in the tissue (Jorrín-Novo *et al.,* 2015). Generally, the TCA/acetone protocol was superior to the phenol protocol and detergent protocol because of the features of the precipitants mentioned above, and it produced a good result and needed less time to complete. All these make the TCA/acetone protocol fit for purpose and was chosen for the extraction of proteins in this study. The critical challenge during protein extraction was to avoid leaf tissue freeze-thaw treatment and working at low-temperature maximum 4 °C, as this causes protein damage and reduces the concentration of total protein.

The results of LC-MS showed there was a huge abundance of protein especially ribulose bisphosphate carboxylase (Rubisco). Rubisco is an enzyme present in plant chloroplasts and in abundance due to it being involved in photosynthesis (Bar-On & Milo, 2019). In the analysed results, the large chain of peptide matched with a sequence large chain (fragment) belonging to *Aesculus carnea*; this species is a hybrid of *A. hippocastanum* and *A. pavia* (Straw & Tilbury, 2006).

The total protein content is a critical physiological parameter in plant development and the immune system. The study of the quality of leaf protein using MS spectrometry or any other highly sensitive techniques is essential, as the leaf is the fastest and most affected plant organ. Recent studies (Kammers *et al.,* 2015; Takos *et al.,* 2008; M. L. Wang *et al.,* 2018) have shown that there are significant changes in the quantity and quality of protein when leaves were exposed to external infection. This is important considering that *A. hippocastanum* is exposed to many leaf infections such as leaf miner, leaf spot and leaf powdery mildew (Hau, 1990; Mark, 2011; Walas *et al.,* 2018; Vilhena *et al.,* 2015). Many proteins of invader organisms may interfere with the proteins of the leaf when isolated. Therefore, the process of studying proteins in leaves without controlling for diseases is questionable only in case of tissue culture study as all other infection is avoidable or under control (Germana & Lambardi, 2016; Tarkowski & Vereecke, 2014; Zhang *et al.,* 2010). Therefore, the emphasis in this study was on the quantity of protein rather than the quality after the success of the process of isolating proteins from the gel and the appearance of a high abundance of proteins, including Rubisco. The difference in the total amount of protein in the model plants compared with previous studies may be due to the fact that plant samples were grown in separate geographic areas with various eco- and agro-environmental conditions.

Furthermore, the method and technique of isolation and purification protein are considered to have a significant effect on the variation in concentration and quality of the isolated protein, so several methods have been tested in this study to select the most appropriate one. This is consistent with other studies to extract protein with different plants (Cilia *et al.,* 2009; Faurobert, Pelpoir, &

Chaïb, 2007; Gómez-Vidal, Tena, Lopez-Llorca, & Salinas, 2008; Méchin, Damerval, & Zivy, 2007; Vilhena *et al.,* 2015). Another reason may be due to the genetic variation in the species estimated (Green *et al.,* 2010). However, in this study, an efficient protein extraction method for proteomic analysis of *A. hippocastanum* was determined and adopted to extract total protein for all samples.

2.5.4 Drought stress responses and triggered

In the drought stress study, biomass, protein content, height of shoots and length of roots were used as useful representative parameters to understand plants response to drought stress. The result showed that the development of infections decreased these parameters in *A. hippocastanum* in conjunction with mild and simple drought stress. At the same time, severe drought stress treatment had a negative effect on plant growth and protein content.

The decreased, or in some cases the lack of, infection in the plant when exposed to drought stress may be due to the plant using mechanisms to maintain or reduce water consumption, including closing the stomata. Therefore, the results show a different response by the plant in different plant species. Bacteria are also known to be present in conductive tissues, which are the first tissues to be affected by drought stress because the conductive tissues contain a small number of parenchymal cells versus fibres and vessels (Aroca, 2013). The studies also showed that *P. syringae* pathovars have acquired genes that may enable them to infect and live within the woody parts of the tree (Green *et al.,* 2010; Green, 2012; Schmidt *et al.,* 2008), and this supports our results which showed a reduction in bacterial infection with drought stress.

Structural and physiological changes to the plant caused by drought may affect parasitic or invader organisms directly by a change in nutrition quality and capability to feed, or indirectly by a variation in signals and host selection. Decreased growth by cell enlargement is the first factor to be affected by moderate water stress (Hsiao *et al.*, 1976). Accordingly, decreased tissue is possible for plants under drought stress: leaves are thicker, waxier, and smaller, possibly making it more difficult for the invader organism to infiltrate and feed on the host plant (Pritchard *et al.*, 2007).

The increase in protein concentration in some treatments, especially 75% of FC, may be due to the accumulation of proline (proteinogenic amino acid) as this protects some protein configurations during dehydration (Fernandez *et al.*, 2006; Percival and Noviss, 2008; Hasheminasab *et al.*, 2012). Proline, glutamic acid and aspartic acid are amino acids stored by plant cells during drought stress. However, under severe drought stress, proteins in cells undergo damage, such as the disruption of their standard structure which produces difficulties in sustaining their activity. In order to survive, cells need to activate processes of protein repair and avoid non-native protein collection (Hamilton & Heckathorn, 2001; Wang *et al.*, 2004). The findings of the current study (severe treatment) are consistent with previous studies that have reported that *P.vulgaris* exposed to drought stress shows more symptoms when infected by *Macrophomina phaseolina* (a fungus that causes damping off), and treatment of detached tomato leaves with exogenously applied ABA increases the susceptibility of wild type plants to the necrotrophic disease *Botrytis cinereal* (Audenaert *et al.*, 2002; Suleman *et al.*, 2001; Ton *et al.*, 2009). The connection between increased proline concentration and drought stress has

been shown in numerous studies (Hasheminasab *et al.*, 2012; De Ronde *et al.*, 2000, Ain-Lhout *et al.*, 2001, Ehmedov *et al.*, 2002, Yamada *et al.*, 2005). Some studies have shown similar results and can explain some of the results obtained during this study. For example, the results reported by Mutava *et al.* (2015) revealed that under drought stress, reduced stomatal conductance of soybean is responsible for the decreased photosynthetic rate in the plant. Drought stress decreases the amount of carbon dioxide (CO_2) from the environment due to the closing of stomata. so that photorespiration is raised, which ensures partial substrate replenishment and maintains the carboxylate role of Rubisco (the primary protein found in horse chestnut leaf tissue by mass spectrometry in this study). Consequently, the utilisation of excess reducing equivalents in chloroplasts causes an increase in oxygen-free radical production leading to oxidative damage in chloroplasts. Most plant biological processes depend on photosynthesis (Manzoni *et al.*, 2011; Lisar *et al.*, 2012). The resistance of *A. hippocastanum* seedlings to drought stress may be due to the tolerance shown by xylem compared with tomato and bean plants, since conductive tissue forms a higher proportion of horse chestnut stems compared to beans and tomatoes (Wang *et al.*, 2012).

The results of drought stress showed that there is an effect on the roots of both *A. hippocastanum* and the model plants (an increase in the length of roots with a decrease in biomass were reported). This can be explained by the plants dynamically adapting and modifying as a result of the drought stress. Many studies have shown that in dry areas, plant seedlings have vertical roots which are several times the length of the above-ground height. With this extensive root system and rooting depth, plants can sustain a higher water potential and a

longer duration of transpiration under drought conditions, which provides further support for their growth and development, and root distribution as volume and depth is essentially controlled by the range and depth of soil moisture (Larcher, 2003; Dixon *et al*., 1980). This variation was reported for root nodes between controls and beans with severe drought treatment. This is perhaps due to the death of root hairs due to severe drought stress which in turn reduced the chances of node formation, where the root hairs are responsible for the formation of the root nodes in the leguminous plants (Teixeira *et al*., 2014).

2.5.5 Damage stress responses and triggered

Plants in nature are often subjected to mechanical wounds caused by different factors such as chewing insects, birds or larger herbivores, or abiotic factors. To attempt to simulate such interactions in the laboratory is difficult. A usual way to induce wounding responses in plants is by causing damage or crush injuries in the leaf tissue. This technique is suitable and applicable for many plants but not all types such as succulent plants which lose a large amount of plant sap following wounding. Some of the disadvantages of this method are that the tissue is not uniformly damaged, and a mix of crushed and intact cells are created; the difficulty of determining the weight of tissue that is damaged; and the problem of wounding or damaging large amounts of plant tissue. Due to this, the results showed a different response between the plants used. The results also showed some convergence between *A. hippocastanum* and tomato plants, which differed somewhat from the beans, especially in the experiments of drought and damage. These differences may be due to the plant type, and the nature of the leaf tissues that play a significant role in the healing of a wound

or damage. Certainly, the palisade parenchyma layer in beans is wider than in tomato plants that have a thin layer of palisade cells (Lulai, 2007; Reymond, 2000).

The results revealed that there was not any infection by the bacteria through the lenticels when using a spraying method on the stems or leaf of *A. hippocastanum*. This is inconsistent with a study conducted by Green *et al.* (2010; 2012) where most of the infections were through the lenticels. This may be due to the young seedlings used having small lenticels compared to the mature plants studied by Green *et al* (2010; 2012). No consistent association was obtained between the presence of mechanical damage and bleeding cankers of *A. hippocastanum*, perhaps because the damage was carried out on the leaves which contain aromatic compounds that may be inhibiting the growth of bacteria and prevent its spread throughout other tissues or cells (Green *et al.,* 2010; Mullett & Webber, 2013; Takos *et al.,* 2008; Thomas *et al.,* 2019). The relationship between the host plant and bacteria has costs to the plant. The bacterial partner obtains carbohydrate and nutrients from the plant, and in return cause damage and make the plant a suitable medium for the development of many fungi and bacteria, which may infect other plants, and perhaps even humans and animals. The damage caused by bacteria usually affects and changes plant tissues and moisture content (Cervilla *et al.,* 2007). However, there is no clear correlation between damage and bacterial infection in the results obtained here, possibly because of the different conditions and age of seedlings used, so additional studies in the future are required with different stages of the seedling will be useful.

2.5.6 Pathogenicity tests and bacteria survival

The re-inoculation test was conducted to confirm the pathogenicity of the *P. syringae* isolates from artificial infected plants. The experiments were carried out by re-injecting the intact plant with isolated bacteria to make sure that the plant has a susceptibility to the bacteria. The model plants were used as well by swapping different strain of bacteria where it was confirmed that bacteria only infect the plant to which it belongs. These results are consistent with those of other studies with different plants (Barrett *et al.,* 2009; Djordjevic & Weinman, 1991; Marcelletti *et al.,* 2011; Van Den *et al.,* 1996). Although high concentrations of bacteria were used with other model plants, to the best of our knowledge, no study reports on swapping different strain of bacteria by artificial inoculation between *A. hippocastanum* and model plants.

For understanding more about how *P. syringae* is dispersed, it would be useful to know whether the bacterium can survive with different level of pH and temperature outside the host. This is especially so because a previous study showed that bacteria have the ability to survive outside the plant for a long period of time in the soil water and in extreme cold (Laue *et al*; 2014). The temperature survival experiments revealed that *P. syringae* pv. *aesculi* is able to grow over a wide range. The most interesting finding is that the bacteria lacked pathogenicity after exposure to high temperatures for a short time, 10 and 15 min. The cause may be the accumulation and deformation of proteins responsible for the disease in bacteria, or maybe due to the loss of the plasmids that are responsible for infection as a result of high temperatures, or its expression sizes were too low to cause disease (Kleitman et al. 2008; Braun *et*

al., 2009). The results of the interaction effect between the growth and the pH levels were not significant. Maybe because pH affected the composition of the medium and led to deposition in some components of the KBA medium at pH 10 and 11. This may have an effect on bacterial growth because of the lack of essential nutrient for bacteria.

Due to next-generation sequencing taking a long time and its cost, the isolated bacterial strains were identified and systematically classified based on their morphological, cultural, physiological and biochemical characteristics, combining the results of 16S rRNA sequence analysis. KB Agar medium was used for growth bacteria and fluorescein detection. The results of the viability of bacteria on the solid KBA medium are very close to the results of growing bacteria in a liquid KB medium using Alamar blue as an indicator. This is because the active bacterial cells have a reducing system able to convert resazurin dye (a safe compound, that can enter bacterial cells easily) from blue colour to a red coloured fluorescent material and its release fluorescent energy can be quantified using a spectrofluorometric device. This method is a highly sensitive indicator, accurately reflecting the activity of the bacterial cells which can quantify down to 50 cells (Léguillier, *et al.*, 2015; Westhrin, *et al.*, 2015; Sarker, *et al.*, 2007).

2.6 Conclusion

Abiotic stress response, in particular, water stress, produces different changes in plants. Certainly, drought stress causes physiological, morphological, molecular and biochemical changes. The physiological effects include stomatal closure, reduced photosynthesis and a decrease in stomatal conductance. Morphological effects include a decrease in leaf area to minimise transpiration loss, reduction in the number of leaves and in growth, and development of the root system to improve water uptake. At the molecular level, the response to water shortage connects with various proteins, in particular, the regulatory and functional proteins. Many drought-related genes such as expansin-like A2 gene, nuclear transcription factor Y subunit B-3 and Late embryogenesis abundant protein 4 (Basu, *et al.*, 2016; Lee *et al.*, 2004; Liu, *et al.*, 2016; Ma *et al*., 2015) are upregulated or downregulated to be expressed in different plants producing an improvement in drought tolerance. The biochemical effects such as the production of reactive oxygen species (ROS), reduction in Rubisco efficiency, etc. (Fang & Xiong, 2015; Feki & Brini, 2016; Gómez-Aparicio, Zamora, Castro, & Hódar, 2008; Khan *et al.*, 2017). The influence of drought stress is likely to be complicated by the fact that it is associated with other factors, such as atmospheric humidity and sunshine levels, increases in temperature and wind. Therefore, these factors can cause damage, change in the pH and temperature of the plant which in turn affect the bacteria as well. The most noticeable overall trend is that the bacteria are not able to make a significant infection in the leaves or xylem of *A. hippocastanum* seedlings. One of the most noticeable results is the loss of bacterial pathogenicity after exposure to high temperatures and for only a short time. However, further

studies *in vivo* are required to find if there is any temperature that plants can survive in order to use this as an effective method to heal infected plants or at least reduce bacterial activity.

3 Chapter 3: Whole transcriptome profiling and bleeding canker study of *A. hippocastanum* by RNA-seq

3.1 Introduction

Aesculus hippocastanum (horse chestnut) is a perennial, deciduous, rapidly growing tree belonging to the Aesculus genus of the Sapindaceae family (Dagmar & Szekely, 2010; *et al.*, 2001). Bleeding canker of *A. hippocastanum* is the most serious pathogen that affects *A. hippocastanum* and other *Aesculus* species (Green *et al.*, 2009). The initial symptoms appear on the main stem and branches of infected trees. Symptoms are normally expressed by the appearance of a black gluey secretion. Advanced phases of the disease usually cause tree damage if the lesions surround the whole trunk. With a warm climate, the symptoms become more severe and visible. (Green *et al.*, 2009; Schmidt *et al.*, 2008; Steele *et al.*, 2010). The symptoms are somewhat similar to those caused by *Phytophthora* spp., but this is uncommon in *A. hippocastanum* (Webber *et al*., 2008).

The disease is caused by *Pseudomonas syringae* pv. *aesculi* (Pánková *et al*., 2015). *Pseudomonas syringae* is a gram-negative, rod-shaped bacterium that contains polar flagella (Horst, 2013a; Palleroni, 1984). As a plant pathogen, *P. syringae* causes disease in hundreds of herbaceous and woody plants including dicots and monocots species all over the world. The infection was also reported on annual plants. *Pseudomonas syringae* pv. *aesculi* has, according to 16S rRNA analysis, been placed under the *P. syringae* group. (Anzai *et al*., 2000) It is named after the *Aesculus* tree, from which it was first isolated (Palleroni, 1984; Webber *et al*., 2008). It was first seen in Britain in 2001/2 and, since

isolates have been seen to be genetically identical, it has probably derived from a single introduction into Britain (Green *et al.,* 2010).

The effect of the bacterial and viral diseases usually reflects on the expression of one or group of genes and then on particular proteins. In general, modifications in the protein profile of organism tissues include two main levels, i.e., transcription and translation. Through transcription, the information data carried on DNA is copied on to messenger RNA (mRNA), which is then matured by removal of the introns (non-coding region) through splicing. Transcription and maturation happen in the nucleus and mRNA is then translocated into the cytoplasm for translation (Liu *et al.,* 2016; Bruce *et al*., 2008). Mature mRNAs transfer sequences are organised in groups of three bases, referred to as codons. There are 64 possible codons (derived from four nucleotide bases A, U, G, C), of which 61 of them designate amino acids. Another three codons UGA, UAA and UAG, designate termination of protein synthesis, whereas AUG encodes methionine amino acid, which also indicates the beginning of protein synthesis. During translation, mature mRNAs are decoded (translated) into proteins, which are molecules that are directly involved in various cellular functions. The procedure of DNA transcription and mRNA translation is referred to as protein expression, and through this expression, responsiveness to external and internal effects such as bacteria, virus and mutations can be detected. On the other hand, controlling the performance of mRNAs translation (transcripts) into proteins is referred to as translation regulation. Next-generation sequencing (NGS) technologies such as the Ion Torrent and Illumina RNA-Seq technology in recent years have provided new opportunities to the field of RNA sequencing (RNA-Seq) (Liu *et*

al., 2016; Bruce *et al.,* 2008). It has revolutionised transcriptomics especially to acquire massive numbers of sequences in a short time and at a modest cost (Mutz *et al.,* 2013; Xiao *et al.,* 2013). More recently, Illumina's digital gene expression (DGE) platform can generate 90 to 100 million reads per run of an eight-lane flow cell using the Genome Analyzer 2x system (www.illumina.com). RNA-Seq is not partial to detecting transcripts that correspond to the existing genomic sequence, which makes RNA-Seq particularly attractive for non-model organisms without genomic sequences (Wang *et al.*, 2012; Zhang *et al.*, 2012).

Current bioinformatic facilities enable such utilities of NGS to aid large-scale transcriptome data even in a lack of a transcriptome sequence or reference genome. These technical capabilities have tremendously increased the applications and revolutionised the progress in the usage of these approaches and analyses. It has stimulated its scope for high-throughput genomic and transcriptomic studies beyond model plants like *Arabidopsis thaliana*, *Triticum aestivum*, *Oryza sativa* etc. (Vidhyasekaran, 2014; Weber *et al.*, 2007). Many bioinformatics engines were developed for quality evaluation of the reads; one of the most common is FastQC (http://www.bioinformatics.babraham.ac.uk/projects/fastqc/) which evaluates sequence quality within the entire read dataset and reports on the read quality, GC distribution, sequencing primers, adaptors, and over-represented sequences. In the present study, we used RNA-Seq technology on the Illumina HiSeqTM platform to investigate the effect of *P. syringae* pv. *Aesculi* on *A. hippocastanum.* We conducted comparative genomics analysis between Infected (sample pieces from the dead /live junction around diseased areas),

Non-infected (sample pieces from healthy tissue of infected trees) and uninfected (healthy pieces tissues from an uninfected tree).

3.2 Aims and objective

The bleeding canker response of horse chestnut is less well understood than that of other plant species. Further, there is a lack of understanding of how plants recover from disease stress and the genetic response during disease progression.

The aims of the current chapter are to characterise the gene expression of horse chestnut to effects caused by *Pseudomonas syringae*. The objective was to study differences in gene expression between tree samples to test whether we could identify large-scale differences in genes that may be identified in the transcriptional response to the disease genetic architecture. This project also aimed to create an RNA library by constructing and sequencing of the non-model *A. hippocastanum* total RNA, as the transcriptome of *A. hippocastanum* is not currently well annotated.

The main objectives of this chapter can be summarised in the following points:

1. to find genes and gene functions which respond to bleeding canker and try to compare levels of genes expression to determine plant response to infection.

2. To develop knowledge about proteins and genes involved in defence against bleeding canker of *A. hippocastanum*. So far little is known concerning the severe disease.

3-To find gene(s) associated or involved with bleeding canker disease or *P. syringae* bacteria and possible roles of some of the proteins identified.

3.3 Materials and Methods

3.3.1 Sampling and storage of phloem tissues

Live *A. hippocastanum* phloem samples were obtained from different trees in Scotland, UK, during November 2017. Samples were collected with help from Dr Sarah Green (Forestry Commission. Edinburgh). The history of tree infection was also known. Samples were selected at random from *A. hippocastanum* trees which were well-known and monitored by Green group (Forestry Commission. Edinburgh). Phloem tissues were sampled from non-infected and from infected phloem of the same tree but different regions and sampled from uninfected trees (Table 3-1). Two samples about 2 cm in diameter were cut from each area. The outer bark was removed immediately using a sterilized scalpel blade. Then, the first group of samples was stored in RNase-free sterile tubes in a polystyrene box container with dry ice. The second group of samples was stored separately in an RNA stabilization solution (RNAlater®, Thermos fisher, AM7022). The location and altitude of each target tree were taken by a GPS Garmin Navigation System in 2017 (GPSMAP,62, Garmin.Ltd.). The diameter and aspect were also recorded. The tree's height was estimated using a TruPulse 200 laser range sensor (LTI TruPulse 200 / 200B, Laser Technology, Inc) (Table 3-1).

Table 3-1 The *A. hippocastanum* samples information. The table shows the number of sample and tree. Height, stem circumference(cm) and location of each tree are also given.

Sample alias	Barcode used of sample	Samples reference	Sample description	No. of tree	No, of the sample in biological pathways	coordinates	Tree height (m)	stem circumference (cm)	Sea level (m)
PRO1708_S1_totRNA	SAM37128:PRO1708_S1_totRNA	AHS 01	Non-infected	7	467	55.477639, -4.551917	6	134	20.22
PRO1708_S3_totRNA	SAM37130:PRO1708_S3_totRNA	AHS 05s	Non-infected	10	468	55.639972, -4.656750	16	211	32.00
PRO1708_S4_totRNA	SAM37131:PRO1708_S4_totRNA	AHS 05	Uninfected	14 k	469	55.639778, -4.663361	9	144	30.65
PRO1708_S5_totRNA	SAM37132:PRO1708_S5_totRNA	AHS 07	Uninfected	12	470	55.639944, -4.656722	8	128	32.35
PRO1708_S6_totRNA	SAM37133:PRO1708_S6_totRNA	AHS 09	Non-infected	2	471	55.639972, -4.656861	12	185	32.35
PRO1708_S7_totRNA	SAM37134:PRO1708_S7_totRNA	AHS 10	Infected	8	472	55.473222, -4.555000	11	164	16.60
PRO1708_S8_totRNA	SAM37135:PRO1708_S8_totRNA	AHS 11	Non-infected	8	487	55.473222, -4.555000	11	164	16.60
PRO1708_S9_totRNA	SAM37136:PRO1708_S9_totRNA	AHS 12	Infected	5	473	55.477361, -4.551917	13	181	19.40
PRO1708_S10_totRNA	SAM37137:PRO1708_S10_totRNA	AHS 13	Uninfected	4	474	55.640083, -4.663639	11	141	29.81
PRO1708_S11_totRNA	SAM37138:PRO1708_S11_totRNA	AHS 15	Non-infected	5	475	55.477361, -4.551917	13	181	19.40
PRO1708_S12_totRNA	SAM37139:PRO1708_S12_totRNA	AHS 16	Infected	7	476	55.477639, -4.551917	6	134	20.22
PRO1708_S13_totRNA	SAM37140:PRO1708_S13_totRNA	AHS 18	Infected	3	477	55.475889, -4.552694	13	146	19.11
PRO1708_S14_totRNA	SAM37141:PRO1708_S14_totRNA	AHS 19	Uninfected	11	478	55.639194, -4.662583	11	162	30.28

PRO1708_S15_totRNA	SAM37142:PRO1708_S15_totRNA	AHS 22	Infected	13k	479	55.639820, -4.663122	7	195	18.13
PRO1708_S16_totRNA	SAM37143:PRO1708_S16_totRNA	AHS 25	Non-infected	6	480	55.63957282 -4.66246709	4.5	147	17.07
PRO1708_S17_totRNA	SAM37144:PRO1708_S17_totRNA	AHS 26	Infected	6	481	55.63957282 -4.66246709	4.5	147	17.07
PRO1708_S18_totRNA	SAM37145:PRO1708_S18_totRNA	AHS 31	Uninfected	1	482	55.639564, -4.664300	12	162	24.06
PRO1708_S19_totRNA	SAM37146:PRO1708_S19_totRNA	AHS 33	Non-infected	9	483	55.639809, -4.664498	7	123	21.93
PRO1708_S21_totRNA	SAM37148:PRO1708_S21_totRNA	AHS 47	Non-infected	15k	484	55.639977, -4.665250	6	131	22.58

3.3.2 RNA isolation

To extract RNA from plant tissue, a plant RNA kit was used (Norgen's Plant RNA/DNA Purification Kit, E4788) As with many commercially available kits, the contents of each contained buffer are not published. To lysate sample tissues preparation, ≤100 mg of plant tissue was placed into a mortar with liquid nitrogen and ground into a fine powder. The plant powder was transferred to a DNase-free 1.7 mL microcentrifuge tube, and then a volume of 600 µL of lysis buffer M was added. The lysate was then pipetted and transferred into an RNase-free microcentrifuge tube and incubated at 65 °C for 10 mins, then mixed occasionally by inverting the tube a few times. After that 100 µL of binding buffer (buffer I) was added, briefly mixed and then incubated for 5 minutes on ice. A filter column with the collection tube was assembled and the lysate was pipetted into the filter column and span for 2 mins at ~14,000 RPM. Next, the clear supernatant from the filtrate was placed into a DNAase-free microcentrifuge tube utilising a pipette. An equal volume

of 70% ethanol was added to the lysate that was collected above and vortexed for ten seconds to mix. For binding nucleic acids to the column, a spin column was assembled with a new collection tube, a volume 600 µL of the clarified lysate with ethanol was applied up onto the column and centrifuged for 1 min at ~6,000 RPM. Then 400 µL of wash solution (solution A) was applied to the column wash and centrifuged for one minute, then the flow-through was discarded and the spin column was reassembled with a new collection tube. Washing step with A 400 µL of wash solution (solution A) was repeated twice and centrifuged for 1 minute and then the spin column was reassembled with its collection tube and the filtrate was discarded. The column was briefly centrifuged for 2 minutes in order to dry the resin and then the collection tube was discarded. After this nucleic acid elution was carried out by placing the column into a fresh 1.7 mL and 50 µL of elution buffer. Following centrifuged for 2 minutes at ~2,000 RPM, followed via spinning for 1 minute at 14,000 RPM and then the RNA was stored at –80°C.

3.3.3 Genomic DNA extraction

Total DNA was isolated from *A. hippocastanum* phloem using a Genomic DNA kit (NucleoSpin®) according to the manufacturer's instructions. One gram of phloem sample was digested using cetyltrimethylammonium bromide (CTAB) isolation buffer in a pre-chilled mortar and pestle. The sample was mixed with a micro-pestle in 7 ml of a pre-chilled Dounce tissue grinder in the presence of 500 µl pre-warmed CTAB buffer at 65 ^{o}C and incubated for 30 min. with grinding at 15 min., then, vortexed for a few seconds. An equivalent volume of chloroform was added into the tube and vortexed for 10 seconds

before being centrifuged at 10,000 g for 12 minutes at room temperature. The tube was vortexed again and centrifuged. The above clear layer was transferred to a new tube and combined with 1 ml of 100% cold ethanol. The tube was incubated at -20ºC for 60 min. After the incubation, the tube was centrifuged, and the supernatant discarded. The precipitation was flooded with 1 ml of 75% (v/v) chilled ethanol and vortexed to mix. The tube was centrifuged, and remaining ethanol was taken out using a micropipette. The precipitation was dissolved in 50 µl deionized distilled water.

3.3.4 Reverse transcription of RNA into cDNA

Reverse transcription (RT) was carried out using a QuantiTect® Reverse Transcription kit from Qiagen. The template RNA, gDNA Wipeout Buffer, Quantiscript® Reverse Transcriptase, Quantiscript RT Buffer, RT Primer were thawed and mixed, RNase free water was thawed as well at room temperature (15–25°C). Each solution was mixed by flicking the tubes, then briefly was centrifuged and then kept on ice. The genomic DNA elimination reaction was preparing on ice according to Table 3-2.

Table 3-2 Genomic DNA elimination reaction components for reverse transcription RNA into cDNA

Component	**Volume/reaction**
gDNA Wipeout Buffer, 7x	2 µl
Template RNA, up to 1 µg*	Variable
RNase-free water	Variable
Total reaction volume	14 µl
* This amount corresponds to the entire amount of RNA present, including any rRNA, mRNA, viral RNA, and carrier RNA present, and regardless of the primers used or cDNA analysed.	

Then the tubes were incubated for 2 min at 42 °C and placed immediately on ice. The reverse-transcription master mix was prepared on ice according to Table 3-3 and mixed and kept on ice. The reverse-transcription master mix (New England Biolabs, cat. no. M0541) contains all components required for first-strand cDNA synthesis except template RNA.

Table 3-3 Reverse-transcription reaction components

Component	**Volume/reaction**
Reverse-transcription master mix Quantiscript Reverse Transcriptase*	1 µl
Quantiscript RT Buffer, 5x†‡	4 µl
RT Primer Mix‡	1 µl
Template RNA Entire genomic DNA elimination reaction	14 µl
Total reaction volume	20 µl
* Also contains RNase inhibitor. / † Includes Mg2+ and dNTPs. ‡ For convenience, premix RT Primer Mix and 5x Quantiscript RT Buffer in a 1:4 ratio if RT Primer Mix will be used routinely for reverse transcription. This premix is stable when stored at –20°C. Use five µl of the premix per 20 µl reaction.	

Then template RNA was added (14 µl) to each tube containing a reverse transcription mixed well and then stored on ice for 15 min at 42°C. They were then incubated for 3 min at 95 °C to inactivate Quantiscript reverse transcriptase. Finally, the reverse-transcription reactions were placed on ice or for long-term storage, reverse-transcription reactions were kept at –20°C.

3.3.5 DNA and RNA quantity and quality

The quantity and quality of all DNA and RNA extracts were determined using a Nanodrop Spectrophotometer (NanoDrop 1000 Spectrophotometer, Thermo Fisher) and the concentration of RNA was detected by Qubit 3.0 Fluorometer (Life Technologies, Carlsbad, CA, USA) using Qubit® dsDNA HS Assay Kits

(Life Technologies, Cat. no. Q32856). The integrity of the extracted RNA was detected by a Bioanalyzer (Agilent).

3.3.6 PCR for housekeeping genes gene (XDH)

Polymerase chain reaction (PCR) was performed on the obtained cDNA samples to ascertain their contents, purity and success of the extraction process. The reaction mixtures are listed in Table 3-4 and were prepared under aseptic conditions in a Cleaver Scientific Clearview UV Cabinet (Thermo Fisher) following a minimum of 30 minutes of UV exposure. All of the pipette tips, reaction tubes and nuclease-free water were also exposed to UV during the 45 minutes, before formation of the mixture, to guarantee there was no contamination of the samples. All the reaction ingredients were kept on ice during preparation to prevent primer dimers forming and random annealing. Before the PCR, the reaction compounds were collected at the bottom of the tubes using a bench-top microcentrifuge. The PCR was completed in an Applied Biosystems Veriti Thermal Cycler (Thermo Fisher) with a heated lid to accurately keep the temperature of the reaction mixture and prevent evaporation. The PCR step setting duration program to amplify DNA were as follows: 98 °C 2:00 mins, 98 °C 0:15 mins, 65 °C 0:30 mins, 72 °C 1:00 mins, 72 °C 5:00 mins. 35 x cycles. The samples were then cooled to 4°C to prevent any further annealing; then the PCR product amplification was analysed on agarose.

Table 3-4 Polymerase Chain Reaction components

Reaction contents	Volume/ µl	Final concentration
GoTaq® Green Master Mix (containing GoTaq® DNA Polymerase, Green GoTaq® reaction buffer, pH 8.5, 400µM of each free nucleotide and 3mM $MgCl_2$)	12.5	1x
forward primer	1- 2	0.1 -1.0 µm
reverse primer	1 - 2	0.1 -1.0 µm
DNA sample (nuclease free-water control)	2	< 250 ng
Nuclease-free water to 25	6.5	N/A
Final reaction volume	25	

3.3.7 Gel electrophoresis

The purity of RNA was determined by gel electrophoresis prior to reverse transcription. Standard agarose gel was prepared by using 2 tablets of agarose (Top Vision agarose tablets, Thermo Scientific) and 50 ml of TAE buffer (Tris base, acetic acid and EDTA with the final composition of 1 mM EDTA, 40 mM Tris-acetate) with pH 8.2 - 8.4 were mixed to obtain gel 2% (w/v). Then, the compounds were microwaved for 2 min on high power. After cooling, the gel was poured into a casting tray (12 combs) after adding 4µl of Ethidium bromide and left to set. Samples of RNAs were prepared by adding 2µl of loading buffer to 1µg of RNA (Final volume 7 µl). The gel was run at 85 V for 45 min using nanoPAC-300 (Cleaver Scientific LTD). DNA ladder 100bp was used (New England BioLabs.inc. N3231S). The gel bands were visualised and photographed in UV lightbox using (GeneSys image capture software).

3.3.8 RNA- Next Generation Sequencing (illumina sequencing to study gene expression)

For RNA-sequencing, samples at a concentration of above 7 µg of total RNA (50 ng/µl in 60 µl) were prepared according to the Earlham Institute (Norwich Research Park, Norwich, UK) and sent to Earlham Institute in the dry ice box. The received quality results were analysed using the Galaxy Web-based platform (Fast QC) version 0.11.6 (downloaded from http://www.bioinformatics.babraham.ac.uk/projects/fastqc/), for bioinformatics analysis database was formed prior to downstream analysis.

3.3.9 Library Preparation and Next Generation Sequencing

Sequence data were generated by the Earlham Institute and was concatenated to produce a large file of sequence data representing all samples. Messenger RNA (mRNA) sequencing libraries were prepared using the Nextera technology RNA kit, and sequenced (Illumina HiSeq 4000) with a paired-end 75nt read metric to obtain approximately 40,000,000 read pairs per sample. Raw sequencing data were trimmed of sequencing adaptors, and low-quality reads removed using the Trim galore package – a wrapper that incorporates cut adapt before downstream analysis.

3.3.10 De novo Transcriptome Assembly

Quality-filtered reads were assembled into candidate transcripts and genes by de novo transcriptome assembly using Trinity version 2.4.0. In order to capture the diversity within our sample population, all reads were initially concatenated

to create a single dataset for assembly. Assembly was performed locally on a Mac Pro 12-core system with 64Gb of RAM and 8TB storage (Apple). To permit efficient computation, 100,000,000 read pairs were randomly selected from the concatenated dataset as input.

3.3.11 Assessment of Transcriptome Quality

The quality of the assembled transcriptome was evaluated using a variety of approaches;

(a) RNA-Seq read representation: the percentage of reads from the entire study represented by the resulting transcriptome was determined by mapping the study reads back to the indexed transcriptome using Bowtie2.

(b) Representation of full-length protein-coding genes: the number of transcripts that represent nearly (>80%) full-length protein-coding genes was determined by mapping the transcriptome against the UniProt database using BLASTX.

(c) Calculation of the Contig Nx statistic: the percentage of transcripts with a length greater than x was determined using the TrinityStats.pl helper script supplied with Trinity version 2.4.0. Data for N10 through N50 were selected for appraisal.

3.3.12 Estimating Transcript Abundance

Following de novo transcriptome assembly, the abundance of each newly described feature was determined in our study samples. For each tree, we mapped RNA-seq reads back to our indexed transcriptome using bowtie2 and

estimated the abundance of each transcript using RSEM. Abundance estimation was performed at the transcript and "gene" level. A data matrix containing abundance estimates for all study samples was subsequently prepared using the abundance estimates to the matrix.pl helper script, packaged with Trinity version 2.4.0.

3.3.13Differential Expression Analysis

Differentially expressed transcripts were identified using the R package edgeR (Bioconductor), with significance defined as those transcripts expressed between treatment and control with Log2 Fold Change ≥ 2.0, and where P, following false discovery rate correction ≤ 0.001.

3.3.14Transcript Annotation

De novo assembled transcripts were annotated using Trinotate (https://github.com/Trinotate/Trinotate.github.io/wiki) through reference to the SwissProt protein database and in addition, through reference to the NCBI nucleotide database (https://www.ncbi.nlm.nih.gov/) using blast in a Linux environment.

3.3.15GO Assignment

Gene ontology terms were assigned to differentially expressed transcripts using GOSeq (R Statistical Language) (the bioinformatic work was done by collaboration with Dr D. Tonge at Keele university).

3.4 Results

3.4.1 DNA Extraction

DNA was extracted to detect the effectiveness of extraction method. The extraction procedure showed successful DNA extraction from both dry ice & RNAlater and the concentration was around 100 ng/µl for each sample. DNA quantity was determined spectrophotometrically using a NanoDrop 1000 Spectrophotometer also showed good purity with A260/280 ~ 2.

3.4.2 Assessing RNA and DNA quality and purity

The purity and the concentrations of the RNA and DNA were measured by a NanoDrop 1000 Spectrophotometer. RNA with a 260/280 nm ratio around ~ 2 and DNA around ~ 1.8 were considered as good quality and pure (Desjardins & Conklin, 2010) (Figure 3-1 and Figure 3-2). The concentrations of RNA and DNA ranged from about 100 to 250 ng/µl.

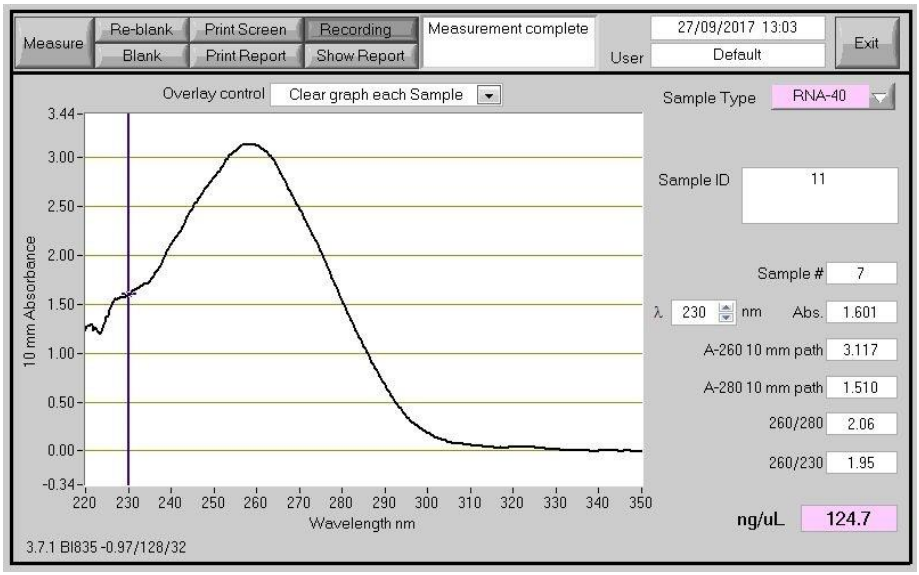

Figure 3-1 An example of nanodrop of isolated RNA profiles. The figure shows a typical RNA tracing shape. RNA concentration is 124.7 ng/µl.

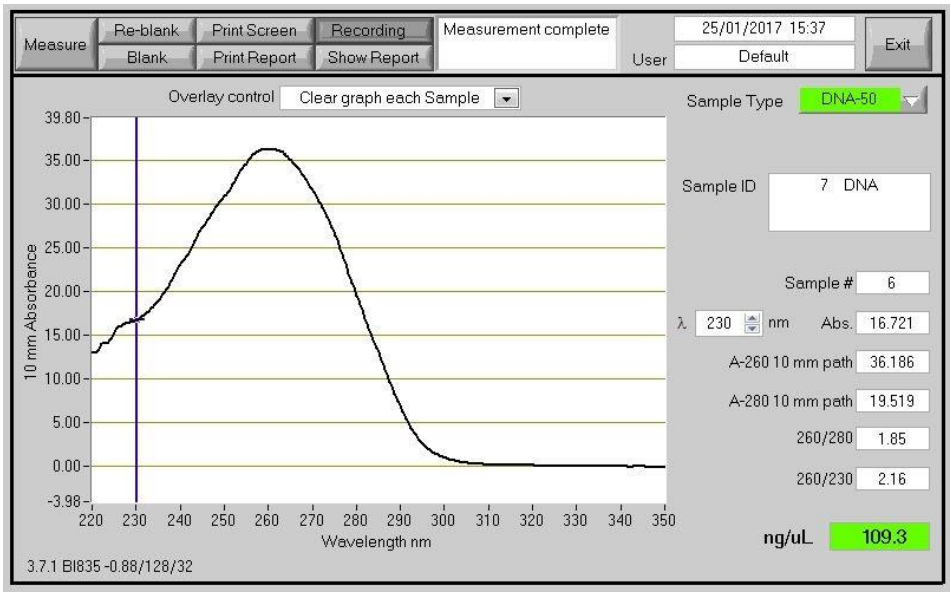

Figure 3-2 An example of Nanodrop of isolated DNA profiles. The figure shows a typical DNA tracing shape. DNA concentration is 109.3 ng/µl.

RNA quantification was achieved with Qubit 3.0 Fluorometer (Thermo Fisher Scientific, USA), results are summarised in Table 3-5. The results of the quality study showed that the samples were all concentrated enough to proceed into library construction, except the samples number AHS 47 and 48, where the concentration is very low, therefore were excluded from the study.

Table 3-5 RNA measuring by Qubit 3.0 Fluorometer. The table shows Qubit 3.0 Fluorometer results Sample used amount was 1 µL, Std 1 RFU (standard 1 relative fluorescence units) was 57.9 and Std 2 RFU was 28180.75

RNA run ID	Sample concentration ng/µl
AHS 01	212
AHS 05s	146
AHS 05	310
AHS 07	216
AHS 09	352
AHS 14	112
AHS 47	212
AHS 11	326
AHS 12	189
AHS 13	268
AHS 15	346
AHS 16	119
AHS 47	300
AHS 19	216
AHS 22	296
AHS 25	222
AHS 26	290
AHS 31	258
AHS 33	380
AHS 47	13
AHS 48	09

3.4.3 Gel electrophoresis of DNA

The DNA extraction process was performed after the failure of the RNA extraction from samples stored in RNAlater stabilization solution, to verify the plant's response to DNA extraction. The integrity of RNA was determined by gel electrophoresis (after obtaining cDNA) which allows the examination of the purity and effectiveness of the isolation and extraction method and ensures no contamination in the samples. The result shows only one size of the banding pattern was observed at a size around 200 bp. The amplification of XDH genes

from other samples with the same primer and polymerase gave consistent results when repeated (Figure 3-3).

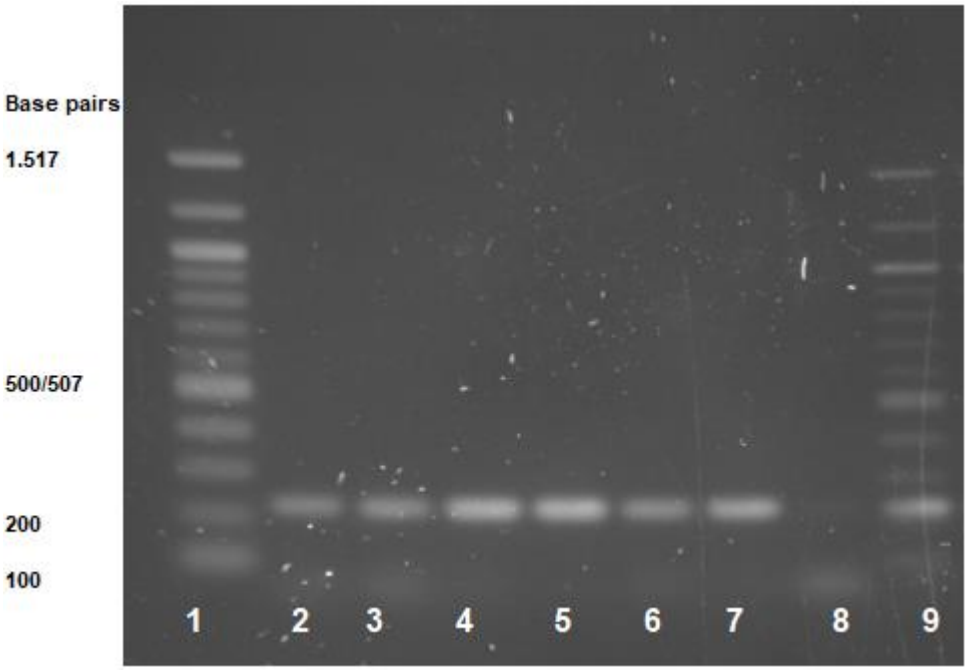

Figure 3-3 Ethidium bromide-stained multiplex PCR products after gel electrophoresis for the housekeeping gene (XDH). DNA molecular size marker used (100 bp. BioLabs.Inc). Lanes: Lane 1and 9 DNA ladder, 2-7 amplified DNA samples; 8: control.

3.4.4 RNA-sequencing quality

In terms, RNA-sequencing quality. The received results were analysed for intact quality using the Galaxy Web-based platform (FastQC) for bioinformatics analysis database. The quality score generally was high for all samples (Figure 3-4).

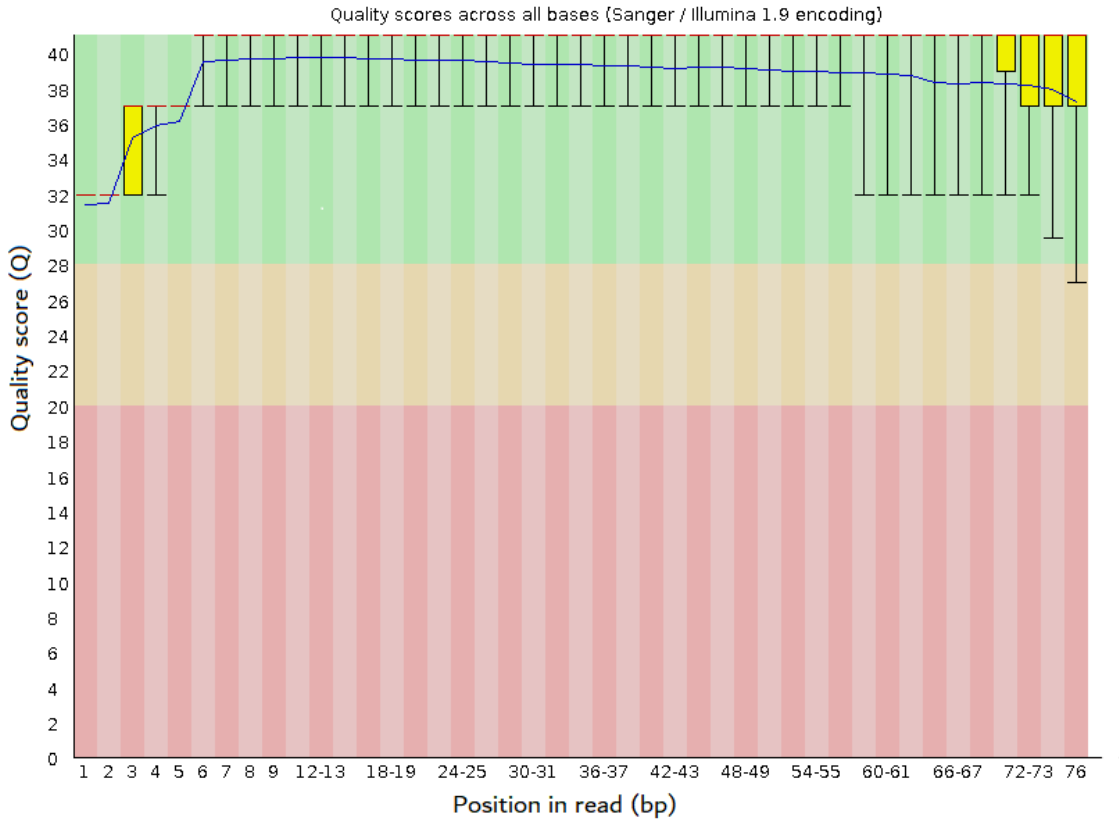

Figure 3-4 Quality control of the genome sequencing data. The figure shows base quality using Phred scores for the data from Illumina sequencing. In the box plots, the whiskers represent the range of quantiles; the yellow boxes show the range between the upper and lower quartiles; the blue line indicates the mean quality. the red lines represent the median. the figure is an example of sample 467 (Table 3-1).

Sequence analysis and assembly were performed to obtain a global overview of the transcriptome and gene activities of *A. hippocastanum* at the nucleotide level.

3.4.4.1 Analysis of assembled transcriptome and differentially expressed genes

To assemble and recognise the genes that were differentially expressed under infection condition in the *A. hippocastanum*, the differentially expressed genes (DEG) profiles of the samples were compared to analyse the gene expression variations.

The comparison revealed that the total number of transcripts were 171,794 (Table 3-6). The total number of hit genes were 56,134. The number of differential expressions of newly annotated transcripts in disease and disease-free trees was 817 genes; 711 genes were significantly up-regulated and 106 genes were down-regulated. Furthermore, 638 infected vs. non-infected area tissues genes were found, of these 624 genes were significantly up-regulated, and 14 genes were significantly down-regulated. The lowest number of DEGs (differentially expressed genes) was found in the non-infected area vs uninfected, were of six genes, five of them were significantly down-regulated (Table 3-7).

Table 3-6 Summary of the assembled *Aesculus hippocastanum* transcriptome

Total number of genes	56,134
Total number of transcripts	171,794
Percentage GC	40.05
Statistics based on the longest isoform per gene only	
Contig N10 (bases)	4558
Contig N20 (bases)	3606
Contig N30 (bases)	2945
Contig N40 (bases)	2448
Contig N50 (bases)	1996
Average Contig length (bases)	978
Total assembled bases	54,875,815
RNA-Seq Read Content (%)	91.07
Proteins represented by full length transcripts*	6412
Trans-rate output	
Longest transcript	14,276
Transcripts (number) > 1Kb	84,164
Transcripts (number) > 10Kb	64
Transcripts (number) with an open reading frame	76,197
*Determined by mapping assembled transcripts to the Swiss-Prot database	

Table 3-7 Differential transcript expression analysis. Differentially expressed transcripts are those expressed at Log2 Fold Change ≥ 2.0 between treatment and control, where P ≤ 0.001 following false discovery rate correction (edgeR).

Comparison	**Differentially Expressed Transcripts**
Uninfected vs Infected	817
Infected vs Non-Infected area	638
Non-Infected area vs Uninfected	6

The clustered heatmap below shows the sample correlation matrix of differentially expressed genes (Log2 Fold Change ≥ 2.0, P ≤0.001) across all comparisons (Figure 3-5).

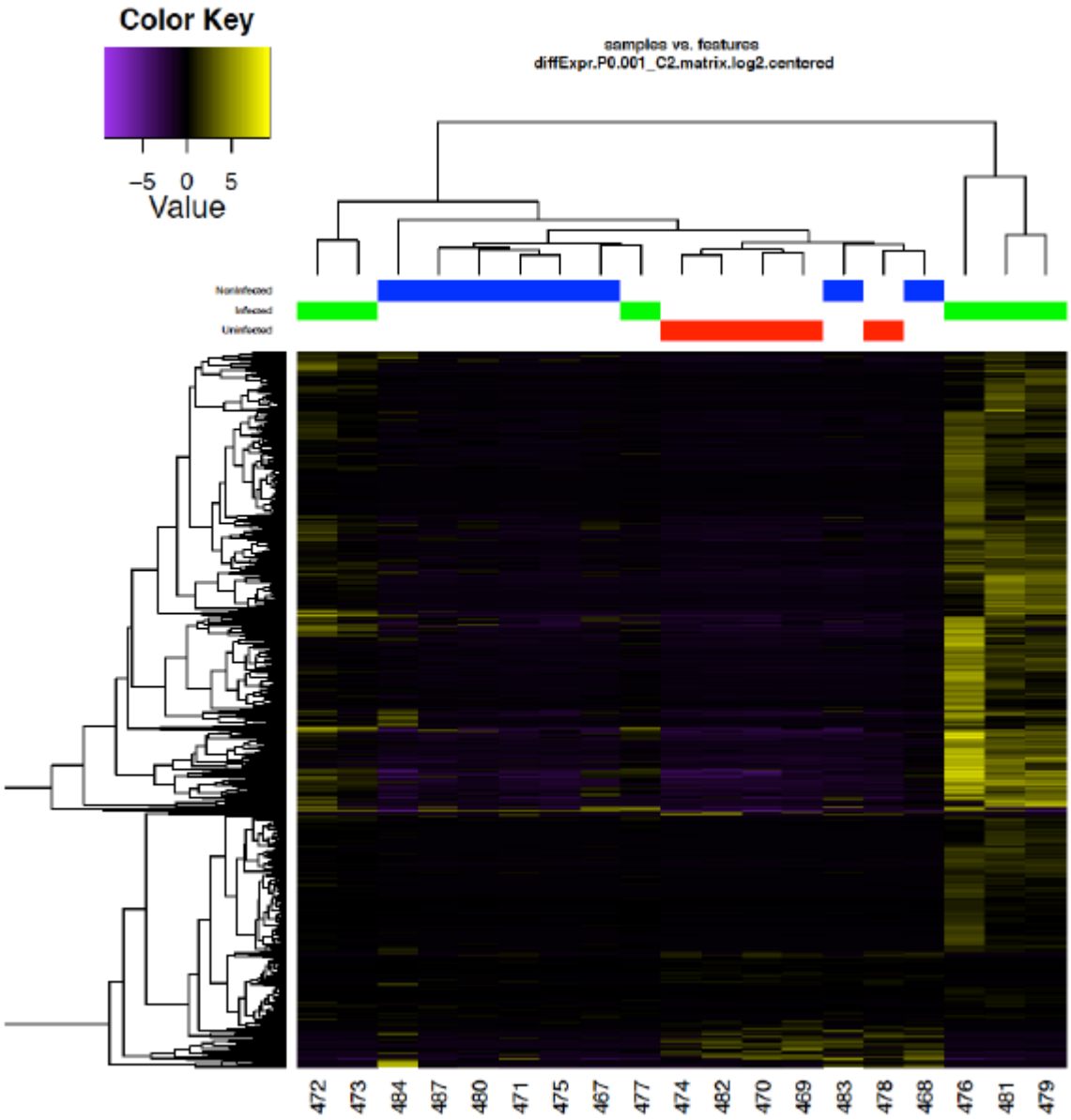

Figure 3-5 Heatmap of the total differentially expressed genes. The heatmap used to cluster the different experimental samples based upon differentially expressed mRNAs (fold change >=2 fold and P < 0.001). The Y-axis clustering represents clusters of genes that have similar expression profiles, the X-axis clustering is experimental samples that have similar expression profiles. The colours bars represent different sample groups. The numbers of samples in biological pathways (the x-axis) are listed in Table 3-1.

In the current study, 1461 related DEGs were found with up- and down-regulated expression under all samples. For the infected vs un-infected group (disease and disease-free), the number of differential expressions of annotated

transcripts was 711 significantly up-regulated genes, and 106 genes were down-regulated. The twenty most abundantly expressed genes that were up-regulated and down-regulated from the infected vs uninfected treatments are listed in Table 3-8.

Table 3-8 Top 20 of up-regulated and down-regulated expressed genes in infected vs uninfected samples. The table shows up- and down-regulation of some identified genes in *A. hippocastanum* in presence or absence of bleeding canker. Log FC value (logarithm of fold change) for each gene is given.

Transcript ID	**gene acronym symbol**	**Gene name**	**Log FC value**
TRINITY_DN15687_c0_g1_i12	CAHC	Carbonic anhydrase, chloroplastic	13.6246099
TRINITY_DN7363_c0_g1_i2	EGC	EG45-like domain containing protein	12.8690239
TRINITY_DN10696_c1_g3_i5	WRK11	Probable WRKY transcription factor 11	12.6571997
TRINITY_DN12080_c2_g2_i7	GH31	Probable indole-3-acetic acid-amido synthetase GH3.1	12.4544412
TRINITY_DN14440_c0_g1_i5	CHIB	Basic endochitinase	11.9962019
TRINITY_DN14168_c1_g1_i24	BGL17	Beta-glucosidase 17	11.9785195
TRINITY_DN14790_c1_g1_i1	C86B1	Cytochrome P450 86B1	11.9331227
TRINITY_DN14433_c2_g1_i18	Y5977	Probable leucine-rich repeat receptor-like protein kinase At5g49770	11.9095447
TRINITY_DN10035_c0_g1_i5	DHQSD	Bifunctional 3-dehydroquinate dehydratase/shikimate dehydrogenase, chloroplastic	11.6006287
TRINITY_DN11316_c0_g1_i7	TPS7	Alpha-farnesene synthase	11.5990597
TRINITY_DN16880_c0_g1_i12	PHL7	Myb family transcription factor PHL7 /ECO	-10.72534192
TRINITY_DN8518_c0_g1_i11	Y2287	GTP-binding protein At2g22870	-11.08552008
TRINITY_DN12908_c2_g1_i11	ASI1	Protein ANTI-SILENCING 1 /ECO	-11.35352101
TRINITY_DN11970_c2_g1_i9	PIF4	Transcription factor PIF4	-11.39409153
TRINITY_DN15530_c0_g1_i1	FTSH2	ATP-dependent zinc metalloprotease FTSH 2, chloroplastic	-11.61634563
TRINITY_DN16136_c0_g1_i21	ZFP34	Probable E3 ubiquitin-protein ligase RZFP34 {ECO	-11.95893969

TRINITY_DN16518_c3_g1_i10	CKL2	Casein kinase 1-like protein 2 /ECO	-12.05447052
TRINITY_DN14784_c1_g2_i6	CBSX5	CBS domain-containing protein CBSX5	-12.07373049
TRINITY_DN16870_c0_g2_i7	OML4	Protein MEI2-like 4	-12.2066161
TRINITY_DN11760_c8_g1_i1	RBOHD	Respiratory burst oxidase homolog protein D	-12.28598252

Regarding the infected vs non-infected group, the number of differential expressions of annotated transcripts was 624 up-regulated genes, whereas 14 genes were down-regulated. The twenty most abundantly expressed genes that were up-regulated and down-regulated in the infected vs non-infected treatments are listed in Table 3-9. in this group, there are some genes such as CBL-interacting serine/threonine-protein kinase 1 (CIPK1), GDSL esterase/lipase At5g22810 (GDL78), Cytochrome P450 86B1 (C86B1) and probable leucine-rich repeat receptor-like protein kinase At5g49770 (Y5977). The last two genes are highly expressed in infected trees but not so in non-infected and uninfected (Table 3-8 and Table 3-9).

Table 3-9 Top 20 of up-regulated and down-regulated expressed genes in infected vs non-infected samples. the table shows up-and down-regulation of some identified genes in *A. hippocastanum* in presence or absence of bleeding canker. Log FC value (logarithm of fold change) for each gene is given.

Transcript ID	**gene acronym symbol**	**Gene name**	**Log FC - value**
TRINITY_DN15178_c0_g1_i3	CIPK1	CBL-interacting serine/threonine-protein kinase 1	13.44547609
TRINITY_DN14790_c1_g1_i2	C86B1	Cytochrome P450 86B1	11.73327652
TRINITY_DN15340_c0_g2_i20	GDL78	GDSL esterase/lipase At5g22810	11.62844375
TRINITY_DN16619_c0_g1_i2	GDL71	GDSL esterase/lipase At5g03610	11.24657368
TRINITY_DN15759_c0_g1_i7	IST1L	IST1-like protein	11.22427259

TRINITY_DN13159_c2_g2_i1	C98A2	Cytochrome P450 98A2	11.16725628
TRINITY_DN10013_c0_g2_i5	MYB15	Transcription factor MYB15 /ECO	11.00562959
TRINITY_DN13120_c0_g1_i5	OFT19	O-fucosyltransferase 19 /ECO	10.74356413
TRINITY_DN14433_c2_g1_i23	Y5977	Probable leucine-rich repeat receptor-like protein kinase At5g49770	10.58437779
TRINITY_DN14570_c2_g1_i6	C75A3	Flavonoid 3',5'-hydroxylase 2	10.45898162
TRINITY_DN7737_c0_g1_i3	PTR50	Protein NRT1/ PTR FAMILY 5.8	-7.437697247
TRINITY_DN16001_c1_g1_i1	IAA13	Auxin-responsive protein IAA13	-7.63785986
TRINITY_DN14489_c0_g2_i2	SEOB	Protein SIEVE ELEMENT OCCLUSION B {ECO	-7.681196567
TRINITY_DN12295_c1_g1_i2	WAT1	Protein WALLS ARE THIN 1	-7.74123786
TRINITY_DN14510_c0_g6_i2	SWT12	Bidirectional sugar transporter SWEET12 {ECO	-8.251601116
TRINITY_DN12557_c2_g2_i6	CAMT3	Probable caffeoyl-CoA O-methyltransferase At4g26220	-8.258691283
TRINITY_DN10277_c0_g2_i1	SEOB	Protein SIEVE ELEMENT OCCLUSION B {ECO	-8.748338878
TRINITY_DN12295_c1_g1_i3	WAT1	Protein WALLS ARE THIN 1	-8.934246218
TRINITY_DN12433_c1_g5_i1	WTR38	WAT1-related protein At5g07050	-8.95380166
TRINITY_DN14110_c1_g2_i27	Y1677	Probable LRR receptor-like serine/threonine-protein kinase At1g67720	-9.157848156

Regarding the genes of the group non-infected vs uninfected samples as differentially expressed genes (DEGs) including one gene up-regulated and five genes down-regulated. the up-regulated gene was calmodulin-binding transcription activator (CMTA5). This gene related to several genes enhanced natural lesions.

In the non-infected vs uninfected group of genes, the result shows that four were down-regulated, from these genes Peptidyl-prolyl cis-trans isomerase CYP18-1 gene (CP18A) which was down-regulated in this study. The CP18A was also down-regulated in infected samples but up-regulated in uninfected. the CP18A (Peptidyl-prolyl cis-trans isomerase CYP18-1) gene was down-regulated in non-infected but up-regulated in uninfected sample.

Transcription factor TGA (TGA3) overexpression in the non-infected sample versus uninfected (Table 3-10).

Table 3-10 The up-regulated and down-regulated expressed genes in non-infected vs uninfected samples. the table shows up-and down-regulation of some identified genes in *A. hippocastanum* in presence or absence of bleeding canker. Log FC value (logarithm of fold change) for each gene is given.

Transcript ID	Gene acronym symbol	Gene name	Log FC - value
TRINITY_DN10384_c0_g1_i1	DGC14	Protein DGCR14	-12.43676024
TRINITY_DN11281_c2_g2_i7			-9.725910512
TRINITY_DN11782_c0_g2_i3	RL34	50S ribosomal protein L34	-8.426628055
TRINITY_DN11504_c0_g1_i1	TGA3	Transcription factor TGA	-8.273575012
TRINITY_DN15937_c0_g1_i7	CMTA5	Calmodulin-binding transcription activator	9.721554148
TRINITY_DN12256_c1_g1_i29	CP18A (g10)	Peptidyl-prolyl cis-trans isomerase CYP18-1	-10.18030078

3.4.5 Identification of genes and the biological pathways

The species distribution of biological pathways revealed that most of the annotated unigenes had high hits with sequences from *Arabidopsis thaliana*, suggesting that the assembly and annotation of *A. hippocastanum* phloem transcriptome are reliable and correct (Figure 3-6). The other best hits were identical with *Morus notabilis*, *Tribolium castaneum* and other miscellaneous organisms. The distribution of gene ontology (GO) terms was in a different category such as Cellular Component (CC) genes category, The Molecular Function (MF) terms “binding” and “catalytic activity” and genes involved in the synthesis of enzymes that degrade pathogenic cell walls etc. (Figure 3-7 and Figure 3-8).

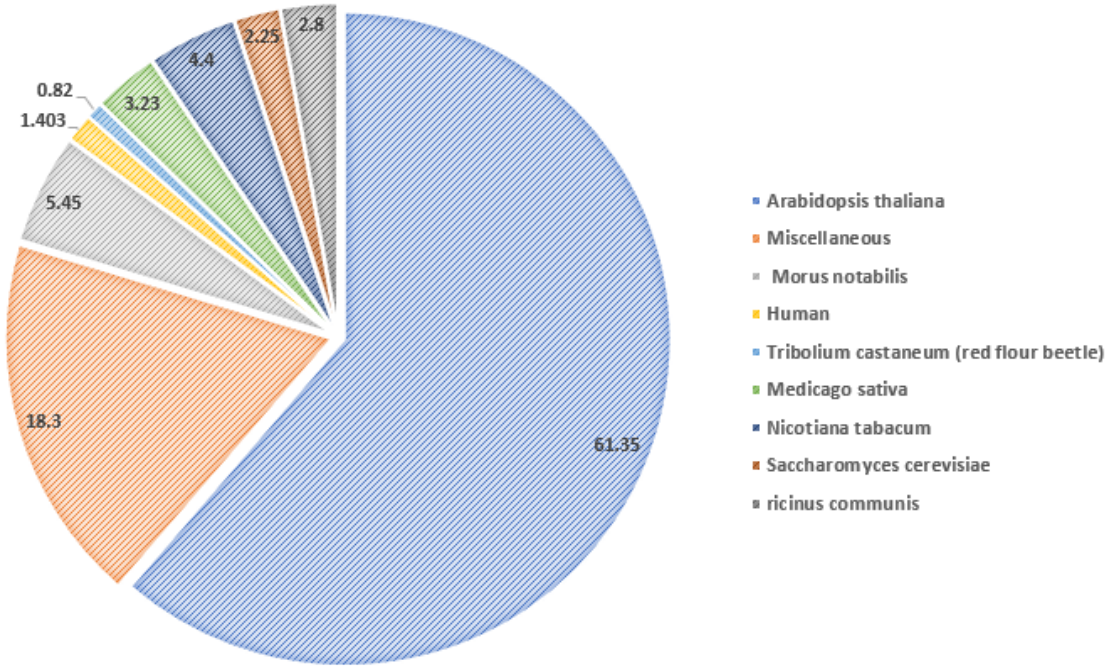

Figure 3-6 The taxonomic hits of *Aesculus hippocastanum* contigs at the transcriptome level. The figure shows species distribution of the top blast hits as a percentage of the total homologous sequences. The pie chart represents 1461 genes.

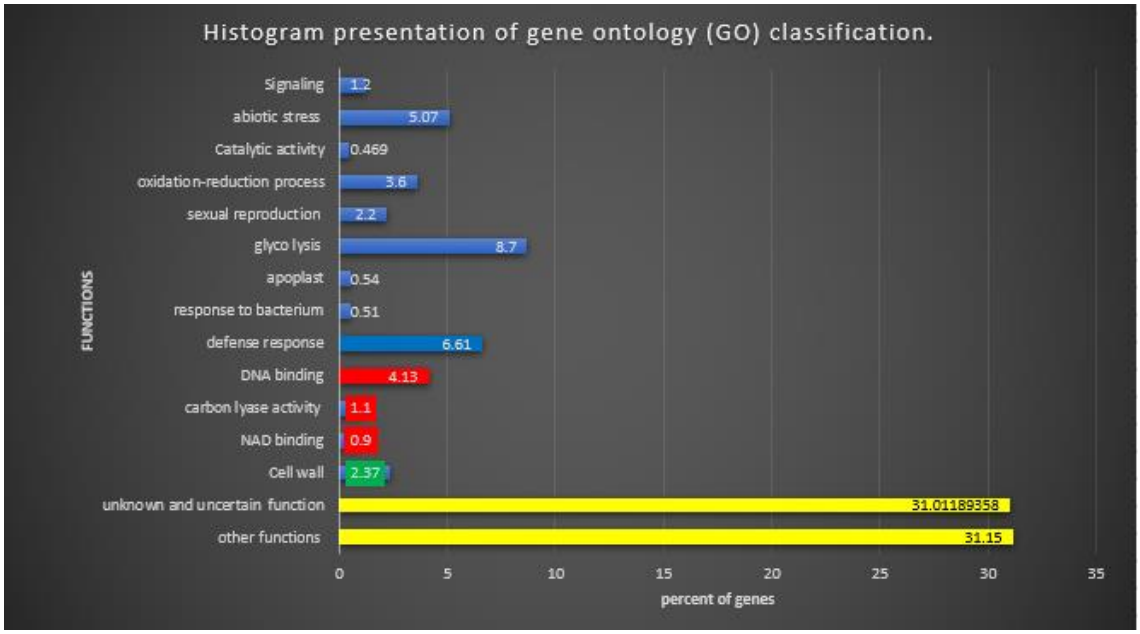

Figure 3-7 Histogram of gene ontology classification. The figure shows functional gene ontology (GO) classification of 638 annotated differentially expressed genes (infected vs non-infected). Sequences with matches were assigned GO terms. The blue colour represents biological process genes, and the red colour represents a molecular function. The green colour represents cellular component genes. The yellow colour refers to different and unknown function genes. The y-axis represents the functions of genes in a category and the x-axis represents the percent of genes.

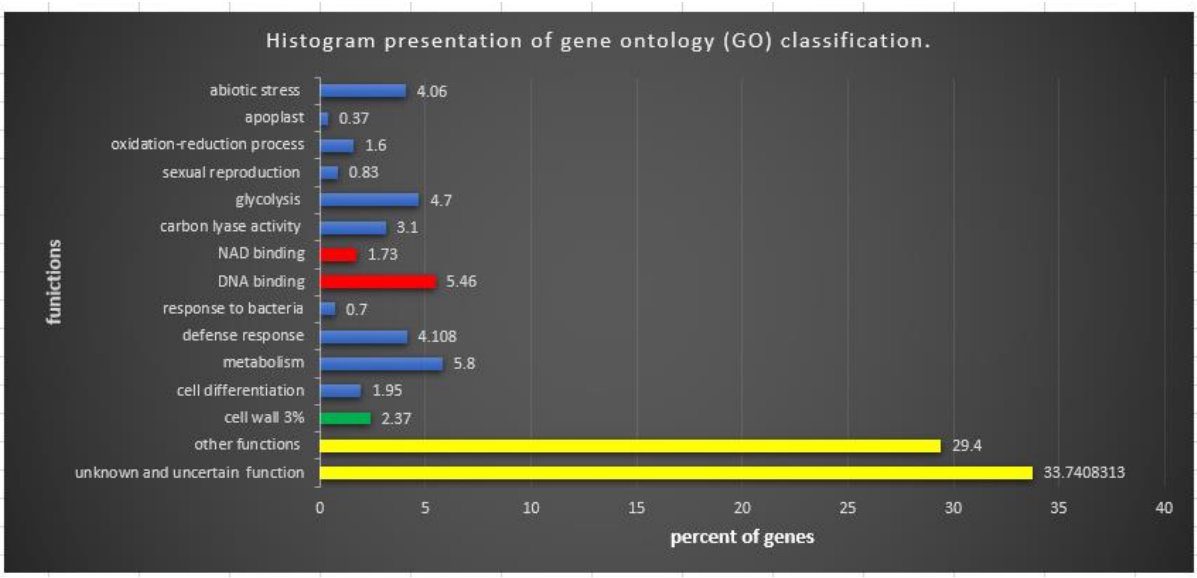

Figure 3-8 Histogram of gene ontology classification. The figure shows functional gene ontology (GO) classification of 817 annotated differentially expressed genes (infected vs Uninfected). Sequences with matches were assigned GO terms. The blue colour represents biological process genes, and the red colour represents the molecular function. The green colour represents cellular component genes. The yellow colour refers to different and unknown function genes. The y-axis represents the functions of genes in a category and the x-axis represents the percent of genes.

3.5 Discussion

3.5.1 DNA extraction of *A. hippocastanum*

The DNA extraction process was performed on frozen samples after the failure of RNA extraction from samples stored in RNAlater® Stabilization Solution, to verify the plant's response to DNA extraction as DNA has more stability than RNA. The results showed successful DNA extraction with a concentration of about 100 ng/µl for each sample. The lack of permeability in the connective tissue of *A. hippocastanum* phloem may be prevented the RNAlater® Stabilization Solution from maintaining the integrity of the RNA.

3.5.2 Assessing DNA and RNA quality using the NanoDrop and Qubit3

The process of extraction and purification of RNA is critical and fundamental to achieving the RNA sequence and finding the expressed genes. The RNA gave absorbance at 260/280 nm indicating purity and with a concentration around ~ 2. This was considered as a good pure quality and suitable for NGS sequencing (Desjardins & Conklin, 2010; Pillai *et al.,* 2017; Zhou *et al.,* 2016). The concentrations ranged from about 100 to 150 ng/µl, and that was also considered enough for sequencing. As absorbance techniques will measure any molecules absorbing at a specific wavelength, some nucleic acid samples require purification before measurement to ensure accurate results. RNA usually absorbs at 260 nm and contributes to the total absorbance. A ratio of ~1.8 is generally accepted as “pure” for DNA; a ratio of ~2.0 is generally accepted as “pure” for RNA. If the ratio is appreciably lower in either case, it may indicate the presence of protein, phenol or other contaminants with DNA

or RNA that absorb strongly at or near 280 nm. The 260/230 ratio was used as a secondary measure of nucleic acid purity and these values for "pure" nucleic acid were regularly higher than the respective 260/280 values. Expected 260/230 values are normally in the range around 2-. If the ratio was far higher or lower, it may show the existence of contaminants in the sample which measured at 230 nm (Desjardins & Conklin, 2010). The results of the nanodrop procedure were also supported and confirmed by using Qubit3.

3.5.3 Analysis of assembled transcriptome and differentially expressed genes (DEGs)

Illumina sequencing technology and de novo transcriptome assembly RNA-seq is a valuable strategy for obtaining a whole set of transcripts from specific plant tissue under specific physiological conditions or at a specific developmental stage (Nie *et al.*, 2016; Wang *et al.*, 2012). In the current work, approximately 40 million reads per sample were requested. It was planned that the transcripts would be assembled to create a first reference list, and this would be used to look at differential expression analysis.

In this study, to perform the comparative genomics analysis, we sequenced the whole transcriptome of *A. hippocastanum* from phloem samples using Illumina RNA-Seq technology. After obtaining Illumina RNA-Seq data, *de novo* assembly was carried out to get unigenes, which were generated with an average length of 978 bp. The strategy of comparative genomics analysis was to directly compare the infected reads with the Non-infected and uninfected samples of phloem. To the best of our knowledge, this study was the first

investigation to characterize the whole transcriptome. This study may also be the first study which has focused on the gene expression in healthy tissue belonging to infected and non-infected trees.

Among the differentially expressed genes found, the most abundantly expressed genes that were up-regulated in the infected vs uninfected treatments are listed in Table 3-8. The results show that the gene that was most common was that encoding the CAHC domain-containing protein Carbonic anhydrase (CA) which catalyses the reversible hydration of CO_2 and it can compensate for the lack of H_2O and CO_2 in plants under stress conditions. This gene was not expressed in intact cells from the uninfected sample. Antioxidative enzymes usually play a crucial role in scavenging reactive oxygen species and in protecting plant cells against the toxic effects of infection (Xiong *et al.,* 2015). The results showed the Cytochrome P450 86B1 gene (C86B1) was also involved, which encodes the Cytochrome P450 86B1 protein that is involved in the stimulation of wound suberization in some tree such as kiwifruit. The C86B1 gene also encodes for the fatty acid ω-hydroxylase activity associated with suberin synthesis, which increased by more than two-fold in infected samples (Chen, *et al.,* 2016; Han *et al.,* 2018). The C86B1 genes were always highly up-regulated within the infected samples. By contrast, the gene expression of C86B1 was down-regulated in both uninfected and non-infected trees. These results are consistent with those of other studies which suggest that C86B1 is up-regulated in plants that are under stress of wound or infection (Han *et al.,* 2018).

The EG45-like domain-containing protein (gene EGC) that encodes a pathogenesis-related EG45-like domain-containing protein was the most up-

regulated in the infected sample while this gene not expressed in uninfected plants. A similar study found that this gene was significantly upregulated in grapevine plants that have been subjected to damage stress as a result of insect feeding (Timm & Reineke, 2015). As is known, bleeding canker bacteria cause significant damage to the infected tissue after the development of infection. The damage makes plant tissues lose water under the influence of drought stress due to the loss of plant sap and cell fluids from the oozing region. Among the top up-regulated genes, the WRK11 gene, which encodes Probable WRKY transcription factor 11protein, is associated with phytohormone genes during normal or stress conditions in apple trees (Krost *et al.,* 2013). This also accords with the stress that occurs to the *A. hippocastanum* under the influence of bacterial disease.

From the most significantly expressed genes, there were a number for which the exact functions of them are not known, such as BGL17 and DGC14. This study found that BGL17 gene was significantly upregulated in infected vs uninfected with a Log FC value of 11.978. This may be strong evidence of the critical role of this gene in the disease function or resistance to bacterial infection of *P. syringae* pv. *aesculi*. Further data collection and studies are required to determine the exact function and role of these genes in bleeding canker disease.

In general, genes responsible for the process of disease resistance made up about 5% of the total genes of upregulated infected samples. These genes work directly or in collaboration with other genes to complete the resistance function and stimulate the plant's immune system, such as Probable WRKY transcription factor 11(WRK11). For instance, the interaction between the

RING-type E3 Ub-ligase EIRP1, and the TF (transcription factors) WRK11 results in suppressed transcriptional activation of WRKY11 target genes AOS (allene oxide synthase) and LOX1 gene, thereby enhancing PTI (pattern-triggered immunity). The RING E3 ligase MIEL1 interacts with the MYB TF MYB30, which results in weakened transcriptional activation of VLCFA-related genes and therefore suppressed HR (hypersensitive response) and defence responses to increase the spread of pathogens. Or the opposite mechanism occurs with the stimulation of the plant to prevent disease spread (Duplan & Rivas, 2014; Ichinose *et al.,* 2013; Park *et al.,* 2015). In the current study, it was found that the Y5977 gene was significantly upregulated in infected vs uninfected and in infected vs non-infected with Log FC value of 11.909 and 10.584, respectively. This may be clear evidence of the significant role of this gene in the disease function or resistance to bacterial infection of *P. syringae* pv. *aesculi*. This matches with earlier studies which reported the effective role of Y5977 gene in disease resistance (Gou *et al.,* 2010; Zhou, *et al.,* 2004).

In regard to the genes of non-infected vs uninfected group, the cell-to-cell communication that motivates local defence responses is largely unknown. A common up-regulated gene was Calmodulin-binding transcription activator (CMTA5). This gene is related to several genes involved in enhanced natural lesions, so the high gene expression may explain the resistance of phloem to bacterial diseases and help in wound healing. In this group of genes, four were down-regulated; from these genes, Peptidyl-prolyl cis-trans isomerase CYP18-1 (CP18A) was down-regulated in this study, but up-regulated under salt stress in another study (Jia *et al.,* 2019). The CP18A was also down-regulated in

infected and non-infected samples but up-regulated in uninfected samples. Sometimes this CP18A gene plays a role as a chaperone gene related to the unfolding of protein in response to salt-tolerant vegetation or other abiotic stress in the plant (Jia *et al.*, 2019).

The 50S ribosomal protein L34 (down-regulated in non-infected vs uninfected group) is considered to produce non-classically secreted, essential, and virulent proteins in the plant, but some studies considered it to be wound-inducible in tobacco leaves, and that benzyl adenine (BA) enhanced the wound-inducible expression of the gene/Ribosomal protein. Protein DGCR14 (DGC14) has an unknown role that appears to play a significant role in the infected samples. The non-infected samples present a very similar transcriptomic picture to that of uninfected samples which suggests that localised transcriptomic changes occur in response to infection. Previous studies have shown that groups of genes work in a contradictory or synergistic way, for example, Contig 9900 was undetected in the *Medicago truncatula* genome suggesting that it might be part of a specific *faba bean* disease resistance gene. In contrast, Contig 3028 showed an important match with the Medtr8g088390 gene, annotated as a protein that physically associates with CBL-interacting serine/threonine-protein kinase 1(CIPK1) (Ocaña-Moral *et al.*, 2017; Ramm *et al.*, 2015).

In general, plant pathology resistance depends partially on the host's ability to reduce pathogen development at the cell-surface level. Structural changes in the host cell wall-associated with defence mechanisms include deposition of lignin-like material, production of Auxin (WAT1 gene which down-regulated in infected vs non-infected group), phenolic compounds, callose, and accumulation of hydroxyproline-rich glycoproteins (Benhamou et al. 1991,

Cantu et al. 2008; Souza *et al.*, 2013). Plants respond to wound and other stress by activating a set of genes such as C86B1 and CHIA. Some of the wound-responsive genes have a defensive function against pathogen infection and insect predation, while others, such as housekeeping genes, may function in wound repair. Therefore, it would be interesting to assess the effects of BGl17, Y5977 and DGC14 genes in detail, which may lead to diagnosis of the main key of bleeding canker in horse chestnut, and probably the key to combatting the disease in an effective way. Identifying these defensive genes would be an essential step towards producing horse chestnut resistant varieties through genetic engineering or breeding. The information given in this work would provide more insights into the mechanism of bleeding canker and wound-healing metabolism in the horse chestnut.

4 Chapter 4: Tracking nanoparticles in plants

4.1 Introduction

In recent years, there has been an increasing interest in nanoparticles (NPs), and they have become more widespread and applicable in many fields in daily life such as agriculture, industry and medicine, in particular using NPs that contain magnetic ingredients of elements such as Fe, Co, Ni, and their chemical compounds. This NP type can be manipulated using magnetic fields for targeted delivery (Cox *et al.,* 2016; Servin & White, 2016; Siddiqui *et al.,* 2015). Engineered NPs have a wide range of functions in plants which vary between species and tissue types. These NPs can be useful for some plant growth while for other plants they may have a negative effect on growth or development (Anjum *et al.,*2013; Doolette *et al.,* 2015).

The importance of NPs is attributed to their unique physicochemical properties such as the surface area, the overall size, charge, colloidal stability, purity, inertness, speed and ease of penetration into the cell or tissue (García-Sánchez *et al.,* 2015; Mousa *et al.,* 2018; Siddiqui *et al.,* 2015). The main problem that affects work with NPs is that these particles tend to aggregate (clump) into larger blocks and this can reduce the available surface area for dissolution and lead to gravitational settling (Wittmaack, 2011). Nanoparticle solubility is assumed to increase as particle size decreases, and size of a NP is considered the main physicochemical property affecting its work (Misra *et al.,* 2012). Characterization of NPs can help in understanding the features that are responsible for NPs toxicity or their useful properties. One of these properties is the dissolution or suspension of NPs, which is considered an important

property because it releases the ionic element from the NP and this increases the possibility of it being in the most toxic form (Mousa *et al.,* 2018; Zhang *et al.,* 2016).

There are a range of factors affecting the mechanisms of how NPs work in plants or other organisms such as dissolution, distribution and accumulation. Moreover, the NP types, concentration, size, and duration of exposure. So, the simple change in some of the characteristics of NPs may alter their effectiveness and impact on the same plant or even between different organs (Anjum *et al.,* 2013; Ma *et al.,* 2016; Wang *et al.,* 2016).

4.2 Aim and objectives

The extensive use of nanoparticles in many applications has raised attention to the possible effects of these particles on the environment and the organisms. So, the main aims and hypothesis of this chapter are to study the effects of nanoparticles on bleeding canker with a view to using them as a therapeutic agent, and to investigate the possibility of these particles entering into the human food chain or even that of animals, especially in edible parts of the plant.

The central objectives of the thesis can be outlined as follows:

1. To produce and characterise Ag and CeO_2 NPs before using them.
2. To evaluate the impact of different NPs on *Aesculus hippocastanum* seed germination and on model plants (*Lycopersicon esculentum* and *Phaseolus vulgaris*).

3. To provide quantitative information about the location, toxicity, behaviour and accumulation of Ag, CeO_2, Fe_3O_4 and TiO_2 NPs in *A. hippocastanum* and model plants.
4. To determine the effect of different NPs on total dry biomass of *A. hippocastanum* and model plants and evaluate any effects on plant growth.
5. To study the effect and behaviour of different nanoparticles core size and type on *Pseudomonas syringae* bacteria.

4.3 Materials and Methods

4.3.1 Types and Sources of Nanoparticles used in this study.

Nanoparticles used in this study were of four types. Titanium dioxide (TiO_2) (Sigma Aldrich, Product Number: 637254) and Iron oxide (Fe_3O_4) (Sigma Aldrich, Product Number: 637106). Cerium oxide (CeO_2) and Silver (Ag) NPs were synthesized in the laboratory.

4.3.2 NPs synthesis and preparation.

4.3.2.1 Chemical synthesis of silver nanoparticles

Silver NPs (Ag NPs) of spherical shape were prepared using chemical reduction of various amounts of silver nitrate ($AgNO_3$). Sodium tetrahydridoborate ($NaBH_4$) was used as a primary reductant and, trisodium citrate dihydrate (TSC), as secondary reductant and stabilizing agent. The reduction procedures were performed at two different temperatures, 60°C, and 91°C, respectively, mediated mainly by $NaBH_4$ and TSC respectively.

A typical synthesis of Ag NPs was carried out as follows: the essential volumes (50 ml) of recently prepared solutions containing $NaBH_4$ and TSC were mixed and heated to 60 °C for half an hour in the dark, with strong stirring to ensure a uniform solution. The required volume of silver nitrate (VWR Analytical) solution was added drop-wise (drop by drop) to the mixture (Table 1). Then, the temperature was further raised to 90 °C. When the temperature reached 90 °C, the pH of the mixture solution was adjusted to 10.5 with 0.1 M sodium hydroxide (NaOH) (Sigma–Aldrich) and left in this

condition for 20 minutes, until a change of colour was obvious. The flask containing the solution suspension was wrapped in aluminium foil to prevent any light penetration and allowed to cool to room temperature. Next, the suspensions were centrifuged at 12 000 RPM for 15 min to remove the unreacted reductants and washed with distilled water with sonication for 30 Sec., the last steps (washing steps) were repeated three times. Finally, the residual was suspended in distilled water and stored at 4 °C for further use. More details about required volumes and times are listed below in Table 1 which shows the standard reaction conditions of the Ag NP synthesis with two different dimensions (Agnihotri *et al.*, 2014).

Table 4-1 Summary of the detailed experimental conditions used for the synthesis of different Ag NPs.

Nanoparticle Size (nm)	Silver nitrate (M)	Sodium borohydride (M)	Trisodium citrate (M)	Ag NPs adding time (min)	Yield (%)
7	0.001	0.002	0.00355	4-7	64.0
25	0.0025	0.001	0.00355	8-11	73.0

4.3.2.2 Biological synthesis of silver nanoparticles

The procedure described below is based on methods described by Çolak *et al.*, (2017) and Espenti *et al.*, (2016), with some modifications. Firstly, fresh leaves of *A. hippocastanum* were selected and collected from the greenhouse at Keele University, then, washed well with deionised water. 25 g of leaves were cut into small fine pieces, then were added to 100ml of deionised water. The temperature was set to 80 °C using a magnetic stirrer for 20 min to obtain the aqueous leaf extract; the reaction flask was wrapped with aluminium foil to

avoid any influence of light, which may cause photodegradation of silver. After the water turned greenish (indicating the release of the leaf extract to deionised water), the extract was filtered through Whatman filter paper grade 1 (Sigma-Aldrich). Next, the extract was filtered using a 0.45 μm filter to get a uniform solution, and the filtrate was collected to use as a reducing agent for NPs synthesis. Then, 10 mg of silver nitrate was added in 50 ml of deionised water. After that, the leaf extract was added dropwise very slowly until a light-yellow colour formed at which point the process was stopped. The light colour indicates the formation of silver NPs in water. These NPs were stored at 4 °C for further use.

4.3.2.3 Synthesis of Cerium nanoparticles

CeO_2 (Ceria) NPs were synthesized according to the amended procedure previously reported by (Zhang *et al.,* 2011), as follows: a solution of 0.05 M hexamethylenetetramine (HMT) was prepared in distilled water and a 0.0375 M of Cerium trinitrate (Ce(NO3)3_6H2O) was prepared and each solution left separately for 30 min on a stirrer at room temperature. The two solutions (25 ml of each solution) were then mixed rapidly and stirred for three hours at 75 °C. After stirring, the solution was centrifuged for 10 min at 10000 g and washed three times with deionised water and dispersed again in distilled water followed by ultrasonication before use. CeO_2 NPs with sizes of 25±3 nm were obtained. For preparing smaller CeO_2 NPs (7 nm), hexamethylenetetramine with a concentration of 0.5 M was used.

4.3.2.4 Determining the yield of synthesised NP

The yield of synthesised NP was determined using inductively coupled plasma optical emission spectrometry (ICP-OES, Optima 7000V DV, PerkinElmer, Wokingham, UK). After the NPs previously formed were harvested by centrifugation for 20 min at 14000 rpm, the precipitation was suspended in 2% HNO3 and sonicated for 30 sec. prior to the ICP-OES analysis of NPs.

4.3.3 Characterisation of Nanoparticles

The prepared and purchased NPs were characterised for their morphological and physicochemical properties prior to their application to *Aesculus hippocastanum* and model plants. The characterisation was carried out by the following methods.

4.3.3.1 Transmission Electron Microscopy (TEM).

Transmission electron microscopy (TEM) (model: Jeol JEM-1230) in the Keele Electron Microscope Facility was used to visualise and characterise the particles. Prior to NP imaging, the TEM ultrathin formvar (Polyvinylformal) coated copper microscopy grids were prepared as follows. Glass slides were dipped in 0.5% formvar (Sigma-Aldrich) and dried using mild heat from a desk lamp. Next, the glass slides edges were scraped by sterile scalpel blades to help raise the film before the glass slides were softly submerged into a wide and shallow glass beaker containing distilled water to separate the film from the glass slide surface. The grids (G2002 Athene 200 mesh thin bar copper 3.05 m) were then carefully placed on the floating formvar film with the dull side down (i.e. facing the film). The next step involved taking a clean glass slide and

slowly slipping the slide over the film so that it attaches to the glass slide surface. The slides were then dried overnight or by using mild heat from a desk lamp. The samples were pipetted (2 µL) onto the grids and left to dry in a closed Petri dish before imaging with TEM. The mean particle size and shapes were determined directly from the TEM images. The size of the particle was characterised by measuring the longest dimension of individual NPs.

4.3.3.2 Sizing of nanoparticles

Hydrodynamic diameter determinations of Ag, CeO_2, TiO_2 and Fe_3O_4 nanoparticles were carried out using a Zetasizer Nano instrument (PCS, Zetasizer Nano-ZS, Malvern Instruments, UK). NP samples were diluted in deionised water prior to analysis and sonicated for 1 min. using Sonoplus ultrasonic homogeniser (Ultrasonic Homogenizer mini20) to break up any aggregates present in the suspensions. The measurements were conducted on 1 ml of each sample at 25℃ held in screw-top glass vials and were run in the Zetasizer Nano. The zeta potential of all the NPs suspensions was then examined to determine their surface charge using the same instrument. All measurements were performed in triplicate, and an average value was determined.

4.3.3.3 Sample preparation for ICP-OES

Inductively coupled plasma optical emission spectrometry (ICP-OES, Optima 7000 DV) was used to determine the concentration of nanoparticle in samples. The concentrations of all NPs contents were calculated numerically based on the content of each NP separately using standard curves. The total content was

calculated using ICP Standard solutions (Sigma Aldrich) for each NP type. Three readings were taken for each sample and the mean were calculated.

4.3.3.4 ICP-OES measurement

The calibration curves were prepared by using standard silver, iron, cerium and titanium solutions 1000 µg/mL (Sigma Aldrich) diluted with deionised water previous to analysis to (10, 5, 1, 0.5, 0.1,0.05,0.01,0.005 µg/mL). The standard calibration equation, R^2 was between 0.998 and 1. ICP-OES analysis for each NP was run 6 times at two different times, showing that the means and standard error of the mean were reliable. A control sample of DW (distilled water) was also run. Silver was analysed at a wavelength of 328.068 nm, iron at 261.187, cerium at 328.048 while titanium was analysed at a wavelength of 336.122 nm, then NPs concentrations were determined according to the calibration curve (see Appendix 2: A, B, C and D).

4.3.4 Bacterial strain and culture media

4.3.4.1 Quantification of Bacterial Growth

The bacterial growth condition are described previously in greater detail in 2.3.3. Briefly, the bacteria were pre-cultivated in King's B agar medium (KB) at 21 °C overnight and inoculated to the same media at a final concentration of 0.1 CFU/ml. The growth of the bacteria was monitored constantly in the entire growth period and phases by measuring the optical densities of the bacterial suspension. Optical densities (OD) were measured using spectrometer (Cecili

CE363) as OD values at a wavelength of 600 nm (King *et al.*, 1954; Tom-Petersen *et al.*, 2001).

4.3.4.2 Effect of NPs on bacterial survival

The disc agar diffusion (DAD) assay was used to evaluate the *in vitro* antimicrobial activity of the NPs. The tested bacteria (*P. syringae* pv *aesculi, P. savastanoi* pv *phaseolicola* and *P. syringae* pv *tomato*) were freshly incubated for 1 h to standardise the culture to 10^4 CFU/mL by serial dilutions. The KBA agar plates were prepared for the cultures, then 250 µl of bacteria were separated on the plate surface. The sterile filter paper discs 6 mm in diameter were placed on these plates, and 25 µl of (0, 250, 500 and 750 mg/k) NPs suspended in deionised water were pipetted onto filter paper discs. Separate sets of media with different concentrations and types of NPs were also inoculated by the streaking method to evaluate the growth of individual colonies on agar plates. Finally, the Petri dishes were incubated at 21 °C for 3-4 days for bacterial growth.

4.3.4.3 Pathogen growth, reproduction and inoculation

Aesculus hippocastanum and model plants (*L. esculentum* and *P. vulgaris*) were inoculated 10 cm above ground level by syringe with 100µl of bacteria suspension (10^4 CFU/ml). The inoculation area was sealed with "Parafilm" to avoid external contamination and any effect of external exposing by NP and to prevent dehydration of the plant at the injection site. For every injection, a new clean disposable syringe (with a needle) was used each time to prevent cross-contamination between inoculated samples. Inoculated plants were then

incubated in the greenhouse under a long-day condition (16 hours light and 8 hours dark, 21-23 ºC, 60% humidity).

4.3.5 Measurement of NP impact on seeds germination and seedling growth (distribution and accumulation)

4.3.5.1 Preparation of particle suspension.

A suspension of a NP was prepared by suspending the particles with distilled water (DW) and dispersed by additional ultrasonic vibration treatment (Crest Ultrasonics, Treniton, NJ) for 10 mins (around 500 KJ) to produce a monodispersed NP suspension. The concentrations used were 0, 250, 500 and 750 mg/kg from each NP type. DW was tested as a negative control. In addition to the steps above designed to prevent precipitation or agglomeration, the NP suspensions in all treatment were stirred vigorously for 3 min and sonicated in a water bath before applying to plants or media. The pH *value* of each suspension was set to 6.8 ± 0.5 by NaOH and 0.1 N HCl before plant exposure. The pH of the DW was also controlled in the same way.

4.3.5.2 Measurement of effect of NPs on seed germination

Seed germination and seedling growth are described in more detail in Chapter 2 (see 2.3.2 and 2.3.2.2). Seeds of *A. hippocastanum* were externally sterilized with 5% NaOCl for 10 min, then washed several times with DW (EPA, 1996). For *Lycopersicon esculentum* (tomato - Ailsa Craig) and *Phaseolus vulgaris* (Bean Dwarf French – Compass) seeds were purchased commercially from Suttons Seed company and used directly after washing in distilled water

several times. Seeds were planted in 1-litre pots, then transferred into a glasshouse and exposed to three concentrations of NPs (250, 500 and 750mg/kg) of each type used in this study separately. The DW was added at the same volume as a control. Each treatment was performed in ten replicates, and after ten days for model plants and 30 days for *Aesculus hippocastanum*, the germination percentage was measured based on normal seedlings (emergence of radicle and plumule).

4.3.5.3 Measurement of effects of NPs on seedlings

4.3.5.3.1 Plants preparation and growth conditions

Seeds were planted in 1-litre pots containing compost soil at 20 ºC in the dark for 2-3 days. The seeds were then transferred to long-day growth-controlled conditions at 15-20 ºC with 16 hours light and 8 hours dark, 50-60% humidity using TOMTECH HC160 auto-environment control computer system. The pots were then exposed to NPs as the following method.

4.3.5.4 Exposing plants to nanoparticles

After five weeks from germination (one week from inoculation by bacteria), NP solutions of either CeO_2, TiO_2, Ag or Fe_3O_4 were used to water the surface of pots in which *A. hippocastanum* or model plants were germinated. The pots were irrigated to the field capacity as earlier described in Chapter 2. The final specific concentration of NPs used were 250, 500, and 750 mg/kg. Distilled water was used as a control group by using the same volume with inoculated and non-inoculated plants as a positive and negative control separately. Each treatment was achieved in four replicates.

4.3.5.5 Injection of infected *Aesculus hippocastanum* by NP

For the injection application method, *Aesculus hippocastanum* seedlings infected by *P. syringae* pv. *aesculi* were used. NP solutions of CeO_2, TiO_2, Ag or Fe_3O_4 were used at the same concentrations used in this study (250, 500, and 750 mg/kg). NPs were injected into the inner bark (phloem) at 5 centimetres above and below the active bacterial lesion separately. To inject the seedlings, small disposable needles with syringes (0.5 mm x 16 mm BD Microlance) were used with all injections. Control groups were conducted by injecting the phloem (intact and infected) on a different plant with distilled water. Each treatment was performed in four replicates and by the end of growth period plants were measured. Infection lesion in four orthogonal directions was estimated to calculate the area (Percival and Banks, 2014) using precision digital Vernier calliper with accuracy resolution of 0.01(±0.03) mm and by using ImageJ software (version 1.52 a).

4.3.5.6 Effect of NPs on biomass, plant height and root length

At harvest time, root and shoot tissues were collected. Plant height (mm) and root length (mm) were determined as the length from the soil surface to the upmost tip of the leaf and from the growth point to the root endpoint, separately. The root hairs and root nodes were examined to check for any difference. The dry weight was used to analyse the effects of the NPs on plant biomass, so the plant components (roots and shoots) at harvest day were separately cut, and were weighed for fresh weight (FW), then dried in an oven

at 80 ± 5 ˚C for 24 hours and again weighed to register dry weight (DW) (Dwivedi *et al.,* 2015; Le Van *et al.,* 2016).

4.3.5.7 Digestion of plant tissues for NP Content Determination

At the end of the growth time (after maturity) the seedlings were harvested and washed cautiously with deionised water, the roots were washed further with 0.01 M HNO_3 and rinsed with Millipore water to remove any NPs loosely associated or adhered to the outer cell surfaces. Then all parts were dried in an oven at 80 °C for 24 hours. Roots and shoots were separated and weighed. 500 mg of dried sample (or equivalent) was milled to a fine powder and digested with a mixture of concentrated HNO_3 and H_2O_2 (1:4 ratio) in a digestion tube on a heating plate or oven for 14-16 hours at 120-130 ºC. After digestion, the sample was diluted to 50 ml. Finally, total NPs contents in the plant tissues were measured by ICP-OES for major and minor NPs contents (Hernandez-Viezcas *et al.,* 2016; Zuverza-Mena, *et al.,* 2016).

4.3.5.8 Transmission electron micrograph (TEM) of bacteria

TEM was also used to visualise *Pseudomonas syringae*. The *P. syringae* culture was removed after four days growth and centrifuged at 5,000 rpm for 5 min, then rinsed twice in 1x phosphate-buffered saline PBS, followed by a wash in PBS (0.5X) and lastly once in DW with centrifugation steps following every washing. After washing the cells were resuspended in ultrapure water. 2µl of the supernatant was then placed on the grid and left overnight at room temperature to dry then was examined in the TEM at accelerating voltage 5-50 kV.

4.3.5.9 Bacterial Genomic DNA extraction

Genomic DNA was isolated from bacteria samples using the PureLink™ Genomic DNA Mini Kit according to the manufacturer's instructions. Briefly, 1 ml of bacterial culture maintained overnight was harvested by centrifugation. The cell pellet was resuspended in 180 µl PureLink™ genomic digestion buffer. 20 µl Proteinase K was added to lyse the cells then mixed well by brief vortexing. The tubes were incubated at 55 °C with occasional vortexing until lysis was completed (30 minutes to up to 4 hours). Next, 20 µl of RNase A was added to the lysate; mixed well by brief vortexing and incubated at room temperature for 2 minutes. 200 µl of binding buffer was added and mixed well by vortex to obtain a regular solution. Finally, 200 µl 96-100% ethanol was added to the lysate, vortexed for 5 seconds to yield a homogenous solution. Then Purification Protocol was completed as stated previously in Chapter 2.

4.3.5.10 Polymerase Chain Reaction (PCR) and Sequencing

To make sure of the identity of bacteria, the 16S rRNA region was amplified using the GoTaq Green DNA (Promega). Forward and reverse primers for DNA amplification were ordered from Eurofins genomics (for sequences see Appendix 3). The sequences genomics reaction was set up as follows: GoTaq® Green Master Mix (Promega) 12.5 µl, forward primer (10 µM) 2.0 µl reverse primer (10 µM) 2.0 µl, template DNA (50-100 ng) 2.0 µl, nuclease-free water 6.5 µl.

The PCR step setting duration program to amplify DNA was as follows: 98 °C 2:00 mins, 98 °C 0:15 mins, 65 °C 0:30 mins, 72 °C 1:00 mins, 72 °C 5:00

mins. 35 x cycles. This was followed by size analysis estimation by running them on agarose gel electrophoresis.

4.3.5.11 Agarose gel electrophoresis of DNA fragments

For analysis of PCR products, DNA was separated on 2.0 % (w/v) agarose gel in 1x TBE buffer. Usually, samples were mixed with 6x loading buffer and migrated on the gel at 85 V for 45 min using NanoPAC-300 (Cleaver Scientific LTD). 100 bp. DNA Ladder (Biolabs TM) was run as the standard DNA marker in the range of 100 – 1517 kb. DNA bands on the gel were identified by placing the gel in a 0.5 µg/ml ethidium bromide solution for 15 mins. Bands were detected in UV light using GeneSys image capture software.

4.3.5.12 Sequencing of DNA (Sanger)

DNA of bacteria sequencing was carried out by the Eurofins genomics service, and the sequencing information received was visualised and processed using NCBI blast database (National Centre for Biotechnology Information, USA) (https://www.ncbi.nlm.nih.gov/)

4.3.6 Statistical analysis

The data in the Figures and Tables of this study is given as means. Error bars represent standard error of the mean (SEM). Statistical analysis was carried out with the GraphPad Prism statistical package to determine the difference between the treatments using one-way analysis of variance (ANOVA) followed by the Bonferroni correction method. Statistically significant differences were considered at $P \leq 0.05$.

4.4 Results

4.4.1 Characterisation and determination of NP yield

The characterisation is crucial for the experimental understanding of the results involving NPs and also for interpretation of their activities - depending on their features and the characteristics of the media they run in. The other issue affecting the NPs are a tendency to aggregate within some biological media (Auffan *et al.,* 2009; Vinković Vrček *et al.,* 2015). The aggregation activities of NPs will change the effective amounts leading to specific concentrations and surfaces that are usually totally different from the original NPs or the behaviours wanted. Therefore, the characterisation of NPs must be the initial step in their estimation, which then can be followed by their risk assessment and biological testing. For the characterisation of synthesised NPs, their main physicochemical properties were analysed and measured, including shape, size, polydispersity and surface charge.

4.4.1.1 Zeta potential measurement

Dynamic light scattering (DLS) was used to quantify the hydrodynamic diameter (the core size of the NPs) and to measure polydispersity and surface charge. For the NPs surface charge, the 7nm Ag NPs possessed a high negative surface charge of -40.5 mV and the rest of the silver NPs also showed negative charge. The TiO_2 NPs also possessed a negative surface charge of -25 mV. The Fe_3O_4 and CeO_2 25 nm possessed a positive surface charge of 22.3 and 20.1 mV, respectively (Table 4-2).

The hydrodynamic radius of three synthesised silver NPs, Ag 7 and 25 chemically synthesised and Ag biological synthesis (AgNPB) synthesised were at about 9.93, 27.62 and 76.08 nm respectively. The hydrodynamic radius of Fe_3O_4 was unexpectedly at 177.92 nm. It has a large diameter because of the inherent magnetic properties in the cores of iron oxide. TiO_2 had the smallest particle size in this group, which could be because of decreased particle aggregation or a large variation in particles sizes, which was reflected in the overall size. The results are listed in Table 4-2.

Polydispersity index of NPs showed that they have a homogeneous distribution except for TiO_2 and biological synthesized AgNPs which was 0.732 and 0.721 respectively, which could be due to the existence of a small fraction of NPs in the formulation, while other NPs were 0.5 or less (Table 4-2). All NP solutions appeared to be tinted, transparent, or semi-transparent in the stable NP suspensions. No particles could be visibly seen, only a cloudy solution. Transparency of NPs solutions changed according to the concentrations. The concentrated solution for Ag and iron tends to be transparent brown, while in contrast, TiO_2 and CeO_2 tend to be with milky white colour.

Table 4-2. The Nanosizer measurements of different types of NPs. The table gives hydrodynamic radius, polydispersity index and zeta potential of NPs measured at 1 mg/ml in DW (n=3, average ± SD). * supposed to be 7n m in size, **NPs were prepared by the biological method.

NPs	Hydrodynamic radius nm ± SD	Polydispersity index ± SD	Zeta potential mV ± SD
Ag (7) *	9.93±0.14	0.570±0.57	-40.5 ± 0.95
Ag (25)	27.62±0.44	0.471±0.55	-35 ± 1.26
Ag b **	76.08±2.93	0.732±0.087	-12±3.44
CeO_2 (7) *	12.44±1.11	0.263±0.13	26.2 ± 0.83
CeO_2 (25)	28.44± 0.90	0.318±0.45	20.1 ± 1.14
TiO_2	24.24±3.63	0.721±0.07	-25.1 ± 1.32
Fe_3O_4	177.92±21.22	0.424±0.97	22.3 ± 1.44

4.4.1.2 TEM imaging

The sizes of the NPs were studied using transmission electron microscopy (TEM). TEM imaging provides a clear and precise view of the NPs shape and size. Throughout the current study, silver and cerium NPs were prepared by chemical reduction (Figure 4-1 and Figure 4-2). The synthesis of AgNPs was carried out using two different approaches, including chemical and biological synthesis methods. For the chemical method, the change in reducing agents ($NaBH_4$ and TSC) with conditions produced Ag NPs of different size and yield. The sizes of Ag NPs depended mainly on the amount of added $AgNO_3$ as mentioned earlier (see 4.3.2.1). The yield of Ag NPs was found to be between 56 to 80%. The chemical method is highly efficient and the most productive. On the other hand, in the biological method, the leaf extract of *Aesculus hippocastanum* was used as a reducing agent for NPs synthesis. Although the biological method was environmentally friendly and succeeded in producing NPs, the yield was insufficient (˜ 20 to 25 %) to use it in the next experiment. Therefore, the chemical method was used and adopted subsequently. The size of Ag NPs which were prepared using chemical reduction were approximately 25 and 7 nm, which show an almost spherical shape (Figure 4-1). Cerium NPs were about 25 nm and mostly cubic or have an irregular shape. (Figure 4-2). The average core sizes of Ag and CeO_2 from a minimum number of 100 particles were found to be in the range between 20 nm to 60 nm and core sizes varying (see details with the standard error of the mean in Figure 4-5). Regarding the synthesis of CeO_2 NPs, the yield was between 60-75%.

The purchased NPs were also examined by TEM microscope. TiO_2 NPs were mostly spherical or near-spherical, with an average size of ≤ 25 nm (Figure

4-4). Whereas Fe_3O_4 NPs were between 100 - 250 nm with mostly cubic or near-spherical shape and usually, NPs of Fe_3O_4 tend to form long chains (Figure 4-3).

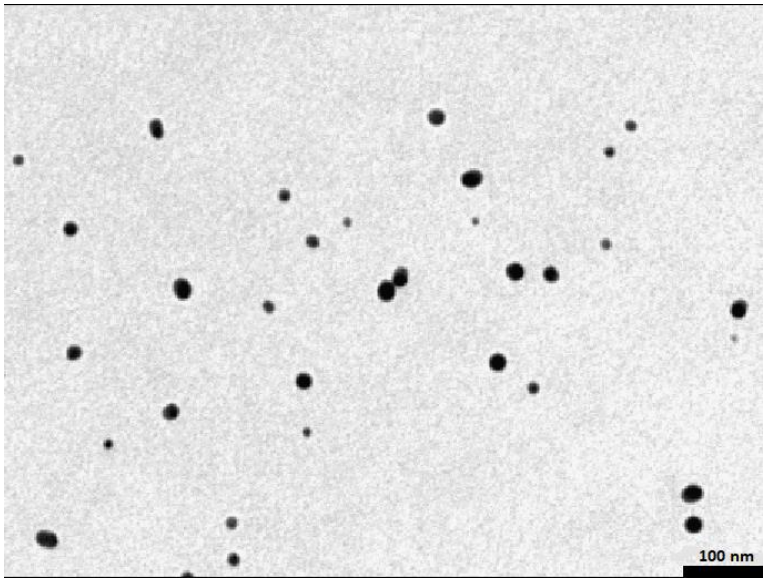

Figure 4-1 TEM image of the chemically synthesised silver nanoparticles. The figure shows NPs of the size 7 nm and 25 nm the figure reveals the same morphologies of the silver nanoparticles. Bar size in the image is 100 nm and analysis was done at 50 kV.

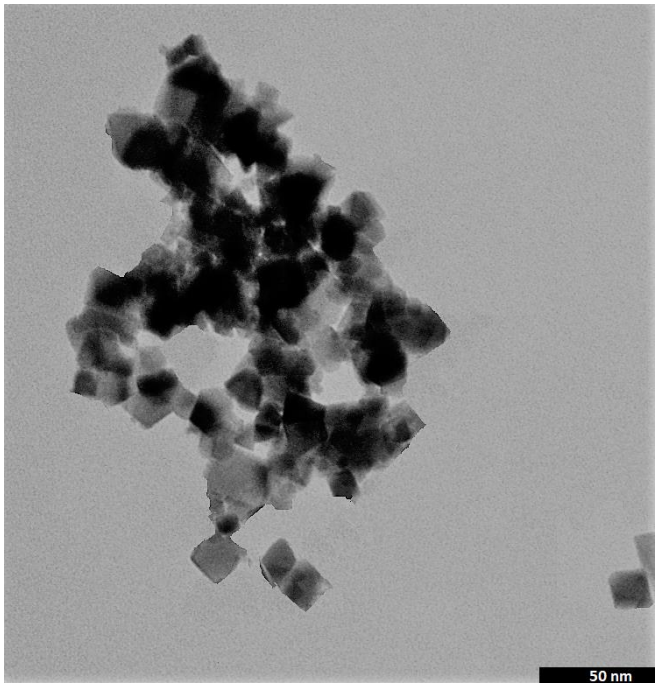

Figure 4-2 TEM image of the chemically synthesised CeO_2 nanoparticles. The figure shows NPs of the size 25 nm. Bar size in the image is 50 nm, and analysis was done at 50 kV.

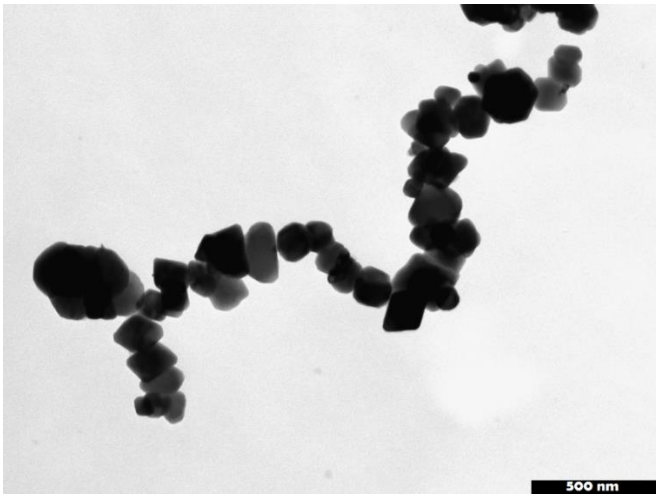

Figure 4-3 TEM images of Fe_2O_3 NPs. The figure shows a different size of Fe_2O_3 NPs under a transmission electron microscope. Bar size in the image is 500 nm, and analysis was done at 50 kV.

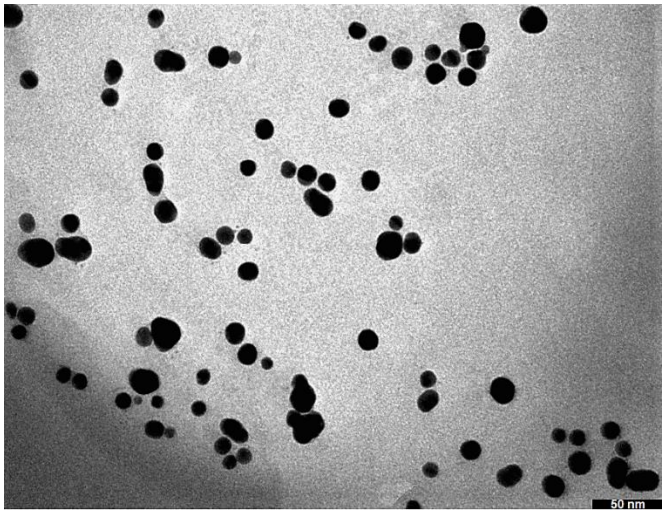

Figure 4-4 TEM images of TiO_2 NPs. The figure shows a different size of TiO_2 NPs under a transmission electron microscope. Bar size in the image is 50 nm and analysis was done at 50 kV.

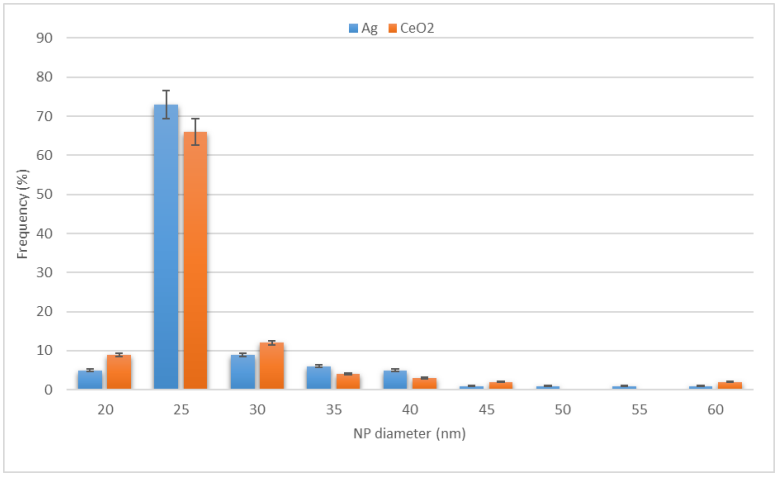

Figure 4-5 Ag and CeO_2 NP sizes distributions. The figure shows the NP sizes distributions from a typical preparation determined from TEM images (a total of 100 particles were measured). Mean size is 25 ±4 and 25 ±5 nm for Ag and CeO_2, respectively (SEM).

4.4.2 Impact of NPs on seed germination

The germination of the seeds is an essential process which indicates the launch of plant development and it shows whether the soil environment is suitable for the plant or not (Cervantes & Emilio, 2006). To determine whether Ag, CeO_2,

Fe_3O_4 and TiO_2 NPs affects the germination and growth of *Aesculus hippocastanum* and model plants, seed germination test was carried out as described earlier in section 4.3.5.2 above.

In the case of *A. hippocastanum* as can be seen from Figure 4-6 A, increasing the Ag or CeO_2 or TiO_2 concentrations did not affect the germination time or the germination frequency of the seeds except for titanium where it had a negative effect on germination especially at high concentration. There was an apparent slight increase in germination with CeO_2 at concentration 250 mg/kg but not significantly. About 80 % of seeds germinated in all treatments. In contrast, Fe_3O_4 at 500 & 750 mg/kg improved germination (100 % of seeds germinated) and accelerated seed germination and growth rate, where the germination of the *A. hippocastanum* seeds began about a week to two weeks before control samples, while seed germination was delayed when TiO_2 NPs were used at 750 mg/kg by around one week (Figure 4-7).

Regarding *Lycopersicon esculentum,* seed germination was not affected by TiO_2 NPs in the studied range of NPs concentrations (250-750 mg/kg), while at 750 mg/kg with Ag and Fe_3O_4 NPs the germination ratio reached 20% and 10%, respectively. The TiO_2 and CeO_2 NPs did not show any effect on germination. (Figure 4-6 B). In contrast, to *Aesculus hippocastanum* and *Lycopersicon esculentum,* the effect of NPs on *Phaseolus vulgaris* seed germination was significant, especially at 750 mg/kg with all NPs types. The germination frequency of the seeds was reduced to 10, 30, 50 and 40% with Ag, CeO_2, TiO_2 and Fe_3O_4 respectively (Figure 4-6 C).

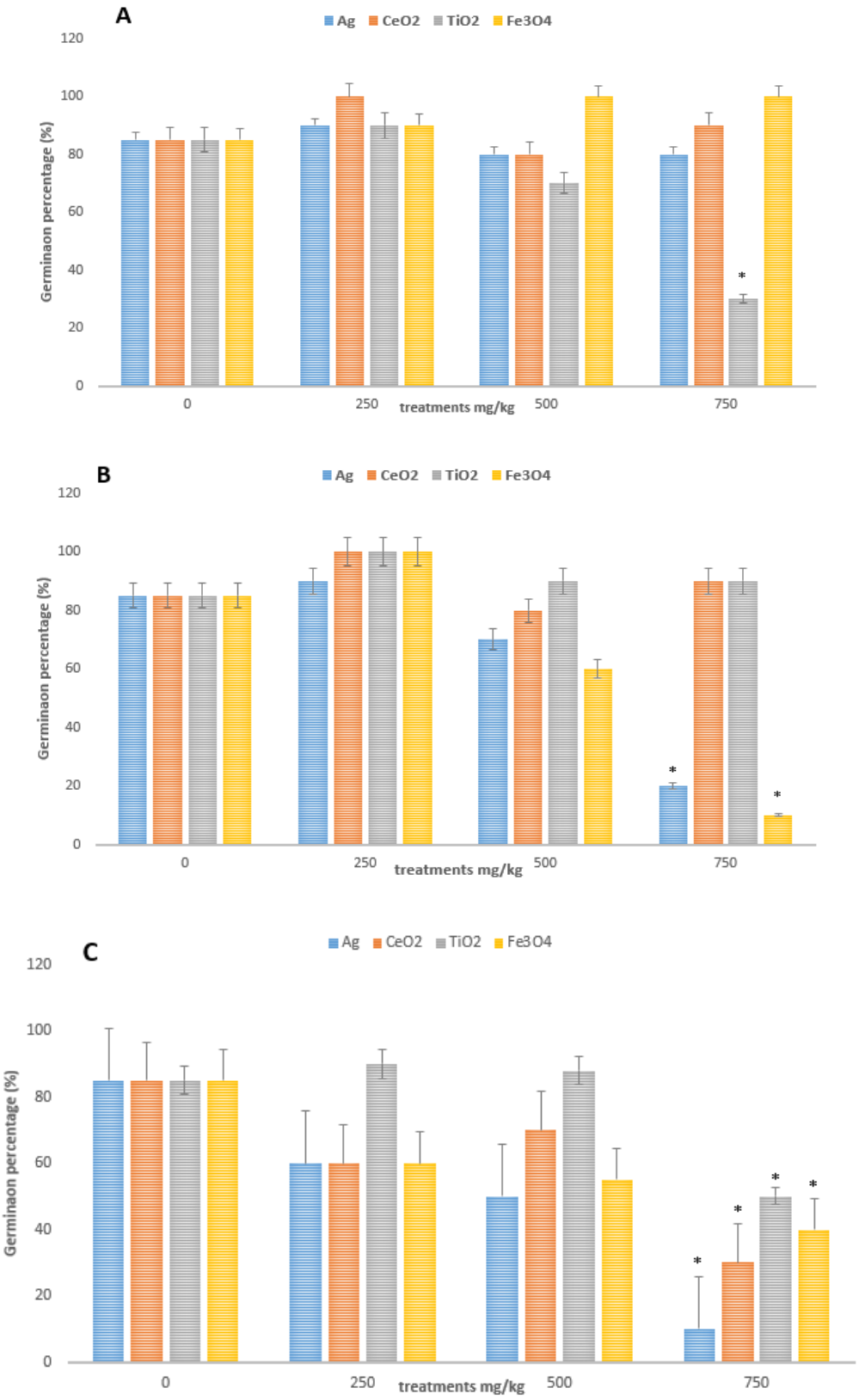

Figure 4-6 Effect of Ag, CeO_2, Fe_3O_4 and TiO_2 NPs at different concentrations (0, 250 500 and 750 mg/kg) on seed germination of A: *A. hippocastanum*. B: *L. esculentum*. C: *Phaseolus vulgaris*. Values are given as mean ± SE, Data are means of ten replicates. Asterisk(s) above bar indicate a significant difference ($p \leq 0.05$).

Figure 4-7 *Aesculus hippocastanum* seedling grown with TiO_2. The figure shows seedlings after germination and growth for eight weeks A: control B: at 500 mg/kg C: at 750 mg/kg. The image showing increasing the concentration of TiO_2 led to slower growth over eight weeks.

4.4.3 Impact of NPs on seedlings growth (distribution and accumulation)

4.4.3.1 Impact of NPs on the growth of *A. hippocastanum* seedlings

To determine whether Ag, CeO_2, Fe_3O_4 and TiO_2 NPs affects the growth of *A. hippocastanum* and model, plants accumulation and dry biomass experiments were carried out as described previously in section (4.4.3).

The results showed an increase in total Ag contents in roots, stem and leaves, of *Aesculus hippocastanum* treated with different concentrations of Ag NPs (250, 500 and 750 mg/kg). The most accumulation was in the roots, then the leaves and the stems, respectively. All treatments increased total Ag concentration in plant tissues. There was a significant increase of Ag uptakes,

especially at 750 mg/kg in stems and leaves, but the increase with the other concentrations was not significant (Figure 4-8).

The results obtained also showed that the majority of Ag NPs were accumulated in the *Aesculus hippocastanum* root. Generally, the concentrations of Ag in the control tissues were lower (or zero) than other treatments. It is apparent from Figure 4-8 that higher uptake appeared to be at concentration 500 mg/kg although it was not significant. In contrast, there were significantly increased of accumulations in root, stem and leaves at 750 mg/kg.

Regarding cerium distribution and accumulation, the results also showed that were accumulations of Ce in the stems and roots at concentration 500, and 750 mg/kg, which reached to 38.65, 57.1 mg/kg in roots and 9.31, 14.45 mg/kg in stems respectively but there was no significant increase in the leaves (Figure 4-9).

The results of *Aesculus hippocastanum* treatment with Fe_3O_4 and TiO_2 also revealed that the highest uptake was in roots and stems. However, there was no significant increase in the leaves at any treatment (Figure 4-10 and Figure 4-11).

In general, the results showed that *Aesculus hippocastanum* was able to translocate Ag from root to above-ground organs (stem and leaf), whereas the translocation of Ce, Fe and TiO_2 to leaves was not recorded.

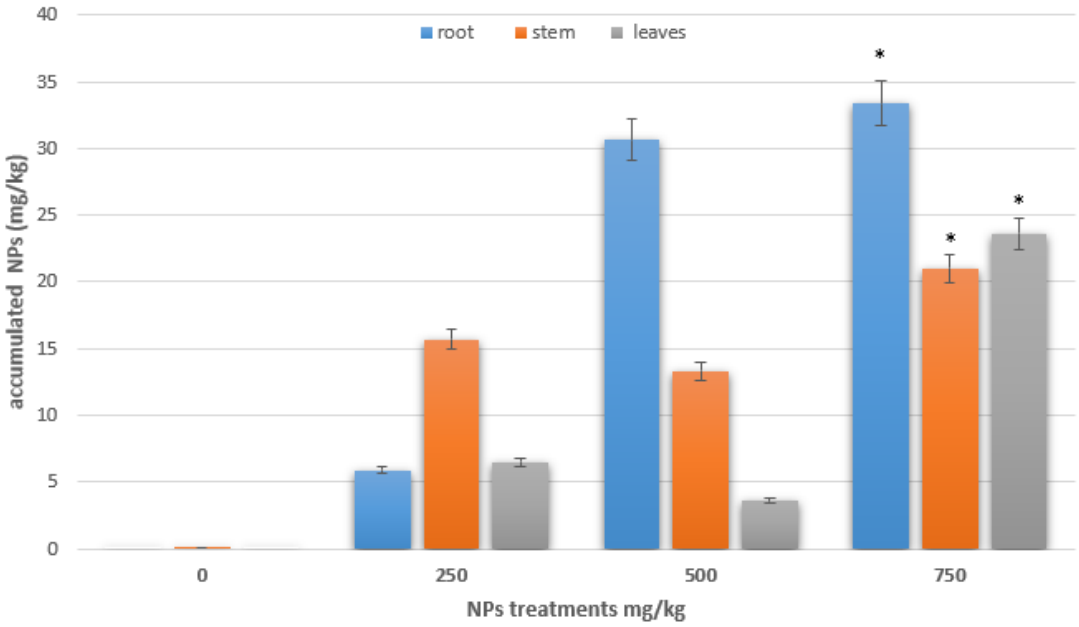

Figure 4-8 Distribution and accumulation of Ag NPs in tissues of *A. hippocastanum.* The figure shows seedlings treated with different concentrations Ag NPs (250, 500 and 750 mg/kg) n = 3 Asterisk (s) represents a significant difference ($p < 0.05$). error bar represents the standard error of the mean.

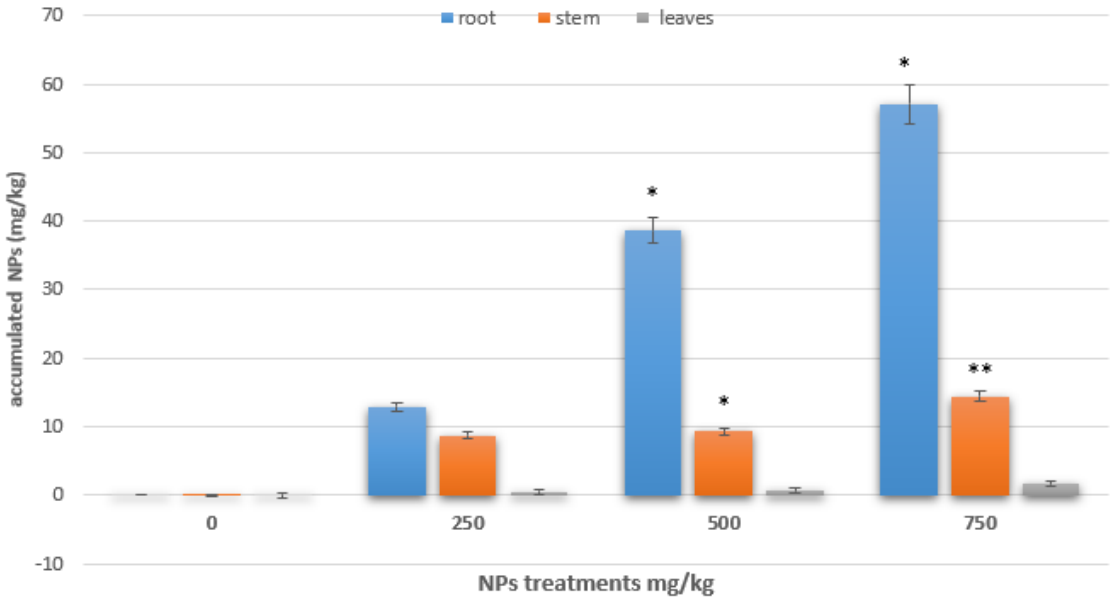

Figure 4-9 Distribution and accumulation of CeO_2 in tissues of *A. hippocastanum.* The figure shows seedlings plants treated with different concentrations CeO_2 NPs (250, 500 and 750 mg/kg) n = 3. Asterisk(s) represents a significant difference ($p < 0.05$). error bar represents the standard error of the mean.

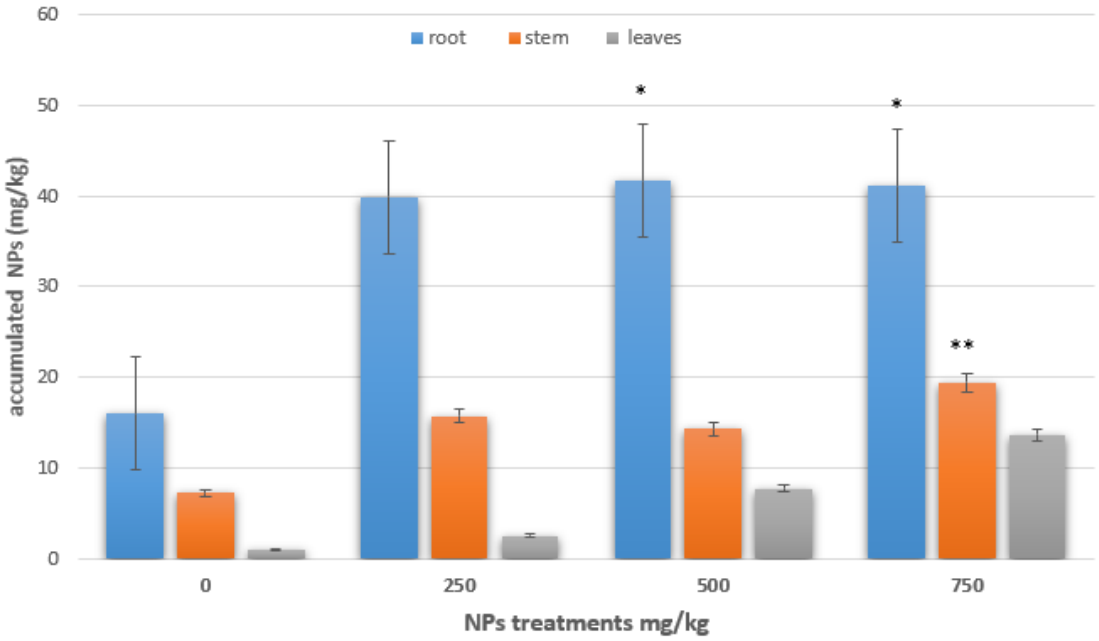

Figure 4-10 Distribution and accumulation of Fe_3O_4 in tissues of *A. hippocastanum.* The figure shows seedlings treated with different concentrations Fe_3O_4 NPs (250, 500 and 750 mg/kg) n = 3. Asterisk(s) represents a significant difference ($p < 0.05$). error bar represents the standard error of the mean.

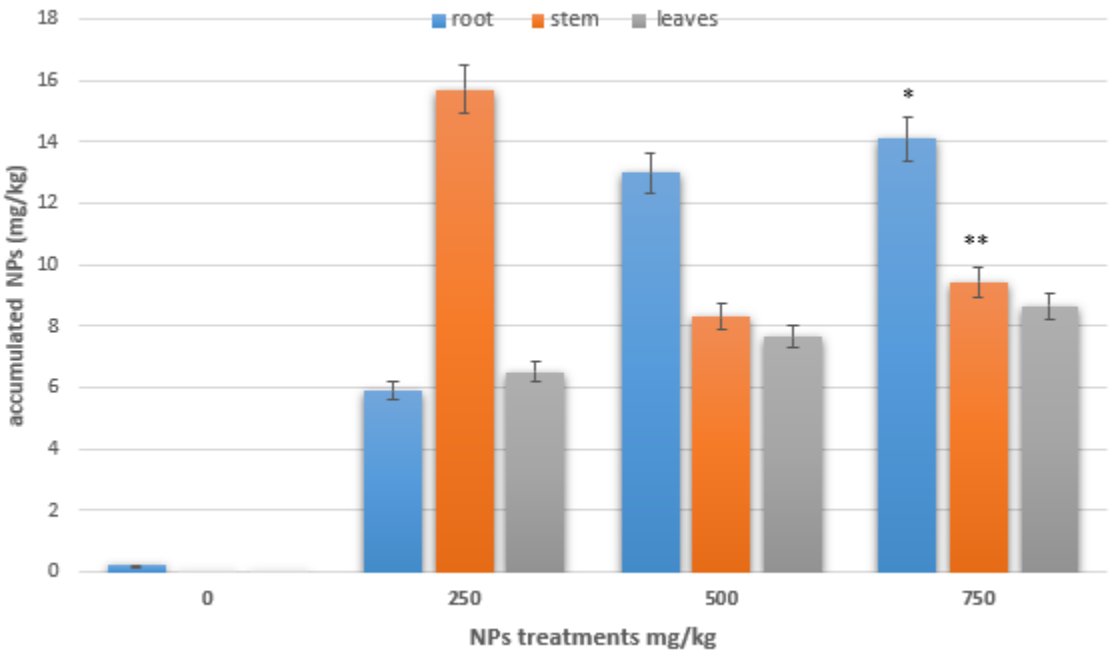

Figure 4-11 Distribution and accumulation of TiO_2 in tissues of *A. hippocastanum.* The figure shows seedlings of *A. hippocastanum* treated with different concentrations TiO_2 NPs (250, 500 and 750 mg/kg) n = 3. Asterisk (s represents a significant difference ($p < 0.05$). error bar represents the standard error of the mean.

The results of the dry biomass and plant growth indicate there was no clear effect for AgNPs on dry weight or elongation or even height, just a small decrease in DW and elongation and height of seedling at concentration 750 mg/kg but not significant (Figure 4-12). A slight increase of 34.53 % and 12% was noticed in DW and height of shoot respectively at concentration 250 mg/kg.

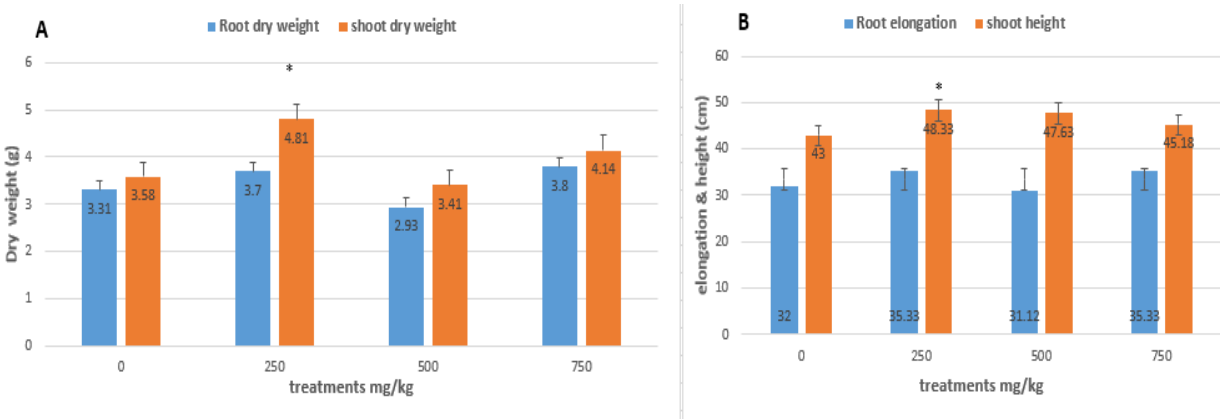

Figure 4-12 Effect of Ag NPs at different concentrations (250, 500 and 750 mg/kg) on *A. hippocastanum* plants grown in pots. Figure A: shows the effect on dry matter of roots and shoots. B: shows the effect on elongation and height. Values are given as mean ± SEM (n=4). Significant differences are marked with * ($P < 0.05$).

Regarding the CeO_2 effect, the results clearly show there was a significant increase in dry weight and height at low concentration (250 mg/kg). P values of dry weight were < 0.05 and 0.001 for root and stem, respectively (Figure 4-13). The titanium also showed positive significant results on dry weight, elongation and height for low concentration and a negative effect when the highest concentration was used (Figure 4-14). In contrast, a high concentration of Fe_3O_4 had a significant positive effect on lengths of roots and stems (Figure 4-15) In addition, there were no significant differences for low concentration of iron NPs, compared with control.

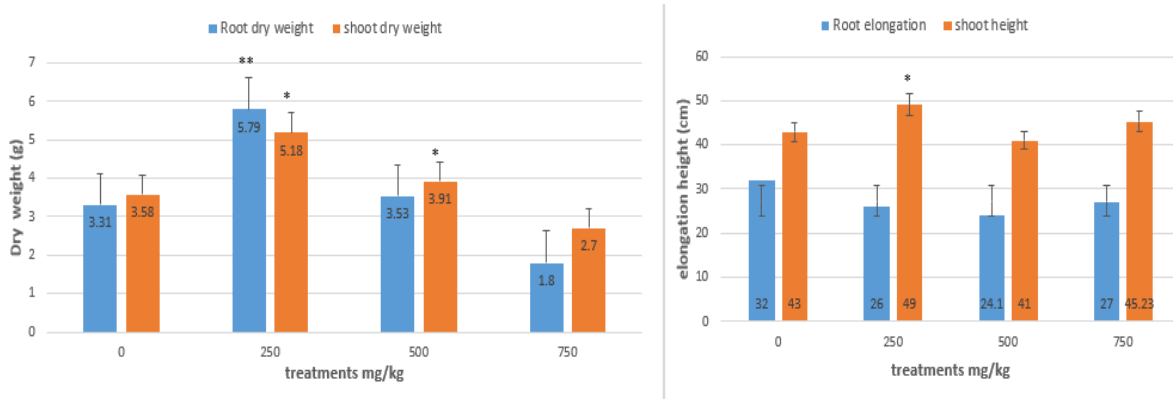

Figure 4-13 The effect of CeO_2 NPs on *A. hippocastanum* plants. The figure shows the effect of CeO_2 NPs at different concentrations (250, 500 and 750 mg/kg) on dry matter of roots, shoots of *A. hippocastanum* plants grown in pots. Values are given as mean ± SE (n=4). Significant differences are marked with *(P < 0.05).

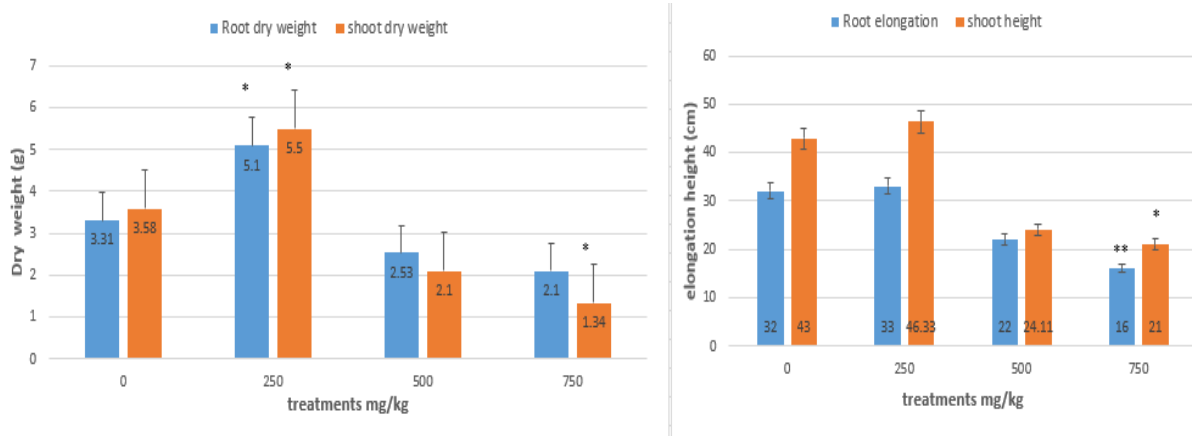

Figure 4-14 The 4effect of TiO_2 NPs on *A. hippocastanum* plants. The figure shows the effect of TiO_2 NPs at different concentrations (250, 500 and 750 mg/kg) on dry matter of roots, shoots of *A. hippocastanum* plants grown in pots. Values are given as mean ± SE (n=4). Significant differences are marked with * (P < 0.05).

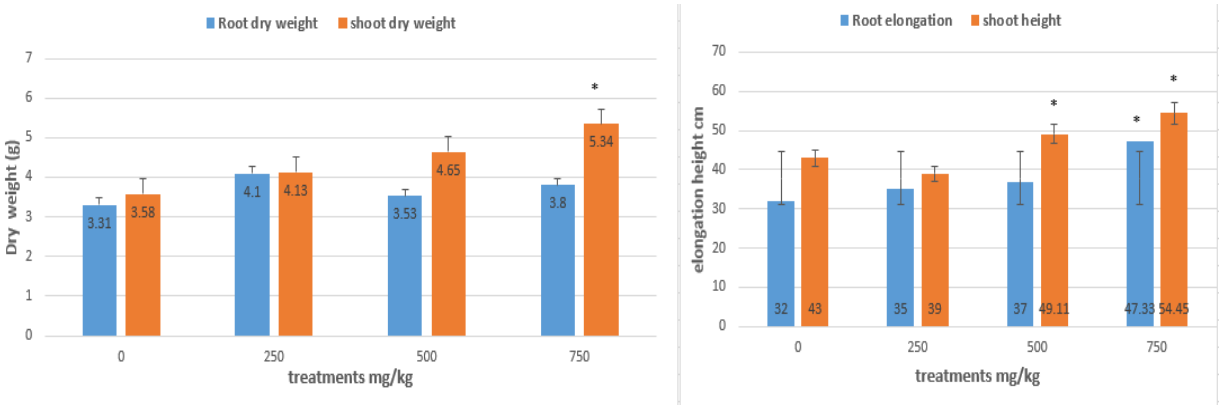

Figure 4-15. The effect of Fe_3O_4 NPs on *A. hippocastanum* plants. The figure shows the effect of Fe_3O_4 NPs at different concentrations (250, 500 and 750 mg/kg) on dry matter of roots, shoots of *A. hippocastanum* plants grown in pots. Values are given as mean ± SEM (n=4). Significant differences are marked with *($P < 0.05$).

4.4.3.2 Impact of NPs on model plants

The distribution and accumulation of NPs in *Lycopersicon esculentum* and *Phaseolus vulgaris* tissues, including their edible parts, could represent a food safety concern. There is no previous study showing the impact of nanoparticles on the *Aesculus hippocastanum*, so we studied it in parallel with above two plants as model plants with the same concentrations to determine accumulation, toxicity and distribution of NPs.

4.4.3.3 Impact of NPs on *Phaseolus vulgaris* seedling growth

The bar charts below illustrate some of the accumulation places in *Phaseolus vulgaris*. Regarding the silver nanoparticles, the results obtained showed that the majority of Ag NP component metals were accumulated in the *Phaseolus vulgaris* root. The mean of concentrations of Ag in the control tissues were lower than other treatments. It is apparent from Figure 4-16 that higher significant uptake was at concentration 500 µg/g with root and stem. A similar

result was found with the root at 750 mg/kg. In contrast, in case of CeO_2 distribution and accumulation, the results showed that were a significant accumulation of Ce at 750 mg/kg even in fruit, also there was significantly increased of accumulation in root and leaves at 500 mg/g (Figure 4-17). Regarding Fe_3O_4, a significant increase of accumulation was recorded with high concentrations (750 mg/kg) in roots, stems and leaves, but no significant increase in fruits was determined (Figure 4-18). In contrast to Fe_3O_4 and CeO_2, with TiO_2 a significant uptake was reported only at low concentration in the stem and root because the growth of seedlings was inhibited the growth of the plant with concentrations 500 and 750 mg/kg (Figure 4-19).

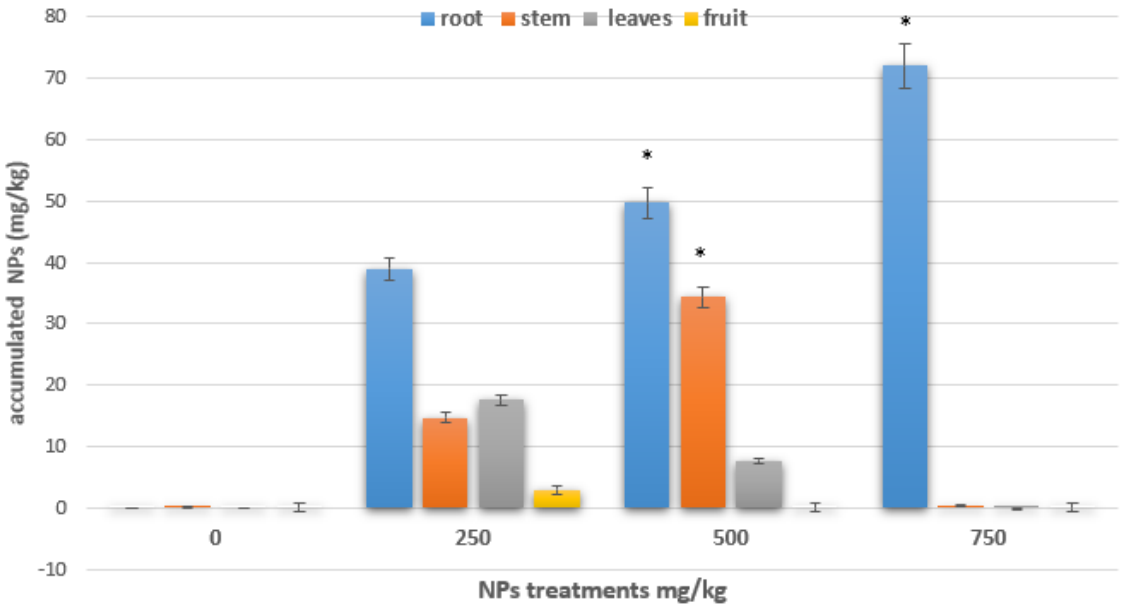

Figure 4-16 Distribution and accumulation of Ag NPs in tissues of *P. vulgaris*. The figure shows plants treated with different concentrations Ag NPs (250, 500 and 750 mg/kg) n = 3. Asterisk(s) above bar indicate significant differences ($P < 0.05$).

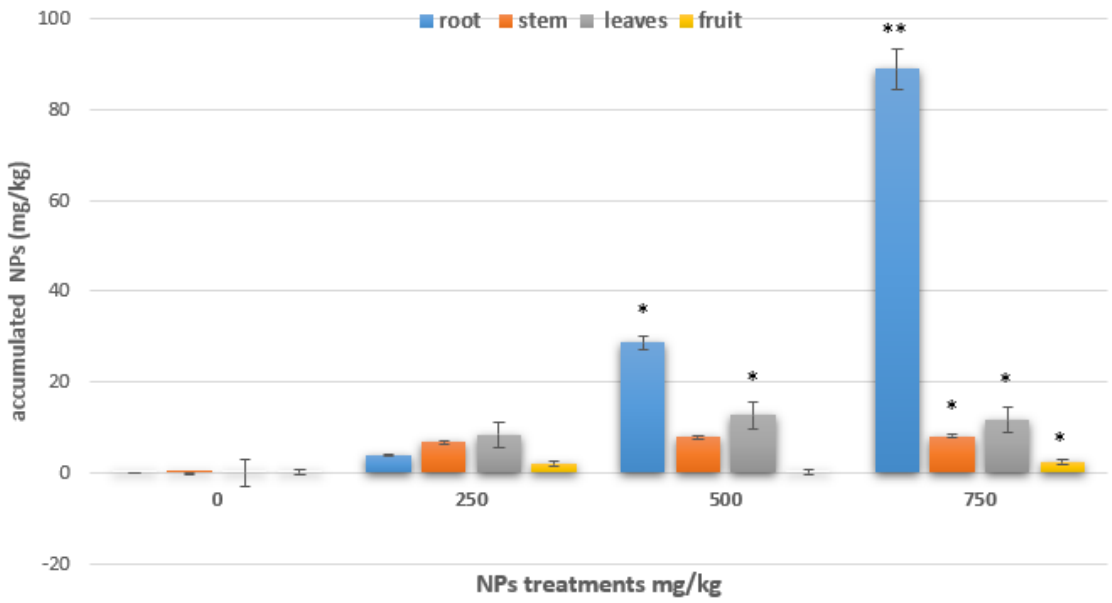

Figure 4-17 Distribution and accumulation of CeO_2 in tissues of *P. vulgaris*. The figure shows plants treated with different concentrations Of CeO_2 NPs (250, 500 and 750 mg/kg) n = 3. Asterisks represents a significant difference ($p < 0.05$). Error bar represents the standard error of the mean.

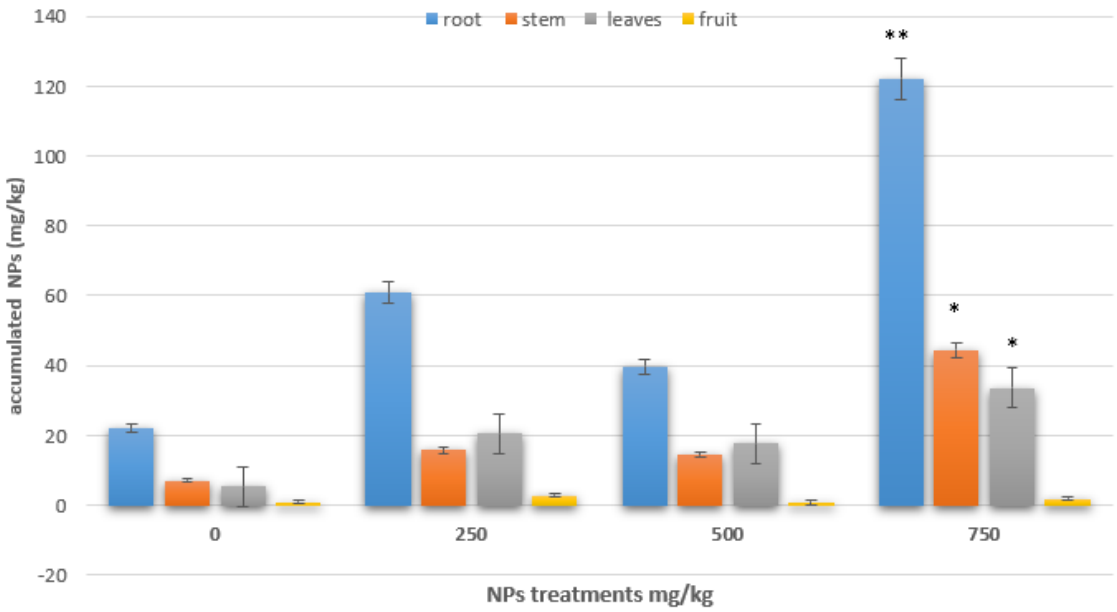

Figure 4-18 Distribution and accumulation of Fe_3O_4 in tissues of *P. vulgaris*. The figure shows plants treated with different concentrations Fe_3O_4 NPs (250, 500 and 750 mg/kg) n = 3. Asterisks represents a significant difference ($p < 0.05$). Error bar represents the standard error of the mean.

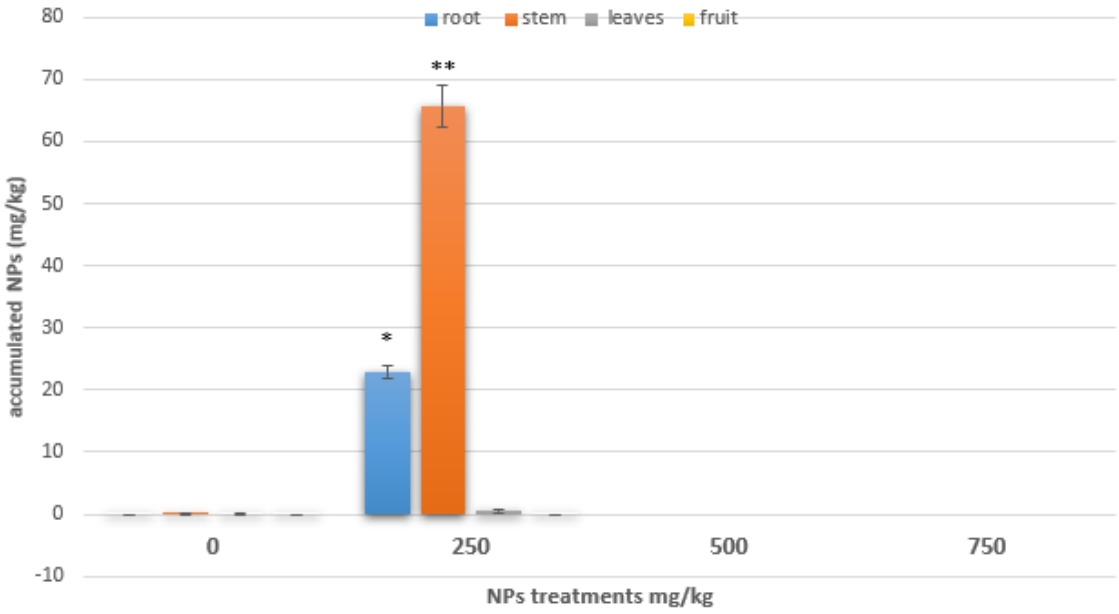

Figure 4-19 Distribution and accumulation of TiO_2 in tissues of *P. vulgaris.* The figure shows plants treated with different concentrations of TiO_2 NPs (250, 500 and 750 mg/kg) n = 3. Asterisks represents a significant difference ($p < 0.05$). Error bar represents the standard error of the mean.

The results of the *P. vulgaris* seedling growth and dry weight indicates there was a clear influence of Ag NPs and TiO_2 on dry weight, elongation and height with seedling exposed to 500 and 750 mg/g (Figure 4-20 and Figure 4-23). The root nodules also did not develop on roots, in particular with the high concentration of silver, and their numbers decreased when the low concentrations of Ag and TiO_2 nanoparticles were used. On the other hand, there were clear nodules on the roots of the control plants (Figure 4-22).

With regard to the effect of iron and cerium NPs on dry weight, elongation and height, the effect of these NPs were positive in increasing and enhancing root, shoot dry weight and elongation of roots and height of shoots were reported as well, (Figure 4-21 and Figure 4-24).

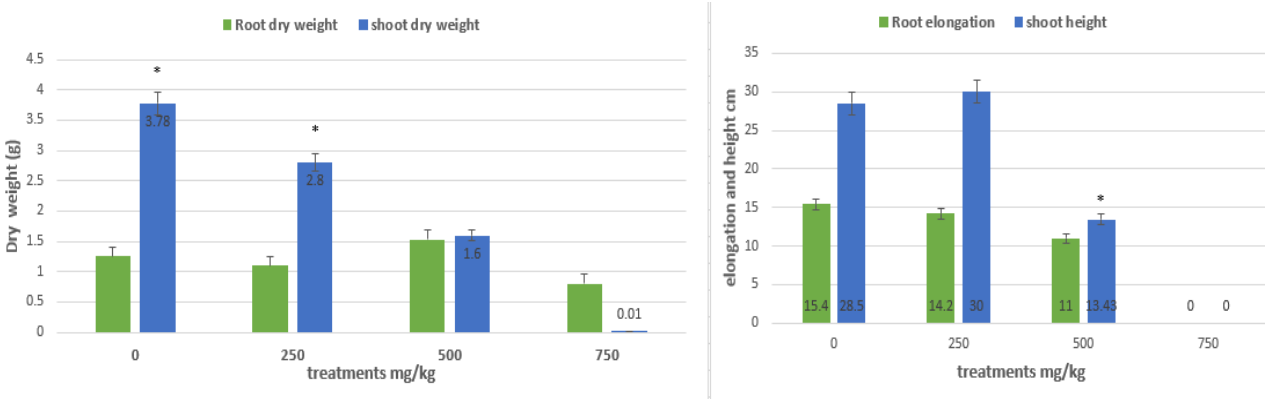

Figure 4-20 The effect of Ag NPs on *P. vulgaris* growth. The figure shows the effect of Ag NPs at different concentrations (250, 500 and 750 mg/kg) on dry matter of roots, shoots and elongation and height of *P. vulgaris*. Values plants grown in pots. Values are given as mean ± SE (n=4). Significant differences are marked at ($P < 0.05$).

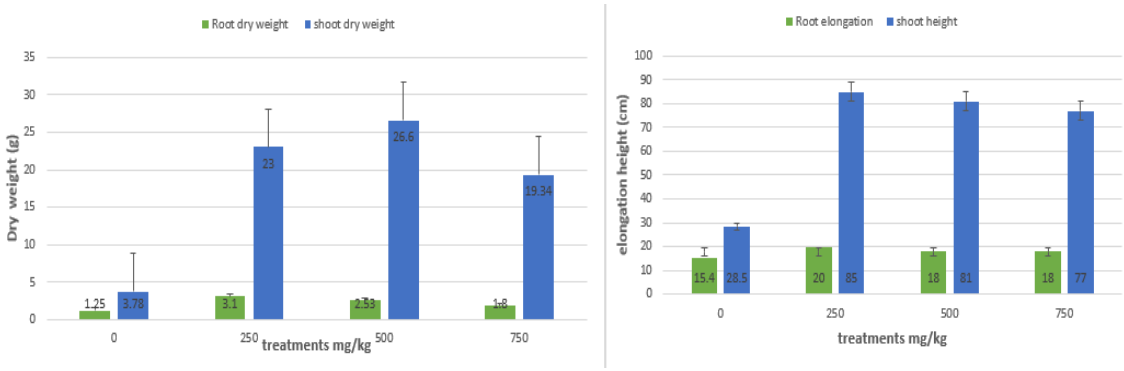

Figure 4-21 The effect of CeO_2 NPs on *P. vulgaris* growth. The figure shows the effect of CeO_2 NPs at different concentrations (250, 500 and 750 mg/kg) on dry matter of roots, shoots and elongation and height of *P. vulgaris*. Values plants grown in pots. Values are given as mean ± SE (n=4). Significant differences are marked at ($P < 0.05$).

Figure 4-22 The root of *Phaseolus vulgaris*. The figure shows root nodules surrounded by yellow circles when untreated with any concentration or type of NPs.

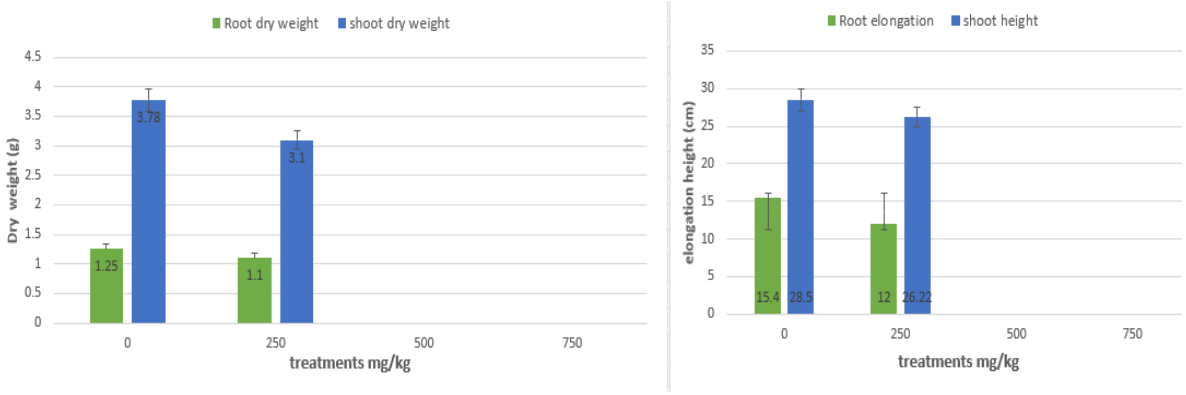

Figure 4-23 The effect of TiO_2 NPs on *P. vulgaris* growth. The figure shows the effect of TiO_2 NPs at different concentrations (250, 500 and 750 mg/kg) on dry matter of roots, shoots of *P. vulgaris* plants grown in pots. Values are given as mean ± SE (n=4). Significant differences are marked with * ($P < 0.05$).

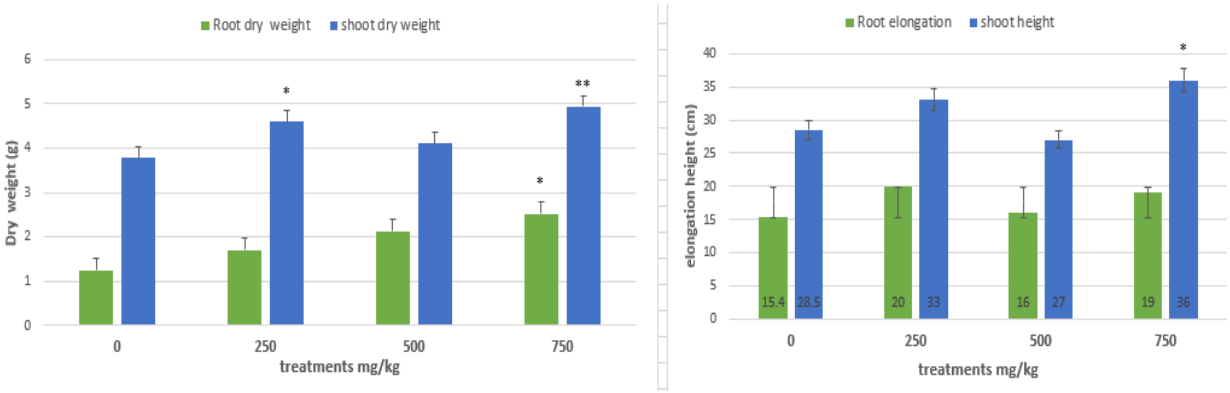

Figure 4-24 The effect of Fe_3O_4 NPs on *P. vulgaris* growth. The figure shows the effect of Fe_3O_4 NPs at different concentrations (250, 500 and 750 mg/kg) on dry matter of roots, shoots of *P. vulgaris* plants grown in pots. Values are given as mean ± SE (n=4). Significant differences are marked with * ($P < 0.05$).

4.4.3.4 Impact of NPs on *Lycopersicon esculentum* seedlings growth

The results of exposing *Lycopersicon esculentum* to NPs showed that the accumulation concentration increased significantly in roots with high concentration when exposed to 750 mg/g. There was a significant increase of Ag uptake likewise in the stem and fruit (Figure 4-25), but it had led to a decline in the shoot and root length as well as in dry weight (Figure 4-29). Regarding cerium, titanium and iron distribution and accumulation in plant tissues, the results also showed increased as nanoparticles concentration was increased in the compost-soil. Interestingly, there were trace elements of cerium and iron in fruit at 4.81 and 5.65 mg/kg, respectively (Figure 4-26 and Figure 4-27). No traces of titanium were recorded in the fruit of *L. esculentum* while the increase was significant in the roots, stems and leaves treated with 750 mg/kg (Figure 4-28).

In general, therefore, it seems that the *Lycopersicon esculentum* was able to translocate Ag, Fe_3O_4 and CeO_2 NPs from root to above-ground organs (stem,

leaf and fruit), whereas the translocation of TiO_2 to fruit was not recorded any significant result.

The results of exposing *Lycopersicon esculentum* to NPs on the dry weight and plant growth indicate there was a significant effect of CeO_2 nanoparticles in increasing the length of roots and shoots and dry weight at the concentration of 500 mg/kg. In contrast, at 250 mg/kg, a non-significant effect was observed on the dry weight of root and shoot even on shoot height (Figure 4-30). In contrast, there was no alteration in root and shoot length or in biomass when TiO_2 NPs (Figure 4-31). In the case of Fe_3O_4 impact on *Lycopersicon esculentum* the results as shown in Figure 4-32, indicated that there is a significant increase in root and shoot length by at least 42% and 29.5%, respectively, with plants treated with a concentration of 500 mg/kg compared to control.

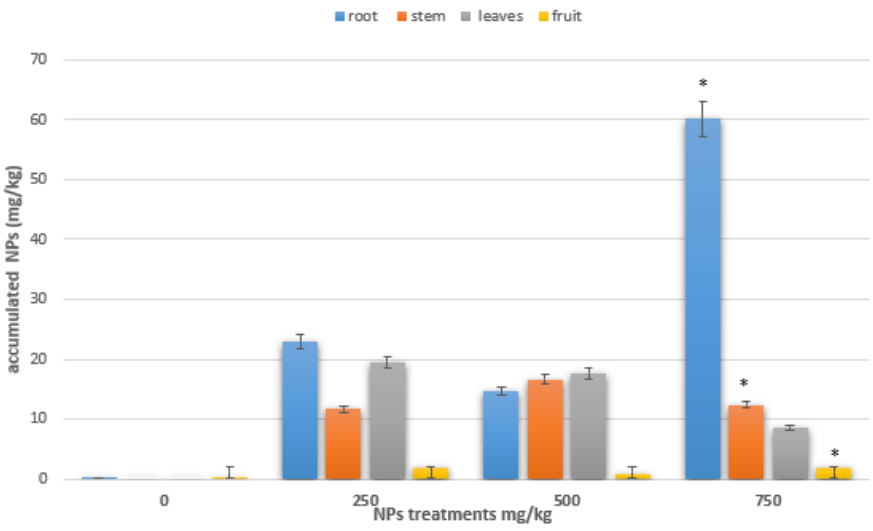

Figure 4-25 Distribution and accumulation of Ag NP in tissues of *Lycopersicon esculentum*. The figure shows plants treated with different concentrations Ag NP NPs (250, 500 and 750 mg/kg) n = 3. Asterisk(s) represents a significant difference ($p < 0.05$). Error bar represents the standard error of the mean.

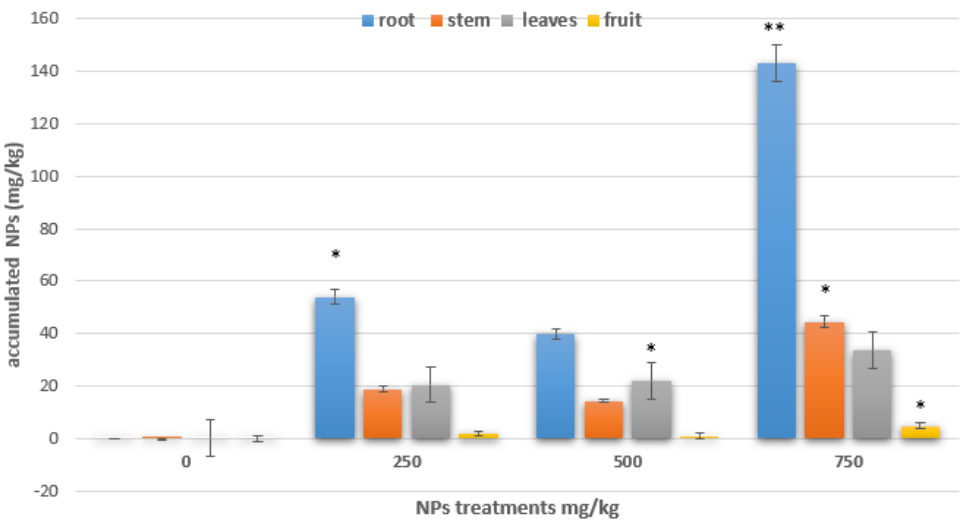

Figure 4-26 Distribution and accumulation of CeO_2 in tissues of *L. esculentum.* The figure shows plants treated with different concentrations CeO_2 NPs (250, 500 and 750 mg/kg) n = 3. Asterisk(s) represents a significant difference ($p < 0.05$). Error bar represents the standard error of the mean.

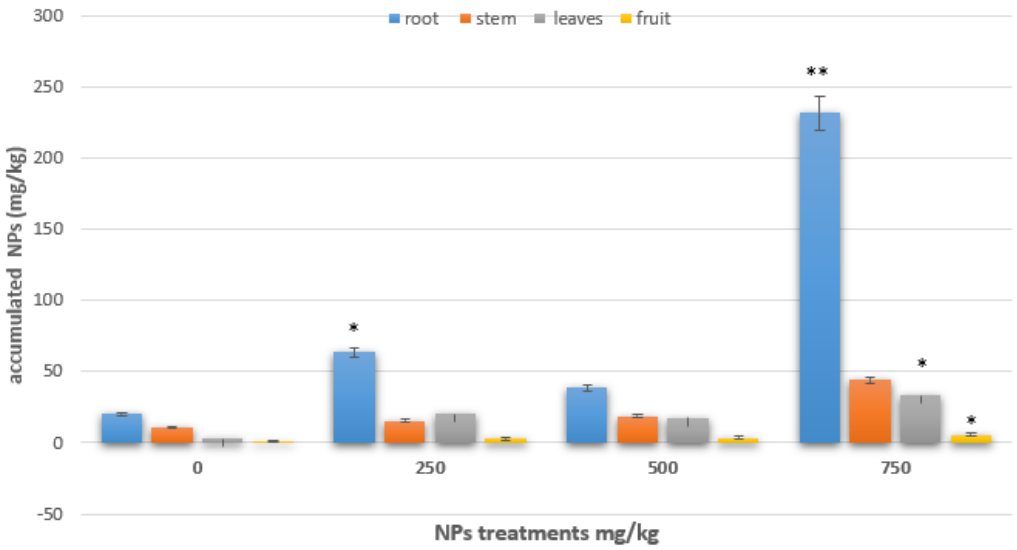

Figure 4-27 Distribution and accumulation of Fe_3O_4 in tissues of *L. esculentum.* The figure shows plants treated with different concentrations Fe_3O_4 NPs (250, 500 and 750 mg/kg) n = 3. Asterisk(s) represents a significant difference ($p < 0.05$). Error bar represents the standard error of the mean.

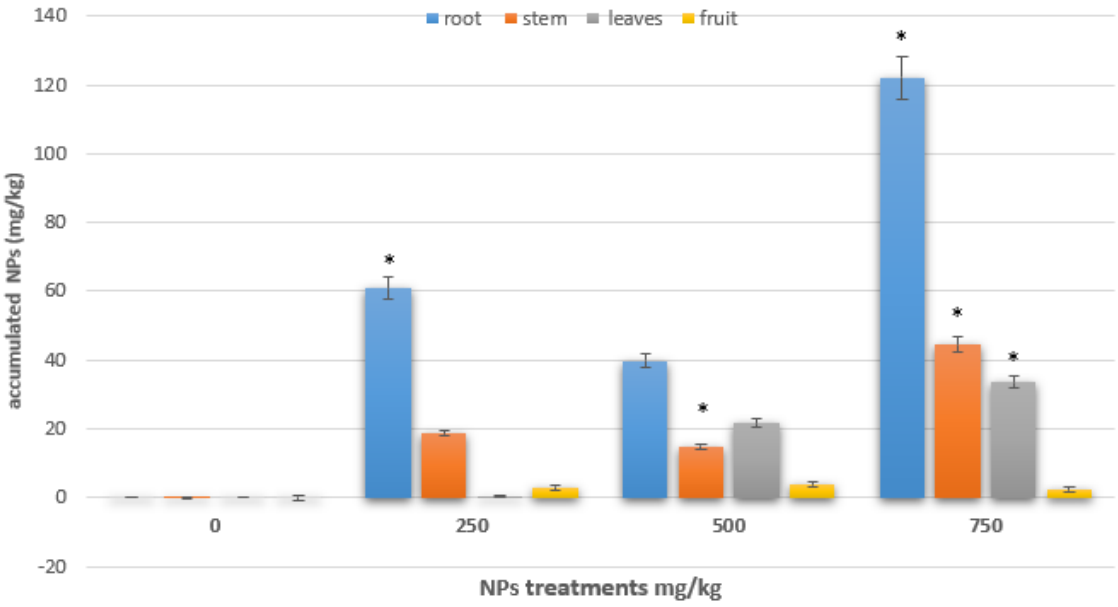

Figure 4-28 Distribution and accumulation of TiO_2 in tissues of *Lycopersicon esculentum*. The figure shows plants treated with different concentrations TiO_2 NPs (250, 500 and 750 mg/kg) n = 3. Asterisk (s) represents a significant difference ($p < 0.05$). error bar represents the standard error of the mean.

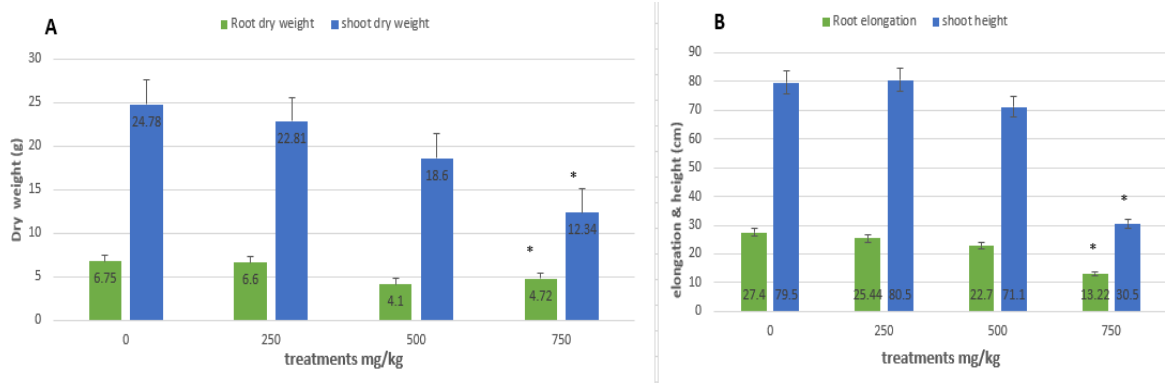

Figure 4-29 The effect of Ag NPs on *L. esculentum* growth. The figure shows the effect of Ag NPs at different concentrations (250, 500 and 750 mg/kg) of L. esculentum plants grown in pots. A: show the effect on dry matter of roots and shoots. B: show the effect on elongation and height. Values are given as mean ± SEM (n=4). Significant differences are marked with * ($P < 0.05$).

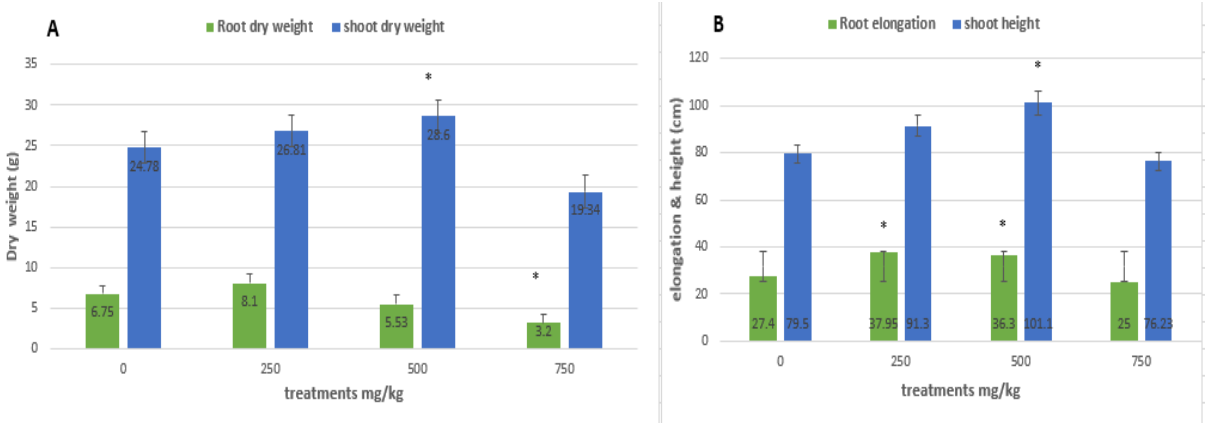

Figure 4-30 The effect of CeO_2 NPs on *L. esculentum* growth. The figure shows the effect of CeO_2 NPs at different concentrations (250, 500 and 750 mg/kg) on *L. esculentum* plants grown in pots A: show the effect on dry matter of roots and shoots. B: show the effect on elongation and height. Values are given as mean ± SE (n=4). Significant differences at ($P < 0.05$).

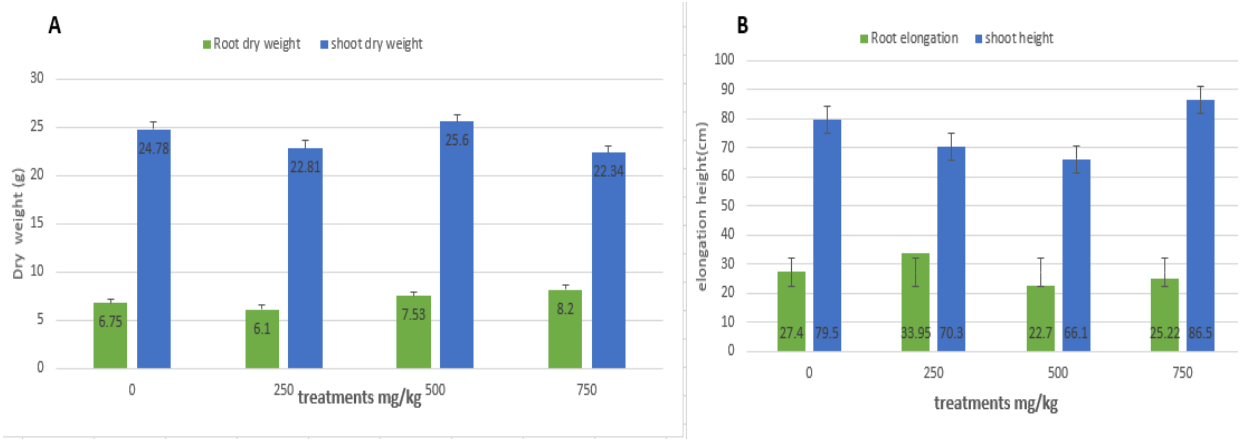

Figure 4-31 The effect of TiO_2 NPs on *L. esculentum* growth. The figure shows the effect of TiO_2 NPs at different concentrations (250, 500 and 750 mg/kg) on dry matter of roots, shoots of *L. esculentum* plants grown in pots. Values are given as mean ± SE (n=4). Significant differences at ($P < 0.05$).

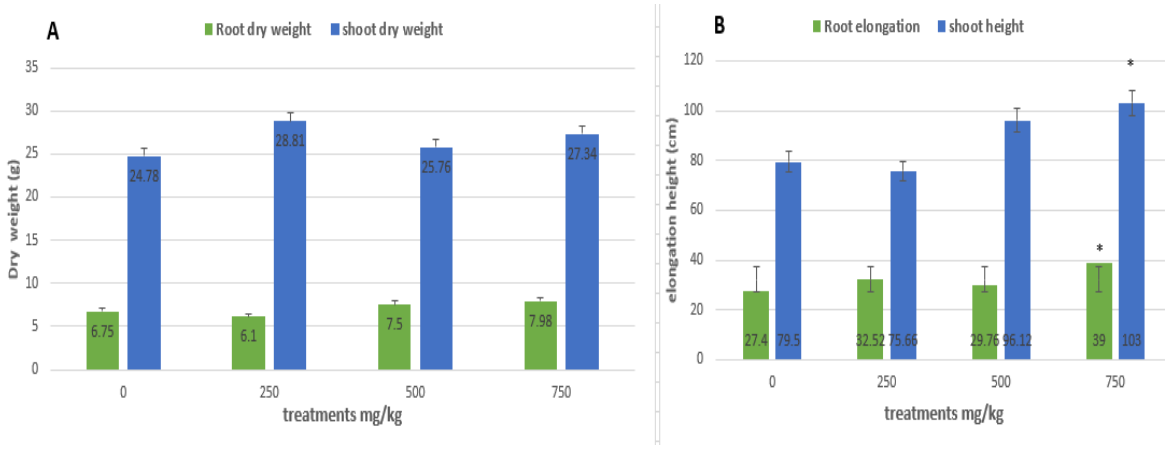

Figure 4-32 The effect of Fe_3O_4 NPs on *L. esculentum* growth. The figure shows the effect of Fe_3O_4 NPs at different concentrations (250, 500 and 750 mg/kg) on dry matter of roots, shoots of *L. esculentum* plants grown in pots. Values are given as mean ± SE (n=4). Significant differences at ($P < 0.05$).

4.4.4 Injection of infected *Aesculus hippocastanum* by NP

As previously described (see 4.3.5.5) *Aesculus hippocastanum* phloem was injected with different concentrations of nanoparticles. Lesion size is considered good evidence of pathogen success or aggressiveness (Thrall *et al.*, 2005). The best results in terms of reducing the number of lesions and the size of the lesion were when titanium used, where the number of lesions decreased by 50% as well as the mean size of the lesions from 6.45 mm to 4.22 mm. This was followed by Ag NPs where the mean size of lesions became 5.34 mm compared to the control of 7.11 mm. The use of cerium did not show any difference or change. In contrast, the effect of iron was negative, where it caused damage to the outer phloem.

4.4.5 Exposing Bacteria to NP

4.4.5.1 Disk diffusion assay

The agar disk diffusion method is not a quantitative but a qualitative assay (Rios, Recio et al. 1988). The NPs showed inhibition zones (IZ) above to 22 mm with Ag NPs agents *P. savastanoi* pv *phaseolicola* compared to the weak antibacterial activity with Fe_3O_4 agents *P. syringae* pv *tomato* (Table 4-3 and Figure 4-36).

Table 4-3 Antibacterial activity of NPs using a disk diffusion assay in triplicate n=3 ± SE. IZ represent an inhibition zone.

Bacterial strains	Mean diameter of IZ mm ± SD, (NPs size nm ˜)						
	AgNP (25)	CeO_2 (25)	TiO_2 (25)	Fe_3O_4 (177)	Ag NPB (76)	AgNP (7)	CeO_2 (7)
P. syringae pv *aesculi*	20.22 ±0.4	7.50±1.3	11.3±0.6	5.70±0.7	9.54±2.6	19.23±1.3	8.59± 0.4
P. savastanoi pv *phaseolicola*	22.14 ±1.6	6.57±0.2	10.43±0.1	3.33±0.9	11.54±2.3	23.21±2.9	7.78± 1.26
P. syringae pv *tomato*	19.79 ±0.41	5.79±1.66	11.84±1.71	2.72±0.48	8.84±1.1	17.55±2.8	5.51± 1.7

Synthesized Ag NPs showed antibacterial activity against all *P. syringae* pv *aesculi* bacteria, especially, with concentration 750 mg/ kg (Figure 4-33), the antibacterial activity including *P. syringae* pv *tomato* and *P. syringae* pv *aesculi* as well, tested by growing bacteria on KBA medium supported by different types of NPs severally at the concentration of 750 mg/kg. Where the KBA supported by Ag NPs inhibit the growth of bacteria of all types (Figure 4-34). In contrast the KBA medium supported by the other nanoparticles did not show any effect and growth was normal.

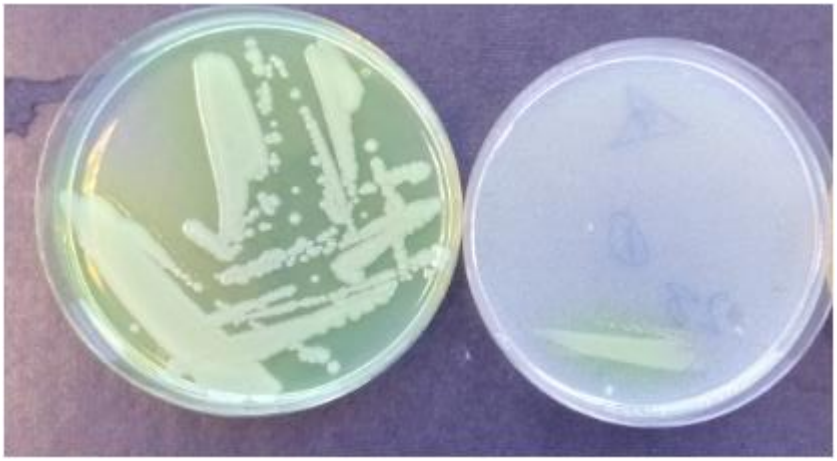

Figure 4-33 The *P. syringae* pv *aesculi* culture. The figure shows Non-growth of *P. syringae* pv *aesculi*, inoculated by streaking method on a KBA medium supported by Ag NPs with a concentration of 750 mg/kg. The petri dish on the right is the treatment, on the left, it is the control.

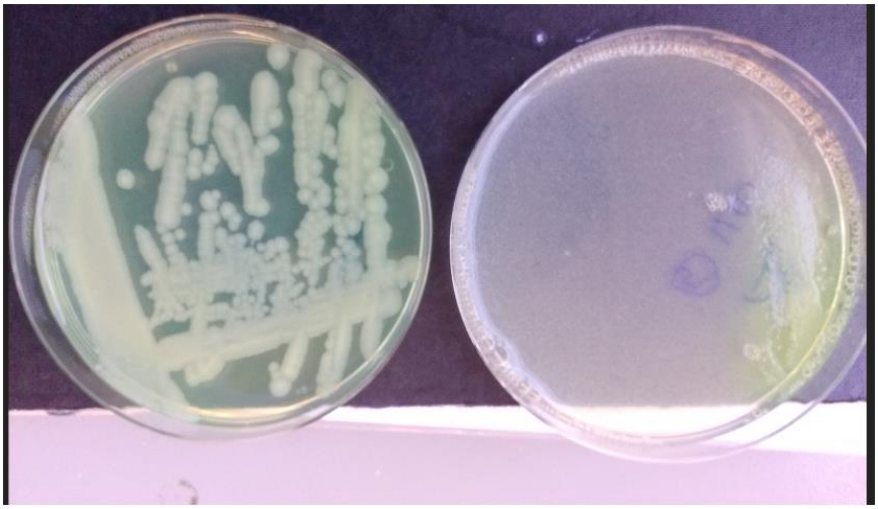

Figure 4-34 The *P. syringae* pv *phaseolicola* culture. The figure shows Non-growth of *P. savastanoi* pv *phaseolicola* on a KBA medium inoculated by streaking method supported by Ag NPs with a concentration of 750 mg/kg. The petri dish on the right is the treatment. other on the left, it is the control.

The results of exposing bacteria to different concentrations of nanoparticles and different times showed the bacteria tended to gather and there was an observed change in the outer shape, especially at 750 mg /l. In high

concentrations or when the time of exposure was increased, after two days, it was not possible to get a clear image of the bacteria. This is evidence of the effect of nanoparticles on bacteria and perhaps the outer surface precisely (Figure 4-35) through which a clear image of the bacterial cell can be observed.

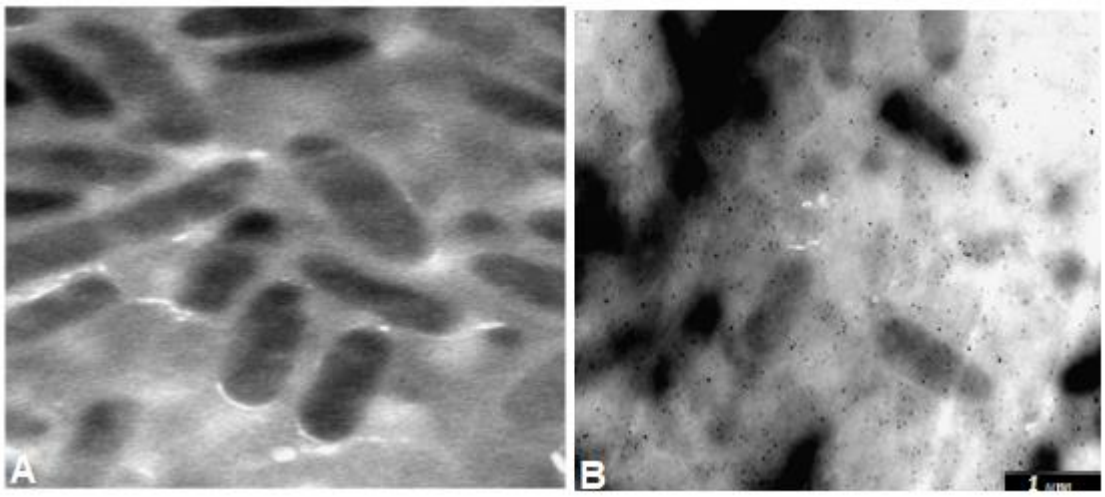

Figure 4-35 TEM images of *Pseudomonas syringae.* The figure shows A: control without NPs. B: *P. syringae* with Ag NPs were exposed to 250 mg/kg for 1 day. In B some agglomeration and change in the size and shape of the bacterial cell can be noted. Bar size in the image is 1 µm and analysis was done at 6 kV.

Figure 4-36 Disc diffusion assay for different types of nanoparticles against *pseudomonas syringae* pv. *aesculi*. The figure shows inhibition zones (IZ) 1: Ag NPs. 2: TiO_2 NPs. 3: control 4: CeO_2 NPs. 5: Fe_3O_4 NPs.

4.4.6 Bacteria diagnosis

The isolated bacterial strains were identified and systematically classified based on their morphological, cultural, physiological and biochemical characteristics, combined with the results of 16S rRNA sequence analysis. Where the tests above have similar results to the original strains, as explained in Chapter 2.

4.4.7 Identification of *bacteria* by restriction fragment analysis of amplified 16S rRNA genes

To ascertain the presence and type of the current bacteria, Sanger sequence was conducted for bacteria strains which re-isolated from infected lesions. 16S rRNA genes from cultures of bacteria gave distinctive banding patterns for each species (Figure 4-37). One band was observed at size 300 bp. The amplification of 16S rRNA genes from bacteria species with the same primer and polymerase gave consistent results when repeated.

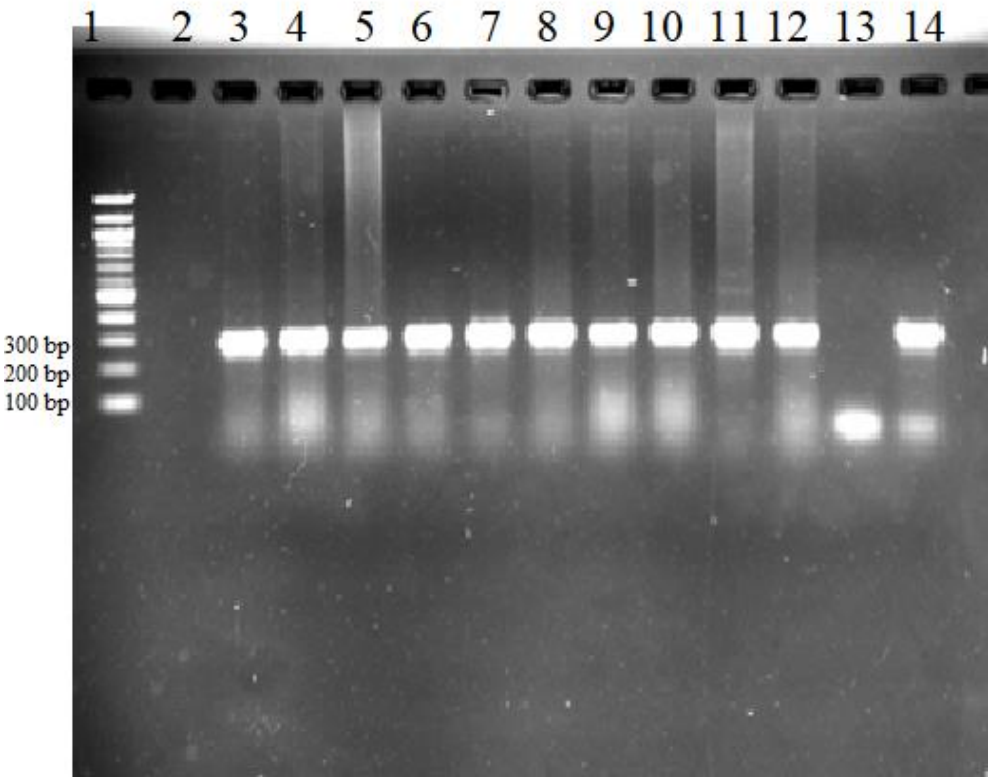

Figure 4-37 Ethidium bromide-stained multiplex PCR products after gel electrophoresis for the 16S rRNA genes. The DNA molecular size marker (100 bp). Lanes: Lane 1 ladder, 3-12, 16S rRNA; 13: control – 14: control + (*E. coli* DNA).

Bacteria clones were tentatively confirmed by the sequencing of 16S rRNA genes (Sanger sequencing Eurofin). The results of the sequence analysis of the 16S rRNA gene from most isolates indicate that the identity of bacteria

matched with *Pseudomonas syringae* strains with more than 60% of the sequences of *Pseudomonas* stored in the NCBI GenBank database (version: BLASTN 2.10.0+).

4.5 Discussion

4.5.1 Characterisation of NPs

Zeta potential is the electrical potential on the sliding outside surface, and it represents a measurement of the stability of the charged nanoparticles. Usually, gathering of the nanoparticles happens when the value of the zeta potential tends to zero (Elimelech *et al.,* 1995). The zeta potential of the NPs maybe showed a little variation, possibly due to variation in types of NPs. The negative charge of Ag NPs and TiO_2 may be the reason for its reaction, and they are a clear influence on the bacteria (Table 4-2). A recent investigation by Spielman-Sun *et al.,* (2017) reported that surface charge affects cellular translocation, uptake and tissue localization in leaves tissues. A study by (Syu *et al.,* (2014), found a large influence of change size, charge and shape of silver nanoparticles on *Arabidopsis* plant growth and gene expression and this impact was significant. The data of NPs size reveal that the variation between the sizes measured with TEM and dynamic light scattering is within the margin of error or because there is a hydrodynamic layer around the nanoparticles when measured by nana sizer.

For the shapes and sizes quantification of the synthesised Ag and CeO_2 nanoparticles at least 100 nanoparticles from each sample were randomly selected throughout the surface of the TEM copper grid and size factor distribution diagrams of the particles were designed and proved (Figure 4-5). TEM examination images corroborated these results and showed the presence of non-uniformly shaped NPs. The electron microscopy images of cerium NPs showed that the results we obtained are very similar to those obtained by Yukui

Rui and his group (Rui *et al.*, 2015) in terms of size and shape of nanoparticles, which have shapes similar to cubes or truncated octahedral.

The hydrodynamic radius of the iron NP was unexpected at 177.92 nm. It may be that a large diameter is obtained because of the inherent magnetic properties in the cores of iron oxide and this feature makes it tend to form long chains (Figure 4-3). The hydrodynamic size values measured by DLS of samples vary a little with TEM in regarding the size values, may because of the water layer surrounding the NPs, which impacts the light scattering measurements (Noureddine *et al.*, 2019).

4.5.2 Impact of NPs on seed germination

Seed germination is one of the most usually used endpoints in nanotoxicological studies. The concept of seed germination has been broadly interpreted, for instance, seed germination has been supposed to have happened when root length is 5 mm long or more (Wang *et al.*, 2012), or a minimum of 1 mm (Lin & Xing, 2007). It is therefore difficult to estimate the growth of seeds in the early stages of germination because it may not last for a long time.

The results showed that different types of nanoparticles have a different influence on seed germination in plant species. From our knowledge, there was not any information described in the literature about the effect of NPs on *A. hippocastanum* seed germination, so this study may be the first which deals with the effect of nanoparticles on *A. hippocastanum*. The negative effect of titanium on seed germination was probably due to changes in the compost-soil microenvironment (Du *et al.*, 2011). In contrast, the positive impact of Fe_3O_4

even though it is simple, maybe because iron is one of the important essential elements for plant growth and development (Sheykhbaglou *et al.,* 2010).

Regarding the influence of nanoparticles on *P. vulgaris* seed germination, the obvious negative effect was with iron and silver nanoparticles at 750 mg/kg. There were no noticeable effects when low concentrations were applied. The findings of the current study are consistent with those of El-Temsah & Joner, (2012) who found similar effects that silver nanoparticles inhibited seed germination of *Lolium* and barley at different lower concentrations.

On the other hand, titanium and cerium nanoparticles did not produce any effect or obvious change. In contrast, the study by (Haghighi & Teixeira da Silva, 2014) indicated the titanium had a positive and stimulant effect for seed growth at concentrations of 100, 200, and 400 mg/kg. Similar results were reported by Vittori Antisari *et al.,* (2014) to our Ag findings despite using a low concentration (20µg/kg). For *L. esculentum* seeds, the most obvious negative effect was at the 750 mg/kg concentration, mainly when Ag nanoparticles were used, causing a clear inhibiting of growth, reaching 80%. The different impacts of NPs on seed germination have been widely reported. For example, in the presence of ZnNPs, Cu NPs, ZnO NPs, CeO_2 NPs, Ag NPs, and Si NPs inhibitory effects on seed germination in different plants were detected as well as the positive effects (El-Temsah & Joner, 2012; Lin & Xing, 2007; Lin *et al.,* 2009; Pariona *et al.,* 2017; Siddiqui & Al-Whaibi, 2014). However, no data are available with the same species; therefore, more studies are needed. Definitely, alterations in the medium, species, size might be considered for the huge difference in results (Anjum *et al.,* 2013).

Some researchers reported the significant effect of pH on the growth and germination of seeds, including the seeds of *L. esculentum* (Thomas, *et al.* 2014), but for our study, we tried to remove this factor by maintaining pH (see 4.3.5). So, there is no doubt about pH, because it was a constant even with the control.

4.5.3 Impact of NPs on seedlings of *Aesculus hippocastanum*

The results of *A. hippocastanum* treatment with Ag NPs revealed there was high uptake by the root, stem and leaves compared to the control. However, to the best of our knowledge, no published report has been found so far using Ag NPs with *A. hippocastanum* or even other types of nanoparticles. In terms of the beneficial presence of nanoparticles or silver in some parts of the plant, proves the possibility of the arrival of silver nanoparticles in the stems and leaves and the possibility of using it the future for the transfer of drugs or as a delivery agent. Similar results reported by (Thuesombat *et al.,* 2014) found an increase in the silver element in the leaves of *Oryza sativa,* despite its clear phytotoxic effect on the rice seedlings. Similar results were also found in another study on *Arabidopsis* where Ag NPs improved root growth and an increase in the accumulation of proteins that are associated with the cell cycle, chloroplast biogenesis, and carbohydrate metabolism (Syu *et al.,* 2014). However, several studies show that significant differences do exist, albeit the findings are slightly different (Agnihotri *et al.,* 2014; Lakshmanan *et al.,* 2018; Metz *et al.,* 2014; Zuverza-Mena *et al.,* 2016).

For example, in *Arabidopsis*, both stimulatory (Syu *et al.,* 2014) and inhibitory (Stampoulis *et al.,* 2009) effects on growth were recorded. Certainly, changes

in the medium, species and NPs size might consider for our differing outcomes (Anjum *et al.,* 2013; Doolette *et al.,* 2015).

The finding related to Fe_3O_4 is consistent with past study results by (Ghafariyan *et al.,* 2013) which reported that superparamagnetic Fe NPs at low concentrations significantly increased the chlorophyll contents in sub-apical leaves of *Glycine max* tested under hydroponic conditions in plants grown in greenhouse condition. This study suggested that *G. max* could use Fe NPs as a source of Fe and decrease chlorotic symptoms of Fe shortage. The influence of using Fe NPs was similar to that of an actual Fe source for the plants. In another study, (Delfani *et al.,*2014) examined foliar application of Fe NPs at 500 mg/kg on black-eyed peas, they found there was a significantly increased number of pods per plant, weight of seeds, and reported increase of iron content in leaves by 34% compared to the control (Delfani *et al.,* 2014). This study provides an important opportunity to advance the understanding of the relationship between *A. hippocastanum* and four types of NPs which were used in this study.

4.5.4 Impact on model plants

The distribution and accumulation of NPs in *L. esculentum* and *P. vulgaris* tissues, including their edible parts, could represent a food security concern.

There is no previous study that shows the impacts of nanoparticles on *Aesculus hippocastanum,* so two plants of economic value were used as a model for the study of NPs impact on *A. hippocastanum,* and the same

nanoparticles were used. The model plants selected have a susceptibility to pathogenic bacteria of the same type (*Pseudomonas*) that affects the *Aesculus hippocastanum*. To determine the accumulation, toxicity, distribution of NPs, we performed this study.

The results showed significant increase of accumulations for all types of NPs, these results match those observed in earlier studies which showed that roots could be the main route of the plant's exposure to NPs, so the main accumulation happened in roots (Anjum *et al.,* 2013; Bradfield *et al.,* 2017; Vittori Antisari *et al.,* 2014). An inhibitory effect of titanium and silver nanoparticles was found on the length, height and the dry weight of *Phaseolus vulgaris* plant. this may be explained due to the effect on the biological effectiveness of Ag NPs and TiO_2 which inhibited the growth of the bacteria which form root nodules that associate with symbiotic nitrogen-fixing bacteria, which in turn reflected on the composition of protein, which is an important element of the growth and development of the plant. The influence of the TiO_2 NPs might result from the minor presence of the NPs in cells or accumulated on the cell walls, which might cause changes in the soil microenvironment (Larue *et al.,* 2014; Vittori Antisari *et al.,* 2014). Another study reported similar results using seedling of *Oryza sativa* exposed to silver NPs, (0.2, 0.5, and 1 mg/L) which showed significant decreases in shoot and root fresh weights as well as root elongation (Nair & Chung, 2014).

The positive results obtained from the effect of cerium and iron on *Lycopersicon esculentum*, which showed significant increases in the shoot and root fresh weights as well as shoot height, may be expected but not with the concentrations used. These positive results of CeO_2 and Fe_3O_4 effect on

Lycopersicon esculentum are consistent with those of other studies (Ma *et al.,* 2016; Rossi *et al.,* 2016). Fe_3O_4 increased root growth for both elongation and dry matter parameters probably because iron is one of the fundamental elements for plant growth, and therefore, the application of Fe_3O_4 on *Lycopersicon esculentum* plants increased the dry weight, and yield which is similar to previous studies on soybean (Sheykhbaglou *et al.,* 2010).

Although the estimation of the influence of NPs on plant nutrient content is in its starting stages, it is very possible that NPs could modify the nutrient profile of food crops and influence the plant's absorption of other essential elements (Gardea-Torresdey *et al.,* 2014).

The possible error factor in calculating the accumulations of NPs is likely to be rare because the experiments here were dependent on a dry weight calculation and the dry weight of any plant body remains constant, but wet mass has variable mass depending upon the water present in the plant organ. So dry weight measurement is useful to determine plant biomass or determine elements (Dwivedi *et al.,* 2015). As is known, plants are the primary producers of biomass on land. Therefore, studying the impact of stress and disease is necessary. Surprisingly, no differences were found in leaf or fruit accumulation in the plants which were treated with Ag NPs, it may be the concentrations of Ag NPs or other NPs in the control tissues were lower or zero than the ICP-OES ability to detect the elements (instrument detection limited).

The positive influence of Ag NPs may be due to the high surface area and the fraction of outside atoms; which as a result have high antimicrobial effect compared to the bulk silver NPs (Nair & Chung, 2014). Many studies have reported the impacts of TiO_2 on bacteria (Larue *et al.,* 2014). Generally,

variations in time, NP type, species and medium might affect the uptake of NPs (Anjum *et al.*, 2013; Gao *et al.*,2017).

In the current study, where different size and concentrations were tried, the results shed some light on using NPs with *A. hippocastanum* and help us to understand the possibility of using these NPs in the future in different functions such as to trigger defence responses, activated by pathogens or carrying RNA or DNA to be delivered to plant cells for their genetic transformation or any wanted drug (Parisi *et al.*, 2015).

4.5.5 Identification of bacteria by restriction fragment analysis of amplified 16S rRNA genes

PCR and running DNA on the agarose gel was used to discover whether v4 region of bacterial 16S rRNA is detectable in the isolated bacteria strains and we found the bacteria in all of these lesions. The negative and positive controls (DNA of *E. coli*) were used, so the absence of bands detected in the negative controls reveals that in protocol environmental contamination did not happen. In addition, current results confirmed that the DNA extracted from bacteria succeeded and this result was confirmed by the first genome sequences (Sanger sequencing).

4.5.6 Disk diffusion assay

Although the agar disk diffusion (Kirby-Bauer disk diffusion) method is a qualitative technique it gave a clear indication for Ag and TiO_2 biological efficacy (Rios & Villaw, 1988). Usually, if antibiotic or active materials

prevents the bacteria from increasing or kills the bacteria, there will be an area around the plate where the bacteria have not grown enough to be obvious; this is called an inhibition zone (IZ). We reported the bigger inhibition zone with Ag NPs then with TiO_2 against *P. syringae* pv. *aesculi*. However, the Fe_3O_4 and CeO_2 showed low antibacterial activity against *Pseudomonas syringae* pv. *aesculus*. The effect of Fe_3O_4 and CeO_2 may be slight due to the small halo around them as a result of changing in the bacterial growth media. There is no complete inhibition zone for growth as is the case with Ag and TiO_2 NPs (where a weak bacterial growth zone can be seen) (Figure 4-36). The findings of the current study are consistent with those studies which reported the high surface area and the fraction of outside atoms of silver nanoparticles give it high antimicrobial effect (Agnihotri *et al.,* 2014; Nair & Chung, 2014). These results indicate that the Ag NPs and maybe TiO_2 have promising antibacterial activity against *Pseudomonas* bacteria. The study of *Pseudomonas syringae* surviving against heat shock and pH is considered a complement for the previous study, that reported *P. syringae* survived cold and seasonality of infection for several years in sterile, refrigerated water without losing viability or pathogenicity (Laue *et al.,* 2014). Outcomes of this study can be adopted as a source for predicting the impact of studied NPs on plants and *Pseudomonas* bacteria.

5 Chapter 5: General Discussion and Conclusions.

5.1 Overview

The European *Aesculus hippocastanum* tree is an important shade plant around the world, in particular in the UK and it also has various pharmaceutical uses. However, little is known about the interaction between the tree and the bleeding canker disease. There has been a rapid global spread of *Pseudomonas syringae*, the causal agent of bacterial canker, which underscores our need for a deeper understanding of pathogen virulence and host specificity. There is also, the possibility of *P. syringae* spreading to other important crops or plants with potential to damage humans lives and other organisms or plants which will have a greater impact on the ecological balance of our planet. *Aesculus hippocastanum* can be used as a model system to understand the interaction between the tree and the bacterium, which may give insights into how diseases can be controlled in other plants.

The mechanisms of adaptation and tolerance of plants to environmental stresses and disease has been studied for a long time by scientists, with the ultimate aim of enhancing stress-tolerant crops (Jenks, 2007; Sharma *et al.*, 2012; Alzwiy, 2013; García-Sánchez *et al.*, 2015). A large amount of research has been conducted to study how plants react to different stresses and whether these can be classified as general and specific responses. The general responses are those produced by signals and signalling components that are shared by multiple pathways in plant cells, whereas the specific responses are those that are produced by factors unique to that particular stress (Jenks, 2007; Alzwiy, 2013). It has become clear that many signalling pathways interact to form a

complex system (Bostock, 2005; Swindell *et al.*, 2006). These networks are linked by different proteins such as kinases, phosphatases and by transcription factors that play very significant roles in plants (Halford *et al.*, 2004; Fujita *et al.*, 2006; Hennig *et al.*, 2010). Moreover, plants have internal defences to plant diseases and to other damaging factors such as drought and physical damage. These are undoubtedly linked to changes in genes expressions, leading to proteins being involved in the immune response. The applications of nanoparticles are now widely studied and used although human activity and pollutants release a lot of accidental nanoparticles into the atmosphere, water and soil. So, considering the positive or negative impact on plants and bacteria has become of undeniable benefit.

In the current study, model plants were also used to study the effects of environmental conditions alongside *A. hippocastanum*, and to determine the accumulation, toxicity and distribution of nanoparticles (NPs). This study was carried out in parallel to the study of *A. hippocastanum*, which, being perennial, requires seedlings in the glasshouse for experimental manipulation rather than mature trees. Therefore, *Lycopersicon esculentum* and *Phaseolus vulgaris* were selected as model plants because of their economic importance for the food and agriculture industry and the fact that the studies could be made easily and quickly on more mature plants while *A. hippocastanum* seeds were collected. Seeds germinate, and seedlings grow fast. The susceptibility of these model plants to *Pseudomonas syringae* was reported. Moreover, the results of the model plants could be compared to *A. hippocastanum* to avoid any mistakes with the real plant.

5.2 Plant vitality assessments

The result of artificial leaf inoculation showed that no bacterial infections occurred on the leaf blade except on the main veins, and any infection on the lamina recovered a few days after developing, maybe because the leaves contain aromatic compounds that inhibit the growth of bacteria and lack abundant lignin which is considered stimulating to bacteria growth (Avtzis *et al.*, 2007; Green, 2012; Dudek-Makuch and Studzińska-Sroka, 2015). This feature can be exploited in the short term in the extraction of active substances from horse chestnut leaves to potentially combat pests or reduce the effects of diseases that infect the plant itself or other plants. Another explanation may be that bacteria have genetic code for the degradation of plant-derived active compounds, such as lignin derivatives and other phenolic complexes. These pathways may enable *P. syringae* to use aromatic substrates as carbon sources, particularly those derived from the woody plant's tissues (Aznar *et al.*, 2015;; Green *et al.*, 2012). It would be useful to investigate inhibiting this target gene or genes to reduce the virulence of bacteria.

The outcome of bacterial inoculation shows that the artificial inoculation in the greenhouse caused a tan/black strip that dispersed along the bark under the stem epidermis towards the bottom of the *A. hippocastanum* seedlings. This is presumably a mark of the passage of the bacteria through the sieve element or parenchyma cells of the phloem, which is the direction of the flow of the plant nutrients that are manufactured in the leaves, as well as evidence that the bacterial infection is superficial, in the bark only. The presence of bacteria was confirmed by different methods such as re-isolation and its development on selective medium and then compared with the original bacterial strain. The

results in this study are consistent with the results of past studies by Steele *et al.,* (2010) who found that lesions produced in the cortex and phloem extended into the cambium to cause cankers, but there was no indication of necrosis in the xylem tissues.

Therefore, the occurrence the bacteria in a specific region such as the bark of the plant helps to reduce or stop its spread, so the experiments carried out in this study, especially heat shock with bacteria, may be useful in developing protocols for eliminating bacteria in these infected areas of the plant. This can be done after studying the effect of heat on the phloem tissues, or even if the infected region in tissue is damaged, it may be a better option than allowing bacteria to spread throughout the entire plant.

5.3 Protein extraction

During any proteomic analyses, sample quality is a crucial determinant, and so the protein extraction method is of prime importance. The typical extraction method should reproducibly capture the most comprehensive repertoire of proteins possible, at the same time, minimising degradation and contamination by non-proteinaceous compounds. Due to the diverse biochemical properties of cellular proteins, including their size, charge, susceptibility to proteolysis, ligand interactions, hydrophobicity and subcellular localization, no single protein extraction protocol can capture the complete proteome (Isaacson *et al.,* 2006; Faurobert *et al.,* 2007; Rao *et al.,* 2018). Protein extraction in the current study at first faced many challenges when attempting to using normal methods or commercial kits. It did not run ‘normally’ within a native gel. There is no extensive information available in the literature regarding the extraction.

Aesculus hippocastanum can be considered to be a recalcitrant plant because it contains many aromatic and phenolic compounds (Otajagić *et al.,* 2012). Therefore, finding a protein extraction method is harder than with some plants. There is thus a need to find a cost-effective, efficient, reproducible and simple protein extraction procedure for proteomics studies if there are many samples to be detected.

The initial results of this study on protein assessment may hopefully shed some light in helping to understand which environmental factors are associated with bleeding canker disease. However, preliminary results showed there was a significant effect of drought stress on the protein content of the plant, while damage stress produced no noticeable effect on the protein content although it did have a clear and significant impact on shoot height and root length. Generally, in this study, the TCA/acetone protocol was superior to the phenol protocol and detergent protocol because of the features of the precipitants mentioned (see Chapter 2), and it produces a good result and needs less time to complete. All these made the TCA/acetone protocol fit for *A. hippocastanum* samples and was chosen for the extraction of proteins in this study. The outcome of protein extraction may pave the way for making related future studies more obvious.

For the in-gel digestion methods, the main challenge was to avoid contamination by keratin or other plant vacuole components which commonly occurs when the cell vacuole is damaged. So, all sample preparation steps were carried out in the laminar hood to avoid contamination from dust which includes skin cells, which contain keratin. Although the method is not used with all samples, the success of the procedure for the first time with our real

plant opens the door for future use, with more pure *A. hippocastanum* samples or for use in *A. hippocastanum* tissue cultures, where further controlled conditions prevail, away from diseases and external influences.

5.4 Sample collection and maintenance

The work presented in this thesis provides new insights into keeping and storing samples. The failure of RNA extraction from samples which were stored in RNAlater® Stabilization Solution confirmed that *A. hippocastanum* is a recalcitrant plant which needs special treatment to extract wanted materials such as protein or nucleic acid. It was found from DNA extraction that the lack of permeability in the connective tissue of *A. hippocastanum* phloem prevented the RNAlater® Stabilization Solution from maintaining the integrity of the RNA. So, this result will help work with this plant in future studies to avoid wasting time, money and rare samples. The storage of samples using a deep freezer or dry ice is more suitable in maintaining samples and avoiding RNA degradation of the recalcitrant woody plants.

5.5 Environmental effects

The interaction between abiotic and biotic stress in plants has been widely studied. There is a close correlation between environmental factors and the host and the pathogen, where one affects the other directly or indirectly, and this causes either the development or the disappearance of the disease. So, the relationship is more three-dimensional (Wanderley-Nogueira *et al.*, 2012; Leslie *et al.*, 2013), and therefore, the environmental effects were addressed in the current study. The results showed that there was no infection by the bacteria when using a spraying method on the stems or leaves of *A.*

hippocastanum through the lenticels or stomata, which is incompatible with a study carried out by Green *et al.,* (2010; 2012) where they confirmed that most infections were through the lenticels. Differences in the results of the two studies are probably due to the age and condition of seedlings (the small seedlings used in this study had smaller lenticels compared to the mature plants studied by Green *et al.,*). No consistent association was obtained between the presence of mechanical damage and bleeding cankers of *A. hippocastanum*. This may be because the damaged leaves contained active aromatic compounds that could have inhibited bacteria growth and prevent its spread throughout tissues (Takos *et al.,* 2008; Green *et al.,* 2010; Mullett and Webber, 2013; Thomas *et al.,* 2019). The damage caused by bacteria usually affects and changes plant tissues, and alters moisture content (Cervilla *et al.,* 2007). However, there was no clear correlation between damage and drought stress maybe due to the high humidity level in the greenhouse. So, when the responses to the drought and damage stress were studied, the effect of drought stress on the *A. hippocastanum* and *L. esculentum* plant was useful and significant, with mild drought stress treatments on biomass and even reduced the bacterial infection. Whereas the effect of drought stress and the damage on *P. vulgaris* was significantly harmful, while no significant effect was observed on *A. hippocastanum* with damage stress.

5.6 Gene expression and RNA sequencing

Through the study of gene expression in plants, any effect of drought or wounds in the plant can be discerned, and the overlap caused by disease-causing bacteria. The current study is considered as a basis for launching more detailed studies. In this work, several million reads per sample were requested,

with plans to assemble the transcripts and create a reference first of all and use this to look at differential expression analysis. To perform the comparative genomics analysis, the transcriptome of *A. hippocastanum* phloem was sequenced using Illumina RNA-Seq technology. In this study, the strategy of the comparative genomics analysis was to directly compare the Infected (sample pieces from the dead /live junction) reads with the Non-infected (infected trees but sample pieces from healthy tissue) and uninfected (uninfected tree, healthy pieces tissues). This study was the first investigation to characterise the whole transcriptome of *A. hippocastanum* using material extracted from the phloem. A set of a hundred genes were found, some of them already reported to have a relationship with wound stress in plants such as the gene C86B1 which encodes the Cytochrome P450 86B1 protein that is involved in the stimulation of wound suberization in some trees. There are also among the high expression genes, unusual genes such as DGC14 which show high up-regulation in uninfected vs non-infected group and BGL17 which high regulated in infected vs uninfected group, the exact function of which is not known but genes such as these could be useful if controlled. Another important finding was that Transcription factor TGA3 (TGA3), this gene show high up-regulation. The TGA3 gene play an central role in transcription factor protein and positively regulates defence PR-1 gene expression and resistance against *P. syringae* and is the TGA3 also reported to strongly interact with the defence regulatory protein NPR1 (Matthes *et al.,* 2010; Pieterse *et al.,* 2012). These results indicate that the DGC14 gene maybe has promising inhibition role activity against *Pseudomonas* bacteria. However, further data collection and studies are required to determine exactly what are the functions and roles of

these genes in bleeding canker disease of *A. hippocastanum*. In the future, the concentration on these genes could be an important key to controlling the disease by up and down-regulation to estimate the role of different genes in the bleeding canker disease response by horse chestnut or eventually other species.

5.7 Nanoparticles studied

The NPs work confirmed that some engineered nanomaterials can exert physical or chemical toxicity on plants depending on their chemical composition, size, surface energy, and the species of plant. Also, plants can absorb NPs without showing any signs of stress. Extensive research on the toxic impacts of nanomaterials could meaningfully help by absorbing and disposing of engineered nanomaterials leading to a reduction of adverse effects in both of agricultural and of environmental systems. Moreover, since NPs are largely non-toxic and move within the plant, there is scope to use them to move to the sites of disease infection where they can target the disease.

The zeta potential of the NPs showed some differences, probably due to variation in types of NPs. For example, the negative charge of Ag and TiO_2 NPs may be the reason for their reaction and their clear impact on the bacteria, whereas others have a positive charge. An investigation by Spielman-Sun *et al.,* (2017) stated that surface charge affects cellular translocation, uptake and tissue localisation in leaves tissues. According to a study by Syu *et al.,* (2014), the size, charge and shape of silver nanoparticles can have a large effect on *Arabidopsis* plant growth and gene expression. The data on NPs size revealed that the variation between the sizes measured with TEM and dynamic light

scattering is in the acceptable error rate or because there is a hydrodynamic layer around the NPs which scatters the light when measured by nana sizer, so the hydrodynamic layer plays an influencing role on size measurement. The size and shape of the synthesised Ag and CeO_2 nanoparticles were confirmed by examining TEM images and agreed with these results and revealed the presence of non-uniformly shaped of NPs. The electron microscopy images of cerium NPs showed that the cuboid shapes found in this study are very similar to those obtained by Rui and his group (Rui *et al.,* 2015) in terms of the size and shape of nanoparticles. The hydrodynamic radius of iron NPs was unexpected at 177.92 nm. Possibly it obtained a large diameter because of the inherent magnetic properties in the cores of iron oxide which tends to make it form long chains. The hydrodynamic size values (measured by DLS) of samples varied a little with TEM in regarding the size values, maybe because of the water layer surrounding the NPs during the measuring. The data presented in this work have demonstrated that TiO_2 is toxic to *P. vulgaris* plants. This toxicity was most obvious in reducing root length and root nodes when seeds were germinated in the presence of TiO_2. However, germination was not inhibited or significantly reduced as with other NPs used with *P. vulgaris* in this study. This demonstrates that NPs need careful selection when considering their use as a potential treatment against the disease.

The current study found that the accumulation of NPs in *L. esculentum* and *P. vulgaris* tissues, including their edible parts, could represent a food security concern. No previous study has proved the impacts of nanoparticles on *A. hippocastanum*, so two model plants of economic value were used as a model during the study of NPs impact on *A. hippocastanum*. The results showed a

significant increase accumulation for all types of NPs, these results resemble those observed in earlier studies showed that roots could be the main route of the plant's exposure to NPs, so the main accumulation happened in roots (Vittori Antisari *et al.,* 2014; Bradfield *et al.,* 2017). Also, an inhibitory effect of titanium and silver nanoparticles on the length, height and the dry weight of *P. vulgaris* plants may be explained by the biological effectiveness of Ag NPs and TiO_2 in inhibiting the growth of the bacteria which form root nodules that are associated with symbiotic nitrogen-fixing bacteria. Moreover, the influence of the TiO_2 NPs might result from the secondary presence of the NPs in cells or as a result of their accumulation in the cell walls, which might cause changes in the soil microenvironment (Larue *et al.,* 2014; Vittori Antisari *et al.,* 2014). Another study reported similar results using seedlings of the rice plant which were exposed to Ag NPs, (0.2, 0.5, and 1 mg /L) and showed significant decreases in the shoot and fresh root weights as well as in root elongation (Nair and Chung, 2014).

Regarding the positive results achieved from the effect of CeO_2 on *L. esculentum* plants, which showed significant improvements in the shoot and fresh root weights as well as shoot height, these may normally be expected but not with the concentrations used. These positive results of Fe_3O_4 and CeO_2 on *L. esculentum* plants agree with previous studies (Ma *et al.,* 2016; Rossi *et al.,* 2016). Fe_3O_4 increased root growth for both elongation and dry matter, presumably because iron is one of the essential nutrients for plant growth, (Sheykhbaglou *et al.,* 2010). Although the estimation of the influence of NPs on plant nutrient content is in the starting stage, it is very possible that NPs could modify the nutrient profile of food crops and affect the plant's absorption

of other essential elements (Gardea-Torresdey, *et al.*, 2014). Surprisingly enough, no differences were found in leaf or fruit accumulation in the plants which were treated with Ag NPs. This may be because the concentrations of Ag NPs or other NPs in the control tissues were zero or lower than the ability of the ICP-OES to detect the elements (instrument detection limited). The positive influence of Ag NPs on bacteria maybe because Ag NPs have a high surface area and so have a high antimicrobial impact compared to the bulkier Ag NPs (Nair and Chung, 2014). However, the different sizes and concentrations used in this study may shed some light on using NPs with *A. hippocastanum* plants and help us to understand the opportunity of using these NPs in the future in different functions such as in triggering defence responses, activated by pathogens, or carrying RNA or DNA to be delivered to plant cells for their genetic transformation, or any required drug. A previous study confirmed that NPs can enhance plant resistance to drought stress through improvement of the rate of photosynthesis and stomatal conductance by SNPs pre-treatments. This also has an effect through the decrease of xylem water potential and malondialdehyde (MDA) content in response to severe and moderate stress. This supports the hypothesis that some NPs have a promised potential in the reduction of the harmful effects of drought on plants (Ashkavand *et al.*, 2015).

5.8 Conclusion

Bleeding canker of *A. hippocastanum* has recently spread throughout Europe and the world. Such a rapid and urgent spread of the disease necessitates a greater understanding of the disease itself. If ways can be found to treat this disease using the immune/protein system of the tree, then this has the potential to transfer to other emerging disease/plant complexes, which may be important for human life.

This study has shown that abiotic stresses including drought stress could be useful with simple treatment (75% soil field capacity) or somewhat mild treatment (50% FC). The positive side was clear in an increase in biomass and a reduced bacterial infection in *A. hippocastanum* seedlings and tomato plants. One of the most important findings was that the bacteria have a high susceptibility for high temperatures that leads them to lose their pathogenicity, which may have potential benefit in controlling the bacteria under field conditions.

The results of the NPs treatments with TiO_2 showed that the effect of TiO_2 nanoparticles on *P. vulgaris* plants was negative and inhibitory for growth, by causing the death of root hairs and inhibiting the formation of root nodules. Conversely, there was no effect of TiO_2 nanoparticles on *L. esculentum* plants. However, the low concentration of TiO_2 nanoparticles had a positive effect on *A. hippocastanum*. The NPs study also shows that there are nanoparticles that may affect seed germination and inhibit germination, but if used after germination, they have little effect and may be useful for growth. In addition to the above, the study could be considered as the basis for deeper studies using

nanoparticles. After this cornerstone work, it was determined that some of the common nanoparticles were suitable for use within *A. hippocastanum* at different concentration. As well as the reverse injection of the plant phloem with nanoparticles, in particular, Ag and TiO_2 NPs gave a promising result that can be used in local treatment to control or stop the spread of bacteria. Results of this study can be used as a reference for predicting the effect of studied NPs on *A. hippocastanum* and model plants, and associated bacteria responses.

The most exciting finding was for RNA sequencing that gave a whole transcriptome for *A. hippocastanum*. With further study, this gene sequence can help to understand the immune system proteins that are used to fight disease and makes *A. hippocastanum* a useful model for a woody plant to understand and diagnose the effects of other diseases in other plants and perhaps even other organisms.

5.9 Future work

This research has thrown up many questions in need of further investigation. However, the major aims of future work are:

- To explore fully all the genes involved in the changes seen resulting from the transcriptome work and investigate the data fully to assess both the gene changes in the plant and the bacteria.
- Study the frequently expressed genes identified or the other unknown genes by up- or down-regulating them to find the target protein.
- To avoid the toxicity of some NPs, use capping by some inactive materials such as to polyvinylpyrrolidone (PVP).

- To ensure the safety of plants, especially the edible parts from the plant (tomato and bean) investigate the accumulation of NPs to ensure that there are acceptable amounts in plant material. The measurement of these should be performed using more sensitive devices such as inductively coupled plasma-mass spectrometry (ICP-MS).
- Further work needs to be carried out to establish whether other types of NPs or even other sizes of NPs, can give a better result to combat diseases.

Reference list

Abuqamar, S., Ajeb, S., Sham, A., Enan, M. R., & Iratni, R. (2013). A mutation in the expansin-like A2 gene enhances resistance to necrotrophic fungi and hypersensitivity to abiotic stress in *Arabidopsis thaliana* Molecular Plant Pathology, 14 (8), 813–827.

Aderiye, B., & OM, A. (2015). How plants respond to microbial infections and some environmental challenges. AASCIT Journal of Bioscience, 1 (3), 47-60.

Agnihotri, S., Mukherji, S. S., & Mukherji, S. S. (2014). Size-controlled silver nanoparticles synthesized over the range 5–100 nm using the same protocol and their antibacterial efficacy. RSC Adv., 4 (8), 3974–3983.

Agrios, G. N. (2005). *Plant pathology*. United States of America: Elsevier Academic Press.

Ain-Lhout, F., M. Zunzunegui, M.C. Diaz Barradas, R. Tirado, A. Clavijo and F. Garcia Novo. 2001. Comparison of proline accumulation in two Mediterranean shrubs subjected to natural and experimental water deficit. Plant Soil 230:175–183.

Allen, C. D., Macalady, A. K., Chenchouni, H., Bachelet, D., McDowell, N., Vennetier, M., Kitzberger, K., Rigling, A., Breshears, D. D., Hogg, E. H., Gonzalez, P., Fensham, R., Zhang, Z., Castro, J., Demidova, N., Lim, J.-H., Allard, G., Running, S. W., Semerci, A., & Cobb, N. (2010) A global overview of drought and heat-induced tree mortality reveals emerging climate change risks for forests. Forest Ecology and Management, 259: 660-684.

Alzwiy, I. A. M (2013) The Interaction between Abiotic and Biotic Stress in *Arabidopsis thaliana*. University of Exeter.

Anderegg, W. R. L., Plavcov.a, L., Anderegg, L. D. L., Hacke, U. G., Berry, J. A., & Field, C. B. (2013) Drought's legacy: multiyear hydraulic deterioration underlies widespread aspen forest die-off and portends increased future risk. Global Change Biology, 19(4), 1188–1196.

Anjum, N. A., Gill, S. S., Duarte, A. C., Pereira, E., & Ahmad, I. (2013). Silver nanoparticles in soil–plant systems. Journal of Nanoparticle Research, 15(9), 1896.

Loenhart, K. K. (2002) The Handsome (and Useful) Horse Chestnut. Anoldia: The Magazine of the Arnold Arboretum, 61 (4): 20-22.

Aroca, R. (2013). Plant responses to drought stress: From morphological to molecular features. Springer, Berlin, Heidelberg, p466.

Aurelio, M. & Arruda, Z. (2007) Trends in Sample Preparation, 1st edn. Nova Science, New York, p 304.

Ashkavand, P., Tabari, M., Zarafshar, M., Tomášková, I., & Struve, D. (2015). Effect of SiO2 nanoparticles on drought resistance in hawthorn seedlings. Forest Research Papers, 76 (4), 350–359.

Assmann, S., & Haubrick, L. (1996). Transport proteins of the plant plasma membrane. Current Opinion in Cell Biology, 8 (4): 458-467

Audenaert, K., De Meyer, G.B. and Höfte, M.M., (2002). Abscisic acid determines basal susceptibility of tomato toBotrytis cinerea and suppresses salicylic acid-dependent signaling mechanisms. Plant Physiology, 128 (2):491-501.

Auffan, M., Rose, J., Wiesner, M. R., & Bottero, J.-Y. (2009). Chemical stability of metallic nanoparticles: A parameter controlling their potential cellular toxicity in vitro. Environmental Pollution, 157(4), 1127–1133.

Ausubel, F. M. (2005). Are innate immune signalling pathways in plants and animals conserved. Nature Immunology, 6 (10), 973-979.

Avtzis, N. D., Avtzis, D. N., Vergos, S. G., & Diamandis, S. (2007). A contribution to the natural distribution of *Aesculus hippocastanum* (Hippocastanaceae) in Greece. *Phytologia Balcanica*, 13(2),183–187.

Aznar, A., Chen, N. W. G., Thomine, S., & Dellagi, A. (2015). Immunity to plant pathogens and iron homeostasis. Plant Science, 240, 90–97.

Baibado, J. T., & Cheung, H. (2010). Seed Extract of Horse Chestnut (*Aesculus hippocastanum* L.) as Effective Medication for Chronic Venous Insufficiency and Other Health Benefits. Hong Kong Pharmaceutical, HY Cheung, 17 (4).156-163.

Ball, S., Colleoni, C., Cenci, U., Raj, J. N., & Tirtiaux, C. (2011). The evolution of glycogen and starch metabolism in eukaryotes gives molecular clues to understand the establishment of plastid endosymbiosis. Journal of Experimental Botany, 62 (6), 1775-1801.

Baltrus, D. A., Nishimura, M. T., Dougherty, K. M., Biswas, S., Mukhtar, M. S., Vicente, J., Dangl, J. L. (2012). The molecular basis of host specialization in bean pathovars of *pseudomonas syringae*. Molecular Plant-Microbe Interactions, 25 (7), 877-888.

Bar-On, Y. M., & Milo, R. (2019). The global mass and average rate of rubisco. Proceedings of the National Academy of Sciences of the United States of America, 116(10), 4738–4743.

Barrett, L. G., Kniskern, J. M., Bodenhausen, N., Zhang, W., & Bergelson, J. (2009). Continua of specificity and virulence in plant host–pathogen interactions: causes and consequences. New Phytologist, 183(3), 513–529.

Bartels D, Sunkar R (2005) Drought and salt tolerance in plants. Crit Rev Plant Sci 24:23–58.

Basu, S., Ramegowda, V., Kumar, A., & Pereira, A. (2016). Plant adaptation to drought stress. F1000Research, 5(0), 1554.

Baucom, R. S., & de Roode, J. C. (2011). Ecological immunology and tolerance in plants and animals. Functional Ecology, 25(1), 18–28.

Bean, W. J. (1970). Trees and shrubs hardy in the British Isles. (Eighth edition fully revised Vol. I. ed.) John Murray, London.

Benhamou N, Mazau D, Grenier J, Esquerré-Tugayé M-T (1991) Timecourse study of the accumulation of hydroxyproline-rich glycoproteins in root cells of susceptible and resistant tomato plants infected by Fusarium oxysporum f. sp. radicis-lycopersici. Planta 184:196–208.

Bellini, E., & Nin, S. (2005). Horse-chestnut: cultivation for ornamental purposes and non-food crop production. Journal of Herbs, Spices & Medicinal Plants, 11, 93-120.

Benson, L. (1979). Plant classification (Second edition ed.). Canada Press.

Bhatt, I., & Tripathi, B. N. (2011). Interaction of engineered nanoparticles with various components of the environment and possible strategies for their risk assessment. Chemosphere 82: 308-317.

Boland, G., Melzer, M., Hopkin, A., Higgins, V., & Nassuth, A. (2004). Climate change and plant diseases in Ontario. Canadian Journal of Plant Pathology, 26 (3), 335-350.

Bostock RM. (2005). Signal crosstalk and induced resistance: straddling the line between cost and benefit. Annual Review of Phytopathology 43, 545-580.

Bour, A., Mouchet, F., Silvestre, J., Gauthier, L., & Pinelli, E. (2015). Environmentally relevant approaches to assess nanoparticles ecotoxicity: A review. Journal of Hazardous Materials 283: 764-777.

Boyer, J.S., 1982. Plant productivity and environment. Science, 218 (4571):443-448.

Bradford, M.M. (1976) A rapid and sensitive method for the quantitation of microgram quantities of protein utilizing the principle of protein-dye binding. Anal. Biochem. 72, 248–254.

Bradfield, S. J., Kumar, P., White, J. C., & Ebbs, S. D. (2017). Zinc, copper, or cerium accumulation from metal oxide nanoparticles or ions in sweet potato: Yield effects and projected dietary intake from consumption. Plant Physiology and Biochemistry, 110, 128–137.

Brashaw, B. K., Ross, R., Wang, X., & Wiemann, M. C. (2012). Wood utilization options for urban trees infested by invasive species. Natural Resources Research Institute, University of Minnesota.

Brasier, C. (2008). The biosecurity threat to the UK and global environment from international trade in plants. Plant Pathology, 57 (5), 792-808.

Braun, Y., Smirnova, A., Weingart, H., Schenk, A., Ullrich, M., Braun, Y., Ullrich, M. S. (2009). Coronatine Gene Expression In Vitro and In Planta, and Protein Accumulation During Temperature Downshift in Pseudomonas syringae. Sensors, 9(6), 4272–4285.

Bray, E. A. (1997). Plant responses to water deficit. Trends in Plant Science, 2 (2), 48–54.

Bray E.A. (2004). Genes commonly regulated by water-deficit stress in *Arabidopsis thaliana*. Journal of Experimental Botany 55**:** 2331-2341.

Bryan, G.,Bowes. (2010). Trees and forests a colour guide biology, pathology, propagation, silviculture, surgery, biomes, ecology, conservation. Spain: Manson Publishing Ltd.

Broadmeadow, M., Webber, J.,Ray, D., Berry, P. (2009). An assessment of likely future impacts of climate change on UK forests. The Stationery Office Limited, Edinburgh, UK.

Bruce Alberts, Dennis Bray, Karen Hopkin, Alexander D Johnson, Julian Lewis, Martin Raff, Keith Roberts, Peter W. (2014). Essential Cell Biology. 4th, Garland science, Taylor & Francis Group, LLC.

Bultreys, A., & Kaluzna, M. (2010). Bacterial cankers caused by *Pseudomonas syringae* on stone fruit species with special emphasis on the pathovars *syringae* and morsprunorum race 1 and race 2. Journal of Plant Pathology, 92(1), S21-S33.

Cantu D, Vicente AR, Labavitch JM (2008) Strangers in the matrix: plant cell walls and pathogen susceptibility. Trends Plant Sci 13:610–617

Campalans, A., Messeguer, R., A. G.-P. P. (1999) undefined. (2nd.). Plant responses to drought, from ABA signal transduction events to the action of the induced proteins. Elsevier. 37(5), 327-340.

Cerezal, J. C. S., & Gutiérrez, L. E. H. (2013). Environmental security, geological hazards and management JC Santamarta. Tenerife, Spain. p 233

Cervantes, E., & Emilio. (2006). Ethylene in Seed Germination and Early Root Development. Global Science Books. 46,429-438.

Cervilla, L. M., Blasco, B., Ríos, J. J., Romero, L., & Ruiz, J. M. (2007). Oxidative stress and antioxidants in tomato (Solanum lycopersicum) plants subjected to boron toxicity. Annals of Botany, 100(4), 747–756.

Chisholm, S. T., Coaker, G., Day, B., & Staskawicz, B. J. (2006). Host-microbe interactions: Shaping the evolution of the plant immune response. Cell, 124 (4), 803-814.

Chellaram, C., Murugaboopathi, G., John, A. A., Sivakumar, R., Ganesan, S., Krithika, S., & Priya, G. (2014). Significance of Nanotechnology in Food Industry. Apcbee Procedia, 8, 109–113.

Chen, J., Mao, L., Lu, W., Ying, T., & Luo, Z. (2016). Transcriptome profiling of postharvest strawberry fruit in response to exogenous auxin and abscisic acid. Planta, 243(1), 183–197.

Chernyshenko, M., Chernyshenko, V., & Musatenko, L. (2016). SDS-PAGE of Ophioglossum vulgatum Proteins. International Journal of Plant & Soil Science, 9(1), 1–7.

Chrispeels, M. J., & Raikhel, N. V. (1991). Lectins, lectin genes, and their role in plant defence. The Plant Cell, 3 (1), 1–9.

Cho, K.-H., Park, J.-E., Osaka, T., & Park, S.-G. (2005). The study of antimicrobial activity and preservative effects of nanosilver ingredient. Electrochimica Acta, 51(5), 956–960.

Cilia, M., Fish, T., Yang, X., Mclaughlin, M., Thannhauser, T. W., & Gray, S. (2009). A Comparison of Protein Extraction Methods Suitable for Gel-Based Proteomic. Journal of Biomolecular Techniques: 20: 201–215.

Çolak, H., Karaköse, E., & Duman, F. (2017). Erratum to: High optoelectronic and antimicrobial performances of green synthesized ZnO nanoparticles using *Aesculus hippocastanum* (Environ Chem Lett, 10.1007/s10311-017-0629-z). Environmental Chemistry Letters, 15(3), 553.

Colmenero-Flores JM, Campos F, Garciarrubio A, Covarrubias AA. (1997).

Characterization of *Phaseolus vulgaris* cDNA clones responsive to water deficit: identification of a novel late embryogenesis abundant-like protein. *Plant Molecular Biology* 35**:** 405

Chunjaturas, W., Ferguson, J. A., Rattanapichai, W., Sadowsky, M. J., & Sajjaphan, K. (2014). Shift of bacterial community structure in two Thai soil series affected by silver nanoparticles using ARISA. World Journal of Microbiology and Biotechnology 30: 2119-2124.

Coakley, S. M., Scherm, H., & Chakraborty, S. (1999). Climate change and plant disease management. Annual Review of Phytopathology, 37 (1), 399-426.

Collinge, D. B., Lund, O. S., & Thordal-Christensen, H. (2008). What are the prospects for genetically engineered, disease resistant plants? European Journal of Plant Pathology, 121 (3), 217-231.

Conde, J., Doria, G., Baptista, P. (2012). Noble Metal Nanoparticles Applications in Cancer. Journal of Drug Delivery,2012. 1-12.

Cos, Paul, Arnold J. Vlietinck Dirk, Vanden Berghe, LouisMaes (2006) 'Anti-infective potential of natural products: How to develop a stronger in vitro "proof-of-concept', Journal of Ethnopharmacology, 106 (3), pp. 290–302.

Cox, A., Venkatachalam, P., Sahi, S., & Sharma, N. (2016). Silver and titanium dioxide nanoparticle toxicity in plants: A review of current research. Plant Physiology and Biochemistry, 107, 147–163.

Cox, A., Venkatachalam, P., Sahi, S., & Sharma, N. (2017). Reprint of: Silver and titanium dioxide nanoparticle toxicity in plants: A review of current research. Plant Physiology and Biochemistry, 110, 33–49.

Curir, P., Galeotti, F., Dolci, M., Barile, E., & Lanzotti, V. (2007). Pavietin, a coumarin from *aesculus pavia* with antifungal activity. Journal of Natural Products, 70 (10), 1668-1671.

Cutler, D. F., Rudall, P., Gasson, P., & Gale, R. (1987). Root identification manual of trees and shrubs. A guide to the anatomy of roots of trees and shrubs hardy in Britain and northern Europe. Chapman and Hall.

D-Vinebrooke, R., L. Cottingham, K., Norberg, Marten Scheffer, J., I. Dodson, S., C. Maberly, S., & Sommer, U. (2004). Impacts of multiple stressors on biodiversity and ecosystem functioning: the role of species co-tolerance. Oikos, 104(3), 451–457.

Dagmar, V., & Szekely, G. (2010). *Aesculus hippocastanum* L. trees in the parks of Timisoara. 14(3), 151–153.

Dangl, J. L., & Jones, J. D. (2001). Plant pathogens and integrated defence responses to infection. Nature, 411 (6839), 826-833.

Dangl, J. L., Horvath, D. M., & Staskawicz, B. J. (2013). Pivoting the plant immune system from dissection to deployment. Science *(*New York, N.Y.), 341 (6147), 746-751.

De Keijzer, J., Van den Broek, Lambertus AM, Ketelaar, T., & Van Lammeren, A. A. (2012). Histological examination of horse chestnut infection by *pseudomonas syringae* pv. aesculi and non-destructive heat treatment to stop disease progression. PloS One, 7 (7), 1-12.

De Magalhães, C. S., & Arruda, M. A. Z. (2007). Sample preparation for metalloprotein analysis: A case study using horse chestnuts. Talanta, 71 (5), 1958–1963.

De Prins, J., De Prins, W., & De Coninck, E. (2003). The pupal morphology of cameraria ohridella compared with that of the genus phyllonorycter (lepidoptera: Gracillariidae). Journal of Pest Science, 76 (6), 145-150.

de Ronde JA, Spreeth MH, Cress WA (2000) Effect of antisense L-Δ1-pyrroline- 5-carboxylate reductase transgenic soybean plants subjected to osmotic and drought stress. Plant Growth Regul 32(1),13–26.

De Schutter, K., & Van Damme, E. (2015). Protein-Carbohydrate Interactions as Part of Plant Defence and Animal Immunity. Molecules, 20 (5), 9029–9053.

Delfani, M., Baradarn Firouzabadi, M., Farrokhi, N., & Makarian, H. (2014). Some Physiological Responses of Black-Eyed Pea to Iron and Magnesium Nanofertilizers. Communications in Soil Science and Plant Analysis, 45(4), 530–540.

Desjardins, P., & Conklin, D. (2010). NanoDrop microvolume Quantitation of Nucleic Acids. Journal of Visualized Experiments: Jove, (45). J. Vis. Exp. (45), e2565.

Dixon R, Wright G, Behrns G, Teskey R, Hinckley T (1980) Water deficits and root growth of ectomycorrhizal white oak seedlings. Can J for Res 10:545–548.

Djordjevic, M. A., & Weinman, J. J. (1991). Factors determining host recognition in the clover-rhizobium symbiosis. Australian Journal of Plant Physiology, 18(5), 543–557.

Doolette, C. L., McLaughlin, M. J., Kirby, J. K., & Navarro, D. A. (2015). Bioavailability of silver and silver sulfide nanoparticles to lettuce (*Lactuca sativa*): Effect of agricultural amendments on plant uptake. Journal of Hazardous Materials, Elsevier, 300 (30),788-795

Du, W., Sun, Y., Ji, R., Zhu, J., Wu, J., & Guo, H. (2011). TiO_2 and ZnO_2 nanoparticles negatively affect wheat growth and soil enzyme activities in agricultural soil. Journal of Environmental Monitoring, 13(4), 822.

Dudek-Makuch, M., & Studzińska-Sroka, E. (2015). Horse Chestnut - Efficacy and safety in chronic venous insufficiency: An overview. Brazilian Journal of Pharmacognosy, 25 (5), 533–541.

Dunphy Guzman, K. A., Finnegan, M. P. & Banfield, J. F. 2006. Influence of Surface Potential on Aggregation and Transport of Titania Nanoparticles. Environmental Science & Technology, 40**,** 7688-7693.

Duplan, V., & Rivas, S. (2014). E3 ubiquitin-ligases and their target proteins during the regulation of plant innate immunity. Frontiers in Plant Science, 5, 1-6.

Dwivedi, R., Singh, V. P., Kumar, J., & Prasad, S. M. (2015). Differential physiological and biochemical responses of two Vigna species under enhanced UV-B radiation. Journal of Radiation Research and Applied Sciences, 8(2), 173–181.

Edwards, S. E., da Costa Rocha, I., Heinrich, M., & Williamson, E. M. (2015). *Phytopharmacy:* An evidence-based guide to herbal medicinal products. John Wiley & Sons.

Ehmedov, V., M. Akbulut and S.T. Sadiqov. 2002. Role of Ca2+ in drought stress signaling in wheat seedlings. Biochemistry 67: 491–497.

El-Temsah, Y. S., & Joner, E. J. (2012). Impact of Fe and Ag nanoparticles on seed germination and differences in bioavailability during exposure in aqueous suspension and soil. Environmental Toxicology, 27(1), 42–49.

Elimelech, M., Gregory, J., Jia, X. & Williams, R. A. 1995. Particle Deposition & Aggregation: Measurement, Modelling and Simulation, Woburn, USA, Butterworth-Heinemann. ELZEY.

Espenti, C. S., Krishna Rao, K. S. V. K., & Madhusudana Rao, K. (2016). Bio-synthesis and characterization of silver nanoparticles using *Terminalia chebula* leaf extract and evaluation of its antimicrobial potential. Materials Letters, 174(02), 129–133.

Fabrega, J., Fawcett, S. R., Renshaw, J. C., and Lead, J. R. (2010). Silver nanoparticle impact on bacterial growth: effect of pH, concentration, and organic matter. Environ. Sci. Technol. 43, 7285–7290.

Fang, Y., & Xiong, L. (2015). General mechanisms of drought response and their application in drought resistance improvement in plants. Cellular and Molecular Life Sciences, 72(4), 673–689.

Faurobert, M., Pelpoir, E., & Chaïb, J. (2007). Phenol extraction of proteins for proteomic studies of recalcitrant plant tissues. Methods in Molecular Biology (Clifton, N.J.), 355(2), 9–14.

Feng Y, Cui X, He Steal (2013) The role of metal nanoparticles in influencing arbuscular mycorrhizal fungi effects on plant growth. Environ Sci Technol 47 (16): 9496–9504

Feki, K., & Brini, F. (2016). Role of proteins in alleviating drought stress in plants. Water Stress and Crop Plants: A Sustainable Approach, 1–2(July), 165–176.

Fernandez, J.A., L. Balenzategui, S. Banon and J.A. Franco. 2006.Induction of drought tolerance by paclobutrazol and irrigation deficit in *Phillyrea angustifolia* during the nursery period. Sci. Hortic. (107):277–283.

Feynman, R. (1959). Engineering and Science. California Institute of Technology. Journal of Ecology, (82) 415-425.

Forestry Commission. (2015). Bleeding canker of horse chestnut: Management. Retrieved from: http://www.forestry.gov.uk/fr/infd-6kyc2w.

Forest, F., Drouin, J. N., Charest, R., Brouillet, L., & Bruneau, A. (2001). A morphological phylogenetic analysis of Aesculus L. and Billia Peyr.

(Sapindaceae). Canadian Journal of Botany-Revue Canadienne De Botanique, 79 (2), 154–169.

Forrest, M. (2006). Landscape trees and shrubs: Selection, use and management CABI. Athenaeum press.

Frazier, M. E., Johnson, G. M., Thomassen, D. G., Oliver, C. E. and Patrinos,

A. (2003). Realizing the potential of the genome revolution: the genomes to life program. Science (300),290-293.

Frey-Klett, P., Burlinson, P., Deveau, A., Barret, M., Tarkka, M., & Sarniguet, A. (2011). Bacterial-fungal interactions: Hyphens between agricultural, clinical, environmental, and food microbiologists. Microbiology and Molecular Biology *Reviews: MMBR*, 75 (4), 583-609.

Fujita M, Fujita Y, Noutoshi Y, Takahashi F, Narusaka Y, Yamaguchi-Shinozaki K & Shinozaki K. (2006). Crosstalk between abiotic and biotic stress responses: a current view from the points of convergence in the stress signalling networks. Current Opinion in Plant Biology (9), 436-442.

Fuller, T. C., & McClintock, E. M. (1986). Poisonous plants of California. University of California Press.

Gašić, K., Prokić, A., Ivanović, M., Kuzmanović, N., & Obradović, A. (2012). Differentiation of *Pseudomonas syringae* pathovars originating from stone fruits. Pesticidi i fitomedicina, 27(3), 219-229.

Lakshmanan G, Sathiyaseelan., A& K., M. (2018). Plant-mediated synthesis of silver nanoparticles using fruit extract of Cleome viscosa L.: Assessment of their antibacterial and anticancer activity. Karbala International Journal of Modern Science, 4(1), 61–68.

Gao, X., Spielman-Sun, E., Rodrigues, S. M., Casman, E. A., & Lowry, G. V. (2017). Time and Nanoparticle Concentration Affect the Extractability of Cu from CuO NP-Amended Soil. Environmental Science and Technology, 51(4), 2226–2234.

García-Sánchez, S., Bernales, I., & Cristobal, S. (2015). Early response to nanoparticles in the Arabidopsis transcriptome compromises plant defence and root-hair development through salicylic acid signalling. BMC Genomics, 16(1), 1–17.

Gardea-Torresdey, J. L., Rico, C. M., & White, J. C. (2014). Trophic Transfer, Transformation, and Impact of Engineered Nanomaterials in Terrestrial Environments. Environmental Science & Technology, 48(5), 2526–2540.

Garrett, K. A., Dendy, S. P., Frank, E. E., Rouse, M. N., & Travers, S. E. (2006). Climate change effects on plant disease: Genomes to ecosystems. Ann. Rev. Phytopathology, 44(1), 489–509.

George, H., Lawrence, H. M. 1951. Taxonomy of vascular plants. Macmillan. New York, NY. 823 pp.

Germana, M. A., & Lambardi, M. (Eds.). (2016). In Vitro Embryogenesis in Higher Plants. Springer. Humana Press, New York, NY

Ghafariyan, M. H., Malakouti, M. J., Dadpour, M. R., Stroeve, P., & Mahmoudi, M. (2013). Effects of Magnetite Nanoparticles on Soybean Chlorophyll. Environmental Science & Technology, Environ. Sci. Technol. 47(18), 10645-10652

Gottschalk, F., & Nowack, B. (2011). The release of engineered nanomaterials to the environment. Journal of Environmental Monitoring 13: 1145-1155.

Gottschalk, F., Sonderer, T., Scholz, R. W. & Nowack, B. 2009. Modeled Environmental Concentrations of Engineered Nanomaterials (TiO2, ZnO, Ag, CNT,Fullerenes) for Different Regions. Environmental Science & Technology, 43**,** 9216-9222.

Gledhill, D. (2008). The names of plants (Foruth edition ed.) Cambridge University Press.

Godzik, S., & Sassen, M. M. A. (1978). A scanning electron microscope examination of *Aesculus hippocastanum* L. leaves from control and air-polluted areas. Environmental Pollution, 17, 13–18.

Gómez-Aparicio, L., Zamora, R., Castro, J., & Hódar, J. a. (2008). Facilitation of tree saplings by nurse plants: Microhabitat amelioration or protection against herbivores? Journal of Vegetation Science, 19(January), 161–172.

Gómez-Vidal, S., Tena, M., Lopez-Llorca, L. V., & Salinas, J. (2008). Protein extraction from Phoenix dactylifera L. leaves, a recalcitrant material, for two-dimensional electrophoresis. Electrophoresis, 29 (2), 448–456.

Gosling Peter. (2007). Raising trees and shrubs from seed. Forest Research, Forestry Commission. Edinburgh.UK, p28.

Gou, X., He, K., Yang, H., Yuan, T., Lin, H., Clouse, S. D., & Li, J. (2010). Genome-wide cloning and sequence analysis of leucine-rich repeat receptor-like protein kinase genes in *Arabidopsis thaliana*. BMC Genomics, 11(1), 19.

Graça, J., 2015. Suberin: the biopolyester at the frontier of plants. Front. Chem. 3, 62.

Green, S., Hendry, S. J., & Redfern, D. B. (2008) Drought damage to pole-stage Sitka spruce and other conifers in north-east Scotland. Scottish Forestry, 62: 10-18.

Green, S., Laue, B., Fossdal, C. G., A'Hara, S. W., & Cottrell, J. E. (2009). Infection of horse chestnut (*Aesculus hippocastanum*) by Pseudomonas syringae pv. aesculi and its detection by quantitative real-time PCR. Plant Pathology, 58(4), 731–744.

Green, S, & Ray, D. (2009). Potential impacts of drought and disease on forestry in Scotland. Cabdirect.Org. Forestry Commission, Edinburgh.UK ,4 pp.

Green, Sarah, Studholme, D. J., Laue, B. E., Dorati, F., Lovell, H., Arnold, D., Kamoun, S. (2010). Comparative genome analysis provides insights into the evolution and adaptation of Pseudomonas syringae pv. aesculi on *Aesculus hippocastanum*. PLoS ONE, 5(4),1-14.

Gui, X., Zhang, Z., Liu, S., Ma, Y., Zhang, P., He, X., Cao, W. (2015). Fate and phytotoxicity of CeO2 nanoparticles on lettuce cultured in the potting soil environment. PLoS ONE, 10(8).

Guo, S. & Wang**,** E. (2011). Noble metal nanomaterials: controllable synthesis and application in fuel cells and analytical sensors. Nano Today, 6(3) 240-247.

Gurel, E., Ustunova, S., Ergin, B., Tan, N., Caner, M., Tortum, O., & Demirci-Tansel, C. (2013). Herbal haemorrhoidal cream for haemorrhoids. *Chinese Journal of* Physiology, 56(5), 253-262.

Haghighi, M., & Teixeira da Silva, J. A. (2014). The effect of N-TiO2 on tomato, onion, and radish seed germination. Journal of Crop Science and Biotechnology, 17(4), 221–227.

Häfeli, OU., Riffle, JS., Harris-Shekhawat, l., Carmichael-Baranauskas, A., Mark, F., Dalley, JP., Bardenstein, D. (2009). Cell uptake and in vitro toxicity of magnetic nanoparticles suitable for drug delivery. Mol Pharm, 6:1417-1428.

Halford NG, Hey S, Jhurreea D, Laurie S, McKibbin RS, Zhang Y & Paul MJ. (2004). Highly conserved protein kinases involved in the regulation of carbon and amino acid metabolism. Journal of Experimental Botany 55, 35-42.

Han, X., Lu, W., Wei, X., Li, L., Mao, L., & Zhao, Y. (2018). Proteomics analysis to understand the ABA stimulation of wound suberization in kiwifruit. Journal of Proteomics, 173(July 2017), 42–51.

Hamilton EW, Heckathorn SA. (2001). Mitochondrial Adaptations to NaCl. Complex I Is Protected by Anti-Oxidants and Small Heat Shock Proteins, Whereas Complex II Is Protected by Proline and Betaine. Plant Physiology 126**:** 1266-1274.

Hardoim, P. R., Overbeek, L. S. van, Berg, G., Pirttilä, A. M., Compant, S., Campisano, A., Sessitsch, A. (2015). The Hidden World within Plants: Ecological and Evolutionary Considerations for Defining Functioning of Microbial Endophytes. Microbiology and Molecular Biology Reviews, 79(3), 293–320.

Herbert L Edlin. (1985). Broadleaves. forestry commission booklet 20 (second edition ed.). London, Her Majesty's Stationery Office.

Hasegawa, P. M., Bressan, R. A., Zhu, J.-K., & Bohnert, H. J. (2000). P LANT C ELLULAR AND M OLECULAR R ESPONSES TO H IGH S ALINITY. Annual Review of Plant Physiology and Plant Molecular Biology, 51(1), 463–499.

Hasheminasab, H., Taghi Assad, M., Aliakbari, A., & Rasoul Sahhafi, S. (2012). Influence of Drought Stress on Oxidative Damage and Antioxidant Defense Systems in Tolerant and Susceptible Wheat Genotypes. Journal of Agricultural Science, 4(8), 20–30.

Hau, B. (1990). Anal Ytic Models of Plant Disease in a Changing Environment. Annu. Rev. Phytopathology, 28 (71), 221–245.

He, X., & Hwang, H. M. (2016). Nanotechnology in food science: Functionality, applicability, and safety assessment. Journal of Food and Drug Analysis, 24(4), 671–681.

Hennig L, Köhler C, Viczián A & Kircher S. (2010). Luciferase and green fluorescent protein reporter genes as tools to determine protein abundance and intracellular dynamics. In Plant Developmental Biology, ed. Walker JM, Humana Press. pp. 293-312.

Hernandez-Viezcas, J. A., Castillo-Michel, H., Peralta-Videa, J. R., & Gardea-Torresdey, J. L. (2016). Interactions between CeO2Nanoparticles and the Desert Plant Mesquite: A Spectroscopy Approach. ACS Sustainable Chemistry and Engineering, 4(3), 1187–1192.

Hirano, S. S., & Upper, C. D. (1990). Population biology and epidemiology of Pseudomonas syringae. Annual Review of Phytopathology, 28(1), 155–177.

Hirano, S., & Upper, C. (2000). Bacteria in the Leaf Ecosystem with emphasis on Pseudomonas syringae: A pathogen, ice nucleus, and epiphyte. MICROBIOLOGY AND MOLECULAR BIOLOGY REVIEWS, 64(3), 624–653.

Hirt, H., & Shinozaki, K. (2004). Plant responses to abiotic stress. 1st edn. Springer. New York, p 108.

Hoagland D. R. 1938. The water-culture method for growing plants without soil, University of California, College of Agriculture, Agricultural Experiment Station. Circular 347.

Horst, R. Kenneth (2013a). Westcott's plant disease handbook (Eighth Edition ed.) Springer Science & Business Media.

Horst, R. Kenneth (2013b). Field manual of diseases on trees and shrubs. Springer, Dordrecht.

Horvat, I., Glavac, V., & Ellenberg, H. (1974). Vegetation Südeuropas. Stuttgard, Germany: Gustav Fischer Verlag.p347

Hsiao, T.C., Acevedo, E., Fereres, E. and Henderson, D.W. (1976). Stress metabolism water stress, growth, and osmotic adjustment. Philosophical Transactions of the Royal Society of London Series B-Biological Sciences, 273, 479–500.

Hutchinson, J. (1959). The families of flowering plants. volume I, dicotyledons. Britain: Oxford University Press.

Hwang, M. S. H., Morgan, R. L., Sarkar, S. F., Wang, P. W., & Guttman, D. S. (2005). Phylogenetic characterization of virulence and resistance phenotypes of *Pseudomonas syringae*. Applied and Environmental Microbiology, 71(9*)*, 5182-5191.

Ichinose, Y., Taguchi, F., & Mukaihara, T. (2013). Pathogenicity and virulence factors of Pseudomonas syringae. Journal of General Plant Pathology, 79(5), 285–296.

Ingram, J., & Bartels, D. (1996). The molecular basis of dehydration tolerance in plants. Annual Review of Plant Physiology and Plant Molecular Biology, 47(1), 377–403.

International Seed Testing Association (ISTA), 1999. International rules for seed testing. Seed Sci. Technol. 27, p333.

Isaacson, T., Damasceno, C.M.B., Saravanan R.S, He, Y., Catala, C., Saladie M., and Rose, J.K.C. (2006). Sample extraction techniques for enhanced proteomic analysis of plant tissues. Nat. Protocols 1, 769-774.

Jacobs, D. I., Van Rijssen, M. S., Van Der Heijden, R., & Verpoorte, R. (2001). Sequential solubilization of proteins precipitated with trichloroacetic acid in acetone from cultured Catharanthus roseus cells yields 52% more spots after two-dimensional electrophoresis. Proteomics, 1(11), 1345–1350.

Jenks, M. a. (2007). Plant Abiotic Stress Edited by. In stress the international journal on the biology of stress ,43(2),257-168.

Jia, T., Wang, J., Chang, W., Fan, X., Sui, X., Song, F., Song, F. (2019). Proteomics Analysis of E. angustifolia Seedlings Inoculated with Arbuscular Mycorrhizal Fungi under Salt Stress. International Journal of Molecular Sciences, 20 (3),788-801.

Johne, A. B., Weissbecker, B., & Schütz, S. (2006). Volatile emissions from *Aesculus hippocastanum* induced by mining of larval stages of cameraria ohridella influence oviposition by conspecific females. Journal of Chemical Ecology, 32 (10), 2303-2319.

Jones, J. D., & Dangl, J. L. (2006). The plant immune system. Nature, 444 (7117), 323-329.

Jorrín-Novo, J. V., Pascual, J., Sánchez-Lucas, R., Romero-Rodríguez, M. C., Rodríguez-Ortega, M. J., Lenz, C., & Valledor, L. (2015). Fourteen years of

plant proteomics reflected in Proteomics: Moving from model species and 2DE-based approaches to orphan species and gel-free platforms. Proteomics 15, 1089–1112.

Kammers, K., Cole, R. N., Tiengwe, C., Ruczinski, I., Spectrometry, M., Facility, P. C., & Hopkins, J. (2015). Detecting significant changes in protein abundance. Euprot, 7, 11–19.

Karlsson, H.L., Gustafsson, J., Cronholm, P. and Möller, L., (2009). Size-dependent toxicity of metal oxide particles-A comparison between Nano- and micrometre size. Toxicology letters, 188(2), 112-118.

Katagiri, F., Thilmony, R., & He, S. Y. (2002). The *Arabidopsis Thaliana-Pseudomonas Syringae* Interaction. The *Arabidopsis* Book, 1(Appendix I), e0039. The, American Society of Plant Biologists.p35.

Kawamura, G., Nogami, M., Matsuda, A. (2013). Shape-Controlled Metal Nanoparticles and Their Assemblies with Optical Functionalities. Journal of Nanomaterials, 2013:1-17.

Keller, A. A., Adeleye, A. S., Conway, J. R., Garner, K. L., Zhao, L., Cherr, G. N., Zuverza-Mena, N. (2017). Comparative environmental fate and toxicity of copper nanomaterials. Nano Impact, 7: 28–40.

Kennelly, M. M., Cazorla, F. M., de Vicente, A., Ramos, C., & Sundin, G. W. (2007). *Pseudomonas syringae* diseases of fruit trees: Progress toward understanding and control. Plant Disease, 91 (1), 4-17.

Khan, M. N., Mobin, M., Abbas, Z. K., AlMutairi, K. A., & Siddiqui, Z. H. (2017). Role of nanomaterials in plants under challenging environments. Plant Physiology and Biochemistry, 110, 194–209.

Kim, B., Kim, J. E., Choi, B.-K., & Kim, H.-S. (2015). Anti-Inflammatory Effects of Water Chestnut Extract on Cytokine Responses via Nuclear Factor-κB-signaling Pathway. Biomolecules & Therapeutics, 23(1), 90–97.

Kimura, H., Ogawa, S., Katsube, T., Jisaka, M., & Yokota, K. (2008). Antiobese effects of novel saponins from edible seeds of japanese horse chestnut (aesculus turbinata BLUME) after treatment with wood ashes. Journal of Agricultural and Food Chemistry, 56 (12), 4783-4788.

King, E. O., Ward, M. K., & Raney, D. E. (1954). Two simple media for the demonstration of pyocyanin and fluorescing. The Journal of Laboratory and Clinical Medicine, 44 (2), 301–307.

Kingdom, U. (1978). Copyright Statement. American Journal of Economics and Sociology, 37 (1), 34–34.

Kleitman, F., Barash, I., Burger, A., Iraki, N., Falah, Y., Sessa, G., Weinthal, D., Chalupowicz, L., Gartemann,K.H., Eichenlaub, R., & Manulis-Sasson, S.

(2008). Characterization of a Clavibacter michiganensis subsp. michiganensis population in Israel. European Journal of Plant Pathology, 121, 463–475.

Konno, K. (2011). Plant latex and other exudates as plant defense systems: roles of various defence chemicals and proteins contained therein. Phytochemistry, 72 (13), 1510–1530.

Kooyers NJ. (2015). The evolution of drought escapes and avoidance in natural herbaceous populations. Plant Science 234, 155–162.

Krost, C., Petersen, R., Lokan, S., Brauksiepe, B., Braun, P., & Schmidt, E. R. (2013). Evaluation of the hormonal state of columnar apple trees (Malus x domestica) based on high throughput gene expression studies. Plant Molecular Biology, 81 (3), 211–220.

Laing, W., & Christeller, J. (2004). Extraction of proteins from plant tissues. *Current Protocols in* Protein Science / Editorial Board, John E. Coligan, Chapter 4, Unit 4.7.

Lamichhane, J. R., & Venturi, V. (2015). Synergisms between microbial pathogens in plant disease complexes: A growing trend. Frontiers in Plant Science, 6, 385.

Larcher W (2003) Physiological plant ecology: ecophysiology and stress physiology of functional groups. springer, Netherlands (4th edu.).

Larue, C., Castillo-Michel, H., Sobanska, S., Trcera, N., Sorieul, S., Cécillon, L., Sarret, G. (2014). Fate of pristine TiO2 nanoparticles and aged paint-containing TiO2 nanoparticles in lettuce crop after foliar exposure. Journal of Hazardous Materials, 273(30), 17-26.

Laue, B. E., Steele, H., & Green, S. (2014). Survival, cold tolerance and seasonality of infection of European horse chestnut (*Aesculus hippocastanum*) by Pseudomonas syringae pv. aesculi. Plant Pathology, 63(6), 1417–1425.

Léguillier, T., Lecsö-Bornet, M., Lémus, C., Rousseau-Ralliard, D.,Lebouvier, N., Hnawia, E., Nour, M., Aalbersberg, W., Ghazi, K.,Raharivelomanana, P. and Rat, P., 2015. The Wound Healing and Antibacterial Activity of Five Ethnomedical *Calophyllum inophyllum* Oils: An Alternative Therapeutic Strategy to Treat Infected Wounds. PLoS ONE, 10(9), 1-20.

Le Van, N., Ma, C., Shang, J., Rui, Y., Liu, S., & Xing, B. (2016). Effects of CuO nanoparticles on insecticidal activity and phytotoxicity in conventional and transgenic cotton. Chemosphere, 144, 661–670.

Lee, C., Wood, M., Ng, K., Andersen, C., Structure, Y. L. (2004). Crystal structure of the type III effector AvrB from Pseudomonas syringae. Elsevier, 12 (3), 487–494.

Leslie, C., Fujita, M., Hasanuzzaman, M., Nahar, K., Pavlousek, P., Ortbauer, M., Showler, A. T. (2013). Abiotic Stress - Plant Responses and Applications in Agriculture.InTec, Croatia, P409.

Leathart, S. (1991). Whence our trees. London, UK: Foulsham.

Li, N. (2015). Toxic Potential of Materials at the Nanolevel. Science, 311 (5761), 622-627.

Li, X., Yang, Y., Gao, B., & Zhang, M. (2015). Stimulation of Peanut Seedling Development and Growth by Zero-Valent Iron Nanoparticles at Low Concentrations. PLOS ONE, 10(4), e0122884.

Lin, D., & B Xing. (2007). Phytotoxicity of nanoparticles: inhibition of seed germination and root growth. Environmental Pollution. Elsevier. 150 (3) 243-250.

Lin, S., Reppert, J., Hu, Q., Hudson, J. S., Reid, M. L., Ratnikova, T. A., Ke, P. C. (2009). Uptake, translocation, and transmission of carbon nanomaterials in rice plants. Small, 5(10), 1128–1132.

Lisar Sys, Motafakkerazad R, Hossain MM, Rahman IMM (2012) Water stress in plants: causes, effects and responses. In: Water Stress, Rahman IMM (Ed.), InTech Publication, pp. 1–14.

Liu, H., Fu, J. M., Du, H., Hu, J., & Wuyun, T. (2016). De novo sequencing of Eucommia ulmoides flower bud transcriptomes for identification of genes related to floral development. Genomics Data, 9, 105–110.

Liu, R., & Lal, R. (2015). Science of the Total Environment Potentials of engineered nanoparticles as fertilizers for increasing agronomic productions. Science of the Total Environment, The, 514, 131–139.

Liu, R., Zhang, H., & Lal, R. (2016). Effects of Stabilized Nanoparticles of Copper, Zinc, Manganese, and Iron Oxides in Low Concentrations on Lettuce (*Lactuca sativa*) Seed Germination: Nanotoxicants or Nanonutrients? Water, Air, and Soil Pollution, 227(1).

Lulai, E. (2007). Skin-set, wound healing, and related defects. Food Chem. 51, 4998.

M Bello. (2018). The effect of major environmental factors on archaeal and bacterial ammonia oxidisers in soil (University of Aberdeen). Retrieved from ethos.bl.uk.

Ma, Xiaowen, Wang, P., Zhou, S., Sun, Y., Liu, N., Li, X., & Hou, Y. (2015). De novo transcriptome sequencing and comprehensive analysis of the drought-responsive genes in the desert plant Cynanchum komarovii. BMC Genomics, 16(1), 1–17.

Ma, Xingmao, Wang, Q., Rossi, L., & Zhang, W. (2016). Cerium Oxide Nanoparticles and Bulk Cerium Oxide Leading to Different Physiological and

Biochemical Responses in Brassica rapa. Environmental Science & Technology, 50(13), 6793–6802.

McMillan Browse. (1982). The propagation of the hardy horse chestnuts and buckeyes. Plantsman, *4*(3), 150-164.

Mansfield, J., Genin, S., Magori, S., Citovsky, V., Sriariyanum, M., Ronald, P., Foster, G. D. (2012). Top 10 plant pathogenic bacteria in molecular plant pathology. Molecular Plant Pathology, 13(6), 614–629.

Manzoni S, Vico G, Katul G, Fay PA, Polley W, Palmroth S, Porporato A (2011) Optimizing stomatal conductance for maximum carbon gain under water stress: a meta-analysis across plant functional types and climates. Funct Ecol, 25: 456–467.

Marcelletti, S., Ferrante, P., Petriccione, M., Firrao, G., & Scortichini, M. (2011). Pseudomonas syringae pv. actinidiae draft genomes comparison reveal strain-specific features involved in adaptation and virulence to Actinidia species. PLoS ONE, 6(11).

Matthes, M. C., Bruce, T. J. A., Ton, J., Verrier, P. J., Pickett, J. A., & Napier, J. A. (2010). The transcriptome of cis-jasmone-induced resistance in *Arabidopsis thaliana* and its role in indirect defence. Planta, 232(5), 1163–1180.

McHale, L., Tan, X., Koehl, P., & Michelmore, R. W. (2006). Plant NBS-LRR proteins: Adaptable guards. Genome Biol, 7 (4), 212.

Méchin, V., Damerval, C., & Zivy, M. (2007). Total protein extraction with TCA-acetone. Methods in Molecular Biology (Clifton, N.J.), 355 (2), 1–8.

Metz, K. M., Sanders, S. E., Miller, A. K., & French, K. R. (2014). Uptake and impact of silver nanoparticles on Brassica rapa: An environmental nanoscience laboratory sequence for a nonmajors course. Journal of Chemical Education, 91 (2), 264–268.

Michelmore, R. W., & Meyers, B. C. (1998). Clusters of resistance genes in plants evolve by divergent selection and a birth-and-death process. Genome Research, 8 (11), 1113-1130.

Misra, S. K., Dybowska, A., Berhanu, D., Luoma, S. N., & Valsami-Jones, E. (2012). The complexity of nanoparticle dissolution and its importance in nanotoxicological studies. Science of the Total Environment, 438, 225–232.

Mitchell, A. (1974). A field guide to the trees of Britain and northern Europe (second edition ed.). south china Printing Co.: Citeseer.

Mitchell, A. (1990). The pocket to guide: Trees of Britain and northern Europe. Italy Press.

Mittler, R. (2002). Oxidative stress, antioxidants and stress tolerance. Trends in Plant Science, 7 (9), 405–410.

Morales-Díaz, A. B., Ortega-Ortíz, H., Juárez-Maldonado, A., Cadenas-Pliego, G., González-Morales, S., & Benavides-Mendoza, A. (2017). Application of nanoelements in plant nutrition and its impact in ecosystems. Advances in Natural Sciences: Nanoscience and Nanotechnology, 8 (1).

Morris, C. E., Sands, D. C., Vinatzer, B. a, Glaux, C., Guilbaud, C., Buffière, A., Thompson, B. M. (2008). The life history of the plant pathogen Pseudomonas syringae is linked to the water cycle. The ISME Journal, 2(3), 321–334.

Morris, C., Kinkel, L., Xiao, K., Infection, P. P.-, and, G., (2007). Surprising niche for the plant pathogen Pseudomonas syringae. Elsevier, 7(1), 84-92.

Mousa, M., Evans, N. D., Oreffo, R. O. C., & Dawson, J. I. (2018). Clay nanoparticles for regenerative medicine and biomaterial design: A review of clay bioactivity. Biomaterials, 159, 204–214.

Mullett, M. S., & Webber, J. F. (2013). Pseudomonas syringae pv. aesculi: Foliar infection of Aesculus species and temperature-growth relationships. Forest Pathology, 43(5), 371–378.

Mushtaq, R., Katiyar, S., & Bennett, J. (2008). Proteomic Analysis of Drought Stress-Responsive Proteins in Rice Endosperm Affecting Grain Quality., 11, 227−232.

Mutava RN, Prince SJK, Syed NH, Song L, Valliyodan B, Chen W, Nguyen HT (2015) Understanding abiotic stress tolerance mechanisms in soybean: A comparative evaluation of soybean response to drought and flooding stress. Plant Physiol Biochem 86: 109–120.

Mutz, K. O., Heilkenbrinker, A., Lönne, M., Walter, J. G., & Stahl, F. (2013). Transcriptome analysis using next-generation sequencing. Current Opinion in Biotechnology, 24 (1), 22–30.

Mork, E. K. (2011) 'Disease resistance in ornamental plants - Transformation of Symphyotrichum Novi-Belgii with powdery mildew resistance genes', unpublished PhD Thesis, Aarhus University.

Nadagouda, M.N., Polshettiwar, V. and Varma, R.S., 2009. Self-assembly of palladium nanoparticles: Synthesis of nanobelts, nanoplates and Nano trees using vitamin B1, and their application in carbon-carbon coupling reactions. Journal of Materials Chemistry, 19(14), 2026-2031.

Nair, P. M. G., & Chung, I. M. (2014). Physiological and molecular level effects of silver nanoparticles exposure in rice (Oryza sativa L.) seedlings. Chemosphere, 112, 105–113.

Nelson, L. S., Shih, R. D. and Balick, M. J. (2007) Handbook of poisonous and injurious plants, Second Edi. New York, NY, Springer, DOI:10.5860/choice.44-6268.

Newton, A. C., Torrance, L., Holden, N., Toth, I. K., Cooke, D. E., Blok, V., & Gilroy, E. M. (2012). Climate change and defence against pathogens in plants. Advances in Applied Microbiology, 81, 89-132.

Nowack, B. & Bucheli, T. D. 2007. Occurrence, behaviour and effects of nanoparticles in the environment. Environmental Pollution, 150**,** 5-22.

Newall, C., Anderson, L., & Phillipson, J. (1996). Herbal medicines: A guide for health-care professionals. London, 296.

Neill, S., & Burnett, E. (1999). Regulation of gene expression during water deficit stress. Springer.29(1-2), 23–33.

Nie, S., Li, C., Xu, L., Wang, Y., Huang, D., Muleke, E. M., … Liu, L. (2016). De novo transcriptome analysis in radish (Raphanus sativus L.) and identification of critical genes involved in bolting and flowering. BMC Genomics, 17(1), 1–16.

Nonami H, Boyer JS. 1990. Wall Extensibility and Cell Hydraulic Conductivity Decrease in Enlarging Stem Tissues at Low Water Potentials. Plant Physiology 93:1610-1619.

Nowack, B. & Bucheli, T. D. 2007. Occurrence, behaviour and effects of nanoparticles in the environment. Environmental Pollution, 150**,** 5-22.

Noureddine, A., Hjelvik, E. A., Croissant, J. G., Durfee, P. N., Agola, J. O., & Brinker, C. J. (2019). Engineering of large-pore lipid-coated mesoporous silica nanoparticles for dual cargo delivery to cancer cells. Journal of Sol-Gel Science and Technology, 89(1), 78–90.

Nowak, D. J., Hirabayashi, S., Bodine, A., & Greenfield, E. (2014). Tree and forest effects on air quality and human health in the United States. Environmental Pollution, 193, 119–129.

Nürnberger, T., Brunner, F., Kemmerling, B., & Piater, L. (2004). Innate immunity in plants and animals: Striking similarities and obvious differences. Immunological Reviews, 198 (1), 249-266.

Ocaña-Moral, S., Gutiérrez, N., Torres, A. M., & Madrid, E. (2017). Saturation mapping of regions determining resistance to Ascochyta blight and broomrape in faba bean using transcriptome-based SNP genotyping. Theoretical and Applied Genetics, 130(11), 2271–2282.

Oljača, R., Govedar Z., & Hrkić Z. (2009). Effects of aeropolution on stomatal density of studied wild horse chestnut (*Aesculus hippocastanum* L.) and birch (Betula pendula roth) species in the area of banjaluka. Proceedings of the International Scientific Conference "Forestry in achieving millennium goals institute of lowland forestry and environment (Ed. S Orlovic). old commerce, Novi Sad, Serbia, 117-123.

Otajagić, S; Dž, Pinjić; Ćavar, S; Vidic, D; Maksimović, M (2012) Total phenolic content and antioxidant activity of ethanolic extracts of *Aesculus hippocastanum* L., Glasnik hemičara i tehnologa Bosne i Hercegovine, 38, 35-39.

Palleroni, N.J. (1984). Genus I. *Pseudomonas* 1894. In Berge's Manual of Systematic Bacteriology, Vol. 1 (Krieg, N. R. and Holt, J. G., eds.). pp. 141-199, Williams and Wilkins, Baltimore.

Pánková, I., Krejzar, V., Mertelík, J., & Kloudová, K. (2015). The occurrence of lines tolerant to the causal agent of bleeding canker, *pseudomonas syringae* pv. aesculi, in a natural horse chestnut population in central europe. European Journal of Plant Pathology, 142 (1), 37-47.

Parida, A. K., Dagaonkar, V. S., Phalak, M. S., Umalkar, G. V., & Aurangabadkar, L. P. (2007). Alterations in photosynthetic pigments, protein and osmotic components in cotton genotypes subjected to short-term drought stress followed by recovery. Plant Biotechnology Reports, 1(1), 37–48.

Pariona, N., Martínez, A. I., Hernandez-Flores, H., Clark-Tapia, R., Martï¿½nez, A. I., Hernandez-Flores, H., & Clark-Tapia, R. (2017). Effect of magnetite nanoparticles on the germination and early growth of Quercus macdougallii. Science of the Total Environment, 575, 869–875.

Parisi, C., Vigani, M., & Rodríguez-Cerezo, E. (2015). Agricultural nanotechnologies: What are the current possibilities? Nano Today, 10(2), 124–127.

Park, H. C., Lee, S., Park, B., Choi, W., Kim, C., Lee, S., Yun, D. J. (2015). Pathogen associated molecular pattern (PAMP)-triggered immunity is compromised under C-limited growth. Molecules and Cells, 38 (1), 40-50.

Park, O. K. (2004). Proteomic studies in plants. Journal of Biochemistry and Molecular Biology, 37 (1), 133–138.

Patlolla, J. M., & Rao, C. V. (2015). Anti-inflammatory and anti-cancer properties of β-escin, a triterpene saponin. Current Pharmacology Reports, 1 (3), 170-178.

Pavan, F., Barro, P., Bernardinelli, I., Gambon, N., & Zandigiacomo, P. (2003). Cultural control of cameraria ohridella on horsechestnut in urban areas by removing fallen leaves in autumn. Journal of Arboriculture, 29 (5), 253-258.

Peçi, D.H., Mullaj, A., & Dervishi, A. (2012). The natural distribution of horse-chestnut (*Aesculus hippocastanum* L) in Albania. Journal of Institute Alb-Shkenca, 5, 153–157.

Peirce, A. The APhA, (1999) Practical Guide to Natural Medicines, Stonesong Press Book, Wm. Morrow & Co., Inc., New York.

Percival, G. C., & Banks, J. M. (2014). Studies of the interaction between horse chestnut leaf miner (Cameraria ohridella) and bacterial bleeding canker (Pseudomonas syringae pv. aesculi). Urban Forestry and Urban Greening, 13(2), 403–409.

Percival, G. C., & Banks, J. M. (2015). Phosphite-induced suppression of Pseudomonas bleeding canker (*Pseudomonas syringae* pv. *aesculi*) of horse chestnut (*Aesculus hippocastanum* L.). Arboricultural Journal, 37(1), 7–20.

Percival, G. C., Barrow, I., Noviss, K., Keary, I., & Pennington, P. (2011). The impact of horse chestnut leaf miner (cameraria ohridella deschka and dimic; HCLM) on vitality, growth and reproduction of *Aesculus hippocastanum* L. Urban Forestry & Urban Greening, 10 (1), 11-17.

Percival, G. C., & Noviss, K. (2008). Triazole induced drought tolerance in horse chestnut (*Aesculus hippocastanum*). Tree Physiology, 28(11), 1685–1692.

Petrova, S., Yurukova, L., & Velcheva, I. (2014). Possibilities of using deciduous tree species in trace element biomonitoring in an urban area (Plovdiv, Bulgaria). Atmospheric Pollution Research, 5(2), 196–202.

Phillips, R. S Grant, T Wellsted (1978). Trees in Britain, Europe and north America. London: Art Resource.

Pieterse, C. M. J., Van der Does, D., Zamioudis, C., Leon-Reyes, A., & Van Wees, S. C. M. (2012). Hormonal Modulation of Plant Immunity. Annual Review of Cell and Developmental Biology, 28(1), 489–521.

Pillai, S., Gopalan, V., & Lam, A. K. Y. (2017). Review of sequencing platforms and their applications in phaeochromocytoma and paragangliomas. Critical Reviews in Oncology/Hematology, 116, 58–67.

Pittler, M. H., & Ernst, E. (2012). Horse chestnut seed extract for chronic venous insufficiency. Cochrane. Database. Syst. Rev, 11.

Prabhu, S., & Poulose, E. K. (2012). Silver nanoparticles: mechanism of antimicrobial action, synthesis, medical applications, and toxicity effects. International Nano Letters, 2: 1-10.

Preston, C. D., Pearman, D. A., & Dines, T. D. (2002). New atlas of the British and Irish flora. Oxford, UK: Oxford University Press.

Pritchard, J., Griffiths, B., & EJ, H. (2007). Can the plant-mediated impacts on aphids of elevated CO2 and drought be predicted? Global Change Biology. 13,1616–1629.

Priester, J. H., Ge, Y., Mielke, R. E., Horst, A. M., Moritz, S. C., Espinosa, K., Gelb, J., Walker, S. L., Nisbet, R. M., An, Y.-J., Schimel, J. P., Palmer, R. G., Hernandez-Viezcas, J. A., Zhao, L., Gardea-Torresdey, J. L. and Holden, P. A. (2012) ‘Soybean susceptibility to manufactured nanomaterials with evidence

for food quality and soil fertility interruption', Proceedings of the National Academy of Sciences, vol. 109, no. 37, 2451–2456.

Puchalski, T. & Prusinkiewicz, Z. (1975). Ecological Basis of Forest Site Classification. Powszechne Wydawnictwo Rolnicze i Leśne, Warsaw, Poland. p 154

Qaim, M., & Zilberman, D. (2003). Yield effects of genetically modified crops in developing countries. Science (New York, N.Y.), 299 (5608), 900-902.

Rabilloud, T., Vaezzadeh, A. R., Potier, N., Lelong, C., Leize-Wagner, E., & Chevallet, M. (2009). Power and limitations of electrophoretic separations in proteomics strategies. Mass Spectrometry Reviews, 28(5), 816–843

Radojevic, L., Marinkovic, N., & Jervremovic, S. (2000). Influence of the sex of flowers on androgenesis in *Aesculus hippocastanum* L. another culture. In Vitro Cellular & Developmental Biology-Plant, 36 (6), 464-469.

Rhodes D, Samaras Y (1994) Genetic control of osmoregulation in plants. cellular and molecular physiology of cell volume regulation, CRC, Tokyo, p361.

Ramm, C., Wachholtz, M., Amundsen, K., Donze, T., Heng-Moss, T., Twigg, P., … Baxendale, F. (2015). Transcriptional Profiling of Resistant and Susceptible Buffalograsses in Response to Blissus occiduus (Hemiptera: Blissidae) Feeding. Journal of Economic Entomology, 108(3), 1354–1362.

Rao, S. P., Tamhane, V. A., Nikam, A. N., Sharan, A. A., & Jaleel, A. (2018). Method for Label-Free Quantitative Proteomics for Sorghum bicolor L. Moench. Tropical Plant Biology, 11(1–2), 78–91.

Rejeb, I., Pastor, V., & Mauch-Mani, B. (2014). Plant Responses to Simultaneous Biotic and Abiotic Stress: Molecular Mechanisms. Plants, 3 (4), 458–475.

Reymond, P. (2000). Differential Gene Expression in Response to Mechanical Wounding and Insect Feeding in Arabidopsis. The Plant Cell Online, 12(5), 707–720.

Ribeiro, F., Gallego-Urrea, J. A., Jurkschat, K., Crossley, A., Hassellöv, M., Taylor, C., et al. (2014). Silver nanoparticles and silver nitrate induce high toxicity to Pseudokirchneriella subcapitata, Daphnia magna and Danio rerio. Sci. Total Environ. 466, 232–241.

Rico, C. M., Majumdar, S., Duarte-Gardea, M., Peralta-Videa, J. R., & Gardea-Torresdeay, J. L. (2011). Interaction of nanoparticles with edible plants and their possible implications in the food chain. Agricultural and Food Chemistry, (59), 3485–3498.

Rios, J. L., & Villaw, A. (1988). Paper screening methods for natural products with antimicrobial activity: a review of the literature. Elsevier, 23, 127–149.

Roloff, A., Korn, S., & Gillner, S. (2009). The Climate-Species-Matrix to select tree species for urban habitats considering climate change. Urban Forestry & Urban Greening, 8 (4), 295–308.

Rossi, L., Zhang, W., Lombardini, L., & Ma, X. (2016). The impact of cerium oxide nanoparticles on the salt stress responses of Brassica napus L. Environmental Pollution, 219, 28–36.

Rui, Y., Zhang, P., Zhang, Y., Ma, Y., He, X., Gui, X., Zhang, Z. (2015). Transformation of ceria nanoparticles in cucumber plants is influenced by phosphate. Environmental Pollution, 198, 8–14.

Salleo, S., Nardini, A., Raimondo, F., Gullo, M., Trees, F. P.-, & 2003, undefined. (2003). Effects of defoliation caused by the leaf miner Cameraria ohridella on wood production and efficiency in *Aesculus hippocastanum* growing in north-eastern. Springer, 17 (4), 367–375.

Sarah Green. (2012). Using genomics to gain insights into the evolution and biology of Pseudomonas syringae pv. aesculi on European horse chestnu. Journal of Agricultural Extension and Rural Development, 4(9), 214–216.

Sarker, S.D., Nahar, L. and Kumarasamy, Y., 2007. Microtitre plate-based antibacterial assay incorporating resazurin as an indicator of cell growth, and its application in the in vitro antibacterial screening of phytochemicals. *Methods* (San Diego, Calif.), 42(4), pp. 321-324.

Schmidt, O., Dujesiefken, D., Stobbe, H., Moreth, U., Kehr, R., & Schröder, T. (2008). Pseudomonas syringae pv. aesculi associated with horse chestnut bleeding canker in Germany. Forest Pathology, 38(2), 124–128.

Șchiopu, E., Șchiopu, T., & Stavrescu-Bedivan, M. (2011). Changes in the structure of *Aesculus hippocastanum* species induced by pollution. Scientific Papers, UASVM Bucharest, 1, 149-153.

Schwarze, F. W., Engels, J., & Mattheck, C. (2000). Fungal strategies of wood decay in trees. Germany: (2nd ed). Springer Science & Business Media.

Sengonca, C., & Arnold, C. (1999). Survey on the distribution of the horse chestnut ScalePulvinaria regalis canard (hom., coccidae) in Germany in the years 1996 to 1998. Anzeiger Für Schädlingskunde, Journal of Pest Science, 72 (6), 153-157.

Servin, A. D., Castillo-Michel, H., Hernandez-Viezcas, J. A., Diaz, B. C., Peralta-Videa, J. R., & Gardea-Torresdey, J. L. (2012). Synchrotron Micro-XRF and Micro-XANES Confirmation of the Uptake and Translocation of TiO 2 Nanoparticles in Cucumber (*Cucumis sativus*) Plants. Environmental Science & Technology, 46(14), 7637–7643.

Servin, A. D., & White, J. C. (2016). Nanotechnology in agriculture: Next steps for understanding engineered nanoparticle exposure and risk. Elsevier, 1, 9-12

Servin, A., Elmer, W., Mukherjee, A., De la Torre-Roche, R., Hamdi, H., White, J. C., Dimkpa, C. (2015). A review of the use of engineered nanomaterials to suppress plant disease and enhance crop yield. Journal of Nanoparticle Research, 17(2), 1–21.

Sharma, P., Jha, A. B., Dubey, R. S., & Pessarakli, M. (2012). Reactive Oxygen Species, Oxidative Damage, and Antioxidative Defense Mechanism in Plants under Stressful Conditions. Journal of Botany, 2012, 1–26.

Sharma, V. K., Filip, J., Zboril, R., & Varma, R. S. (2015). Natural inorganic nanoparticles-formation, fate, and toxicity in the environment. Chemical Society Reviews, 44(23), 8410–8423.

Sheykhbaglou, R., SEDGHI, M., SHISHEVAN, M. T., & SHARIFI, R. S. (2010). Effects of Nano-Iron Oxide Particles on Agronomic Traits of Soybean. Notulae Scientia Biologicae, 2(2), 112.

Shi, J., Peng, C., Yang, Y., Yang, J., Zhang, H., Yuan, X., … Hu, T. (2014). Phytotoxicity and accumulation of copper oxide nanoparticles to the Cu-tolerant plant Elsholtzia splendens. Nanotoxicology, 8(2), 179–188.

Siddiqi, K. S., & Husen, A. (2017). Plant Response to Engineered Metal Oxide Nanoparticles. Nanoscale Research Letters, 12(1).

Siddiqui, M. H., & Al-whaibi, M. H. (2014). Role of nano-SiO 2 in germination of tomato (Lycopersicum esculentum seeds Mill.). Saudi Journal of Biological Sciences, 21(1), 13–17.

Siddiqui, M. H., Al-Whaibi, M. H., & Mohammad, F. (2015). Nanotechnology and plant sciences: Nanoparticles and their impact on plants. Nanotechnology and Plant Sciences: Nanoparticles and Their Impact on Plants, 1–303.

Singh, H., Kaur, S., Batish, D., Sharma, V., & N Sharma. (2009). Nitric oxide alleviates arsenic toxicity by reducing oxidative damage in the roots of *Oryza sativa* (rice). Elsevier. 53: 65– 73.

Singh, H. P., Batish, D. R., Kohli, R. K., & Arora, K. (2007). Arsenic-induced root growth inhibition in mung bean (Phaseolus aureus Roxb.) is due to oxidative stress resulting from enhanced lipid peroxidation. Plant Growth Regulation, 53(1), 65–73.

Sirtori, C. R. (2001). Aescin: Pharmacology, pharmacokinetics and therapeutic profile. Pharmacological Research, 44(3), 183-193.

Snieskiene, V., Stankeviciene, A., Zeimavicius, K., & Balezentiene, L. (2011). *Aesculus hippocastanum* L. state changes in Lithuania. Polish Journal of Environmental Studies, 20(4), 1029–1035.

Souza, A. A. De, Takita, M. A., Kishi, L. T., & Machado, M. A. (2013). RNA-Seq analysis of Citrus reticulata in the early stages of Xylella fastidiosa infection reveals auxin- related genes as a defence response. BMC Genomic, 14:676

Sparks, D. L. (2014). Advances in agronomy (First edition ed.). USA: Academic Press.

Sparks, T., Jeffree, E., & Jeffree, C. (2000). An examination of the relationship between flowering times and temperature at the national scale using long-term phenological records from the UK. International Journal of Biometeorology, 44 (2), 82-87.

Sparks, T., & Smithers, R. (2002). Is spring getting earlier? Weather, 57 (5), 157-166.

Spielman-Sun, E., Lombi, E., Donner, E., Howard, D., Unrine, J. M., & Lowry, G. V. (2017). Impact of Surface Charge on Cerium Oxide Nanoparticle Uptake and Translocation by Wheat (*Triticum aestivum*). Environmental Science & Technology, 51 (13), 7361–7368.

Spoel, S. H., & Dong, X. (2012). How do plants achieve immunity? defence without specialized immune cells. Nature Reviews Immunology, 12 (2), 89-100.

Sproll, C., Ruge, W., Andlauer, C., Godelmann, R., & Lachenmeier, D. W. (2008). HPLC analysis and safety assessment of coumarin in foods. Food Chemistry, 109 (2), 462-469.

Stankeviciene, A., Snieskiene, V., & Lugauskas, A. (2010). *Erysiphe flexuosa*– the new pathogen of *Aesculus hippocastanum* in Lithuania. Phytopathologia, 56, 67-71.

Steele, H., Laue, B. E., MacAskill, G. A., Hendry, S. J., & Green, S. (2010). Analysis of the natural infection of European horse chestnut (*Aesculus hippocastanum*) by Pseudomonas syringae pv. aesculi. Plant Pathology, 59(6), 1005–1013.

Street, N. R., Skogström, O., Sjödin, A., Tucker, J., Rodríguez-Acosta, M., Nilsson, P., Taylor, G. (2006). The genetics and genomics of the drought response in Populus. Plant Journal, 48(3), 321–341.

Straw, N., & Bellett-Travers, M. (2004). Impact and management of the horse chestnut leaf-miner (*cameraria ohridella*). Arboricultural Journal, 28 (1-2), 67-83.

Straw, N., & Tilbury, C. (2006). Host plants of the horse-chestnut leaf-miner (cameraria ohridella), and the rapid spread of the moth in the UK 2002–2005. Arboricultural Journal, 29 (2), 83-99.

Straw, N. A., & Williams, D. T. (2013). Impact of the leaf miner cameraria ohridella (lepidoptera: Gracillariidae) and bleeding canker disease on horse-chestnut: Direct effects and interaction. Agricultural and Forest Entomology, 15 (3), 321-333.

Strouts, R., Winter, T., & Parry, W. (1995). Diagnosis of ill-health in trees. Forestry, 68 (2), 169-170.

Studholme, D. J. (2011). Application of high-throughput genome sequencing to intrapathovar variation in *Pseudomonas syringae*. Molecular Plant Pathology, 12 (8), 829-838.

Šućur, K. M., Aničić, M. P., Tomašević, M. N., Antanasijević, D. Z., Perić-Grujić, A. A., & Ristić, M. Đ. (2010). Urban deciduous tree leaves as biomonitors of trace element (as, V and cd) atmospheric pollution in belgrade, serbia. Journal of the Serbian Chemical Society, 75 (10), 1453-1461.

Suleman, P., Al-Musallam, A., & Menezes, C. A. (2001). The Effect of Solute Potential and Water Stress on Black Scorch Caused by Chalara paradoxa and Chalara radicicola on Date Palms. Am Phytopath Society, 85(1), 80–83.

Sun, T. Y., Gottschalk, F., Hungerbühler, K., & Nowack, B. (2014). Comprehensive probabilistic modelling of environmental emissions of engineered nanomaterials. *Environmental Pollution* 185: 69-76.

Syu, Y. yu, Hung, J. H., Chen, J. C., & Chuang, H. wen. (2014). Impacts of size and shape of silver nanoparticles on Arabidopsis plant growth and gene expression. Plant Physiology and Biochemistry, 83(October), 57–64.

Swindell, W.R. The association among gene expression responses to nine abiotic stress treatments in *Arabidopsis thaliana*. Genet. Soc. Am. 2006, 174, 1811–1824.

Tabata, S. (2002). Impact of genomics approaches on plant genetics and physiology. *Journal of Plant Research* 115: 271-275.

Tabashnik, B. E., Brévault, T., & Carrière, Y. (2013). Insect resistance to beet crops: Lessons from the first billion acres. Nature Biotechnology, 31 (6), 510-521.

Takos, I., Varsamis, G., Avtzis, D., Galatsidas, S., Merou, T., & Avtzis, N. (2008). The effect of defoliation by Cameraria ohridella Deschka and Dimic (Lepidoptera: Gracillariidae) on seed germination and seedling vitality in *Aesculus hippocastanum* L. Forest Ecology and Management, 255 (3–4), 830–835.

Talgo, V., Spies Perminow, J., Sletten, A., Brurberg, M. B., Herrero, M., Stromeng, G., & Stensvand, A. (2012). Fungal and bacterial diseases on horse chestnut in Norway. J.Agricult.Extention and Rural Devel, 4 (9), 256-258.

Taniguchi, N. (1996). Nanotechnology: integrated processing systems for ultra-precision and ultra-fine products. Oxford University Press, USA.

Tao, X., Mao, L., Li, J., Chen, J., Lu, W., & Huang, S. (2016). Abscisic acid mediates wound-healing in harvested tomato fruit. Postharvest Biology and Technology, 118, 128–133.

Tarkowski, P., & Vereecke, D. (2014). Threats and opportunities of plant pathogenic bacteria. Biotechnology Advances, 32(1), 215–229.

Tattar, T. A. (1989). Diseases of shade trees. USA: Academic Press.INC.

Teixeira, E. M. B., Carvalho, M. R. B., Neves, V. A., Silva, M. A., & Arantes-Pereira, L. (2014). Chemical characteristics and fractionation of proteins from Moringa oleifera Lam. leaves. Food Chemistry, 147, 51–54.

Thalmann, C., Freise, J., Heitland, W., & Bacher, S. (2003). Effects of defoliation by horse chestnut leafminer (*Cameraria ohridella*) on reproduction in *Aesculus hippocastanum*. Trees - Structure and Function, 17(5), 383–388.

Thomas, P. A. (2014). Trees: Their natural history, 2nd ed. Cambridge, UK: Cambridge University Press.

Thomas, P. A., Alhamd, O., Iszkuło, G., Dering, M., & Mukassabi, T. A. (2019). Biological Flora of the British Isles: *Aesculus hippocastanum*. Journal of Ecology, 107(2), 992–1030.

Thomas, P. J., Carpenter, D., Boutin, C., & Allison, J. E. (2014). Rare earth elements (REEs): Effects on germination and growth of selected crop and native plant species. Chemosphere, 96, 57–66.

Thrall, P. H., Barrett, L. G., Burdon, J. J., & Alexander, H. M. (2005). Variation in pathogen aggressiveness within a metapopulation of the Cakile maritima-Alternaria brassicicola host-pathogen association. Plant Pathology, 54(3), 265–274.

Thuesombat, P., Hannongbua, S., Akasit, S., & Chadchawan, S. (2014). Effect of silver nanoparticles on rice (Oryza sativa L. cv. KDML 105) seed germination and seedling growth. Ecotoxicology and Environmental Safety, 104(1), 302–309.

Tilbury, C., Evans, H.F., 2003. Horse Chestnut *Leafminer Cameraria* ohridella Desch. & Dem. (*Lepidoptera: Gracillariidae*). Forestry Commission, Edinburgh, UK, 4pp.

Timm, A. E., & Reineke, A. (2015). First insights into grapevine transcriptional responses as a result of vine mealybug *Planococcus ficus* feeding. Arthropod-Plant Interactions, 8, :495–505.

Tolaymat, T., Genaidy, A., Abdelraheem, W., Dionysiou, D., & Andersen, C. (2017). The effects of metallic engineered nanoparticles upon plant systems: An analytic examination of scientific evidence. Science of the Total Environment, 579, 93–106.

Tomaševič, M., Vukmirovič, Z., Rajšič, S., Tasič, M., & Stevanovič, B. (2008). Contribution to biomonitoring of some trace metals by deciduous tree leaves in urban areas. Environmental Monitoring and Assessment, 137(1-3), 393-401.

Tom-Petersen, A., Hosbond, C., & Nybroe, O. (2001). Identification of copper-induced genes in Pseudomonas fluorescens and use of a reporter strain to monitor bioavailable copper in soil. FEMS Microbiology Ecology, 38(1), 59–67.

Ton, J., Ent, S., Hulten, M. van, & Pozo, M. (2009). Priming as a mechanism behind induced resistance against pathogens, insects and abiotic stress. IOBC/Wprs Bulletin, 44, 3–13.

Tosetti, R., Tardelli, F., Tadiello, A., & V. Z. (2014). Molecular and biochemical responses to wounding in mesocarp of ripe peach (*Prunus persica* L. Batsch) fruit. Elsevier. 90(April),40-51.

Trigiano, R. N., & Mark T. Windham, Alan S. Windham. (2006). Plant pathology, concepts and laboratory exercises, Boca Raton, US: Taylor & Francis e-Library.

Tripathi, D. K., Tripathi, A., Shweta, Singh, S., Singh, Y., Vishwakarma, K., Chauhan, D. K. (2017). Uptake, accumulation and toxicity of silver nanoparticle in autotrophic plants, and heterotrophic microbes: A concentric review. Frontiers in Microbiology, 8(JAN), 1–16.

Tsiroukis, A. (2008). Reproductive biology and ecology of horse-chestnut (*Aesculus hippocastanum* L.). Unpublished PhD Thesis, National & Kapodistrian University of Athens, Athens, Greece.

Van Den Ackerveken, G., Marois, E., & Bonas, U. (1996). Recognition of the bacterial avirulence protein AvrBs3 occurs inside the host plant cell. Cell, 87(7), 1307–1316.

Vasconcelos, É. a. R., Nogueira, F. C. S., Abreu, E. F. M., Gonçalves, E. F., Souza, P. a. S., & Campos, F. a. P. (2005). Protein Extraction from Cowpea Tissues for 2-D Gel Electrophoresis and MS Analysis. Chromatographia, 62 (7-8), 447–450.

Vidhyasekaran, P. (2014). PAMP Signals in Plant Innate Immunity. In PAMP Signals in Plant Innate Immunity: Signal Perception and Transduction, Signalling and Communication in Plants (Vol. 21). Springer, Dordrecht.

Vilagrosa, A., Chirino, E., Peguero-Pina, J. J., Barigah, T., Cochard, H., & Gil-Pelegrín, E. (2012). Plant Responses to Drought Stress. Plant Responses to

Drought Stress: From Morphological to Molecular Features, (Chapter 13), 63–109.

Vilhena, M. B., Schmidt, D., Carvalho, G., Azevedo, R. A., Franco, M. R., Schmidt, D., Azevedo, R. A. (2015). Evaluation of protein extraction methods for enhanced proteomic analysis of tomato leaves and roots. Anais Da Academia Brasileira de Ciências, 87(3).

Vinković Vrček, I., Pavičić, I., Crnković, T., Jurašin, D., Babič, M., Horák, D., Gajović, S. (2015). Does surface coating of metallic nanoparticles modulate their interference with in vitro assays? RSC Advances, 5 (87), 70787–70807.

Vittori Antisari, L., Carbone, S., Gatti, A., Vianello, G., & Nannipieri, P. (2014). Uptake and translocation of metals and nutrients in tomato grown in soil polluted with metal oxide (CeO2, Fe3O4, SnO2, TiO2) or metallic (Ag, Co, Ni) engineered nanoparticles. Environmental Science and Pollution Research, 22 (3), 1841–1853.

Von Maltitz, I. (2003). Black powder manufacturing, testing & optimizing American Fireworks News. American Fireworks News.

Walas, Ł., Dering, M., Ganatsas, P., Pietras, M., Pers-Kamczyc, E., & Iszkuło, G. (2018). The present status and potential distribution of relict populations of *Aesculus hippocastanum* L. in Greece and the diverse infestation by Cameraria ohridella Deschka & Dimić. Plant Biosystems, 152 (5), 1048–1058.

Walter, A., Silk, W., & U Schurr. (2009). Environmental Effects on Spatial and Temporal Patterns of Leaf and Root Growth. Annual Review of Plant Biology, 60(1), 279–304.

Walthelm, U., Dittrich, K., Gelbrich, G., & Schopke, T. (2001). Effects of saponins on the water solubility of different model compounds. Planta Medica, 67 (1), 49-54.

Wanderley-Nogueira, A. C., Kido, E. A., Soares-cavalcanti, N. M., Bezerra-Neto, J. P., Burnquist, W. L., Chabregas, M. S., Benko-iseppon, A. M. (2012). Insight on pathogen defense mechanisms in the sugarcane transcriptome. Functional Plant Science and Biotechnology, 6 (2), 134–148.

Wang, M. L., Harrison, M. L., Tonnis, B. D., Pinnow, D., Davis, J., & Irish, B. M. (2018). Total leaf crude protein, amino acid composition and elemental content in the USDA-ARS bamboo germplasm collections. Plant Genetic Resources: Characterisation and Utilisation, 16 (2), 185–187.

Wang, P., Lombi, E., Zhao, F. J., & Kopittke, P. M. (2016). Nanotechnology: A New Opportunity in Plant Sciences. Trends in Plant Science, 21(8), 699–712.

Wang, Q., Ma, X., Zhang, W., Pei, H., & Chen, Y. (2012). The impact of cerium oxide nanoparticles on tomato (Solanum lycopersicum L.) and its implications for food safety. Metallomics, 4 (10), 1105–1112.

Wang, S., Wang, X., He, Q., Liu, X., Xu, W., Li, L., Wang, F. (2012). Transcriptome analysis of the roots at early and late seedling stages using Illumina paired-end sequencing and development of EST-SSR markers in radish. Plant Cell Reports, 31(8), 1437–1447.

Wang, W., Meng, B., Ge, X., Song, S., Yang, Y., Yu, X., Yu, J. (2008). Proteomic profiling of rice embryos from a hybrid rice cultivar and its parental lines. PROTEOMICS, 8(22), 4808–4821.

Wang, W. N., Tarafdar, J. C., & Biswas, P. (2013). Nanoparticle synthesis and delivery by an aerosol route for watermelon plant foliar uptake. Journal of Nanoparticle Research, 15(1). 1417.

Wang W, Vinocur B, Shoseyov O, Altman A. (2004)**.** Role of plant heat-shock proteins and molecular chaperones in the abiotic stress response. Trends in Plant Science 9**:** 244-252.

Warren, J. M., Norby, R. J., & Wullschleger, S. D. (2011) Elevated CO2 enhances leaf

senescence during extreme drought in a temperate forest. Tree Physiology, 31: 117-130.

Wang, X., Han, H., Liu, X., Gu, X., Chen, K., Nanoparticle, D. L.-J. of, & 2012, U. (2012). Multi-walled carbon nanotubes can enhance root elongation of wheat (Triticum aestivum) plants. Journal of Nanoparticle Research, 14:841.

Wang, Z., Xie, X., Zhao, J., Liu, X., Feng, W., White, J. C., & Xing, B. (2012). Xylem-and phloem-based transport of CuO nanoparticles in maize (*Zea mays* L.). Environmental Science & Technology 46: 4434-4441.

Warren, J., Norby, R., & Wullschleger, S. (2011). Elevated CO2 enhances leaf senescence during extreme drought in a temperate forest. Academic.Oup. Com, 31, 117-130.

Webber, J., Parkinson, N., Rose, J., Stanford, H., Cook, R., & Elphinstone, J. (2008). Isolation and identification of *pseudomonas syringae* pv. aesculi causing bleeding canker of horse chestnut in the UK. Plant Pathology, 57 (2), 368-368.

Weber, A. P. M., Weber, K. L., Carr, K., Wilkerson, C., & Ohlrogge, J. B. (2007). Sampling the Arabidopsis Transcriptome with Massively Parallel Pyrosequencing. Plant Physiology, 144(1), 32–42.

Weiner, M. (1980). Earth medicine-earth food: plant remedies, drugs, and natural foods of the North American Indians. p 230.

Westhrin, M., Xie, M., Olderøy, M.Ø, Sikorski, P., Strand, B.L. and Standal, T., 2015. Osteogenic Differentiation of Human Mesenchymal Stem Cells in Mineralized Alginate Matrices. PLoS ONE, 10 (3), 1-16.

Whatmore, R. W. (2006). Nanotechnology—what is it? Should we be worried? Occupational Medicine 56: 295-299.

Wigginton, N. S., Haus, K. L. & Hochellajr, M. F. (2007). Aquatic environmental nanoparticles. Journal of Environmental Monitoring, 9**,** 1306-1316.

Williams, A. G., & Whitham, T. G. (1986). Premature leaf abscission: An induced plant defence against gall aphids. Ecology, 1619-1627.

Wittmaack, K. (2011). Excessive delivery of nanostructured matter to submersed cells caused by rapid gravitational settling. ACS Nano, 5(5), 3766–3778.

Wood AJ. (2005). Eco-physiological adaptations to limited water environments. In:

Jenks MA, Hasegawa PM, eds. *Plant Abiotic Stress*. Blackwell Publishing, 1–13.

Xiong L, Schumaker KS, Zhu JK (2002) Cell signalling during cold, drought, and salt stress. Plant Cell 14:165–183

Xiao, M., Zhang, Y., Chen, X., Lee, E. J., Barber, C. J. S., Chakrabarty, R., … Sensen, C. W. (2013). Transcriptome analysis based on next-generation sequencing of non-model plants producing specialized metabolites of biotechnological interest. Journal of Biotechnology, 166(3), 122–134.

Xiong, S. J., Wen, X. Y., He, H. G., Lu, G. Q., Wu, Y. Y., Wang, Y., & Sun, W. H. (2015). Different mechanisms of photosynthetic response to drought stress in tomato and violet orychophragmus. Photosynthetica, 54(2), 226–233.

Yilmaz, R., Sakcali, S., Yarci, C., Aksoy, A., & Ozturk, M. (2006). Use of *Aesculus hippocastanum* L. as a biomonitor of heavy metal pollution. Pak.J.Bot, 38(5), 1519-1527.

Yamada, M., H. Morishita, K. Urano, N. Shiozaki, K. Yamaguchi- Shinozaki, K. Shinozaki and Y. Yoshiba. 2005. Effects of free proline accumulation in petunias under drought stress. J. Exp. Bot. 56:1971–1985.

Yang, H., Tong, M., & Kim, H. (2013). Effect of Carbon Nanotubes on the Transport and Retention of Bacteria in Saturated Porous Media.*Environ. Sci. Technol.* 47, 20, 11537-11544.

Yigit, N., Cetin, M., Sevik, H., & Aricak, B. (2018). Variation of some micro-morphological characters of leaves of *Aesculus hippocastanum* based on growing environment. 4, 45–52.

Yu, Y., Huang, W., Chen, H., Wu, G., Yuan, H., Song, X., Guan, F. (2014). Identification of differentially expressed genes in flax (Linum usitatissimum L.) under saline-alkaline stress by digital gene expression. Gene, 549 (1), 113–122.

Zhang, X.-F. F., Liu, Z.-G. G., Shen, W., & Gurunathan, S. (2016). Silver nanoparticles: Synthesis, characterization, properties, applications, and therapeutic approaches. International Journal of Molecular Sciences, 17 (9), 1534.

Zhang, Y., Zhang, S., Han, S., Li, X., & Qi, L. (2012). Transcriptome profiling and in silico analysis of somatic embryos in Japanese larch (Larix leptolepis). Plant Cell Reports, 31(9), 1637–1657.

Zhang, Zhi, Shen, W., Xue, J., Liu, Y., Liu, Y., Yan, P., Tang, J. (2018). Recent advances in synthetic methods and applications of silver nanostructures. Nanoscale Research Letters, 13(5),1-18.

Zhang, Zhiyong, He, X., Zhang, H., Ma, Y., Zhang, P., Ding, Y., & Zhao, Y. (2011). Uptake and distribution of ceria nanoparticles in cucumber plants. Metallomics, 3 (8), 816–822.

Zhang, Zhizhen, Li, S., & Lian, X.-Y. (2014). An Overview of Genus Aesculus L.: Ethnobotany, Phytochemistry, and Pharmacological Activities. Pharmaceutical Crops, 1(1), 24–51.

Zhang, Zhizhen, Li, S., Lian, X., Temple, A., & State, S. F. A. (2010). An Overview of Genus Aesculus L.: Ethnobotany, Phytochemistry, and Pharmacological Activities. Pharmaceutical Crops, (1), 24–51.

Zhou, A., Wang, H., Walker, J. C., & Li, J. (2004). BRL1, a leucine-rich repeat receptor-like protein kinase, is functionally redundant with BRI1 in regulating Arabidopsis brassinosteroid signaling. The Plant Journal, 40(3), 399–409.

Zhou, D., Gao, S., Wang, H., Lei, T., Shen, J., Gao, J., Liu, J. (2016). De novo sequencing transcriptome of endemic Gentiana straminea (Gentianaceae) to identify genes involved in the biosynthesis of active ingredients. Gene, 575(1), 160–170.

Zhu JK (2002) Salt and drought stress signal transduction in plants. Annu Rev Plant Biol 53:247–273.

Zipfel, C., & Felix, G. (2005). Plants and animals: A different taste for microbes. Current Opinion in Plant Biology, 8 (4), 353-360.

Zuverza-Mena, N., Armendariz, R., Peralta-Videa, J. R., & Gardea-Torresdey, J. L. (2016). Effects of Silver Nanoparticles on Radish Sprouts: Root Growth Reduction and Modifications in the Nutritional Value. Frontiers in Plant Science, 7, 1-11.

Appendices:

Appendix 1: Hoagland's Nutrient Solution ingredients

Component	Stock Solution	mL Stock Solution/1L
Macronutrients		
2M KNO_3	202 g/L	2.5
2M $Ca(NO_3)_2 \cdot 4H_2O$	236 g/0.5L	2.5
Iron (Sprint 138 iron chelate) Ferric tartrate	15 g/L	1.5
2M $MgSO_4 \cdot 7H_2O$	493 g/L	1
1M NH_4NO_3	80 g/L	1
1M KH_2PO_4 (pH to 6.0)	136 g/L	0.5
Micronutrients		
H_3BO_3	2.86 g/L	1
$MnCl_2 \cdot 4H_2O$	1.81 g/L	1
$ZnSO_4 \cdot 7H_2O$	0.22 g/L	1
$CuSO_4 \cdot 5H_2O$	0.051 g/L	1
$H_2MoO_4 \cdot H_2O$ or	0.09 g/L	1
$Na_2MoO_4 \cdot 2H_2O$	0.12 g/L	1
deionized water		800 mL

Appendix 2: - Calibration curve of NPs.

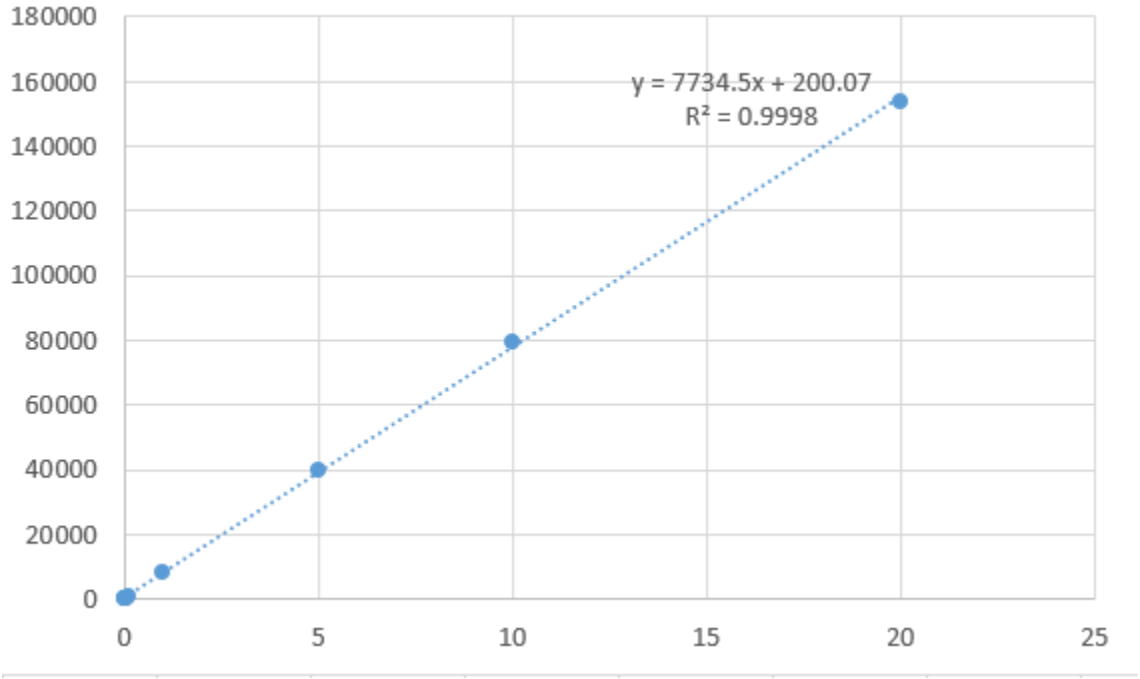

A: Calibration curve of AgNP.

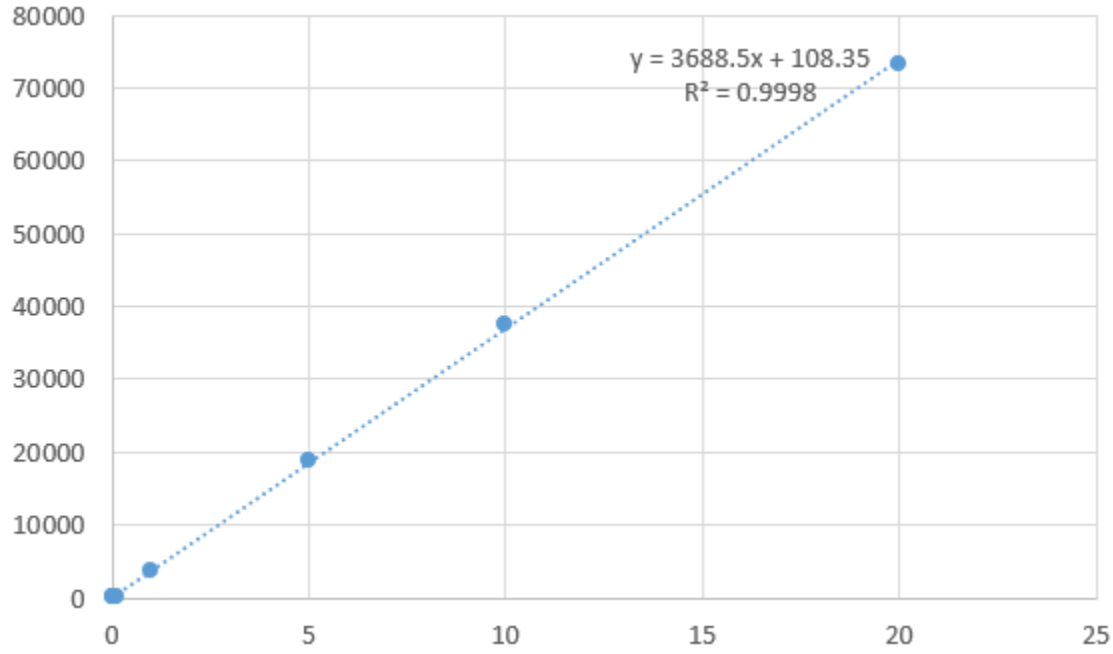

B: Calibration curve of CeO_2 NP.

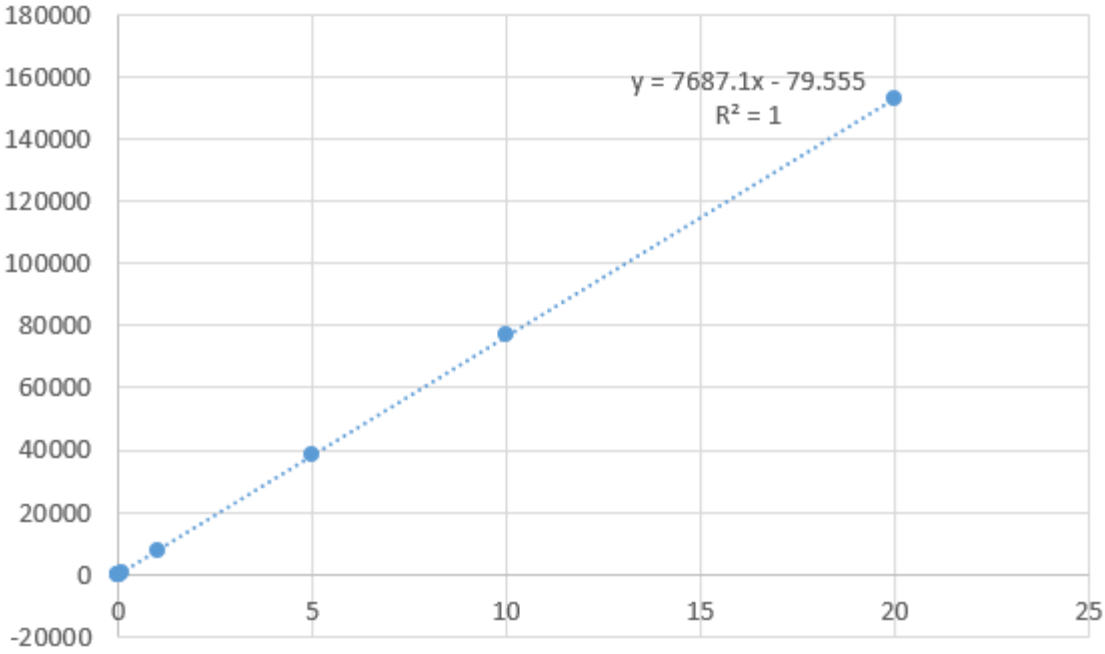

C: Calibration curve of TiO_2 NP

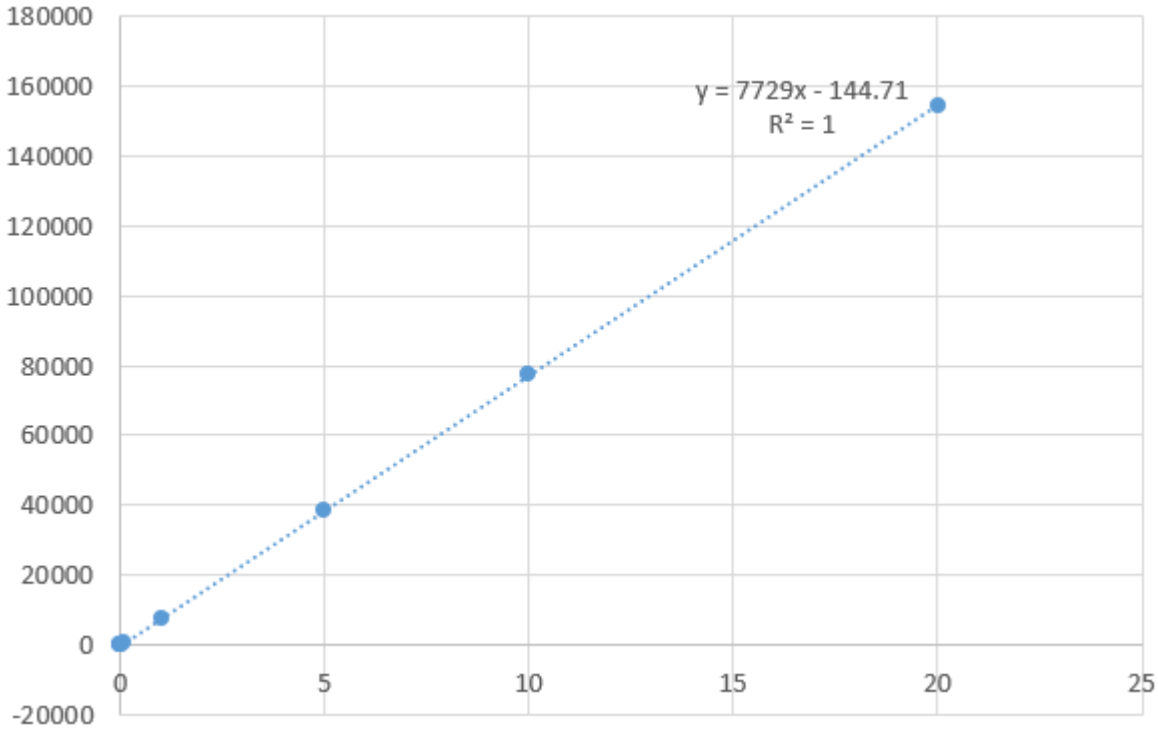

D: Calibration curve of Fe_3O_4 NP

Appendices 3: -

Forward and revers primers for DNA amplification were ordered from Eurofins genomics.

EU264404_F Unmodified DNA Oligos
5'-ATCCCTTGCCGGGAATTTGT-3' HPSF
0.01

EU264404_R Unmodified DNA Oligos
5'-CTCTTGCCACAGGTCACACT-3' HPSF
0.01